MECHANISTIC AND SYNTHETIC ASPECTS OF THE ANODIC OXIDATION OF SUBSTITUTED BENZENES

A thesis submitted for the degree of
Doctor of Philosophy
in the University of Southampton.

by

Olga Pérez de Márquez

July 1981.

To Jairo,

Kira

and Keyla.

UNIVERSITY OF SOUTHAMPTON

ABSTRACT

FACULTY OF SCIENCE

CHEMISTRY

Doctor of Philosophy

MECHANISTIC AND SYNTHETIC ASPECTS OF THE ANODIC OXIDATION OF SUBSTITUTED BENZENES

by Olga Pérez de Márquez

The mechanisms of the anodic oxidation of a series of alkylbenzenes and alkoxybenzenes in dry acetonitrile are discussed. Electrochemical techniques, assisted by analysis of the products, were used to determine the mechanisms. Modulated Specular Reflectance Spectroscopy was used to identify the major intermediates formed during the oxidation of the aromatic compounds.

An ECE type of mechanism is proposed for the oxidation of both, the alkylbenzenes and the alkoxybenzenes. Hexaethylbenzene and 1,4-Dimethoxybenzene are taken as examples to explain the mechanisms for the oxidation of alkyl and alkoxybenzenes, respectively. Reversible oxidation waves were observed in dry acetonitrile for either hexaethylbenzene and 1,4-dimethoxybenzene. All the other compounds oxidized irreversibly under the same conditions.

Decay of the cation radical of the alkylbenzenes occurs due to a side chain proton loss, whilst radical cations from the alkoxybenzenes are attacked on the aromatic ring by the acetonitrile. In all cases, the formation of a nitrilium ion is suggested.

For many of the compounds it was found that preparative electrolyses at constant potential were unsuccesful due to electrode fouling and very poor yields of products. A method of pulsed electrolysis was developed which, in conjunction with the presence of a cationic exchange resin, enabled a high yield of product to be obtain in a relatively clean reaction. This technique greatly extends the utility of the electrochemical method for the functionalization of aromatic compounds.

Acknowledgments

I would like to express my sincere gratitude to my supervisor, Dr. Alan Bewick, for his guidance and advice throughout the course of this work.

Thanks are due to Dr.J. Mellor for fruitful discussions, and Dr. D. Pletcher for his kindness and hospitality.

I would also like to thank the other members of chemistry department, in particular Mr. F. Viloria, Mrs. D. Milano and Dr. V. Solis for their invaluable help.

I am indebted to Mr. J.Castillo and Mr. Miguel Toro for their enthusiastic and great help to finish typing this thesis.

I am grateful to all the people who have been working in this group since I joined it for providing a friendly atmosphere in which to work. Special mention should be done to Dr. K.Kunimatsu and Dr. J. Russell. The technical assistence of the staff of electronic workshop and glassblowing, and in particular Mr. C. Godden and Mr. T. Young, is gratefully appreciated .

I am indebted to 'La Universidad de Los Andes' for its economical support.

Without the collaboration and unfailing encouragement of my husband , Jairo , this research would not possibly be completed.

Thanks are due to miss L. McKeogh for her patience to type most of this thesis.

I am also grateful to all my friends for their continuos encouragement.

CONTENTS

CHAPTER 1: INTRODUCTION

1.1. ELECTROCHEMICAL REACTIONS.

Electroorganic Chemistry has developed considerably in the last few years. This development has involved both, electroorganic syntheses and mechanistic studies of organic reactions. A great number of these reactions are with ion radical intermediates, and electrochemical methods provide very convenient means for generating such intermediates.

An extremely wide variety of electrochemical conversions can be carried out using relatively simple and inexpensive equipment, usually, with the further advantages of speed, good yields and simplicity of work up. It is possible to carry out electrochemically many redox processes, reductions and oxidations, far more efficiently than with the aid of conventional reducing or oxidizing agents.

Oxidations and reductions, particularly those involving fast rates of formation and reaction of intermediates in redox processes can be studied in considerably greater detail electrochemically than is usually possible with chemical oxidants, reductants and conventional kinetic methods. There are several features supporting the utility of electrochemistry in syntheses as the electrode is an incomparable electron source, making it possible to carry out "clean" reactions without polluting the environment with disposal of oxidants or reductants which may produce an ecological inequilibrium , and by controlling potential or current conditions, selective reactions can be performed.

Anodic oxidation is a powerful way to functionalize aromatic compounds. Such reactions involve the participation of cationic intermediates whose stabilities and mechanisms of formation are very

interesting subjects. The behaviour of such reactions can be studied over a wide range of potentials. The intermediates can be detected and, sometimes, identified by their oxidation potentials.

Optical methods have been developed to detect, in situ, electrochemically generated intermediates. Kinetic information can be obtained by analysis of the optical absorption against time responses following a potential step perturbation.

1.2. HOMOGENEOUS REACTIONS IN ELECTROCHEMISTRY.

The Polarographic School of Czechoslovakia was the first place to carry out investigations of coupled chemical reactions in electrochemical systems in the decade of the 40's. Since then, a great deal of the theory and applications of electroanalytical techniques to the study of such systems has been worked out.

If we represent an electron transfer by E and a homogeneous chemical reaction by C and if association of both E and C represent the sequence in which such reactions occur, various combinations of possible mechanisms could be enumerated.

i) CE reaction

$$Y \rightleftharpoons O$$

$$O + ne^- \rightleftharpoons R$$

In this case, O is the species which undergoes electrochemical reaction and it is generated in the reaction media by a chemical reaction

prior to the electron transfer.

ii) EC reaction

$$O + ne^- \rightleftharpoons R$$

$$R \rightleftharpoons X$$

For this sequence, the species formed as a result of the electrode reaction, suffers a further chemical reaction to give a non-electroactive product within the range of potential where the reduction of O is occurring.

iii) catalytic EC^1 reaction

$$O + ne^- \rightleftharpoons R$$

$$R + Z \rightleftharpoons O + Y$$

This is a special case of ii. This mechanism takes place when the product of an electrochemical reaction is reconverted to the starting material at the electrode surface through reaction with a second species which is itself electroinactive within the potentials used. Since the starting material, O, is regenerated at the electrode surface, it may be reduced again and the experiment may fall into a vicious circle These types of mechanism are not very common in organic electrochemistry but they are, quite often met in inorganic systems.

iv.) E.C.E. reaction

$$O_1 + n_1e^- \rightleftharpoons R_1 \qquad E_1^0$$

$$R_1 \xrightarrow{(+z)} O_2$$

$$O_2 + n_2e^- \rightleftharpoons R_2 \qquad E_2^0$$

Here, the chemical reaction follows a previous electron transfer, and produces species which are electroactive at potentials of the O_1/R_1 electron transfer reaction. Thus a second electron transfer reaction can take place. ECE processes are very common in organic electrochemistry,[11] but in most of these, the reduction of O_2 is possible at a less negative potential than that required for O_1, for example $E_2^0 > E_1^0$. In such cases, there can be a competition between homogeneous electron transfer reactions and electron transfer involving the electrodes directly, therefore it is necessary to distinguish between E.C.E. processes and mechanisms involving disproportionation reactions (DISP). This cannot be made by ordinary electrochemical techniques, but it is possible by means of Modulated Specular Reflectance Spectroscopy (MSRS).

This mechanistic complication is met in the anodic oxidation of hydrocarbons. The competing process can be represented by the following generalized reaction scheme.

$$\{1\} \quad RH \overset{E_1}{\rightleftharpoons} RH^{+\cdot} + e^-$$

$$\{2\} \quad RH^{+\cdot} \xrightarrow{k} R^{\cdot} + H^+$$

$$\{3\} \quad R^{\cdot} \overset{E_2}{\rightleftharpoons} R^+ + e^-$$

$$\{4\}\quad R^{+} + \text{nucleophile} \longrightarrow \text{products}$$

$$\{5\}\quad RH^{+\cdot} + R \rightleftharpoons RH + R^{+}$$

If the sequence {1}, {2}, {3}, takes place, then a pure E.C.E. mechanism occurs, while the {1}, {2}, {5} sequence is a pure DISP mechanism. Of course, in general, a mixture of these two limiting cases would be expected depending upon the magnitude of the rate constant for step {5}.

Saveant and co-workers have given a theoretical analysis for disproportionation and E.C.E. mechanisms and their applications to several systems. They discuss diagnostic criteria and rate determination in such systems,[2-5] as well as dimerization reactions.[6,7] It was, however, in this laboratory,[8] that it was shown for the first time that Specular Reflectance Spectroscopy could be used to make a clear mechanistic assignment in E.C.E./DISP cases; thus demonstrating the power of this technique. Bewick and co-workers[9] using hexamethylbenzene as an example, have proposed the following kinetic scheme:

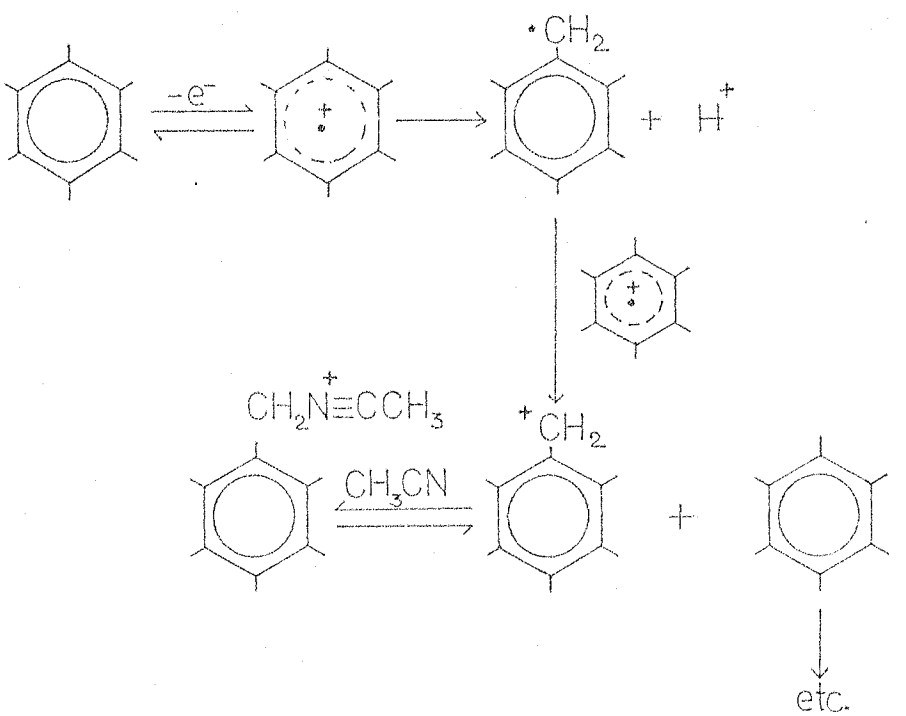

The rate of the oxidation of the neutral radical by the cation radical was sufficiently fast (diffusion controlled) to effectively prevent the oxidation taking place directly at the electrode.

1.3. AROMATIC HYDROCARBONS.

When a solution containing an aromatic hydrocarbon is oxidized, a great number of reactions can take place as a function of the structure of the aromatic compound and the environmental conditions.

The most common reactions observed in anodic oxidation of aromatic compounds have been classified as: a) side chain substitution[10], b) nuclear substitution[11], c) addition[12], d) dimerization[13]. Typical examples have been given by the authors:

a) 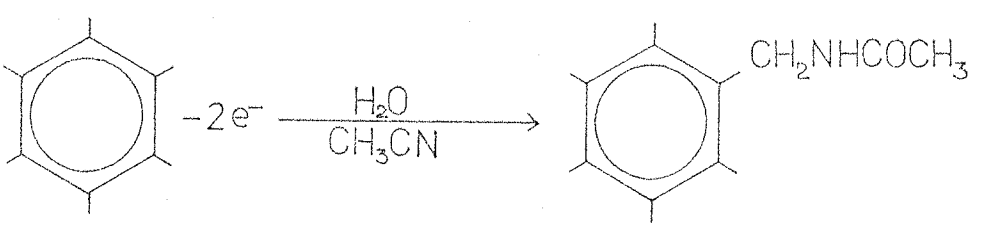

b) 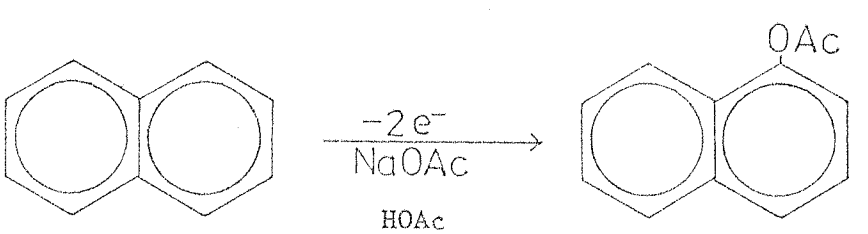

c) 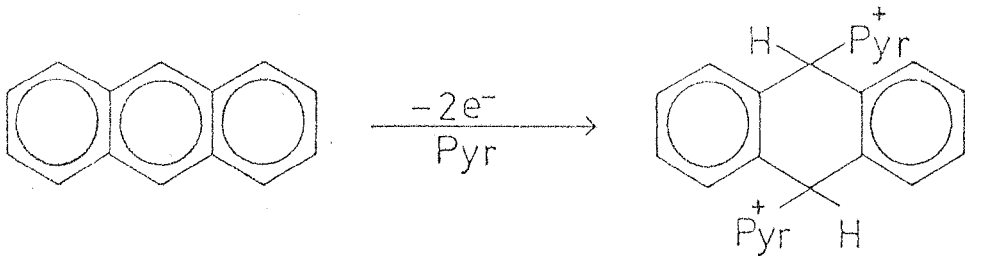

d) 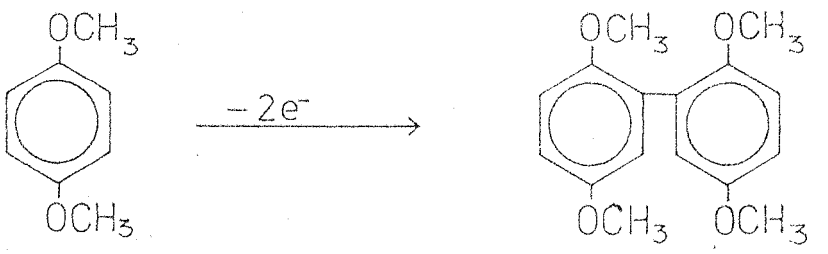

If experimental conditions are suitably chosen, the course of an oxidation could be shifted to favor any of these processes.

Most organic compounds are insoluble in aqueous solutions, consequently, the use of an appropriate non-aqueous solvent is necessary; the solvent must be chosen to be able to dissolve a sufficient quantity of supporting electrolyte as well as the substrate of interest. Of great importance is the dielectric constant of the solvent, since electrolytic conductivity will always be necessary. Values of a dielectric constant larger than 10 are necessary to avoid experimental difficulties. When a solvent with smaller dielectric constant is used, it is necessary to have quite high concentrations of supporting electrolyte to achieve

reasonable conductivities. Solvent viscosity is also important for voltammetry and chronoamperometry. Mass transfer by diffusion is more easily maintained in a viscous medium. For large scale work, where rapid transport to the electrode is desirable, low viscosity is advisable. When coupled chemical reactions are considered, as is usually the case for organic electrochemical reactions, the ability of the solvent to behave as a nucleophile and participate in the reaction can be useful. These electrophile-nucleophile combination reactions have been discussed in detail by Ritchie[26].

Acetonitrile is an excellent solvent. It is quite difficult to oxidize and reduce; ion radicals are more stable in acetonitrile than they are in water. A very important requirement for the solvent as well as for the supporting electrolyte is that it should be stable in the presence of the electrode reaction.

Many cases are known to undergo reaction with the solvent to form stable compounds, Eberson and Nyberg[14] working with hexamethylbenzene in acetonitrile obtained an N-benzylacetamide:

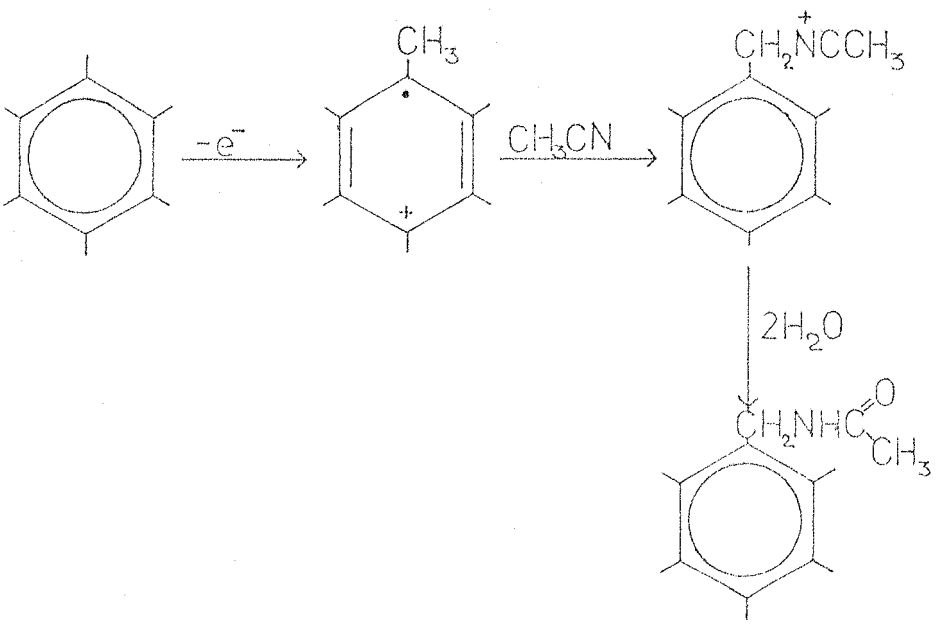

A later work carried out by Nyberg and co-workers[14], used benzene, toluene, p-xylene and mesitylene (all of them with higher oxidation potentials under the same conditions) and using methylene chloride as the solvent and tert-butylammonium tetrafluoroborate as supporting electrolyte with added trifluoroacetic acid or methane sulphonic acid to ensure that the methylene chloride would not be reduced to Cl^- at the counter electrode. When the reaction was carried out without other hydrocarbons with hexamethylbenzene, this was oxidized to form pentamethylbenzyltrifluoroacetate, in a very high yield. When hydrocarbons were added, at least five different kind of products were observed, showing competitive reactions with the intermediates produced as a consequence of the anodic oxidation of hexamethylbenzene.

More interesting studies have been made of the oxidation of alkylbenzenes [15, 16] leading to functionalized derivatives. Bewick et al[16-18] have studied the mono- and poly-functionalization of alkylbenzenes, reporting their synthetic and mechanistic results. Oxidation of hexamethylbenzene was also studied by them [16, 18] in dry acetonitrile. Voltammetry of hexamethylbenzene showed six separate anodic waves. The first wave (+1.25 V.) is associated with the transfer of two electrons leading to a high concentration of the nitrilium ion,

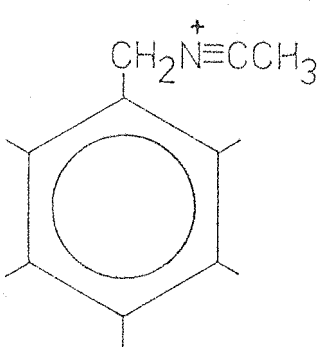

which, in the presence of water, formed N-(2,3,4,5,6-pentamethyl-benzyl)-acetamide with a high yield.

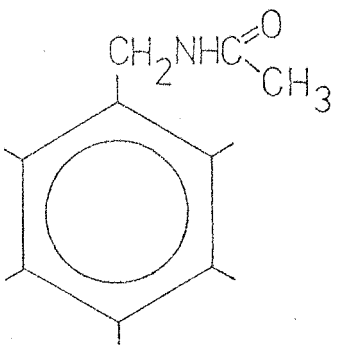

At the second voltammetric wave (1.70 V), 1,3- bis (acetamide methyl)-2,4,5,6-tetramethylbenzene is the main product. The monoamide being a minor product. The transfer of two additional electrons was observed to be associated with the second wave. They concluded that the mono and difunctionalization can be succesful although, in some cases, the preparative oxidation was not very sucessful because some polymers were also obtained.

Mechanistic schemes have been proposed. Eberson[19] suggested the formation of a cation radical as the initial oxidation product of alkylbenzenes in acetonitrile. They propossed that if a cation radical is formed and then diffuses to the bulk of the solution, a proton could be lost to form the neutral radical with the further dimerization. But if the cation radical loses the proton in the interface, the neutral radical so formed would be oxidized to the cation with two further possibilities:either reaction with water to give alcohols or with the solvent (acetonitrile) to form amides. The half-life of the pentamethyl-benzene cation radical was calculated[20] to be, approximately 25 msec

by using Nicholson and Shain's method [21]. By using E.S.R. [8], hexamethylbenzene cation radical half-life time was found to be 10^3 times longer than the other methylbenzenes cation radicals. Bewick and co-workers [17.23] proved the existence of ion and radical intermediates in the anodic oxidation of methylbenzenes in acetonitrile using Modulated Specular Reflectance Spectroscopy. In a posterior work[9] they studied the mechanism for the anodic oxidation of methyl benzenes in acetonitrile and, by spectroelectrochemical methods, they were able to distinguish clearly between ECE and DISP mechanisms.

As in organic reactions, specially in organometallic syntheses and controlled catalysis, the use of polymer bound reagent has being producing good results to prepare compounds under controllable conditions[24], and to find whether it would be possible to extend such applications of the polymer to electrodic reactions. Bewick et al [25] investigated the electrooxidation of the methylbenzenes by following a typical scheme for durene: (see the following page)

They found that using a good quality polystyrene polymer based resin (in their case, Dowex 50 w-x 8, with sulphonic acid groups bound to the polystyrene matrix), they were able to remove, from the solution, the nitrilium ion formed when methylbenzenes were oxidized in acetonitrile, inhibiting subsequents reactions. In this way, they could select the conditions to functionalize methylbenzenes in acetonitrile to produce amides. With this method, they improved yields of products, which proved that the carbonium ion is converted to the nitrilium ion very rapidly and so trapped by the resin. They suggested that this new method will be very useful in industrial processes.

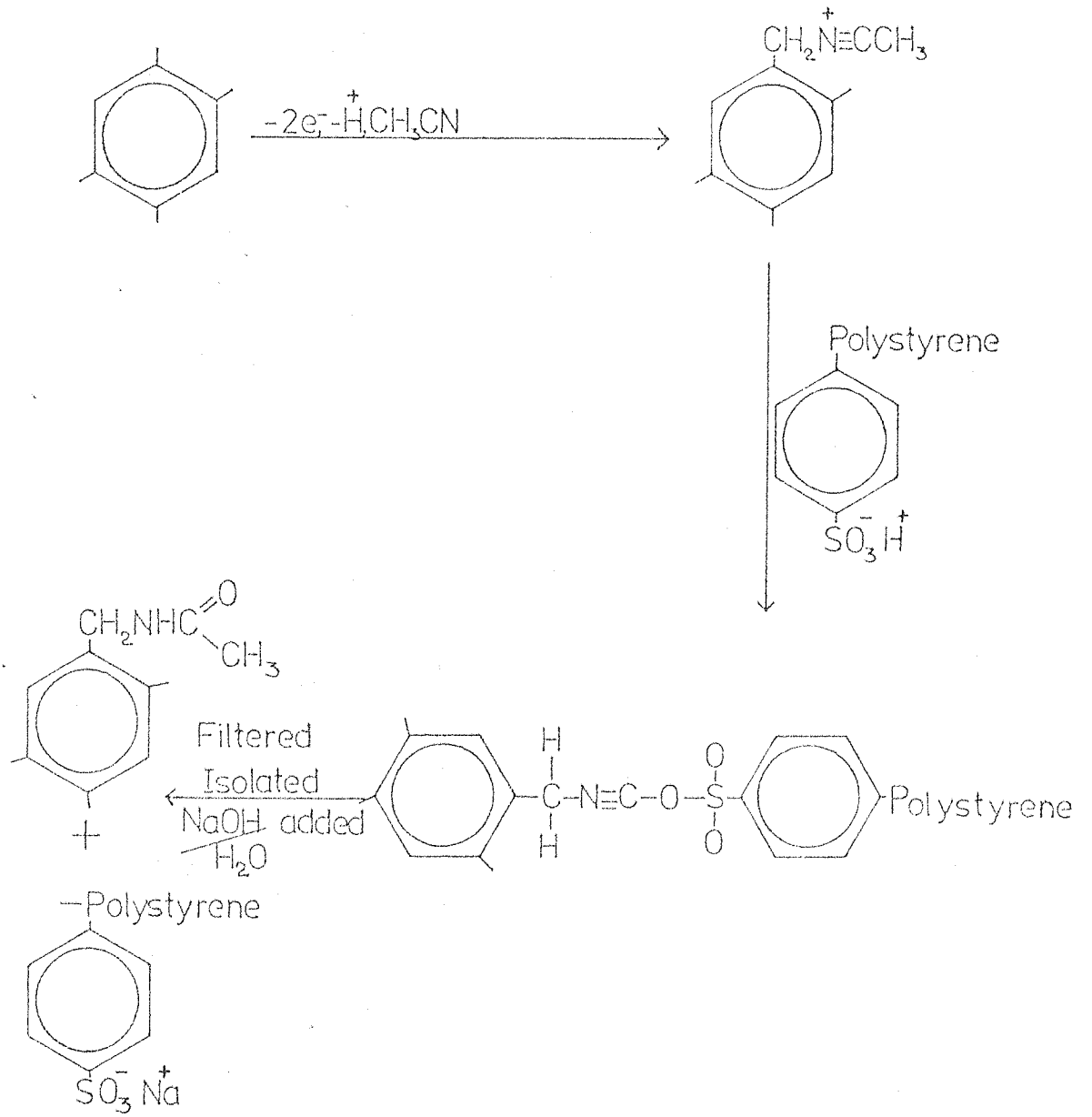

In this work, the functionalization of longer chain substituted alkylbenzenes in acetonitrile will be described. The application of a pulse technique for preparative electrolysis was coupled with the use of polymer bound reagents to improve the yields of the production of acetamides in the anodic oxidation of hydrocarbons in acetonitrile.

1.4. ALKOXY AROMATICS.

Methoxy substituted aromatics comprises a type of compound with electron-rich molecular π orbitals. The substituent interacts strongly with the ring and the high symmetry of benzene derivatives, simplifies theoretical treatment of their properties. Those properties make them strong candidates to be studied. Due to the relatively high stabilities of their cation radicals, E.S.R. spectra have been obtained of the radicals which were produced by oxidation with sulphuric acid, pulse radiolysis, photochemically, or electrochemically.

Much of the difference between the oxidative behavior of simple aromatic hydrocarbons and oxygenated aromatics, is due to the powerful stabilizing effect of oxygen upon cationic intermediates.

Andreades and Zahnow[27,28] studied cyanation of organic compounds, performing electrolyses in CH_3CN/Et_4CN and in $CH_3OH/NaCN$, under controlled potential conditions. Without the aromatic present, electrochemical oxidation of cyanide ion in CH_3CN gave no evidence of cyano radical. In the presence of aromatic alkoxy compounds, electrolyses gave products resulting from aromatic, substitution of hydrogen or methoxy groups by nitrile.

They suggested that the products may be predicted on the basis of spin density distribution calculated from E.S.R. spectra of the cation radical. Later in the section, a list with the values of calculated spin densities reported in the literature, will be given. They suggested the following mechanism for cyanation of 1,4-dimethoxybenzene:

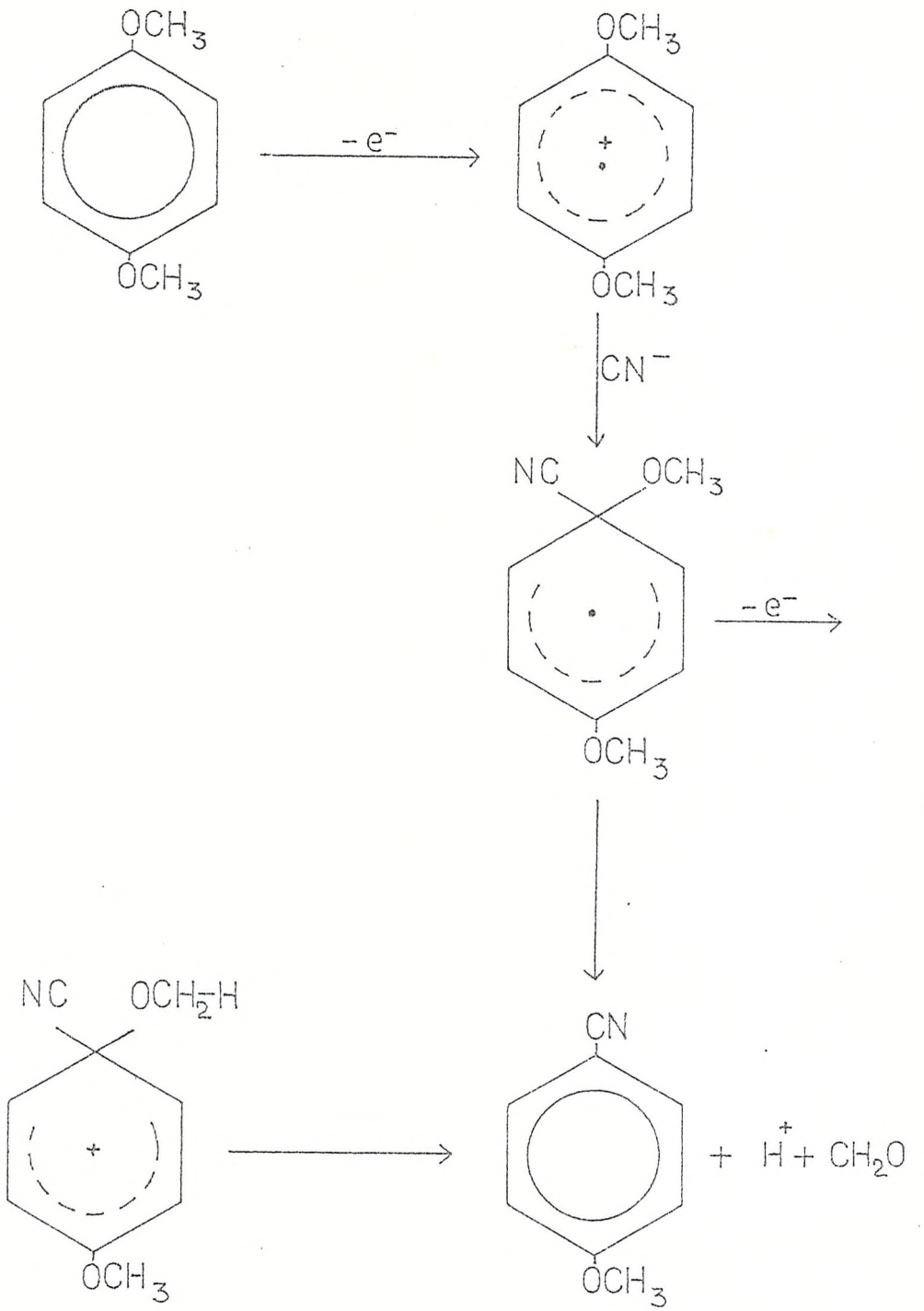
OCH3
OCH3
-e⁻
OCH3
OCH3
CN⁻
NC
OCH3
-e⁻
OCH3
NC
OCH2H
OCH3
CN
OCH3
+ H⁺ + CH2O

Electrolysis of anisole[29,30] in CH_3OH/KCNO at 1.8 V. against S.C.E. gave a product of substitution of an aromatic hydrogen atom.

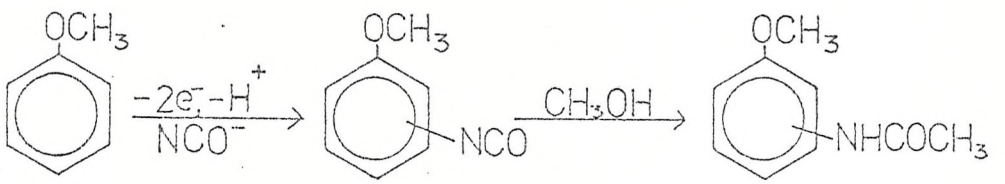

Aromatic substitution was not observed at 1.0 V vs. SCE, but only at more positive potentials. They had evidence for a reaction involving discharge of the aromatic, followed by nucleophilic attack of cyanate ion.

The following mechanism scheme has been proposed[5] for the oxidation of 1,3 -dimethoxybenzene in CH_3OH:

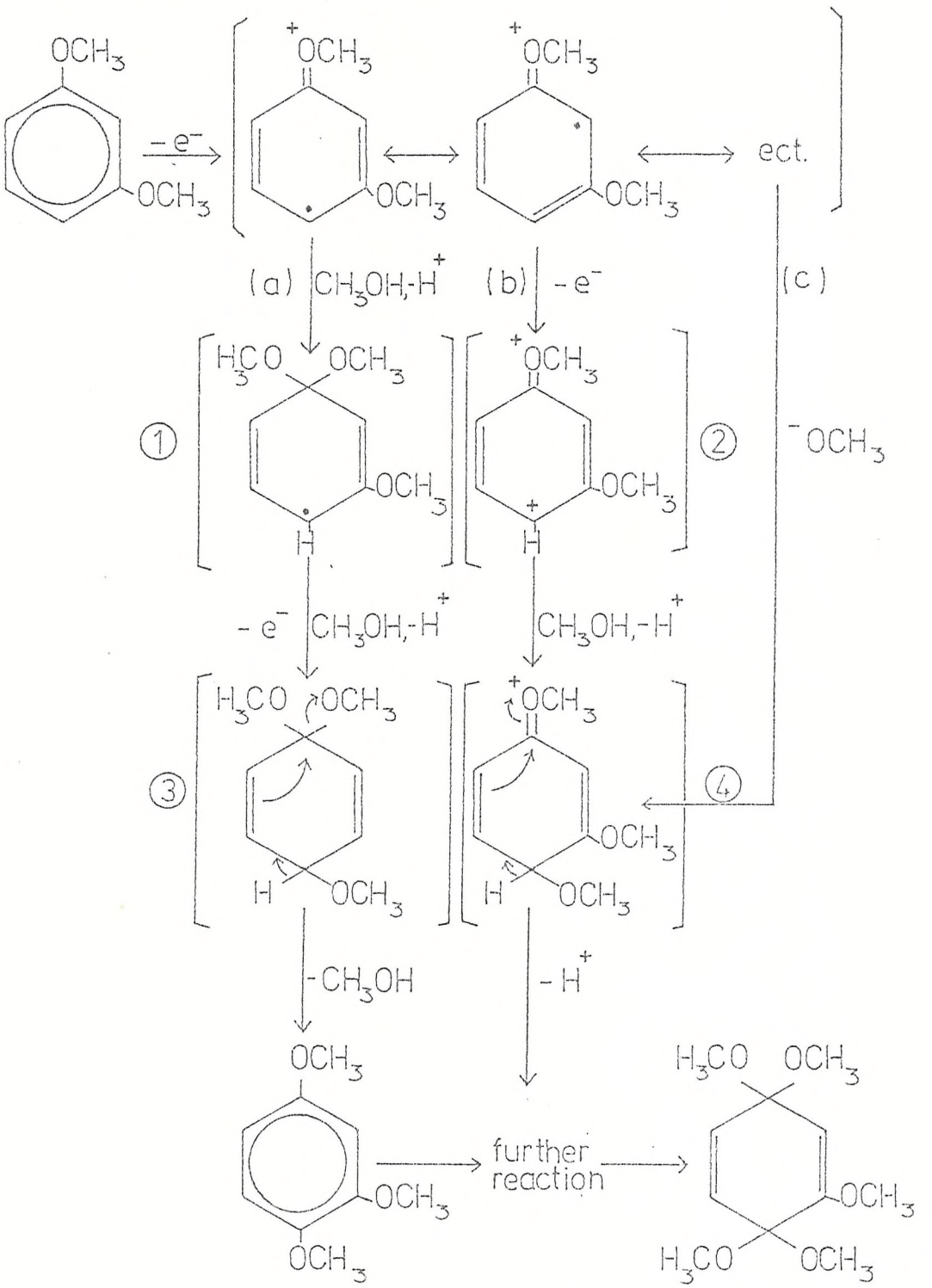
OCH3
-e⁻
ect.
(a) CH3OH,-H+
(b) -e⁻
(c)
H3CO
①
②
-OCH3
-e⁻ CH3OH,-H+
CH3OH,-H+
③
④
H
-CH3OH
-H+
further reaction

To explain the scheme above, they carried out experiments using 1,3-dimethoxybenzene labeled with $O^{14}CH_3$. Those experiments did not show a decrease in the specific radioactivity of (3), excluding the possibility of mechanism (a) and favouring (b) or (c).

Methoxylation of 1,2-dimethoxybenzene (veratole)[31] gave, apart from the products obtained for the oxidation of 1,3-dimethoxybenzene, 5,5,6,6-tetramethoxy-1,3-cyclohexadiene (I) and hexamethyl-cis,cis-othomuconate (II):

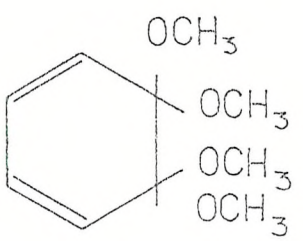

I

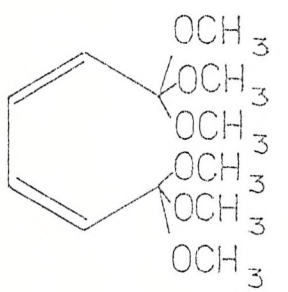

II

The author confirmed that(II) is obtained from (I) by electrolysis of (I) to give (II) in 77% yield. They proposed the following reaction:

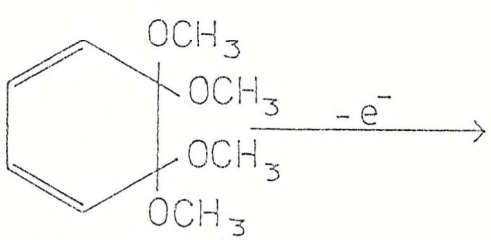

I

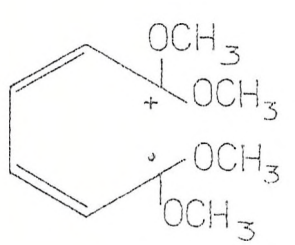

III

suggesting that the intermediate species III is not long-lived and that an adsorption process may be involved in maintaining the cis-cis configuration.

Anodic acetoxylation and methoxylation of anisole[32] gave o, m, and p-products, in both cases, m-products were found in low yield. For the O- and p-products, the rate methoxylation/acetoxylation, was found to be 39/67.4 and 58/29.1.

Eberson[33] suggested a concerted mechanism involving a two-electron transfer from anisole with formation of a C-O bond for the acetoxylation. This suggestion is consistent with that proposed for electrophilic aromatic substitution in homogeneous solution[34] A preponderance of the ortho isomer has been proposed[35] in the photochemical methoxylation of anisole.

Oxidation of methoxybenzenes in acetonitrile at platinum electrode was performed[36] and E.S.R. spectra obtained at controlled potential in situ in H_2SO_4 96%.Polarographic data were obtained using dry acetonitrile at a rotating disc electrode. Tetra n-propylammonium perchlorate was used as supporting electrolite and the SCE as reference electrode. They made molecular orbital calculations to help to explain their results. All the methoxybenzenes, under controlled potential oxidation, displayed E.S.R. spectra when the potential was adjusted to the peak of their first oxidation wave. Results for the 1,4-dimethoxybenzene, suggested two different radical species and they attributed it to the possibility of cis-trans isomerism.

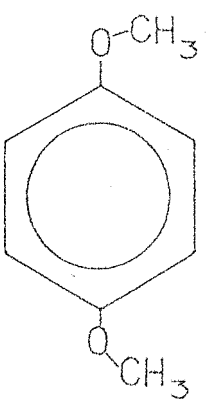

cis

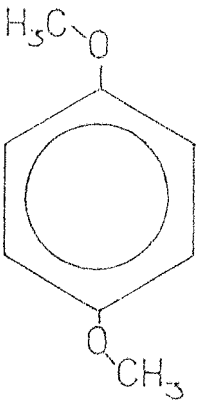

trans

They observed E.S.R. spectra at 1.0 V against SCE, and as the potential was increased the shape of the spectra changed. From 1,3-dimethoxybenzene the spectrum obtained was found unlikely to be due to the cation radical. 1,2-dimethoxybenzene (veratrole), and anisole, showed a single line for E.S.R.

Norman and Thomas[37] compared acetoxylation for o-m- and p-dimethoxybenzene. They found m-dimethoxybenzene to be less reactive than the others, probably because in that reaction, where the aromatic compounds donates one electron to an electrophilic reagent, the energy of its highest filled molecular orbital is greater than those of its isomers. They extended their expectation to a reaction in which the aromatic compound donated two electrons. The observed order of reactivity was found to be p>o>m , for acetoxylation. They suggested aromatic substitution.

Similar studies of acetoxylation were carried out by Yoshida and co-workers[38]. They oxidized, anodically, p-dimethoxybenzene under a nitrogen atomosphere using a platinum foil anode in glacial acetic acid containing sodium acetate and at a constant current of

0.1 A; 2,5-dimethoxy-phenylacetate (68% yield) was the main product. They attributed the primary step of the oxidation to a direct discharge of the aromatic at the anode, from a cation radical intermediate. The second stage is the combination of the cation radical intermediate with the nucleophile. In each case, the methoxyl displacement by cyanide ion occurs at the position of highest spin density, but acetoxylation does not show the same behavior. Yoshida[38] attributed this to the unstability of an acylol type of intermediate, because acetate ion is a better leaving group than the methoxide ion. They proposed the following mechanism:

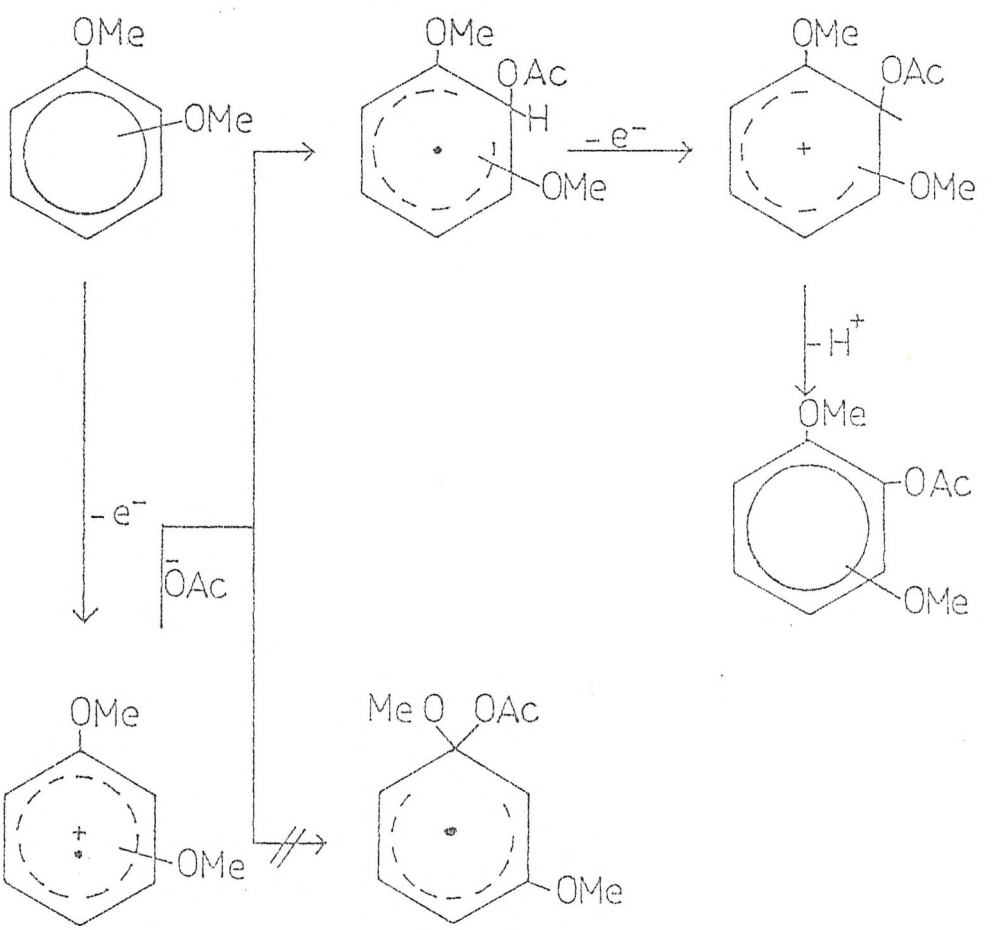

Cation radical pairing has been postulated[13] as the mechanism for anodic coupling of aromatic compounds. Since methoxy aromatic compounds are far more nucleophilic than hydrocarbons, the coupling mechanism would appear to be even more plausible for these substrates.

Potential dependent competitive cyanation and methoxylation of 1,4-dimethoxybenzene was studied by Weinberg et al[31]. They oxidized p-dimethoxybenzene in NaCN-CH_3OH, and suggested, in both cases, the formation of a cation radical. By voltammetry, they found n=2 electrons per molecule of p-dimethoxybenzene. They stated that relatively stable carbonium ions, will react about 40 times faster with methoxide ions than with cyanide ions in methanol solution. The following sequence was proposed:

Mech. I

$$R \overset{E_1}{\rightleftharpoons} R^{+}\cdot + e^{-}$$

$$R^{+}\cdot \overset{E_2}{\rightleftharpoons} R^{+2} + e^{-} \qquad E_2 > E_1$$

Mech. II Disproportionation

$$R \rightleftharpoons R^{+}\cdot + e^{-}$$

$$2R^{+}\cdot \rightleftharpoons R + R^{+2}$$

there is much support from literature for this mechanism.

Mech. III Competitive reaction of

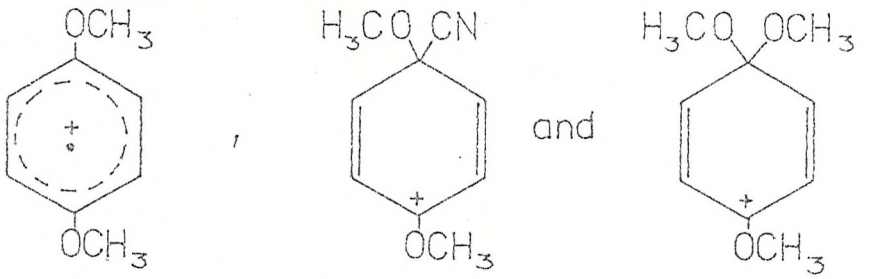

with CN^- and CH_3O^- ions following the scheme:

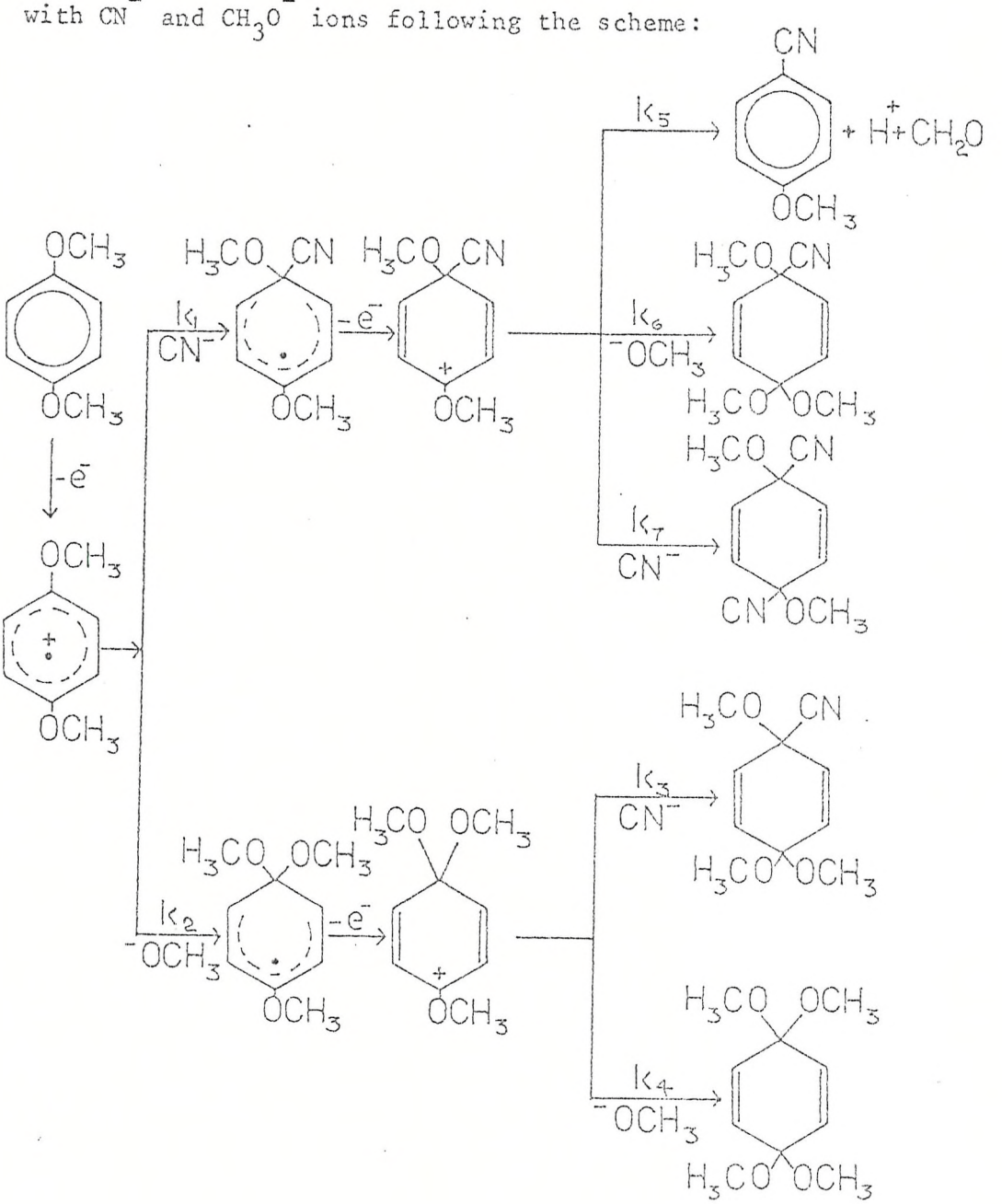

The cation radicals of alkoxy aromatics have been found to be remarkably stable in trifluoroacetic acid. Veratrole[40] was oxidized in TFA acid, and trimer cation radical was observed.

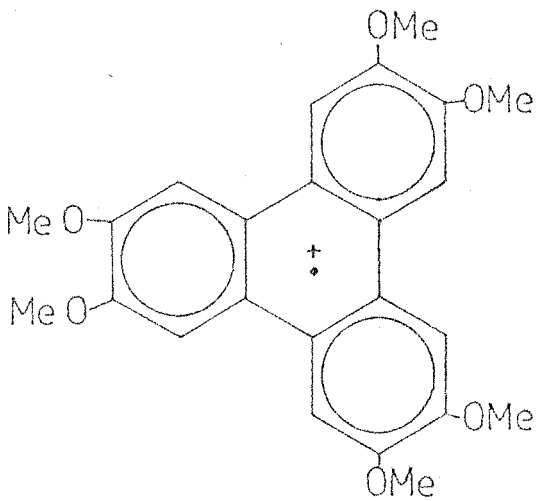

P. O'Neill and co-workers[41] studied the sequences: anisole, 1,2-; 1,3-; and 1,4-dimethoxybenzene and 1,2,3-; 1,2,4,-; and 1,3,5-trimethoxybenzene using optical and conductometric pulse radiolysis and in situ radiolysis E.S.R. for detection. They produced the radicals cation by pulse irradiation of 10^{-3}M Tl_2SO_4 solutions saturated with H_2O at pH 4 containing 10^{-4}M of the methoxy aromatic and suggested the decay to follow a second order kinetics with rate constants ranging from 4×10^3 to $1 \times 10^9 M^{-1}$ sec^{-1}; depending on the position of the methoxy groups relative to each other. At 5°C, they monitored the E.S.R. spectra for cis and trans isomers of p-dimethoxybenzene- in contrast, ortho and meta dimethoxybenzene E.S.R. spectra showed no evidence for the existence of more than one isomer. The cation radicals were found to decay more rapidly in the case of anisole, 1,3-dimethoxybenzene and 1,3,5-trimethoxybenzene than those of 1,2- and 1,4-dimethoxybenzene. In agreement with these kinetic results, the stationary concentration of the cation radicals of anisole and 1,3-dimethoxybenzene, was found,

for E.S.R., to be considerably lower than that of 1,2- and 1,4-dimethoxybenzene, respectively. They used p-dimethoxybenzene as an example to explain the mechanism they proposed, assuming that the mechanism is also applicable to the other methoxylated benzenes.

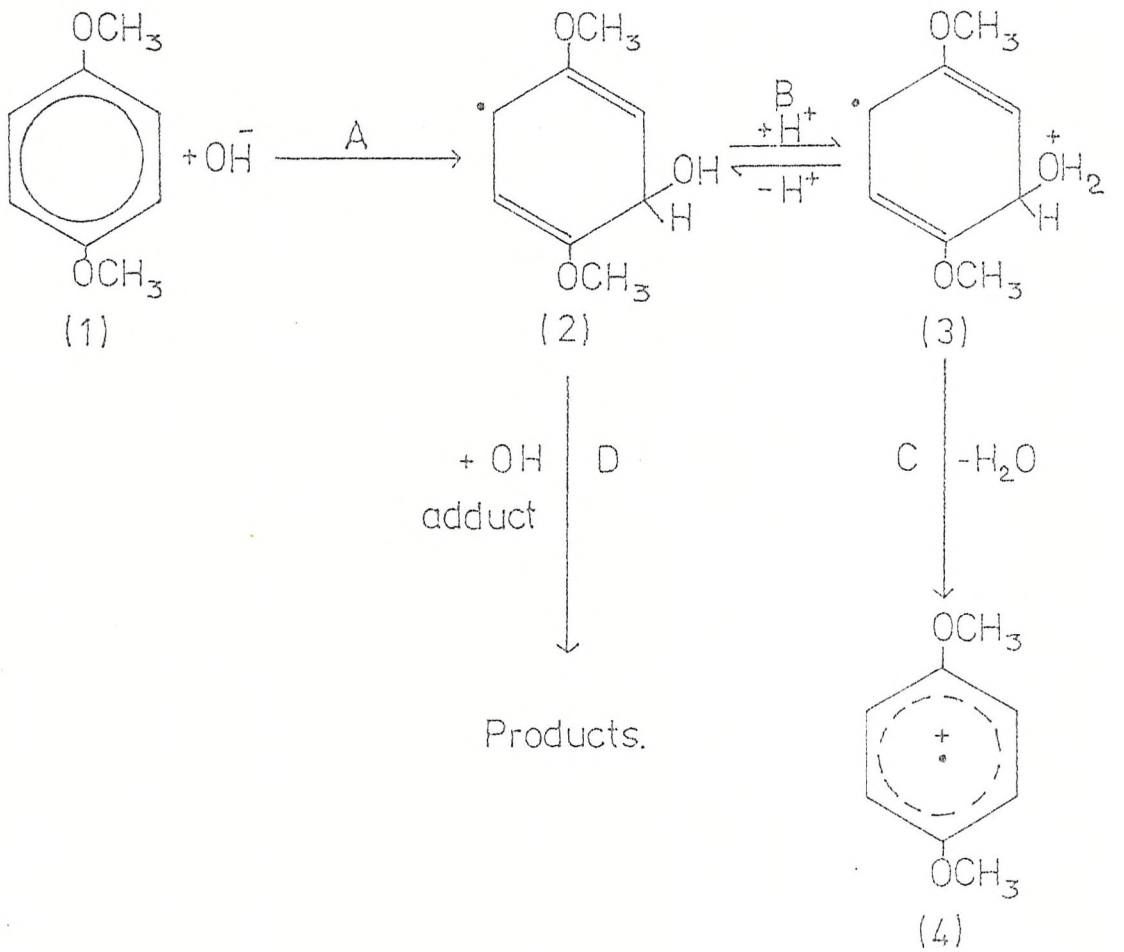

As they changed the pH, they found rate constant for the decay of the cation radicals to be dependent on pH and when the pH was increased over 4, the decay tended to follow a first order behavior. From the scheme above, they proposed that electron transfer from radical (2) to cation radical, may result in a carbonium ion:

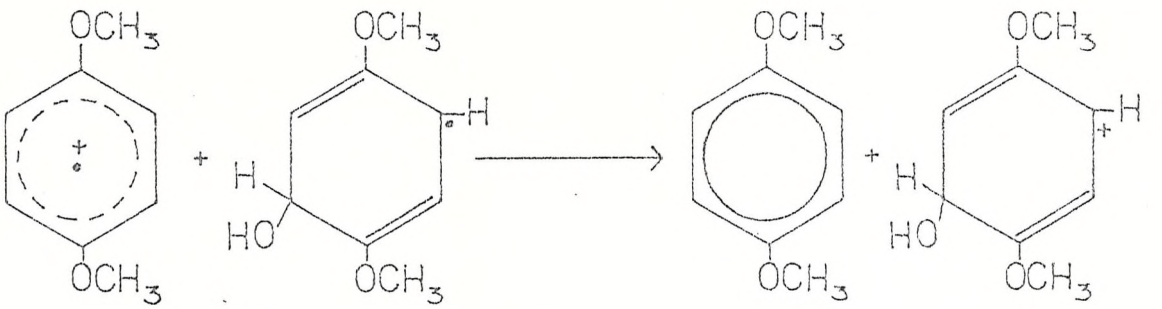

but that it could also form a dimeric product:

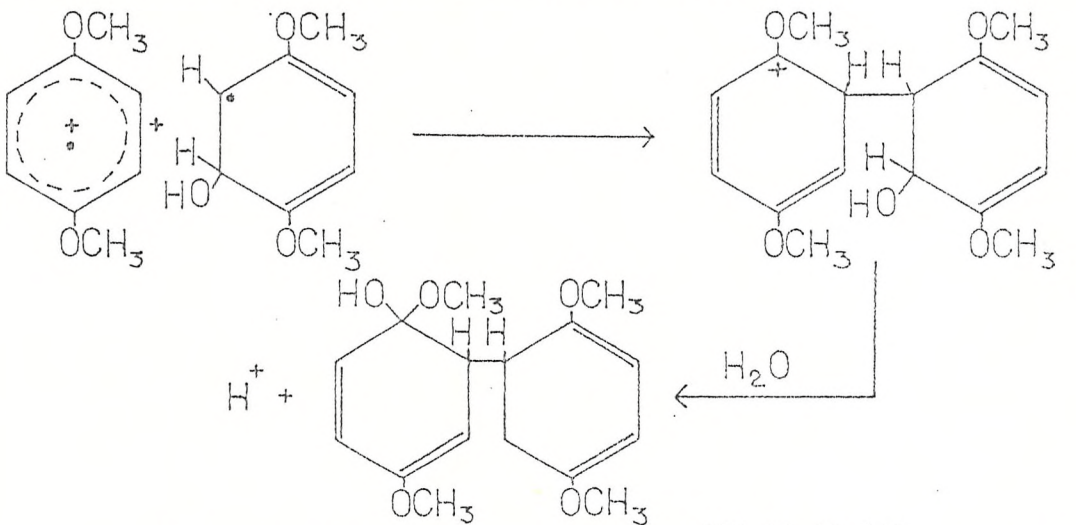

As we can see from the literature,[27,36,42-44] a great number of E.S.R. studies have been done to the alkoxyaromatics in order to explain their behavior by molecular orbitals consideration of spin densities. A summary of such data is shown below:

Reactant	Position	Spin densities for cation radical
Anisole	1	0.258
	2,6	0.122
	3,5	0.048
	4	0.282
	oxygen	0.120
1,2-dimethoxy benzene	1,2	0.233
	3,6	0.012
	4,5	0.162
	oxygen	0.092

1,3-dimethoxy-benzene	1,3	0.161
	2	0.000
	4,6	0.270
	5	0.000
	oxygen	0.069
1,4-dimethoxy-benzene	1,4	0.241
	2,3,5,6	0.084
	oxygen	0.090
1,3,5-trimethoxy-benzene	1,3,5	0.107
	2,4,6	0.180
	oxygen	0.046

Raman spectroscopy has been combined with E.S.R.[45] to study alkoxy aromatics: 1,4-dimethoxybenzene cation radical was generated in acidic aqueous solution by oxidation with Cerium IV[45] The free radical was studied in steady-state conditions by Raman spectroscopy .

A free radical species, at very low concentrations, can produce a strong band in a solution spectrum.

They determined the optical parameters and calculated the half time of the cation radical at different experimental conditions, and it was found to be within a range of 2.2 to 3 sec.

The effect of an alkyl substituent in alkoxy aromatics has been also considered[45-47]: Electrochemical oxidation of methylanisoles in methanol containing sodium cyanide was investigated by Yoshida[46]. In the case of ortho and meta substitutions nuclear cyanation took place preferentially,with p-methylanisole, side chain methoxylation compound was formed as the main product. They propose then the following mechanism scheme:

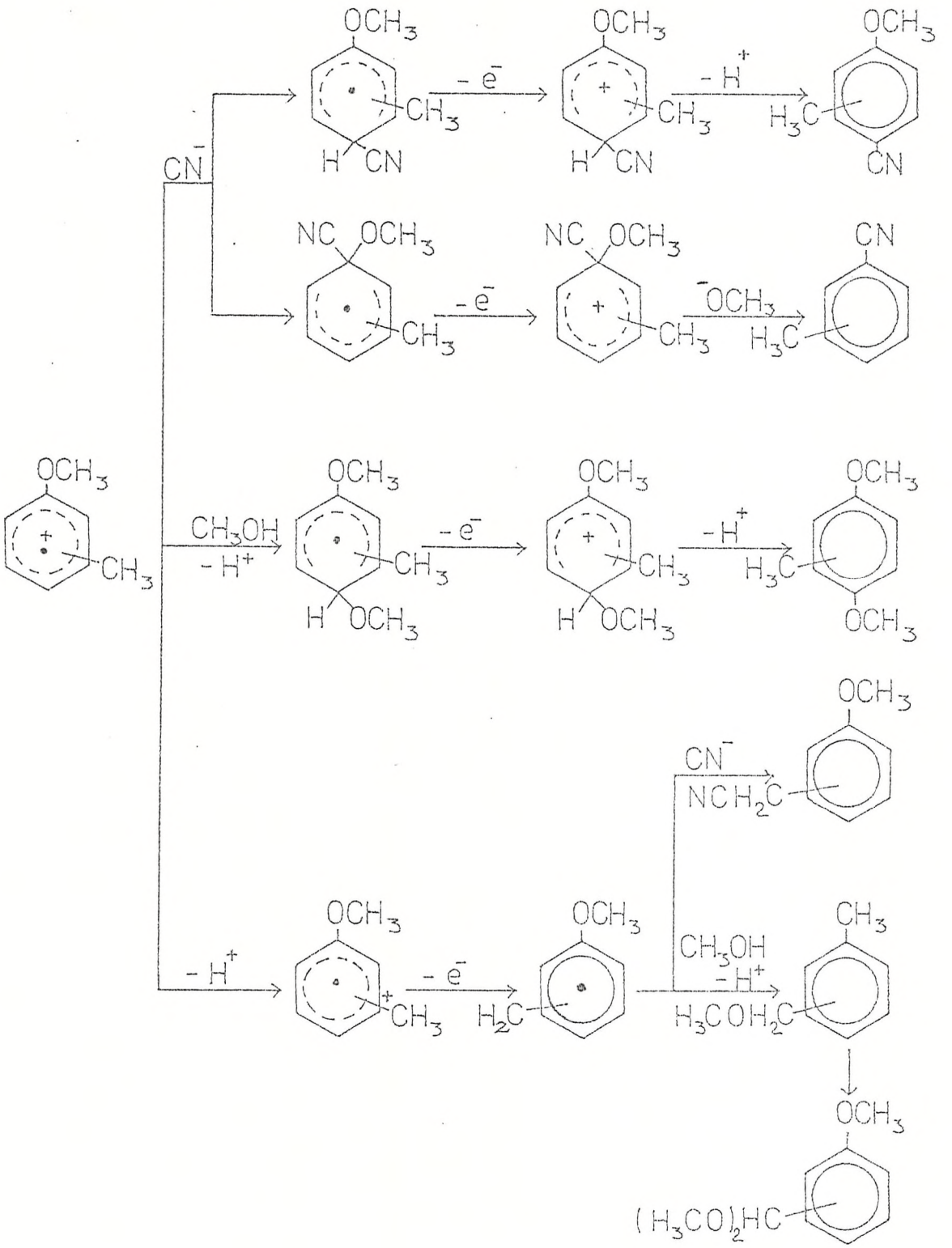
OCH3
CH3
CN⁻
- e⁻
- H⁺
H CN
NC OCH3
⁻OCH3
H3C
CN
CH3OH
- H⁺
H OCH3
CN⁻
NCH2C
CH3OH
H3CO H2C
(H3CO)2HC

In any case, for the scheme above, they proposed the scheme: cation radical-neutral radical-carbonium ion, whether the substitution is on the ring or on the side-chain. In an earlier paper Yoshida and co-workers[47] demonstrated that there are two esentially important stages for anodic cyanation of aromatic compounds: firstly, the electrochemical oxidation of organic compounds to cation radicals and secondly, the reaction of the combination of the cation radical with the CN^- ion. The second stage being apparently assisted by larger positive charge localized on the carbon atoms in the cation radical. They calculated such charge distribution and the results are shown below.

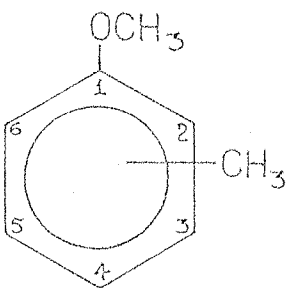

Reactant	Position	Charge
2-methyl-anisole	1	0.1284
	2	0.0335
	3	0.0418
	4	0.1264
	5	0.0525
	6	0.0694
	7	0.0476
	oxygen	0.5000
3-methyl-anisole	1	0.1326
	2	0.0647
	3	0.0064
	4	0.1259
	5	0.0505
	6	0.0798
	7	0.0393
	oxygen	0.5013

4.methyl-	1	0.1312
anisole	2,6	0.0744
	4	0.0459
	3,5	0.0817
	7	0.0557
	oxygen	0.0491

For the p-methylanisole, they proposed the reaction of the cation radical to lose a proton. Also, an attack of a nucleophile on the aromatic ring was proposed to compete with the side chain reaction when a relatively reactive nucleophile is used. They found that the relative degree of positive charge on the carbon atoms with an aromatic hydrogen in p-methylanisole cation radical is less than that for the o- and m- methylanisole.

Oxidation of anisole in MeOH [51] has shown:

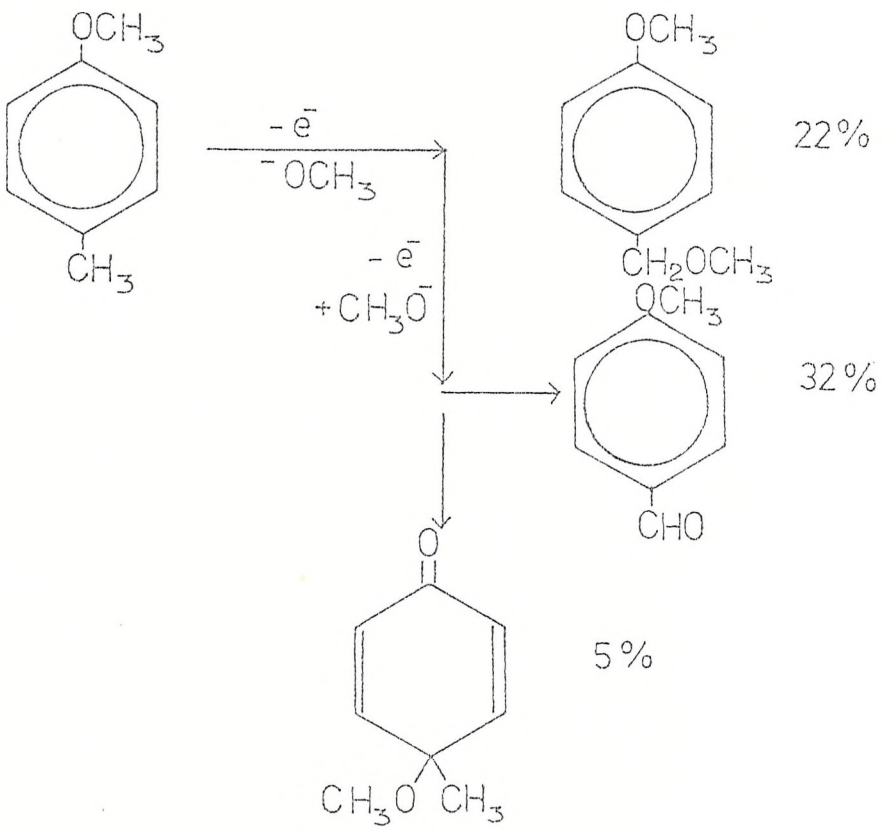

1.5. REFERENCES

(1) G.S. Alberts and I. Shain, Anal. Chem., 35, 1859 (1963).

(2) M. Mastragostino, L. Nadjo and J.M. Saveant Electrochimica Acta, 13, 721 (1968).

(3) M. Mastragostino and J.M. Saveant. Electrochimica Acta, 13, 751 (1968).

(4) L. Nadjo and J.M. Saveant. Electrochimica acta, 16, 887 (1971).

(5) L. Nadjo and J.M. Saveant, J. Electroanal Chem., 48, 113 (1973).

(6) L. Nadjo and J.M. Saveant, J. Electroanal Chem., 33, 419 (1971).

(7) C.P. Andrieux and J.M. Saveant, J. Electoanal. Chem., 33, 453 (1971).

(8) B.S. Pons. Phd. Thesis. University of Southampton 1979.

(9) A. Bewick, J.M. Mellor and B.S. Pons, Electrochimica Acta., 25, 931 (1980).

(10) L. Eberson and B. Olofsson, Acta Chem. Scand., 23, 2355 (1969).

(11) M. Leung, J. Herz and H.W. Salzberg. J. Org. Chem. 30, 310 (1965).

(12) H. Lund, Acta Chem. Scand., 11, 1323 (1957).

(13) W.D. Parker and R.N. Adams, Tetrahedrom lett., 1721 (1969).

(14) K. Nyberg and A. Trojanek, Coll. Czech. Chem. Comm., 40, 526 (1975).

(15) M. Baizer, Organic Electrochemestry, Dekker, New York. 1973.

(16) A. Bewick, G. Edwards and J. Mellor, Liebigs Ann. Chem., 41 (1978).

(17) A. Bewick, G. Edwards and J. Mellor, Electrochim. Acta., 21, 1101 (1976).

(18) A. Bewick, G. Edwards and J. Mellor; J. Chem Soc. Perkin Trans., 2, 1952 (1977).

(19) L. Eberson and B. Oloffson. Acta Chem. Scand., 23, 2355 (1969).

(20) L. Boyd, L. Miller and D. Pletcher, Tet. letters 2419 (1972).

(21) R. Nicholson and I. Shain, Anal. Chem., 36, 706 (1964).

(22) Does not exist.

(23) A Bewick, J. Mellor and S. Pons., Electrochem. Acta., 23, 77 (1978).

(24) P. Hodge, Chemistry in Britain, 14, 237 (1978).

(25) A. Bewick, J. Mellor and B.S. Pons. J.C.S. Chem. Com., 178, 738 (1977).

(26) C.D. Ritchie, J. Am. Chem. Soc., 97, 110 (1975).

(27) S. Andreades and E.W. Zahnow. J. Am. Chem. Soc., 91, 4181 (1969).

(28) S. Andreades, U.S. 3, 431, 184 (1969) (chem. abs.).

(29) V.D. Parker and B.E. Burgert, Tetrahedrom lett., 3341 (1968).

(30) E.T. Blues, Brit., 1, 141, 638 (1969) (chem. abs.).

(31) B. Belleau and N.L. Weinberg, J. Am. Chem. Soc., 85, 2525 (1963).

(32) N.L. Weinberg Ed., "Thechniques of Electroorganic Synthesis". volume V, Part II John Wiley & Sons. p.24

(33) L. Eberson, J. Am. Chem. Soc., 89, 4669 (1967).

(34) E.S. Gould. "Mechanism and Structure in Organic Chemistry", Henry Holt, New York, 1959.

(35) J.D. Mec, D.W. Heseltime and E.C. Taylor. J. AM. Chem. Soc., 92, 5814 (1970).

(36) A. Zweig, W.G. Hodgson and W.H. Jura. J. Am. Chem. Soc., 86, 4124 (1964).

(37) R.O.C. Norman and C.B. Thomas J. Chem. Soc., B, 241 (1970).

(38) K. Yoshida, M. Shigi, T. Kanbe and T. Fuerro J. Org. Chem. 40, 25, 3305 (1975).

(39) M. Sainsburg. J. Chem. Soc. 2888 (1971).

(40) K. Bechgaard, V.D. Parker. J. Am. Chem. Soc. 84, 13, 4749 (1972).

(41) P. O'Neill, S. Steenken and D. Schulte-Frohlinde. J. Phys. Chem. 79, 25, 2773 (1975).

(42) W.T. Dixon and D. Murphy, J. Chem. Soc. Faraday 11, 135 (1976).

(43) W. T. Dixon and D. Murphy. J. Chem. Soc. Faraday 11 1976, 1221.

(44) W.T. Dixon and D. Murphy. J. Chem. Soc. Farday 11, 1823 (1976).

(45) E. Ernstbrunner, R.B. Girling, W.E.L. Grossman and R.E. Wester. J. Chem. Society. Perkin 11, 177 (1978).

(46) K. Yoshida, M. Shigi and T. Fuerro. J. Org. Chem., 40, 1 (1975).

(47) K. Yoshida and T. Fueno, J. Org. Chem., 37, 4145 (1972).

(48) M. Rakout, D Michelet, B Brossaro and J. Varagnat.

Tetrahedron Letters, 39, 3723 (1979).

(49) J. Holeman and Knud Sehesied. J Phys. Chem., 80, 14 (1976).

(50) G. Grabner, W. Rauscher, J. Zechner and N. Getoff. J. Chem. Soc. Chem. Comm. 222 (1980).

CHAPTER 2: TECHNIQUES

2.1. General introduction to voltammetry.

- 2.1.1. Single sweep voltammetry.
- 2.1.2. Cyclic voltammetry.
- 2.1.3 Mathematics considerations for voltammetry
- 2.1.4. Diagnostic criteria for voltammetry
- 2.1.5. Chemical Reaction coupled to Electron Transfer.

2.2. General introduction to potential step methods.

- 2.2.1. Chronoamperometry.
- 2.2.2. Double potential step chronoamperometry.
- 2.2.3. Mathematics considerations for chronoamperometry.
- 2.2.4. Diagnostic Criteria for chronoamperometry.

2.3. General introduction to Coulometry.

- 2.3.1. Coulometry law.
- 2.3.2. Controlled potential Coulometry.

2.4. Spectroelectrochemistry.

- 2.4.1. General considerations of spectroelectrochemistry.
- 2.4.2. Modulated specular reflectance spectroscopy. (MSRS).

2.1. GENERAL INTRODUCTION TO VOLTAMMETRY.

Voltammetry is the general term applied to the study of current-potential relationships upon the application of a potential to a working electrode.

2.1.1. SINGLE SWEEP VOLTAMMETRY.

In single-sweep peak voltammetry, a rapidly changing ramp potential > 10mV/sec is applied to the working electrode and the resulting current is measured as a function of the potential. The solution is unstirred and mass transport is a result of diffusion alone. Unlike steady-state techniques where the limiting current becomes constant, the current in peak voltammetry increases to a maximum and then decays, yielding a peak shaped curve. The rate of the reaction increases as the potential is increased through the region where the electrochemical reaction occurs. However, because the solution is unstirred, the region in the vicinity of the electrode is depleted of electroactive substance, and the size of the diffusion layer increases. A peak potential is thus reached where the increase in reaction rate is balanced by the depletion effect. At potentials beyond this point, the current decreases as the depletion effect becomes dominant. The potential at which the peak current occurs, E_p, can be related to the $E_{\frac{1}{2}}$ potential for a reversible system. At 25°C, the relationship is:

$$E_p = E_{\frac{1}{2}} - \frac{0.029}{n} \text{ Volts} \qquad \{2 - 1\}$$

The peak potential is 0.029/n volts more cathodic than $E_{\frac{1}{2}}$ for an anodic process, and 0.028/n volts more anodic than $E_{\frac{1}{2}}$ for a cathodic process. Another parameter which is useful in describing the shape of a peak voltammogram is the difference between the peak potential and the potential at which the current is one half the maximum value, $E_{p/2}$. For a reversible system, this is given by:

$$E_p - E_{p/2} = \frac{0.057}{n} \text{ Volts} \qquad \{2 - 2\}$$

That means that the peak voltammogram of a reversible system is quite sharp. A simple relationship exists between E_p and $E_{p/2}$ for irreversible systems:

$$E_p - E_{p/2} = \frac{0.048}{\alpha n_\alpha} \text{ Volts} \qquad \{2 - 3\}$$

Where α is the electron transfer coefficient and n_α is the number of electrons up to and including the rate determining step. The shape of the voltammogram for the irreversible system is dependent on the product αn_α, and the voltammograms for these systems are very often spread out.

The peak current for a reversible system at 25°C is given by:

$$I_p = 2.72 \times 10^5 \times n^{3/2} D^{1/2} A C^\infty \nu^{1/2} \qquad \{2 - 4\}$$

Where A is the electrode area in cm^2, and ν is the potential scan rate in Volts/s

The peak potential for a reversible system is independent of the sweep rate and it is related to $E_{\frac{1}{2}}$ by equation {2 - 1}. The peak current for an irreversible system is smaller than that for the reversible system. This difference can, under certain conditions, be used to determine the reversibility of a system.

The peak current for an irreversible system, at $25^{o}C$ is given by:

$$I_p = 3.01 \times 10^5 \, n(\alpha n_\alpha)^{1/2} \, A \, D^{1/2} \, C^{\infty} \, \nu^{1/2} \qquad \{2 - 5\}$$

In this case, the peak potential is dependent on the sweep rate, and it shifts by about $30/\alpha n_\alpha$ per tenfold change in sweep rates.

The control settings for single-sweep voltammetry, are as follows: The potential range should be selected to include all the electrochemical reactions of interest,and the selected sweep rate should be rapid enough to achieve peak voltammograms, usually, greater than 10 mV/sec.

2.1.2. CYCLIC VOLTAMMETRY

This technique differs form single-sweep voltammetry in that the ramp potential function is replaced by a triangular potential function. In this technique, the current is measured over the entire potential scan: both, anodic and cathodic current are measured. The potential scan rates employed are about the same as those used for single-sweep voltammetry.

Figure 2.1 shows a typical cyclic voltammogram for a reversible case.

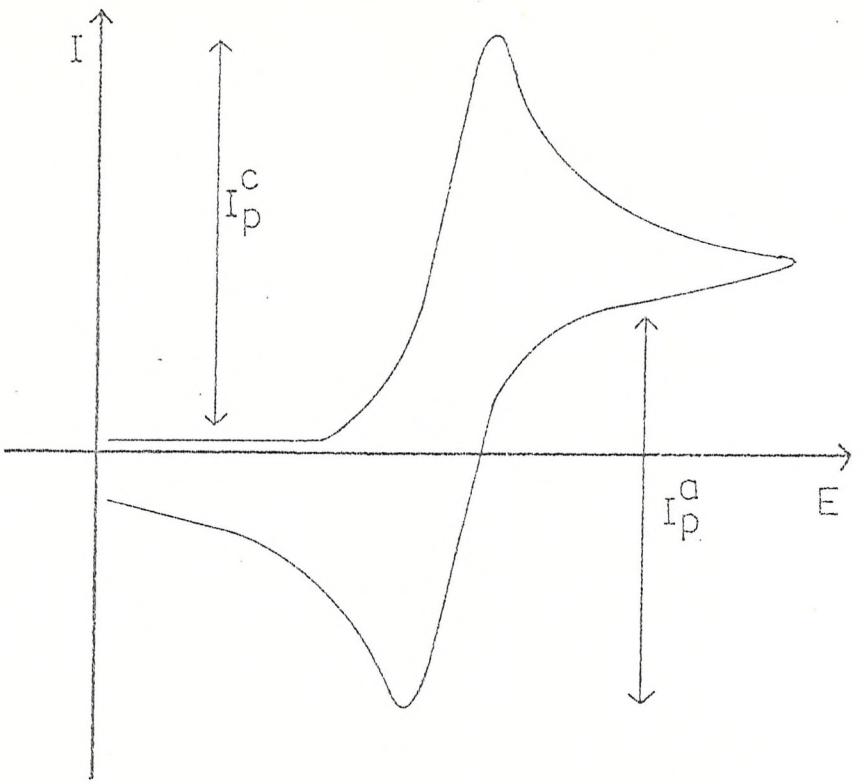

Fig 2.1.

For an electrochemically reversible system, the anodic and cathodic peaks are separated by approximately 0.058/n Volts, and the peak separation is independent of the sweep rate.

As the system becomes less reversible, the current peak spreads and the separation between the anodic and cathodic peaks increases. The peak separation for the irreversible systems is dependent on the scan rate.

For a reversible system, the peak separation may be greater than the 0.058/n Volts predicted by theory if the potential at which the scan is reversed is close to the peak potential. This happens because even at the potential of peak current, the concentration of the oxidized or reduced species undergoing reaction at the electrode, is not zero, and a gradient of concentration is present in the system,

so, conditions during the forward scan to the reverse scan may differ. The result is a shift in the peak potential. When the sweep is carried 200 or 300 mV past the peak potential, the reverse peak is relatively unaffected by the potential.

Cyclic voltammetry provides a very good tool for an estimate of heterogeneous rate constant, k_f. Care must be taken when working at fast sweep rates to insure that the change in peak separation is not due to IR loss. Modern potentiostats such as the one used in this work, have built-in positive feedback IR compensation.

Cyclic voltammetry is very useful for studying overall processes occuring at the electrode surface. Very often we can observe (specially with organic systems) that the initial cycle is quite different from the second and succeeding cycles, due to chemical reactions coupled with the electrode process. In our case this phenomenon was observed and the electrode was flamed each time before the run (more details of the treatment will be given in chapter 3).

2.1.3. MATHEMATICS CONSIDERATIONS FOR VOLTAMMETRY.[2-4,6,8-17]

Earlier in this chapter, expressions for the peak current in both, reversible and irreversible cases, were given (eqs.{2-4} and {2-5}). The aim of this section is to provide more details about the considerations and assumptions made in the derivation of such expressions.

If we consider a simple electrode process of species O undergoing electrochemical reaction to give species R:

$$O \underset{}{\overset{ne^-}{\rightleftharpoons}} R$$

and, if we assume linear diffusion of the species from a plane electrode

surface to the bulk of the solution, the potential-time {E(t)} function can be written as

$$E(t) = E_i - \nu t \qquad \{2 - 6\}$$

where ν is the sweep rate (dE/dt) and E_i the initial potential.

If the reaction follows a Nernstian behaviour, i.e. the reaction is completely reversible, eq {2 - 6} can be rewritten as:

$$E(t) = E_i - \nu t = E^o + \frac{RT}{nF} \ln \frac{C_O(o,t)}{C_R(o,t)} \qquad \{2 - 7\}$$

where C_O and C_R are concentration of species O and R, respectively.

The ratio of the concentrations $C_O(o,t)/C_R(o,t)$ is then a function of time:

$$\frac{C_O(o,t)}{C_R(o,t)} = f(t) = \exp\left[\frac{nF}{RT}(E_i - \nu t - E^o)\right] \qquad \{2 - 8\}$$

The diffusion equations to be solved in this case are:

$$\frac{\delta C_O(x,t)}{\delta t} = D_O \frac{\delta^2 C_O(x,t)}{\delta x^2} \qquad \{2 - 9\}$$

$$\frac{\delta C_R(x,t)}{\delta t} = D_R \frac{\delta^2 C_R(x,t)}{\delta x^2} \qquad \{2 - 10\}$$

Initial conditions: species R initially absent:

$$C_O(x,o) = C_O^{\infty}$$

$$C_R(x,o) = 0$$

Flux balance and boundary conditions:

$$D_O \left(\frac{\delta C_O(x,t)}{\delta x} \right)_{x=o} + D_R \left(\frac{\delta C_R(x,t)}{\delta x} \right)_{x=O} = O \qquad \{2 - 11\}$$

$$\lim_{x \longrightarrow \infty} C_O(x,t) = C_O^{\infty} \qquad \{2 - 12\}$$

$$\lim_{x \longrightarrow \infty} C_R(x,t) = 0 \qquad \{2 - 13\}$$

From equation {2 - 8} we can write down:

$$\frac{C_O(o,t)}{C_R(o,t)} = \theta e^{-at} = \theta s(t) \qquad \{2 - 14\}$$

where

$$\theta = \exp \left[(nF/RT) (E_i - E^{\circ}) \right]$$

$$a = \left(\frac{nF}{RT} \right) \nu$$

and $$s(t) = e^{-at}$$

The Laplace transform solution to the diffusion equations and boundary conditions are:

$$S\,\overline{C_O}\,(x,s) - C^{\infty} = D_O \frac{d^2\,\overline{C_O}\,(x,s)}{dx^2} \qquad \{2 - 15\}$$

$$S\,\overline{C_R}\,(x,s) = D_R \frac{d^2\,\overline{C_R}\,(x,s)}{dx^2} \qquad \{2 - 16\}$$

$$\frac{d^2\,\overline{C}\,(x,s)}{dx^2} - \frac{s}{D}\,\overline{C}\,(x,s) = -\frac{C^{\infty}}{D} \qquad \{2 - 17\}$$

Considering ordinary differential equations:

$$\overline{C_O}\,(x,s) = \frac{C^{\infty}}{S} + A'(s)\,\exp\{-(S/D_O)^{1/2}\,x\} +$$

$$+B'(s)\exp\{(S/D_O)^{1/2}\,x\} \qquad \{2 - 18\}$$

Since $\lim_{x \to \infty} \overline{C_O}\,(x,s) = \frac{C^{\infty}}{S}$, then $B' = 0$ and eq {2 - 18} becomes

$$\overline{C_O}\,(x,s) = \frac{C^{\infty}}{S} + A'(s)\exp\{-(S/D_O)^{1/2}x\}$$

$$\{2 - 19\}$$

Futhermore, as

$$J_o(o,t) = \frac{i(t)}{nFA} = D_O \left(\frac{\delta C_O(x,t)}{\delta x} \right)_{x=o} \qquad \{2 - 20\}$$

Where J_o is the flux of species O, and expression for the current can be written:

$$\bar{i}(s) = nFA\ D_O \left(\frac{\delta \bar{C}_O(x,s)}{\delta x} \right)_{x=o} \qquad \{2 - 21\}$$

combining eqs {2 - 19} and {2 - 21} :

$$\left(\frac{\delta \bar{C}_O(x,s)}{\delta x} \right)_{x=o} = -A'(s)\ (S/D_O)^{1/2} = \frac{\bar{i}(s)}{nFA\ D_O}$$

$$A(s) \left(\frac{\delta \bar{C}_O(x,s)}{\delta x} \right)_{x=o} = 0$$

Then, the value A'(s) can be determined:

$$A'(s) = -\frac{\bar{i}(s)}{nFA\ D_O\ (S/D_O)^{1/2}} \qquad \{2 - 22\}$$

putting {2 - 22} into {2 - 19} :

$$\bar{C}_O(x,s) = \frac{-\bar{i}(s)}{nFA\ D_O(S/D_O)^{1/2}} \exp\left(-\left(\frac{S}{D_O}\right)^{1/2} x \right)$$

The inverse transformation can be made by using the convolution formula[12,13]:

$$\int_0^{at} \frac{\chi(z)\,dz}{(at-z)^{1/2}} = \frac{1}{1 + (D_O/D_R)^{1/2}\,\theta(at)} \qquad \{2 - 23\}$$

where: $z = a\tau$, τ is a dummy variable arising from use of the convolution theorem on the Laplace transformed diffusion equations.

$$\chi(z) = \frac{g(z)}{C_O^{\infty}\,(\pi D_O a)^{1/2}} = \frac{i(at)}{nFA\,C_O^{\infty}\,(\pi D_O a)^{1/2}}$$

and

$$i = nFA\,C_O^{\infty}(\pi D_O a)^{1/2}\;\chi\;(at) \qquad \{2 - 24\}$$

The solution of equation {2 - 23}has been found by a series solution[8,9] and analytically[10,11]. The function $\pi^{1/2}\,\chi(at)$ and, hence, the current reaches a maximum (at 25°C) at $n\left(E_p - E_{p/2}\right)$ = −28.5 mV. At that point, $\pi^{1/2}\,\chi(at) = 0.4463$. If we fit this value into eq. {2 - 24}, the peak current is:

$$I_p = 2.7 \times 10^5\, n^{3/2}\, A\, D_O^{1/2}\, \nu^{1/2}\, C_O^{\infty}$$

which is the same equation {2 - 4}.

The same treatment is valid for the peak potential. If at the maximum of current function, at 25°C, $n\left(E_p - E_{p/2}\right) = -28.5$ mV, we can write:

$$E_p - E_{p/2} = E_p - E^o + \frac{RT}{nF} \ln\left(\frac{D_O}{D_R}\right)^{1/2} = -1.1 \frac{RT}{nF} = \frac{-28.5}{n} \text{ mV}$$

$$E_{p/2} = E_{1/2} + 1.1 \frac{RT}{nF} = E_{1/2} + 28.0n \text{ mV}$$

and

$$\left|E_p - E_{p/2}\right| = 2.2 \frac{RT}{nF} = \frac{56.5}{n} \text{ mV}$$

For a totally irreversible reaction:

$$O + n\bar{e} \longrightarrow R$$

The Nernstian boundary condition is replaced by

$$\frac{\bar{i}}{nFA} = D_O \left(\frac{\delta C_O(x,t)}{\delta x}\right)_{x=o} = k_f(t)\, C_O(o,t) \quad \{2 - 25\}$$

where

$$k_f(t) = k^o \exp\left[-\alpha n_\alpha f \{E(t) - E^o\}\right]$$

$$K_f(t)\, C_O(o,t) = K_{fi}\, C_O(o,t)\, e^{bt}$$

where

$$k_{fi} = k^{o} \exp\left[- \alpha n_{\alpha} f(E_i - E^{o}) \right]$$

$$b = \alpha n_{\alpha} f \nu$$

$$f = \frac{F}{RT}$$

Following the procedure as before:

$$i = nFA\, C_0^{\infty}\, D_0^{1/2}\, \nu^{1/2} \left(\frac{\alpha n_{\alpha} F}{RT} \right)^{1/2} \pi^{1/2}\, \chi(bt) \qquad \{2 - 26\}$$

The function $\pi^{1/2}\, \chi(bt)$ goes through a maximum at $\pi^{1/2}\, \chi(bt) = 0.496$.

If we reptace this value in eq {2 - 26}, the peak current is:

$$I_p = 3 \times 10^5\, n\, (\alpha n_{\alpha})^{1/2}\, A\, C_0\, D_0^{1/2}\, \nu^{1/2}$$

which is equation {2 - 5}.

This value occurs when

$$\alpha n_{\alpha} (E_p - E^{o}) + \frac{RT}{F} \ln\left(\frac{(\pi D_0 b)^{1/2}}{K^{o}} \right) = -5.34\text{mV}$$

$$E_p - E_{p/2} = \frac{1.857\, RT}{\alpha n_{\alpha} F} = \frac{47.7}{\alpha n_{\alpha}}\ \text{mV at } 25^{o}\text{C}$$

2.1.4. DIAGNOSTIC CRITERIA FOR VOLTAMMETRY.

Paragraphs 2.1.1. and 2.1.2. describe the information that could be taken from a voltammogram. In this section we will summarize those diagnostic criteria.

(i) The ratio $I_p/\nu^{1/2}$ should be a constant value for a simple electron transfer process not coupled to any chemical steps.

(ii) For a reversible process, if the potential at which the potential reverses is not very close to the peak potential, the difference between the peak potential for the forward reaction and the reverse peak potential should be $\frac{59}{n}$ mV and independent of sweep rate. The peak potential, E_p, should also be independent of the sweep rate.

(iii) The shape of the voltammogram could give further information about reversibility, so, a reversible peak band width should be about twice $\frac{57}{n}$ mV.

(iv) The peak potential is related to the half wave potential, $E_{1/2}$, by the expression:

$$E_p = E_{1/2} - \frac{28.5}{n} \text{ mV}$$

(v) For a reversible process, the ratio I_{PO}/I_{PR} is equal to unity.

2.1.5. CHEMICAL REACTION COUPLED TO ELECTRON TRANSFER.

More complicated mechanisms[3,18,19] can be analyzed by cyclic voltammetry. As it was described in Chapter 1, when there are chemical reactions coupled with the electrochemical process, a series of different mechanisms could take place. In organic electrochemistry, the most important is the ECE. It was first studied by Hawley and Feldberg;[20-22] Nicholson and Shain[3] and Saveant *et al*[6,23-27] have done a great deal on the numerical solutions of the integral equations describing ECE mechanism.

A typical ECE scheme[3] is shown below:

$$O \underset{}{\overset{n_1 e^-}{\rightleftharpoons}} R \qquad E_1^{\theta} \qquad \{2 - 27\}$$

$$R \underset{k_{-1}}{\overset{k_1}{\rightleftharpoons}} Y \qquad \{2 - 28\}$$

$$Y \underset{}{\overset{n_2 e^-}{\rightleftharpoons}} X \qquad E_2^{\theta} \qquad \{2 - 29\}$$

Species Y may be more easily oxidized or reduced than species O and, therefore, the electron transfer involving species Y may occur homogeneously (DISP).

The equilibrium constant Keq ($=k_1/k_{-1}$) for reaction {2 - 28} is given by[29],

$$\frac{RT}{F} \ln K_{eq} = E_2^{\theta} - E_1^{\theta}$$

If species O is more easily oxidized than species Y in an oxidation reaction, then $E_1^\theta < E_2^\theta$ and K_{eq} is high and the reaction does not enter much in disproportionation. However, if Y is much more easily oxidized than O, then $E_2^\theta << E_1^\theta$ and K_{eq} is very small, so, species R, diffusing away from the electrode, is capable of reducing Y in the bulk solution.

Equation {2 - 28} is considered to be irreversible. The change transfer reactions could be either reversible (r) or irreversible, so, four different posibilities could happen: R - R, R - I, I - R or I - I.

The diffusion equations to be solved, could be obtained from:

$$\frac{\delta C_O}{\delta t} = D_O\left(\frac{\delta^2 C_O}{\delta x^2}\right) \qquad \{2 - 30\}$$

$$\frac{\delta C_R}{\delta t} = D_R\left(\frac{\delta^2 C_R}{\delta x^2}\right) + K_{-1} C_y - K_1 C_R \qquad \{2 - 31\}$$

$$\frac{\delta C_y}{\delta t} = D_y\left(\frac{\delta^2 C_y}{\delta x^2}\right) + K_1 C_R - K_{-1} C_y \qquad \{2 - 32\}$$

$$\frac{\delta C_x}{\delta t} = D_x\left(\frac{\delta^2 C_x}{\delta x^2}\right) \qquad \{2 - 33\}$$

By putting $k_{-1} = 0$ and $k_1 = k$, and assuming that all the diffusion coefficients are equal, we can write:

$$\frac{\delta C_O}{\delta t} = D\left(\frac{\delta^2 C_O}{\delta x^2}\right) \qquad \{2 - 34\}$$

$$\frac{\delta C_R}{\delta t} = D\left(\frac{\delta^2 C_R}{\delta x^2}\right) - k C_R \qquad \{2 - 35\}$$

$$\frac{\delta C_y}{\delta t} = D\left(\frac{\delta^2 C_y}{\delta x^2}\right) + k C_R \qquad \{2 - 36\}$$

$$\frac{\delta C_x}{\delta t} = D\left(\frac{\delta^2 C_x}{\delta t^2}\right) \qquad \{2 - 37\}$$

The initial and boundary conditions are:

$$t = 0, \quad x \geq 0: \quad C_O = C_O^b, \quad C_R = C_y = C_x = 0 \qquad \{2 - 38\}$$

$$t > 0, \quad x \longrightarrow \infty: \quad C_O \longrightarrow C_O^b, \quad C_R = C_y = C_O \longrightarrow 0 \qquad \{2 - 39\}$$

$$t>0, \quad x=0: \quad D\left(\frac{\delta C_O}{\delta x}\right) + D\left(\frac{\delta C_R}{\delta x}\right) = 0 \qquad \{2 - 40\}$$

$$D\left(\frac{\delta C_y}{\delta x}\right) + D\left(\frac{\delta C_x}{\delta x}\right) = 0 \qquad \{2 - 41\}$$

$$C_O,\ C_R,\ C_y,\ C_x = f(E,t) \qquad \{2 - 42\}$$

where f(E,t) describes the nature of the experiment and follows Nernstian behaviour for reversible reactions and the Butler-Volmer equation[30] for irreversible reactions.

If $C = C_R + C_y$ and the diffusion equations given above are Laplace transformed, subject to boundary conditions, inverse transforms yield the following integrals for the concentrations of all the species involved in terms of the fluxes of O and Y at the electrode surface:

$$C_O(o,t) = C_O^b - \Delta_O \qquad \{2 - 43\}$$

$$C_R(o,t) = \Delta'_O \qquad \{2 - 44\}$$

$$C_y(o,t) = \Delta_O - \Delta y - \Delta'_O \qquad \{2 - 45\}$$

$$C_x(o,t) = \Delta y \qquad \{2 - 46\}$$

where

$$\Delta_i = \left(\int_o^t \left[f_i(\tau)\ (t-\tau)^{1/2} \right] d\tau \right) \Big/ \pi^{1/2}\ D^{1/2} \qquad \{2 - 47\}$$

$$\Delta'_O = \left(\int_o^t \left[e^{-K(t-\tau)}\ f_o(\tau)\ (t-\tau)^{1/2} \right] \right) \Big/ \pi^{1/2}\ D^{1/2} \qquad \{2 - 48\}$$

$$f_i(t) = D\left(\frac{\delta C_i}{\delta t}\right)_{x=d} \qquad i \equiv o \text{ or } y$$

so, the expression for the current will be:

$$i = n_1 FA\, f_o(t) + n_2 FA\, f_y(t) \qquad \{2 - 49\}$$

If equations {2.43 - 46} are put into eq {2 - 42}, dimensionless current functions for reversible charge transfers could be expressed like:

$$\chi(at) = f_o(t) / C_O^b\, \pi^{1/2}\, D^{1/2}\, a^{1/2} \qquad \{2 - 50\}$$

$$\phi(at) = f_y(t) / C_O^b\, \pi^{1/2}\, D^{1/2}\, a^{1/2} \qquad \{2 - 51\}$$

and for irreversible reactions as similar functions: $\{\chi(bt), \phi(bt)\}$, where a and b have been defined in section 2.2. Nicholson and Shain[3] have solved the equations for all the variants described above, and presented tables for theoretical current functions.

They have published values of $\pi^{1/2}\, \phi\chi(at)$ in tabular form for many electrode mechanisms. Suitable values for ECE mechanism were plotted by B.S. Pons[31] as a function of k_f/a (fig 2.2). By combining equations {2 - 20}, {2 - 21} and {2 - 24} , we obtain the relation

$$\frac{I}{FA\,(Da)^{1/2}\,CA} = \pi^{1/2}\,\{\chi(at) + \phi(at)\} \qquad \{2 - 52\}$$

if there is one electron transfered in each step {2 - 27} and {2 - 29}. The left hand side of the equation above, is obtained from experiments for different values of sweep rates. As values of χ and ϕ are listed in literature as functions of k_f/a (where k_f is the pseudo-first order rate constant for the homogeneous reaction), after choosing arbitrary values of k_f, k_f/a is calculated for several values of ν. The values of $\chi(at)$ and $\phi(at)$ are taken from the tables and the sum of both functions is plotted versus ν, to obtain the theoretical working curves.

Theoretical working curves in this work have been constructed by using this method and assuming $E_2^{\theta} < E_1^{\theta}$, both charge transfer reversible and the chemical step irreversible $\chi(at)$ and $\phi(at)$ were found for several values of k_f/a from Fig 2.2. The function sum $\chi(at) + \phi(at)$, was plotted against sweep rate, ν, and theoretical working curves were obtained for various values of rate constant. Experimental current functions (left hand side of equation {2 - 52}) against ν were fitted into the same graphs and the closest fit for k_f was found.

Since the time of the experiment is low compared with k_f, at slow sweep rates, the plot will show two electrons behaviour. As sweep rate is increased, the behaviour is changing from two electron transfer to one electron transfer process. A crossover region is observed and it is characteristic of the coupled chemical reaction and, therefore, of the value of k_f.

2.2. GENERAL INTRODUCTION TO POTENTIAL STEP METHODS.

In a typical potential step experiment, electrode potential is stepped from a value E_1, at which no Faradaic processes are taking

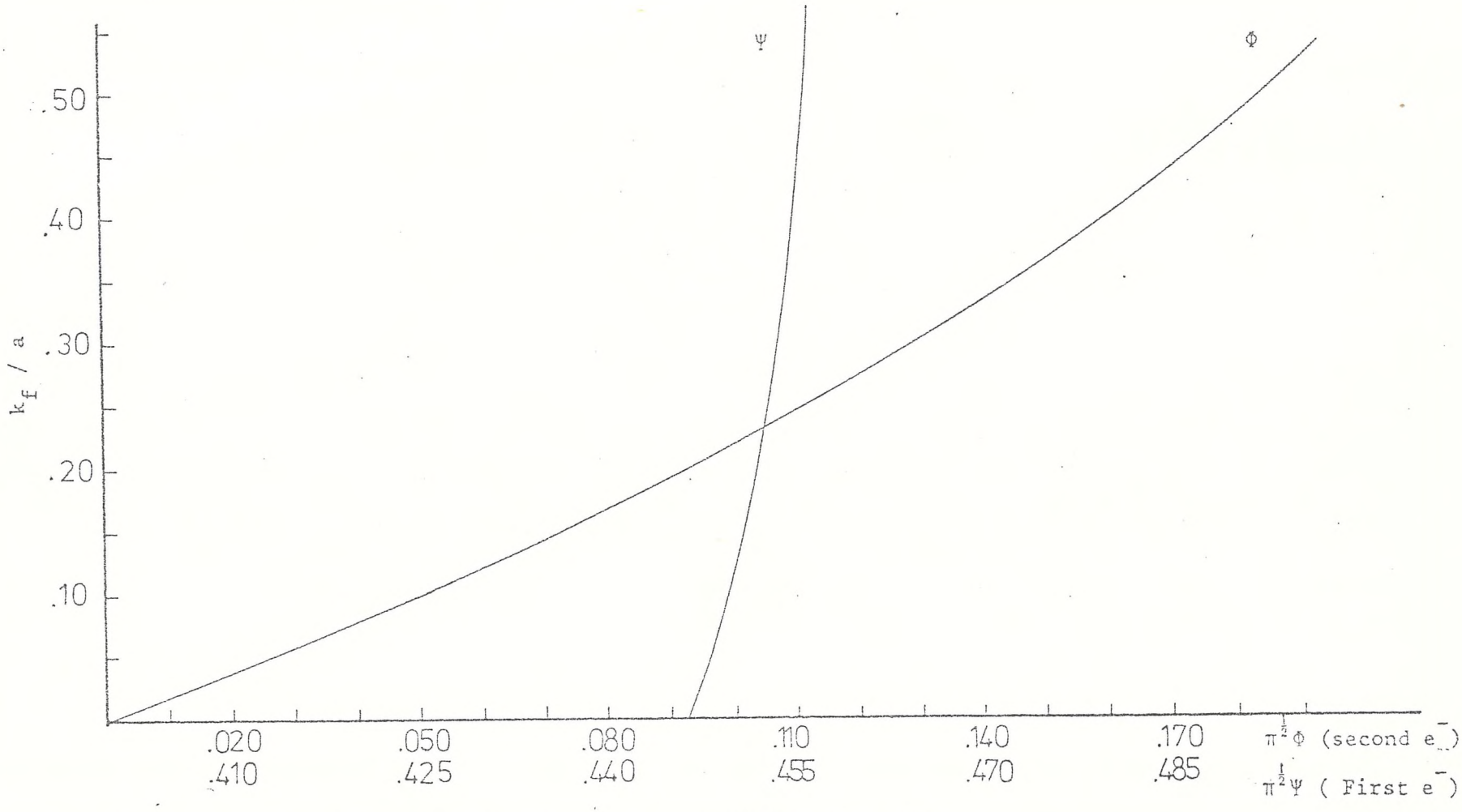

Fig. 2.2 ECE - DISP 1 Current functions for cyclic voltammetry taken from reference 31.

place, up to a value E_2, at which reaction takes place. Either the resultant current/time transient is recorded and analyzed, chronoamperometry; or the charge/time transient is used, chronocoulometry. In this work, we are concerned with chronoamperometry.

2.2.1. CHRONOAMPEROMETRY. (1, 32-37)

In chronoamperometry, a potential step function is applied to the working electrode, and the resulting current is measured as a function of time. The potential step is selected such that at the initial potential, E_1, no Faradaic current flows, and at the final potential, E_2, the current is diffusion controlled. With semi-infinite linear diffusion control, the instantaneous current, I_t, is given by the Cot equation.

$$I_t = \frac{n\,FA\,D^{1/2}C}{\pi^{1/2}\,t^{1/2}} \qquad \{2 - 53\}$$

where C is the bulk concentration and t is the time since the application of the potential step. The other terms have their usual significance.

From equation {2 - 53} it is apparent that the product $I_t\,t^{1/2}$ is constant. Therefore, the diffusion coefficent can be obtained, providing the n value and electrode area are known. In this work, we used the geometrical area of the electrode; but the real area can be obtained by using a standard solution, such as ferricyanide, for which the diffusion coefficient is well known.

Chronoamperometry is a good tool for the study of electrode reaction kinetics and chemical reaction, coupled to electrode process

kinetics. At very short times, a linear relationship exists between I_t and $t^{1/2}$. These data can be used to study electrode reaction kinetics, and chemical reactions which follow an electrochemical reaction. For these studies, working curves must be used. Details of the working curves will be given later in this chapter.

2.2.2. DOUBLE POTENTIAL STEP CHRONOAMPEROMETRY.

This technique is just an extension of chronoamperometry in that at some time, τ, after application of the potential step, the potential is returned to E_1. That is: a potential pulse is applied to the working electrode and the current-time transient is monitored. This technique is quite useful in the study of chemical reactions which follow an electrochemical process. During the initial potential step, the oxidation or reduction of the electroactive species takes place at a diffusion controlled rate. The product of such reactions then suffers a chemical reaction while diffusing away from the electrode surface. Reversal of the potential step then results in the electrochemical reaction of unreacted portion of this species.

The control setting for potential step experiments is as follows:

The initial potential is usually set to a potential such that no electrode process takes place, and hence, no Faradaic current is observed. The final potential is set to a potential where the reaction is diffusion limited. If double potential step has been performed, a suitable pulse duration should be chosen.

Chronoamperometry has been found to be particularly useful

to measure homogeneous rate constant for an ECE process[3,38].

2.2.3. MATHEMATICS CONSIDERATIONS FOR CHRONOAMPEROMETRY.[13-16, 19,39-41].

If we consider a system with a small value for the ratio electrode area/volume of solution[40], in which the mass transport of electroactive species occurs only under diffusion conditions, and if we also consider the more general case: The potential is stepped from a potential where the working electrode reaction:

$$O + ne^- \underset{\overleftarrow{K}}{\overset{\vec{K}}{\rightleftharpoons}} R$$

has a negligible rate to a value where its rate has a finite value[19]. The initial condition involves only species O. The diffusion equations to be solved are:

$$\frac{\delta C_O}{\delta t} = D \frac{\delta^2 C_O}{\delta x^2} \qquad \{2 - 54\}$$

$$\frac{\delta C_R}{\delta t} = D \frac{\delta^2 C_R}{\delta x^2} \qquad \{2 - 55\}$$

Initial and boundary conditions:

$t=o \quad \forall x,$

$$C_O = C_{o\,\infty} \qquad \{2 - 56\}$$

$$C_R = 0 \qquad \{2 - 57\}$$

$x=o$

$$D\left(\frac{\delta C_O}{\delta x}\right)_{x=o} = -D\left(\frac{\delta C_R}{\delta x}\right)_{x=o} =$$

$$= \vec{k}\, C_O^{\sigma} - \overleftarrow{k}\, C_R^{\sigma} = \frac{I}{nF} \qquad \{2-58\}$$

where C_O^{σ} and C_R^{σ} are the concentrations of O and R at the interface, respectively, and $\vec{k}$ and $\overleftarrow{k}$ are the potential dependent rate constants for the electron transfer processes.

$x=\infty$

$$C_O = C_O^{\infty}$$

$$C_R = 0$$

Laplace transforming the above equations[13], we obtain:

$$S\,\overline{C}_O - C_O^{\infty} = D\,\frac{d^2\,\overline{C}_O}{dx^2} \qquad \{2-59\}$$

$$S\,\overline{C}_R - 0 = D\,\frac{d^2\,\overline{C}_R}{dx^2} \qquad \{2-60\}$$

at $x=o$

$$D\left(\frac{d\,\overline{C}_O}{dx}\right)_{x=o} = -D\left(\frac{d\,\overline{C}_R}{dx}\right)_{x=o} =$$

$$= \vec{K}\, C_O^{\sigma} - \overleftarrow{K}\, C_R^{\sigma} \qquad \{2-61\}$$

$x=\infty$

$$\overline{C}_O = \frac{C_O^\infty}{S} \qquad \{2 - 62\}$$

$$\overline{C}_R = 0 \qquad \{2 - 63\}$$

Equation {2 - 60} can be solved by considering ordinary differential equation[39] and then we can write:

$$\overline{C}_O = A \exp\left(\frac{S}{D}\right)^{1/2} x + B \exp -\left(\frac{S}{D}\right)^{1/2} + \frac{C_O^\infty}{S} \qquad \{2 - 64\}$$

$$\overline{C}_R = C \exp\left(\frac{S}{D}\right)^{1/2} x + E \exp -\left(\frac{S}{D}\right)^{1/2} + 0 \qquad \{2 - 65\}$$

According with the initial and boundary conditions, the constants could be found:

$$A = C = 0 \qquad \{2 - 66\}$$

$$B = -E \qquad \{2 - 67\}$$

and

$$B = \frac{-\vec{k}\ C_O^\infty}{D^{1/2}\ S\left(S^{1/2} + (\vec{k} + \vec{k})/D^{1/2}\right)} \qquad \{2 - 68\}$$

Putting equations {2 - 66} and {2 - 68} into {2 - 64}, we obtain:

$$\bar{C}_O = \frac{-\vec{k}\, C_O^{\infty} \exp - (S/D)^{1/2}\, x}{D^{1/2}\, S\left(S^{1/2} + (\vec{k} + \overleftarrow{k})/D^{1/2} \right)} + \frac{C_O^{\infty}}{S} \qquad \{2 - 69\}$$

If we transform equation {2 - 58}

$$\bar{I} = nFD \left(\frac{d\, \bar{C}_O}{dx} \right)_{x=o} \qquad \{2 - 70\}$$

$$\bar{I} = \frac{n\, F\, \vec{k}\, C_O^{\infty}}{S^{1/2}\left(S^{1/2} + (\vec{k} \quad \overleftarrow{k})/D^{1/2} \right)} \qquad \{2 - 71\}$$

Inverting equation {2 - 71} to a time dependent function again:

$$I = n\, F\, \vec{k}\, C_O^{\infty} \exp \frac{(\vec{k} + \overleftarrow{k})^2 t}{D} \operatorname{erf} \frac{(\vec{k} + \overleftarrow{k}) t^{1/2}}{D^{1/2}} \qquad \{2 - 72\}$$

which represents the current transient over all the time scale. Let us now consider ECE mechanism:

Numerical analysis has been used to solve the Laplace transformed equation[38], and the current is given by:

$$I = FA\, D^{1/2}\, C\, \pi^{-1/2}\, t^{-1/2} \{n_1 + n_2\, (1 - e^{-kt})\} \qquad \{2 - 73\}$$

where I is the observed current at time t, K_f is the pseudo-first

order rate constant, and n_1 and n_2 are the number of electrons lost in the first and second electron transfer, respectively.

2.2.4. DIAGNOSTIC CRITERIA FOR CHRONOAMPEROMETRY.

(i) As for cyclic voltammetry, the effect of a coupled chemical reaction is shown in a graph of I against $t^{-1/2}$.

(ii) At short times, $\{1-e^{-k_f t}\}$ tends to zero and the slope of the plot is determined by n_1 electrons.

(iii) At long times, $\{1-e^{-k_f t}\}$ tends to one and the slope is determined by $(n_1 + n_2)$ electrons.

(iv) At intermediates time , the current shifts from one limit to the other, the time at which this change occurs being proportional to the rate constant.

(v) The profile of the crossover from one electron process to that for two electron process can be represented in time by:

$$2 - \{1-\exp(-kt)\} \ /2kt \qquad \{2 - 74\}$$

for the particular case in which the second electron transfer takes place by disproportionation[41,42]

(vi) The crossover profile for ECE mechanism is:

$$2 - \exp(-kt) \qquad (2-75)$$

and the current:

$$I = n\,FA\,D^{1/2}\,C\,\pi^{-1/2}\,t^{-1/2}\,(2-e^{-kt})$$

for the case in which one electron is involved in each electron transfer step.

(vii) The number of "apparent" electrons (n_{app}) transfered during the time between one electron transfer and the second, is given by:

$$n_{app} = n\,\frac{I}{I_{k=o}}$$

In this work, the systems gave and overall 2 electron reaction. It was assumed $n_1 = 1$ and $n_2 = 2$ and theoretical working curves were constructed by plotting I vs $t^{-1/2}$, the limiting cases being given by k=o (for one electon process) and K =∞ (for two electron processes). A changeover region was found between the two boundaries. Experimental plots of I vs $t^{-1/2}$ were fitted into the theoretical working curves, and the rate constant values determined by a best fit method.

2.3. GENERAL INTRODUCTION TO COULOMETRY.

2.3.1. COULOMETRY LAW. (43-48)

Faraday's law states that 96484 coulombs are consumed per equivalent of substance electrolyzed. The number of coulombs, Q,

consumed in an electrolysis, can be measured with considerable accuracy and precision. At constant E, the fraction of the total amount which has been electrolyzed after time t is independent of its initial concentration. The decay of electrolysis current with time for a given cell arrangement follows the relationship $i = i_o e^{-kt}$, being an exponential decay. Q is obtained through integration of the current-time curve

$$Q = \int_o^t i \, dt \qquad \{2 - 76\}$$

where t is the time at which the electrolysis current has decayed to a level indistinguishable from the background current. An operational amplifier integrator built in this laboratory was used in this work to measure the charge Q.

In analysis by coulometry, the species that is determined is quantitatively electrolyzed in a portion of the sample solution, and the amount present is calculated from the quantity of coulombs passed during the electrochemical reaction:

$$W = \frac{W_{eq}}{F} \int_o^t i \, dt \qquad \{2 - 77\}$$

Where W and W_{eq} are weight of material electrolyzed and its equivalent weight, respectively.

2.3.2. CONTROLLED POTENTIAL COULOMETRY.

The concept of controlled potential electrolysis has revolutionized electroorganic syntheses since 1942 when Hickling[43] constructed the potentiostat. The use of controlled potential avoids the formation of many by-products and makes the achievement of selective syntheses much simpler. The fast response of modern potentiostats has allowed the development of powerful non-steady state methods for elucidating reaction mechanisms and this has established the basis for the possibility of improving product yields by pulse techniques. The use of nonaqueous solvents has removed the limitation on the range of electrode potential, allowing a wider potential range, and therefore, making possible the study of systems which were not able to be studied before. The use of tetrafluoroborate or hexafluorophosphates instead of more common salts as supporting electrolyte, makes it possible to extend the potential range in acetonitrile[44].

2.4. SPECTROELECTROCHEMISTRY.

2.4.1. GENERAL CONSIDERATIONS OF SPECTROELECTROCHEMISTRY.

The study of electrochemical systems by conventional methods is hampered by constraints of the kind of information which is accessible. Such limitations have led to the development of a number of more sophisticated associated techniques to assist in the elucidation of mechanisms and the identification of intermediates. *In situ* spectroscopic methods have been developed for the detection, the characterisation and the kinetic monitoring of intermediates [49-54, 59-64] as well as for

study of the electrode surface properties. Contributions have also been made in the areas of photoelectrochemical cells.[55-58] Internal reflection and conventional transmission spectroscopy have been used to monitor an absorbing species[49-53,64] but their use is limited by the material of the electrodes (they must be optically transparent to light in the frequence range under study). Modulated Reflectance Spectroscopy, however, overcomes such problems and can be used extensively.

2.4.2. MODULATED SPECULAR REFLECTANCE SPECTROSCOPY (MSRS).[65-71]

2.4.2.1. GENERAL CONSIDERATIONS OF SPECULAR REFLECTANCE.

Measurements of specular reflectance involve the intensities of light reflected from the surface of interest. Usually, the incident light is polarized either parallel or perpendicular to the plane of incidence, and a detector such as a photodiode or a photomultiplier monitors the intensity of the reflected beam. Fig. 2.3. shows how an incident beam is reflected from a specular surface.

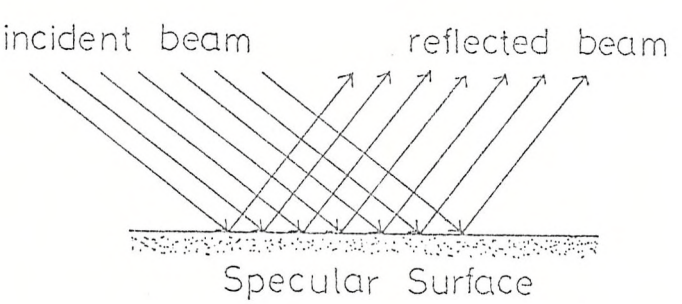

Fig. 2.3.

The surface should be smooth and any irregularities in it should be small compared to a wavelength. Reflection is obviously a surface effect. In fact, it involves only those atoms in a layer about $\lambda/2$ deep. Figure 2.4. shows the reflection and transmission of an incident monochromatic light.

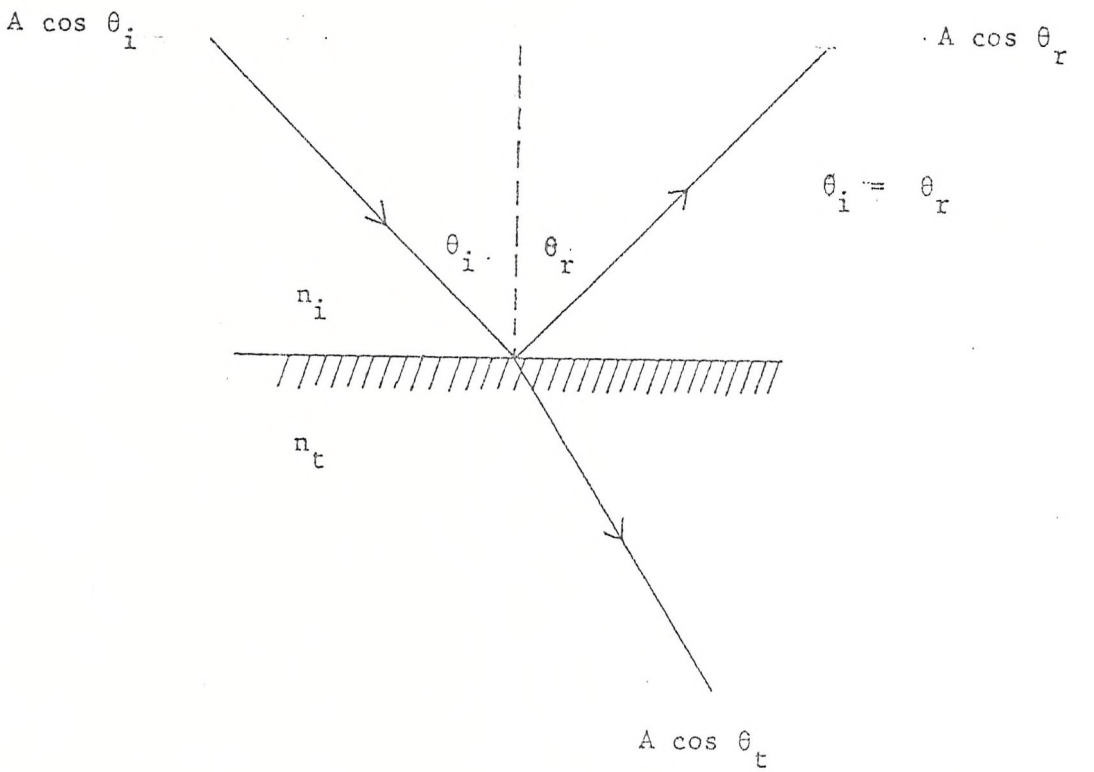

Fig. 2.4

If we let I_i, I_r and I_t be the incident, reflected and transmitted flux densities, respectively, accordingly, the portion of the energy incident normally on a unit area of the boundary per second is: $I_i \cos \theta_i$. Similarly, $I_r \cos \theta_r$ and $I_t \cos \theta_t$ are the energies per second leaving a unit area of the boundary normally on either side. The reflectance, R, is the ratio of the reflected

over the incident flux:

$$R \equiv \frac{I_r \cos \theta_r}{I_i \cos \theta_i} = \frac{I_r}{I_i} \qquad \{2 - 78\}$$

While the transmittance, T, is the ratio of the transmitted over the incident flux and is given by:

$$T \equiv \frac{I_r \cos \theta_t}{I_i \cos \theta_i} \qquad \{2 - 79\}$$

So, reflectance, R, is defined as the ratio of the reflected light intensity to the intensity of the incident beam. Absolute reflectances are difficult to measure and are not necessarily of interest More interesting is to know the change in reflectance ΔR induced by some change in the system.

Electrochemical modulation spectroscopy is a powerful method for characterizing the state of an electrode surface in situ. It offers to the electrochemist the possibility of determining the electronic energy levels (relative to the Fermi level) of adsorbed species, and determining the nature of the chemisorption bond.[72] The surface specificity of this technique, combined with the very high fields that can be generated in the electrical double layer, can be utilized to advantage in studying the electronic structure of metal surfaces.[65] It can be used for chemical identification of adsorbed species, with the help of theoretical understanding and the use of digital deconvolution techniques. Its wavelength selectivity, polarization sensitivity, and

the rapid response makes electrochemical modulation spectroscopy a versatile technique for studying the kinetics and mechanism of electrosorption processes.

2.4.2.2. GENERAL CONSIDERATIONS OF MODULATED SPECULAR REFLECTANCE SPECTROSCOPY.

Modulated peflectance spectroscopy was used in this work to monitor absorbing species which have been produced at the electrode.

The use of reflectance methods, allows performance *in situ* of absorption spectroscopy in the U.V, visible, near IR region and, now, in this laboratory, very succesful experiments are going on in the whole I.R. range[73-75]. Such experiments permit one to obtain information for the detection and the identification of reaction intermediates within the normal limits of spectroscopy in the range of wavelength to be covered. With the help of high sensitivity means of detection and signal averaging techniques, 10^{-13} mole of intermediate per cm^2 of electrode area can be detected.

To measure intensity changes, the Beer-Lambert law[76] is used:

$$I = I_o \exp -\varepsilon \cdot c \cdot l \qquad \{2 - 80\}$$

where I_o is the intensity of reflected beam when the electrode is in the reference state, I is the intensity of the reflected beam, ε is the extinction coefficient, c is concentration of absorbing species and l is the longitude of the light path.

In electrochemistry, reflectance experiments in which a species is generated at the electrode and it exists with a time, t,

and a distance,x, dependent profile C(x,t), the equation {2 - 80} can be expressed like:

$$I(t) = I_o \exp-\left(\int_o^{\infty} \varepsilon \; C(x,t)\; dx\right) \qquad \{2 - 81\}$$

where I(t) is the time dependent intensity of the reflected beam after the electrode process has been initiated and x is the coordinate of the light path.

The light travels twice through the profile at an angle of incidence θ, so,

$$C_x l = \frac{2}{\cos\theta} \int_o^{\infty} C(x,t)\; dx$$

$$\therefore \quad I(t) = I_o \exp-\left(\frac{2\varepsilon}{\cos\theta} \int_o^{\infty} C(x,t)dx\right) \qquad \{2 - 82\}$$

2.4.3. MATHEMATICS CONSIDERATIONS FOR M.S.R. (65,69,78-82)

Let us consider the dimension under the actual experimental conditions. If we have a close view of what is going on inside the optical cell:

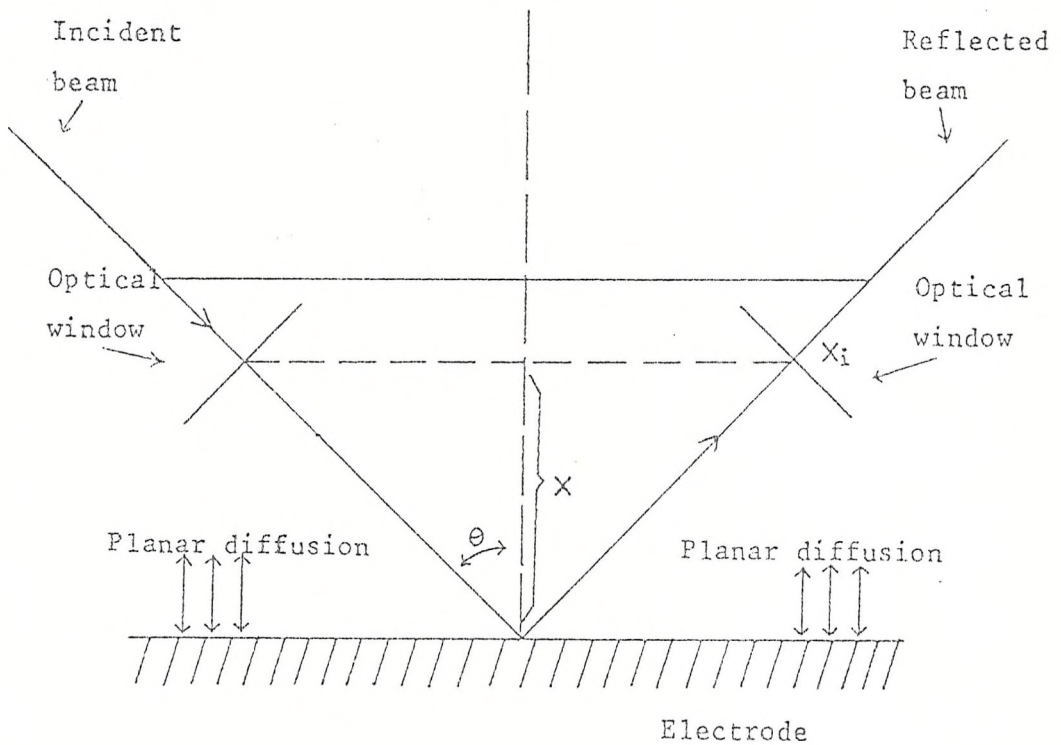
Incident
beam
Reflected
beam
Optical
window
Optical
window
X_i
X
Planar diffusion
θ
Planar diffusion
Electrode

Fig. 2.5

Where x is the width of the cell, θ is the angle of incidence of the monochromatic light. x_i is the value of x in which the concentration of absorbing species is equal to zero.

The concentration profile for such cell will be:

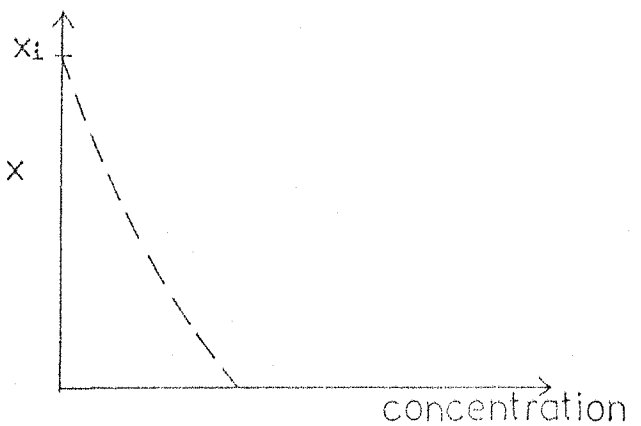

Fig. 2.6

It has been stated[77] that the number of molecules undergoing energy transfer per length dx parallel to the light path per second, can be expressed like:

$$\omega_{fi} = \frac{\pi I(\nu) \left|\overline{P}_{BA}\right|^2}{3\,\varepsilon_o\,\hbar^2} \times n'dx \qquad \{2-83\}$$

where ω_{fi} is the transition rate, $I(\nu)$ is the frequency dependent light intensity, ε_o is the permitivity, h is the Planck constant and n' is the number of molecules per cm^3. $\left|\overline{P}_{BA}\right|$ is the matrix element of the electric dipole moment of the absorbing molecule.

It was also stated that the energy released by the beam in each transition, is equal to the loss of intensity -dI:

$$- dI(\nu) = \frac{\pi I(\nu) \left| \overline{P}_{BA} \right|^2}{3 \varepsilon_o \hbar^2} n' h\nu \, dx \qquad \{2 - 84\}$$

The real light path due to the incidence angle θ, in the cell shown in figure 2.4, is related to the cell width, x, and as the light passes twice through the cell, the actual path length is:

$$q = \frac{2x}{\cos\theta} \qquad \{2 - 85\}$$

If we substitute{2 - 85}into {2 - 84}, the new expression for the loss of intensity will be:

$$- dI(\nu) = \frac{\pi I(\nu) \left| \overline{P}_{BA} \right|^2 n' h\nu \, d\left(\frac{2x}{\cos\theta}\right)}{3 \varepsilon_o \hbar^2} \qquad \{2 - 86\}$$

$$n' = 10^{-3} NC \qquad \{2 - 87\}$$

Where N is Avogadros number and C is molar concentration, so eq {2 - 86}can be converted as a function of molar concentration by substituting{2 - 87}into{2 - 86}:

$$- dI(\nu) = \frac{\pi I(\nu) \left| \overline{P}_{BA} \right|^2 10^{-3} NCh\nu \, d\left(\frac{2x}{\cos\theta}\right)}{3 \varepsilon_o \hbar^2} \qquad \{2 - 88\}$$

Integrating between the limits of incident and reflected intensities I_o and I respectively, and along the light path coordinates from o to x, the following expression is obtained:

$$\frac{I}{I_o} = \exp- \left(\frac{\pi \left| \overline{P}_{BA} \right|^2 10^{-3} N h\nu}{3 \varepsilon o \hbar^2 (2.303)} \frac{2}{\cos\theta} \left(\int_o^x C dx \right) \right) \qquad \{2 - 89\}$$

The first term in brackets has been found[77] to be extinction coefficient ϵ.

If we now assume semi-infinite linear diffusion, and if we work in the basis of that the concentration of the species varies with the distance x and with the time, t, equation{2 - 89}can be rewritten as:

$$\frac{I(t)}{I_o} = \exp- \left(\frac{2\varepsilon}{\cos\theta} \int_o^\infty C(x,t)\, dx \right) \qquad \{2 - 90\}$$

If we define ΔI as:

$$\Delta I = I_o - I(t)$$

we can then write:

$$\frac{I_o - \Delta I}{I_o} = 1 - \frac{\Delta I}{I_o}$$

The ratio $\frac{\Delta I}{I_o}$ is equivalent to $\frac{\Delta R}{R}$ if we think in terms of reflectivities,

so,

$$\frac{I(t)}{I_o} = 1 - \frac{\Delta R}{R}$$

ΔR has been defined by the quantity$(R_2 - R_1)$ where R_1 is the reflectivity of the most cathodic part of the pulse, and R_2 was that at the most anodic potential. Equation {2 - 90} can be expressed as:

$$1 - \frac{\Delta R}{R} = \exp - \left(\frac{2\varepsilon}{\cos\theta} \int_o^\infty C(x,t)\, dx \right) \qquad \{2 - 91\}$$

If the exponential term is expanded and if we work at low concentrations so that $C(x,t)$ is small enough, we have:

$$1 - \frac{\Delta R}{R} \simeq 1 - \frac{2\varepsilon}{\cos\theta} \int_o^\infty C(x,t)\, dx \qquad \{2 - 92\}$$

which is the same as:

$$\frac{\Delta R}{R} = \frac{2\varepsilon}{\cos\theta} \int_o^\infty C(x,t)\, dx \qquad \{2 - 93\}$$

As in the equation above, the concentration is dependent on the time, a comparison of the optical transients with mathematical expression can be made, providing that we know the extinction coefficient of the chromophore and the concentration profile with time. For semi-infinite linear diffusion e.g. for the diffusion controlled generation

of a stable absorbing species at constant potential in a potential step experiment, the current density is given by:

$$i = \frac{C^{o} D^{1/2}}{\pi^{1/2} t^{1/2}} \qquad \{2 - 94\}$$

and the total amount of species formed is:

$$\int_{o}^{\infty} C(x,t)\, dx = \int_{o}^{\infty} i dt = 2\pi^{-1/2}\, C^{o}\, D^{1/2}\, t^{1/2}$$

therefore,

$$\frac{\Delta R}{R} = \frac{4\epsilon}{\cos\theta}\, \pi^{-1/2}\, C^{o}\, D^{1/2}\, t^{1/2} \qquad \{2 - 95\}$$

If a plot of $\frac{\Delta R}{R}$ against $t^{1/2}$ behaves linearly, ϵ can be determined from the slope.

Mathematical treatment has been made[82] for the single potential step in a diffusion controlled reaction considering a charge transfer process:

$$R \longrightarrow O + n\bar{e}$$

The diffusion of the two species of the redox couple to a planar surface may be given by

$$\frac{\delta C_R}{\delta t} = D \frac{\delta^2 C_R}{\delta x^2} \qquad \{2 - 96\}$$

and

$$\frac{\delta C_O}{\delta t} = D \frac{\delta^2 C_O}{\delta x^2} \qquad \{2 - 97\}$$

Where $D = D_R = D_O$. If the potential at the working eletrode is stepped from a value where no Faradaic reaction occurs to a value where the reaction proceeds at a diffusion controlled rate, the following initial and boundary conditions are valid:

$$C_O(x,o) = O$$

$$C_R(x,o) = C_R^o \qquad \{2 - 98\}$$

$$C_R(o,t) = O; \left(\frac{\delta C_O}{\delta x}\right)_{x=o} = -\left(\frac{\delta C_R}{\delta x}\right)_{x=o} \qquad \{2 - 99\}$$

$$C_O(x \longrightarrow \infty, +) = O \; ; \qquad C_R(x \longrightarrow \infty, +) = C_R o \qquad \{2 - 100\}$$

Where $C_R o$ is the bulk concentration of R.

Solution of eq. {2 - 96} and {2 - 97} by the method of Laplace transformation shows that the concentration of the product of the electrode reaction, O, is given in the transform plane by

$$\overline{C}_O(x,s) = \overline{C}_O(o,s) \exp\left[-\left(\frac{S}{D}\right)^{1/2} x\right] \qquad \{2 - 101\}$$

The absorbance of species O, A_O, may be related to the diffusion equations through Beer's Law

$$A_O(\lambda,t) = \varepsilon o(\lambda) \int_o^\infty C_O(x,t)\, dx \qquad \{2 - 102\}$$

Where εo is the molar absorptivity of O. Transformation of eq {2 - 102} gives

$$\overline{A}_O(\lambda,s) = \varepsilon o \int_o^\infty \overline{C}_O(x,s)\, dx \qquad \{2 - 103\}$$

Substitution of equation {2 - 101} into equation {2 - 103} and performance of the indicated integration yield

$$\overline{A}_O(\lambda,s) = \varepsilon o(\lambda)\ D^{1/2}\ s^{-1/2}\ \overline{C}_O\ (o,s) \qquad \{2 - 104\}$$

Inversion of the above expression gives the result[78] for the time dependence of the absorbance of the product of a diffusion controlled charge-transfer process.

$$\overline{A}_O(\lambda,t) = 2\pi^{-1/2}\ \varepsilon o(\lambda)\ C_R^{\,o}\ D^{1/2}\ t^{1/2} \qquad \{2 - 105\}$$

Kuwana and co-workers[82] evaluated first order and pseudo first order homogeneous reactions following charge transfer.

They used the pulse and pulse relaxation[72,82] methods, to follow electrogenerated species, both during the applied electrochemical perturbation and then during a subsequent open-circuit.

In this work, the method proposed by Bewick et al[83] for evaluating the homogeneous rate constant was used. The method will be described in chapter 4.

2.4.4. INFORMATION THAT ARISES FROM MSRS EXPERIMENTS.

(i) The complete UV-visible spectra from all species involved in the electrochemical reaction can be obtained.

(ii) If the absorbance at a value of λ_{max} is due predominantly to one species then kinetic and mechanistic information can be readily obtained from the analysis of the absorbance/time transients resulting from a potential step experiment.

(iii) For the cation radical produced in the primary step of an anodic oxidation, a plot of the absorbance/time transient as absorbance vs. $t^{\frac{1}{2}}$ should be linear at short times where the intermediate can be considered stable. From the slope of this plot, the extinction coefficient can be obtained.

(iv) At longer times the absorbance vs. $t^{\frac{1}{2}}$ plot will deviate from linearity and from this deviation, the rate constant for the decay of the cation radical can be calculated.(see chapter 4).

(v) More detailed mechanistic and kinetic information on further steps in the reation can be obtained by careful fitting of the absorbance/time transients for the secondary intermediates. In general, the experimental transients need to be fitted, to calculate transients derived by digital methods, from the set of partial differential equations, governing the diffusion/reation scheme corresponding to the particular mechanism being fitted.

REFERENCES

(1) R.N. Adams, "Electrochemistry at Solid Electrodes". Marcel Dekker Inc., New York (1969).

(2) R.S. Nicholson and I. Shain, Anal. Chem. 36, 706 (1964).

(3) R.S. Nicholson and I. Shain, Anal. Chem. 37, 178 (1965).

(4) R.S. Nicholson, Anal. Chem. 37, 1351(1965).

(5) D.S. Poleyn and I. Shain, Anal. Chem. 38, 370 (1966).

(6) J.M. Saveant, Electrochim. Acta, 12, 999 (1967).

(7) D.S. Poleyn and I. Shain, Anal. Chem., 39, 376 (1966).

(8) A. Sevcick, Collect. Czech. Chem. Comm., 13, 34 (1948).

(9) W.H. Reinmuth, J. Am. Chem. Soc., 79, 6358 (1957).

(10) H. Matsuda and Y. Ayabe, Z. Electrochem., 59 ,494 (1955)

(11) Y.P. Gokshtein, Dolk. Akad. Nauk. S.S.S.R., 126, 598 (1955)

(12) G.E. Roberts and M. Kaufman. "Table of Laplace Transforms, Saunders, Philadelphia, Pensylvania (1966).

(13) F. Oberhettinger and L. Badu, "Tables of Laplace Transforms"., Springer-Verlag. Berlin (1973).

(14) D.D. MacDonald. "Transient Techniques in Electrochemistry". Plenum Press (1977).

(15) L. Antropov. "Theoretical Electrochemistry. English Edition- Mir. Publisher. Moscow (1977).

(16) K.J. Vetter. "Electrochemical Kinetics". Theoretical Aspects. Academic Press. New York-London (1967).

(17) J. Crank. "The Mathematics of Diffusion". Second edition Clarendon Press- Oxford (1975).

(18) Weissberger and Rossiter, editors, "Physical Methods of Chemistry". Part II A: Electrochemical Methods. Interscience (1971).

(19) Advanced Instrumental Methods in Electrode Kinetics. The Department of Chemistry, University of Southampton (1975).

(20) D. Hawley and S. Feldberg, J. Phys. Chem., 70, 3459 (1966).

(21) S. Feldberg, J. Phys. Chem., 73, 1238 (1969).

(22) D. Hawley and S. Feldberg, J. Phys. Chem., 71, 85 (1967).

(23) J.M. Savéant, Compt. Rend. 256, 4017 (1964).

(24) L. Nadjo and J.M. Savéant, J. Electroanal. Chem. 47, 146 (1973).

(25) L. Nadjo and J.M. Savéant, Electrochim. Acta., 16, 887 (1971).

(26) C.P. Andrieux and J.M. Savéant. J. Electroanal. Chem., 42, 189 (1973).

(27) Ibid., 50, 141 (1974).

(28) J.C. Imbeaux and J.M. Savéant, J. Electroanal. Chem., 31, 183 (1971).

(29) H.N. Blount. Electroanalytical Chemistry and Interfacial Electrochemistry, 42, 271 (1973).

(30) J. O'M. Bockris. A.K.N. Redy. "Modern Electrochemistry" Volume 2 (1973).

(31) B.S. Pons. PhD. thesis. Southampton University (1979).

(32) Y. Okinaka, S. Toshima and H. Okaniwa, Talanta., 11, 203 (1964).

(33) K.B. Oldham and R.A. Osteryoung J. Electroanal. Chem. 11, 397 (1966).

(34) P.J. Lingane and J.H. Christie, J. Electroanal. Chem., 10, 284 (1965).

(35) K.B. Oldham, J. Electroanal. Chem., 11, 171 (1966).

(36) W.M. Schwarz and I. Shain, J. Phys. Chem., 69, 30 (1965).

(37) R.F. Nelson and S.W. Feldberg, J. Phys. Chem., 73. 2623 (1969).

(38) G. Alberts and J. Shain, Anal. Chem., 35, 1859 (1963).

(39) H.F. Weinberg. "Partial Differential Equations" Xerox. College Publishing, Lexington, Massachusetts, Toronto (1965).

(40) A.J. Bard and L.R. Faulkner., "Electrochemical Methods". John Willey & Sons., INC. U.S.A. (1980).

(41) C. Amatore and J. Saveant, J. Electroanal. Chem., 44, 169 (1973).

(42) D. Evans, T. Rosanske, and P. Jimenez, J. Electroanal. Chem., 51, 449 (1974).

(43) A. Hickling, Trans Faraday soc., 38, 27 (1942).

(44) M. Fleishman and D. Pletcher, Tetrahedrom Letters., 60, 6255 (1968).

(45) J.J. Lingane "Electroanalytical Chemistry" Second edition, Interscience, INC., New York (1958).

(46) L. Meites "Polarographic Techniques". Second edition, Interscience, INC., New York (1965).

(47) G.H. Rechnitz. "Controlled-Potential Analysis", The Macmillan Co., New York (1963).

(48) N.L. Weinberg Ed. "Technique of Electroorganic Synthesis" Vol. 5., Part I. John Wiley & Sons. New York. London. Sydney. Toronto (1974).

(49) B.S. Pons, J. Manson, L. Winston and H. Mark Jr. Anal. Chem., 39, 685 (1967).

(50) N. Winograd and T. Kuwana, Electroanal. Chem, 7, 1 (1974).

(51) T. Kuwana and W.R. Heineman Acc. Chem. Res., 9, 241 (1976).

(52) W.R. Heineman, Anal. Chem., 50, 390 A (1978).

(53) R. Cieslinki and N.R. Armstrong, Anal. Chem., 49, 1395 (1977).

(54) R.H. Müller, Adv. in Electrochemistry and Electrochemical Engeneering, Vol 9, Wiley , Interscience, New York (1973).

(55) G.H. Brilmyer and A.J. Bard, Anal. Chem., 52, 685 (1980).

(56) A. Fujishima, H. Masuda, K. Honda and A.J. Bard, Anal. Chem., 52, 682 (1980).

(57) A. Fujishima, G.H. Brilmyer and A.J. Bard. "Semiconductor Liquid Junction Solar Cells"., A. Heller Ed., Electrochemical Society, Princeton (1977).

(58) A. Fujishima, Y. Maeda, K. Honda, G.H. Brilmyer and A.J. Bard. J. Electrochem. Soc., 127, 840 (1980).

(59) H.A. Szmanski, Ed., "Raman Spectroscopy", Plenum., New York (1970).

(60) M. Fleishmann, P. Hendra and J. Mc. Quillan, Chem. Phys. Letters, 26, 163 (1974).

(61) J.B. Goldberg and A.J. Bard "Magnetic Resonance in Chemistry and Biology". J.N. Herak and K.J. Adamic, eds., M. Dekker, INC., New York (1975).

(62) T.M. McKinney, Electroanal. Chem., 10, 97 (1977).

(63) (a) B. Kastening Prog. Polarog., 3, 195 (1972).
(b) Ibid Chem. Ing. Tech., 42, 190 (1970).

(64) H. Mark, Jr. and B.S. Pons., Anal. Chem., 38, 119 (1966).

(65) J.D.E. McIntyre, Adv. Electrochem, Electrochem Engr., 9, 227 (1973).

(66) R.H. Müller, Ibid p. 167.

(67) B.D. Cahan, J. Horkans and E. Yeager, Symp. Faraday Soc., 4, 36 (1970).

(68) M.A. Barrett and A. Parsons, Ibid, p. 72.

(69) J.D.E. McIntyre and D.M. Kolb, IIbid p. 99.

(70) A. Bewick and A.M. Tuxford, Ibid p. 114.

(71) W. J. Plieth, Ibid., p. 137.

(72) J.M. Baker and D.E. Eastman. J. Vac. Sci. Technol., 10, 223 (1973).

(73) A. Bewick, K. Kunimatsu. Surf. Sci., 101, 131 (1980).

(74) A. Bewick, K. Kunimatsu and B.S. Pons, Electrochim Acta, 25, 465 (1980).

(75) A. Bewick, K. Kunimatsu, J. Robinson and J.W. Russell. J. Electronal. Chem., 119, 175 (1981).

(76) E. Hecht., A. Zajac "Optics". Addison Westey Publishing Co. Second Printing (1977).

'77) R. Moss., "Interaction of Radiation with Matter". Lecture. University of Southampton (1978).

(78) J. Strojek, T. Kuwana, and S. Feldberg, J. Am. Chem. Soc., 90, 85 (1972).

(79) G.A. Gruver and T. Kuwana, J. Electroandl. Chem., 36, 85 (1972).

(80) S.W. Feldberg "Electroanalytical Chemistry". A. Bard. Ed. VolIII, Marcel Dekker, New York (1969).

(81) G. C. Grant and T. Kuwana, J. Electroanal. Chem., 24, 11 (1970).

(82) N. Winograd, H.N. Blount, and T. Kuwana. J. Physical Chemistry, 73, 3456 (1969).

(83) A. Bewick, J.M. Mellor and B.S. Pons. Electrochim. Acta . 25 , 931 (1980).

CHAPTER 3: EXPERIMENTAL

3.1. REAGENTS

Hexaethylbenzene (Eastman-Kodak); 1-Phenyloctane (Aldrich); 1-Phenylnonane(Aldrich); n-Propylbenzene (Aldrich); tert-Butylbenzene (BDH); 1,2-Dimethoxybenzene (Aldrich); 1,3-Dimethoxybenzene (Aldrich); 4- Methylanisole (Aldrich); Ethoxybenzene,Phenetole,(BDH); 3-Methylphenetole(Eastman-Kodak); 1,3,5-Trimethoxybenzene (Aldrich); Anisole (Koch - Light), were used without further purification.

Toluene (BDH) was purified by vacuum distillation. Acetonitrile (Fisons) was purified as described later; 1,4-Dimethoxybenzene (BDH) was recrystallized from ethanol; Tetra-n-butylammonium tetrafluoroborate ($Bu^n_4 NBF_4$) was prepared by a modified procedure of Clark, Fleischmann and Pletcher [1] which will be described later in this section.

3.3.3. PURIFICATION OF ACETONITRILE

Fisons' far UV grade acetonitrile was distilled on P_2O_5 at atmospheric pressure (boiling point 81.5°C). The distillate was collected into a flask containing $KMnO_4$, and re-distilled at about 5 ml. per minute, discarding the first 10 and the last 50 ml. The distillate was then collected into a conical flask containing Woelm Super grade neutral alumina and stored until use.

3.1.2. PREPARATION OF SUPPORTING ELECTROLYTE.

Tetra-n-butylammonium hydrogen sulphate (Labkemi, Goteborg, Stocholm) (339 g.) was dissolved in triply distilled water (2 l.) and sodium tetrafluoroborate (110 g.) was dissolved in water (1 l.). The two aqueous solutions were added and immediately, a white fluffy precipitate of tetra-n-butylammonium fluoroborate dropped out of solution. The precipitate was filtered, only the first batch of crystals being collected. The precipitate was then dissolved in dichloromethane (200 ml.) and this solution washed three times with water (300 ml.). The dichloromethane solution was filtered and poured into ether. Pure crystals of $Bu^n_4NBF_4$ precipitated. Only the first crystals were collected and purified twice by dissolving in dichloromethane, washing with triply distilled water and pouring into ether. The precipitate was vacuum dried at 80°C for 48 hours.

3.2. GLASSWARE CLEANING.

All glassware was washed with acetone, rinsed with distilled water, and then, boiled during 5 min, in a mixture (1:1) of concentrated Nitric and Sulphuric acids. After cooling the acid mixture, it was rinsed with hot running water and then boiled for 10 min. in triply distilled water, rinsed again with distilled acetone and vacuum dried at 100°C for at least one hour prior to use.

3.3. ANALYSIS.

Infrared spectra were recorded on a Pye Unicam SP 200 Spectrometer for samples in Nujol on a NaCl window.

N.M.R. spectra were recorded on a Perkin Elmer R 12, Varian Associates HA 100 or XL 100 spectrometer.

Thin Layer Chromatography (TLC) were run on 20 x 20 glass plates with 1 mm thick silica gel coat.

Gas-liquid chromatography (GLC) was performed using Pye Unicam GCD gas chromatograph fitted with a flame ionisation detector, and using 2m OV1 on chromosorb GAW DMCS 100-200 mesh (5% w/w) column.

Mass spectra were carried out in a Kratos M5 30 mass Spectrometer (sometimes, coupled to a gas chromatograph).

3.4. CYCLIC VOLTAMMETRY EXPERIMENTS.

Cyclic Voltammetry experiments were performed using a Hi-Tek potentiostat type DT 2101 and a Hi-Tek waveform generator type PP R1. The voltammograms were recorded either directly on a Hewlett Packard 7015B x-y recorder at slow sweep rates, or via a Gould Advance OS4100 Digital storage oscilloscope/waveform Digitizer at those sweep rates higher than 0.7 Vs^{-1}.

IR compensation was not necessary with the arrangement used in these experiments.

The working electrode was 0.2 cm^2 platinum wire. The secondary electrode was a cylindrical platinum gauze surrounding the working electrode, to ensure good cylindrical geometry.

All measurements were taken against a silver wire held in an acetonitrile-$Bu^n_4NBF_4$ (0.1 M) solution containing silver nitrate (0.01 M). A frit separated the silver wire from the reference compartment and a Luggin capillary isolated the reference electrode from the working compartment. The voltammetric cell is shown in fig. 3.1.

To assure that the ramp points matched the digital store points on the oscilloscope, a dummy cell was used, and the scope controls were adjusted until a straight diagonal line was obtained on the display of the oscilloscope. This was done for each sweep rate.

For quantitative studies, only the first sweep was recorded and the working electrode was flamed before each run. Concentrations were between 5×10^{-3} and 1×10^{-3} M.

The system provided a range of sweep rate from 10 mV s^{-1} to 500 V s^{-1}.

3.5. CHRONOAMPEROMETRY EXPERIMENTS.

The potential step experiment for obtaining current-time transients, was performed by using the same setting up as that for fast cyclic voltammetry. (fig 3.2.) , and the same range of concentrations. The starting potential was chosen from 200-300 mV cathodic to the oxidation peak, to 100-200 mV anodic to this peak; depending upon the shape of the voltammogram.

The transients were monitored and stored in the digital storage oscilloscope, and then plotted out on an x-t recorder, the time scale

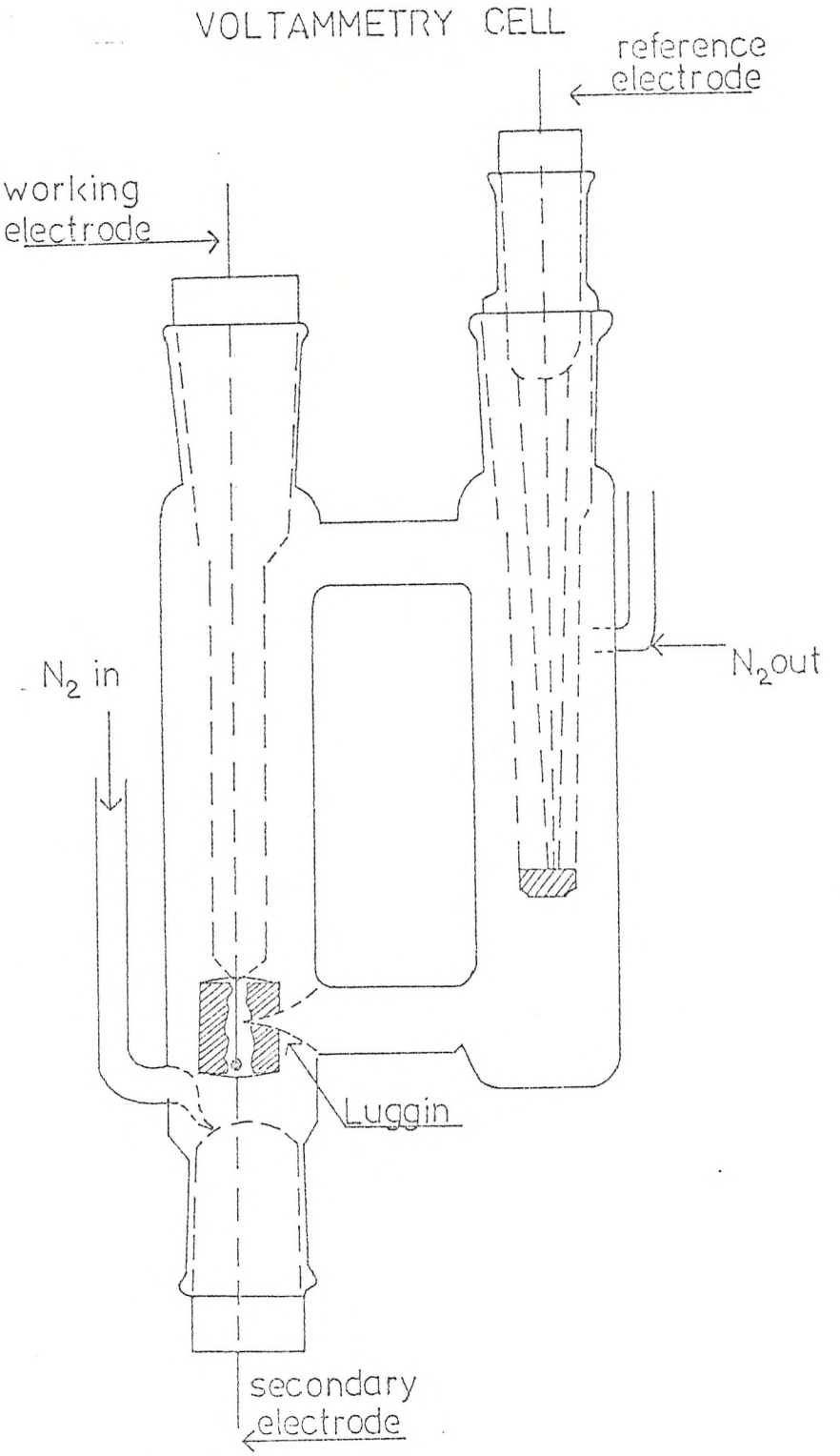
VOLTAMMETRY CELL
reference electrode
working electrode
N_2 in
N_2 out
Luggin
secondary electrode

Fig. 3.1

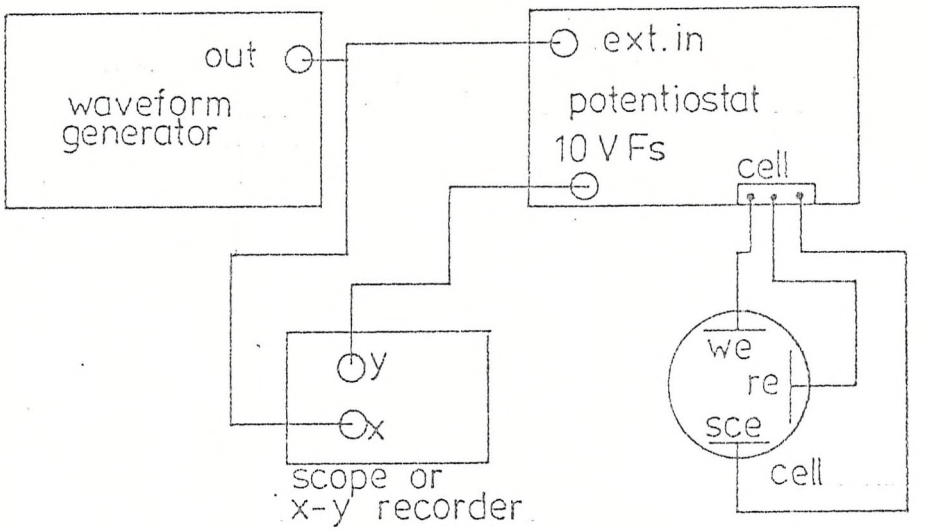

(a)

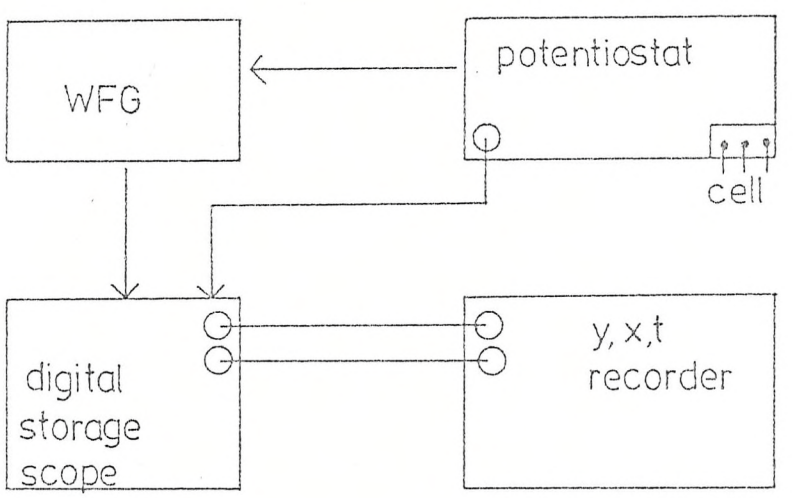

(b)

Fig. 3.2

Block diagram for (a) slow cyclic voltammetry. (b) fast cyclic voltammetry and chronoamperometry

of the recorder being syncronized with the plotting scale of the oscilloscope.

A dummy cell was used to adjust the scope controls until the desired pulse length was obtained, to ensure that the pulse points matched the digital store points on the oscilloscope.

The cell used in these experiments was the same as that used for cyclic voltammetry.

3.6. PREPARATIVE COULOMETRY EXPERIMENTS.

Preparative coulometry experiments were performed using a three compartment electrolysis cell (fig. 3.3.). Both, the working and the secondary electrodes were 2 cm^2 geometrical area platinum gauzes. The anolyte and catholyte compartments were separated by two number 3 sintered frits, leaving a small space in between filled with the same solution, in order to minimize migration from the working to the secondary compartment. The reference electrode was as described before, and it was conected to the working electrode by the Luggin capillary.

For all the experiments, the anolyte and catholyte were solutions of acetonitrile-$Bu^n_4 NBF_4$ (0.10 M). The anolyte was continuously stirred magnetically.

A cationic resin (DOWEX 500 W-X8, 100-200 mesh) was added to the working electrode compartment before the start of the electrolysis, to trap the intermediate and to simplify the reaction.

The resin was continuously washed with CH_3CN in a Soxhlet

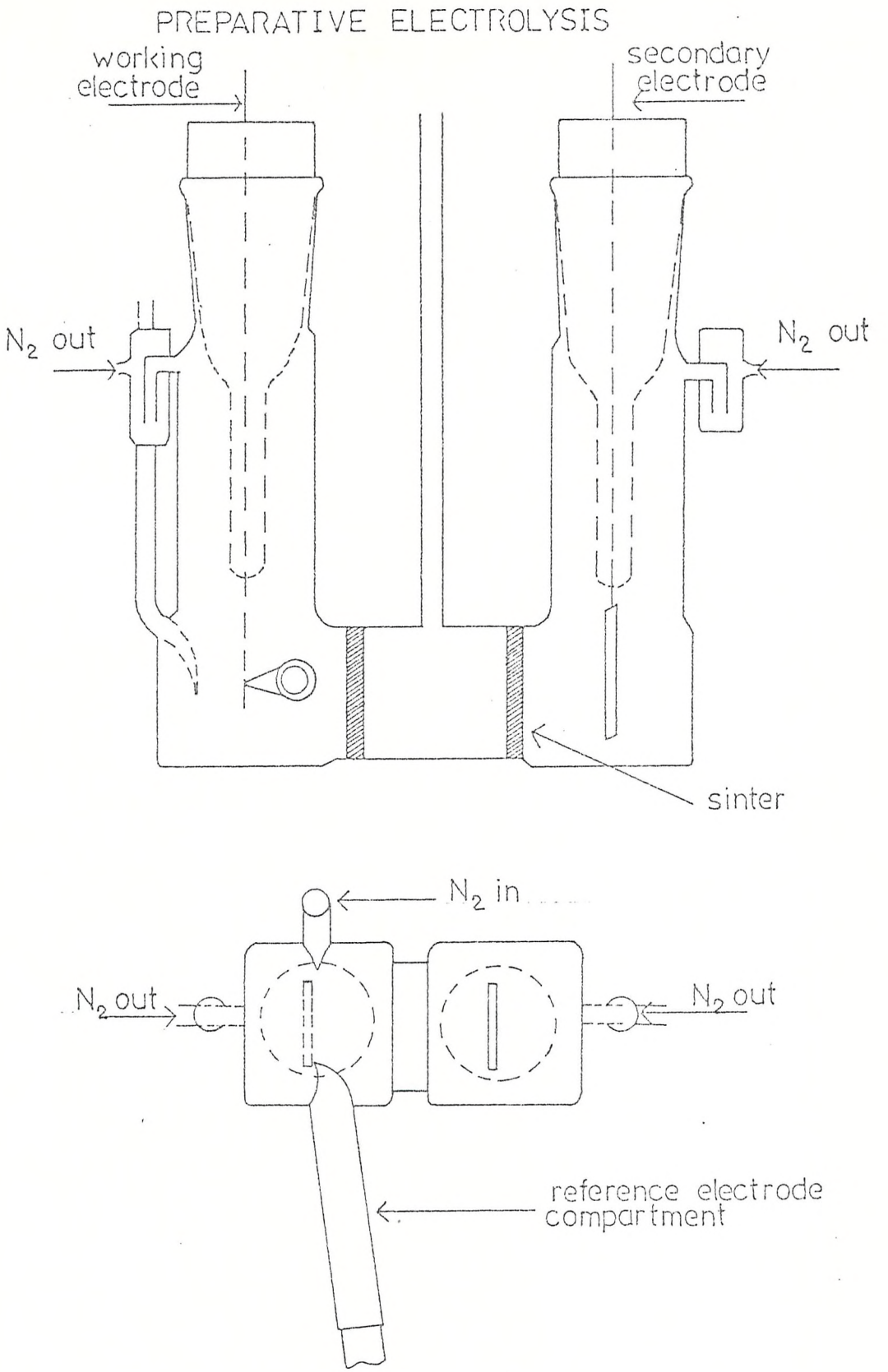
PREPARATIVE ELECTROLYSIS
working electrode
secondary electrode
N_2 out
N_2 out
sinter
N_2 in
N_2 out
N_2 out
reference electrode compartment

Fig . 3.3

extractor for 24 hours and then vacuum dried during 24 hours at 80°C prior to use.

After the reaction finished, the anolyte was filtered and the resin separated, washed with CH_3CN and poured into 1 M NaOH solution, leaving it to stand for 1 hour, stirring magnetically. It was then filtered and the resin poured into CH_2Cl_2 for 2 hr. The aqueous solution was neutralized with HCl and extracted with CH_2Cl_2. Both, CH_2Cl_2 extracts were put together, dried with sodium sulphate, the solvent evaporated, the residue taken up in ethylacetate (5 ml) and recrystallized from ethanol.

The solvent of the anolyte solution was evaporated, the residue washed three times with triply distilled water, and the product extracted with diethylether.

Both, steady state and pulsing preparative coulometry experiments were performed during this work. In the first case, potentials were set at the peak voltammetric potential. For the second case, consecutive pulses were applied instead of a constant potential: the potential was modulated with a square wave from 0.00 V up to the peak potential, the time potentials being maintained for 0.1 s each. This latter procedure allowed high currents to be maintained when severe electrode fouling was encountered using a steady fixed potential.

Background currents were measured with solvent-supporting electrolyte solution; they were found to be very low. (0.05 mA), compared with the value for the reaction (20-30 mA).

A Hi-Tek Potentiostat type DT 2101 was used to maintain a constant potential applied to the working electrode. Coupled to the

potentiostat, a Hi-Tek waveform generator type PPR1 was used for stepping the potential for the pulsing coulometry. A current integrator (made in the department workshop) was used to measure the amount of coulombs passed during the electrolysis.

3.7. THE OPTICAL SYSTEM.

Modulated Specular Reflectance Spectroscopy (MSRS) was used to detect optically absorbing intermediates at the electrode.

The light source was a 200 watt Hg-Xe arc (Engelhard Hanovia 901-B1) in a special housing (Oriel Optical Corp. 6165) with a fan incorporated. The lamp was coupled with a Bausch & Lamb (Grating 1200 Grooves/mm) monochromator. The monochromator output beam was focussed with a 2.5 cm focal length lens (Thermal Syndicate Ltd.), to allow the beam to pass through the 45° optical cell window onto the platinum electrode mirror surface. The monochromatic light out was equally focussed with a similar lens to bring the beam onto the detector. Both, a EMI 6256 B Photomultiplier and a UDT 500 photodiode were used as detectors. The photomultiplier was fed from a high voltage source (Brandenberg 472 R).

All optical components, except the detectors, were set up using adjustable mounts on a long optical bench. The detector, preceded by the lens, was mounted on a short optical bench positioned perpendicular to the long bench.

The optical arrangement, except the lamp and the monochromator, were enclosed in a black box.

A Brookdeal 401A Lock-in amplifier was used to monitor the reflectivity difference, ΔR, (produced by a change ΔE in potential) for the reflectance spectra. A low noise differential amplifier was used for monitoring ΔR in the optical transient experiments. The optical transients were stored in a Hi-Tek AA1 signal averager.

The block diagrams for both MSRS spectra scanning and optical transients measurements are illustrated in fig. 3.4. and 3.5. respectively.

3.7.1. OPTICAL CELL AND ELECTRODES.

Optical experiments were carried out in a typical optical cell (fig. 3.6.). It was made of pyrex glass except the optical windows which were made with "spectrosil" discs.

The monochromatic light was focussed onto the platinum mirror working electrode, and the reflected beam taken onto the detector as it was described before.

The working electrode consisted of a platinum disc welded onto the end of a syringe barrel (fig. 3.6.)

The secondary electrode was a platinum mesh held parallel to the working electrode at a distance of 3 cm from it. The reference electrode was the same as for the other experiments; it was also mounted in a syringe barrel to allow correct positioning. The Luggin was positioned at about 1 mm from the working electrode. To reduce impedance in the Luggin arrangement, a platinum wire was inserted between the Luggin and the two way tap which isolated the reference compartment. A 0.1μF capacitor was arranged in parallel between the reference electrode and the platinum wire.

SPECULAR REFLECTANCE
BLOCK DIAGRAM

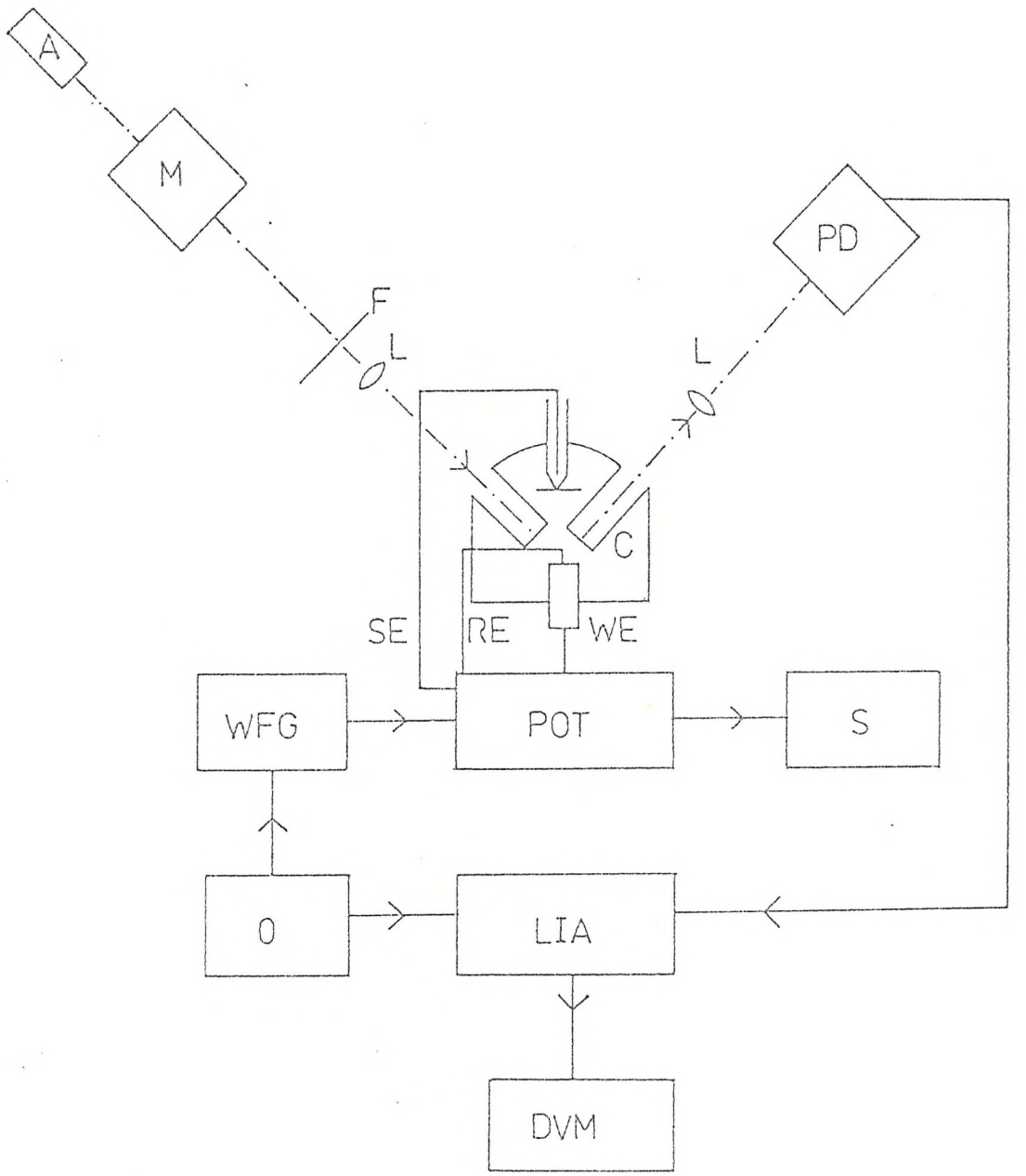

A=lamp ; M=monochromator; F=filter ; L=lens ; SE=secondary electrode ; RE=reference electrode ; WE=working electrode. PD=photodiode ; POT=potentiostat ; WFG=wavefor generator. S=oscilloscope ; O=oscillator ; LIA=lock-in amplifier; C=cell. DVM=digital voltmeter

Fig. 3.4

OPTICAL TRANSIENT EXPERIMENT
BLOCK DIAGRAM

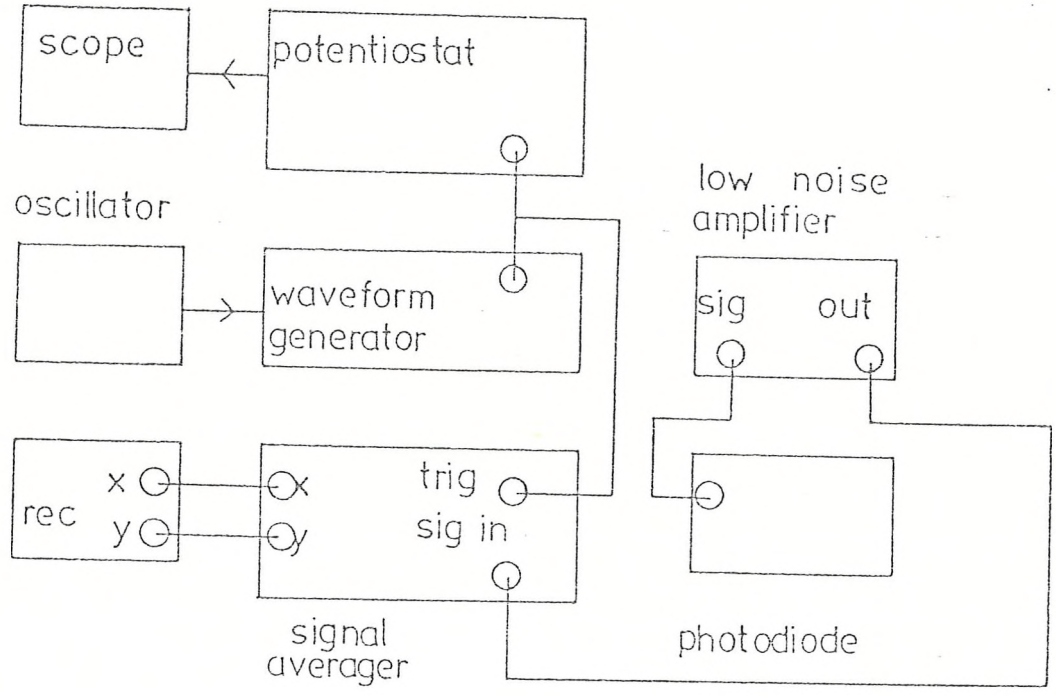

Fig. 3.5

OPTICAL ELECTRODE AND CELL DIAGRAM

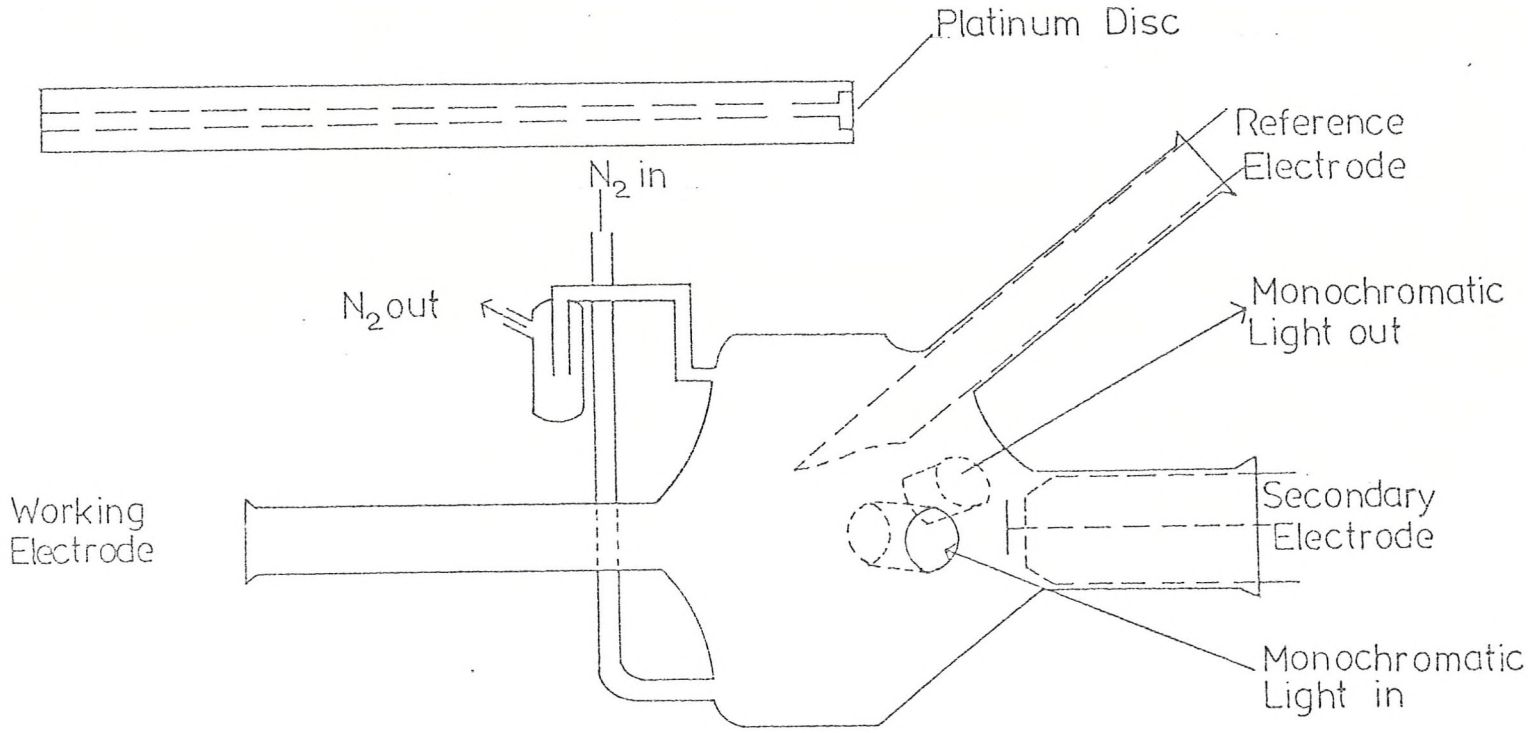

Fig . 3.6

The cell was held such that the angle of incidence of the beam on the electrode surface was 45^{o}.

The working electrode was polished with alumina of successively decreasing grades (0.3μ, 0.1μ, 0.05μ) on a polishing cloth lubricated with distilled water. Then, it was placed into a 1:1 concentrated nitric and sulphuric acid mixture for about 15 min (the mixture was kept just under the boiling point), rinsed off with triply distilled water and vacuum dried at 30^{o}C during two hours before use. The secondary electrode was flamed each time before use.

3.7.2. THE OPTICAL EXPERIMENTS.

The MSRS spectra were monitored using phase sensitive detection. The waveform generator was triggered by the oscillator and the square wave pulse length was adjusted to finish at the same time on both the oscillator and the waveform generator. This pulse train was applied to the working electrode via the potentiostat, giving a modulated reflected light beam, which was converted into a.c. voltage by the photodetector. The lock-in amplifier (referenced by the waveform generator pulse trigger) received the signal sent by the detector, shifted the reference signal into phase with the potential modulation at the electrode. Finally the lock-in amplifier delivered a d.c. output voltage proportional to the change in reflectivity ΔR.

The amplitude of the square wave was chosen according to the cyclic voltammogram for each particular system; for a system exhibiting a smooth cyclic voltammogram, the pulse was from a potential where no

electrochemical reaction was taking place, to a point where the reaction was completely diffusion controlled. For those with a cyclic voltammogram showing a rather complex behavior, the pulse was from a potential of no faradaic reaction to the voltammetric peak potential, to avoid the appearence of complicated species. For a better resolution of the spectra it is desirable to make the modulation potential range as short as possible.(2)

Care must be taken to choose the pulse length for the experiments: it is necessary to work away from the main line frequency (50 Hz in our case) and any odd harmonic frequency of it, to avoid interferences and noise. If the pulse is too short, any species formed in a future chemical step could be missed. If the pulse is too long, poisoning of the electrode in some organic systems may occur, spoiling the mirror properties of the electrode surface, and the signal may not be seen.

What is observed as a result of this experiment is the variation of $\Delta R/R$ as a function of the wavelength. The value $\Delta R/R$ can be defined as the quantity $(R_2 - R_1)/R_1$, where R_1 was the reflectivity of the most cathodic part of the pulse, and R_2 is that at the most anodic potential. Therefore, for oxidations where intermediates species absorb, $R_2 < R_1$ and ΔR are negative.

Once we had the MSRS spectra, optical transients at each well-defined peak wavelength could be stored digitally in a Hi-Tek signal averager (triggered to start at the same time as the waveform generator pulse started) which was fed by the signal coming from the photodetector, passing through a low-noise amplifier.

Proper choice of the time of data input must be made, taking

into account the life time of the intermediates (if known) and trying to include part of the species decay.

For all the experiments in this work, the following arrangement was used:

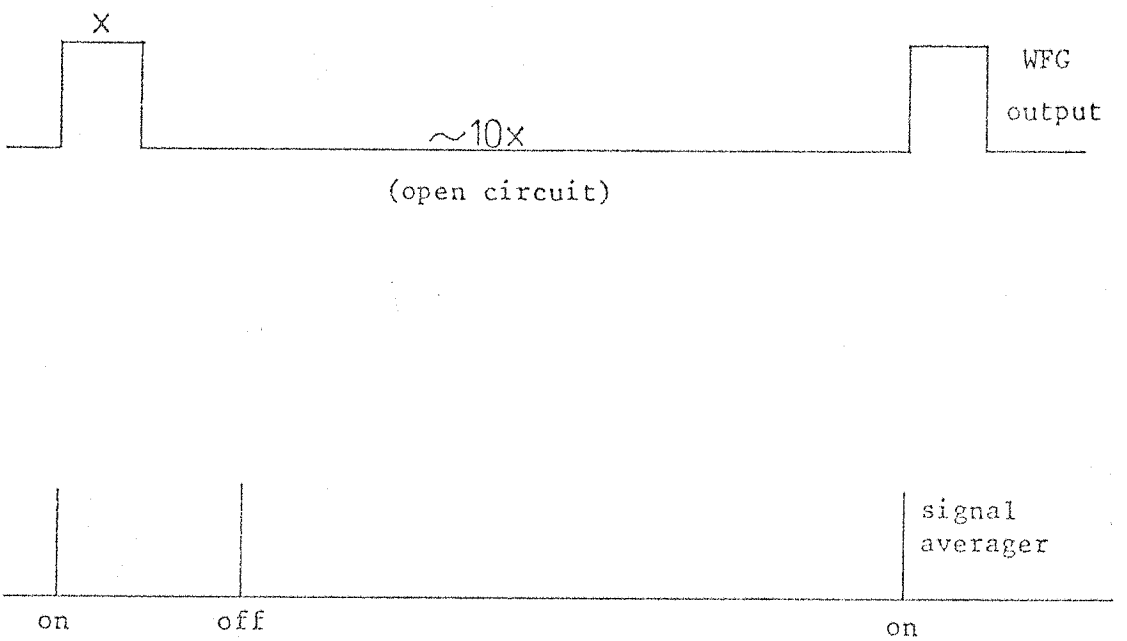

The shape of the transient observed depended on the nature of the system under study and the intermediates.

The open circuit time was chosen 10 times longer than the oxidation pulse length, to allow the system to reach initial conditions before the start of the next pulse.

For some of the systems studied here, the working electrode

became completely covered by a dark film, so it was necessary to take it out to be cleaned and polished by the procedure described before, washing it with distilled acetone followed by solvent-supporting electrolyte solution (5 ml), to avoid contamination of the solution when replaced back to the cell. Reproducible transients were found by this procedure.

As a result of this experiment, a ΔR vs time transient was plotted out on a x-y recorder.

Values of R were measured for each transient to build the plot $\Delta R/R$ vs time from the recorded transients.

In all the cases, signal averaging of 512 transients was carried out.

The experimental parameters for the spectra of most compounds were:

Frequency of modulation: 80Hz

Modulation pulse height:

Base Potential: see tables 4.7. and 5.4.

Recorded sensitivity: 1 V/inch

Lock-in amplifier time constant: 1 s

Lock-in amplifier sensitivity: (100-300) μ V

And for transient experiments:

Time of data input: 10 m s.

Modulation peak height:

Base potential: see tables 4.7 and 5.4

Signal averager sensitivity: ($\pm$0.5, $\pm$1) Volts

Amplifier gain: 40-60 dB

Amplifier frequency range: 10 Hz-1KHz

3.8. REFERENCES.

(1) M. Fleischmann and D.Pletcher, Tetrahedron Letters., 60, 6255 (1968).

(2) M. Cardona. "Modulation Spectroscopy" Solid State Physics Academic Press - New York- London (1969).

CHAPTER 4 : ANODIC OXIDATION OF ALKYLBENZENES

4.1. CYCLIC VOLTAMMETRY RESULTS FOR ANODIC OXIDATION OF HYDROCARBONS.-

All voltammetry experiments were performed using the cell described in section 3.4, and shown in figure 3.1. The composition of the solutions used for voltammetry are described on the voltammograms.

The voltammetry of hexaethylbenzene will be described separately because it showed a different behaviour, compared with the other hydrocarbons discussed in this chapter, while 1-Phenyloctane , 1-Phenylnonane , n-Propylbenzene and tert-Butylbenzene showed certain similarities in their behaviour.

At a sweep speed of 40 mV. $s.^{-1}$, hexaethylbenzene gave an oxidation wave with only a barely defined peak. As the sweep rate was increased,a well defined anodic reversible peak developed at + 1.360 V. ; the cathodic reverse peak was at + 1.300 V. Figure 4.1 shows the hexaethylbenzene cyclic voltammogram at several sweep rates. The potentials of both the anodic and the cathodic peaks did not change with the sweep rate.

Theoretical working curves were constructed as described in chapter 2,section 2.1.5,and compared with the experimental data by fitting the curves in the same graph (fig. 4.2). The pseudo-first order rate constant ,k_f, was estimated. A list of the experimental rate constants of all the members of this series, will be given later in this chapter.

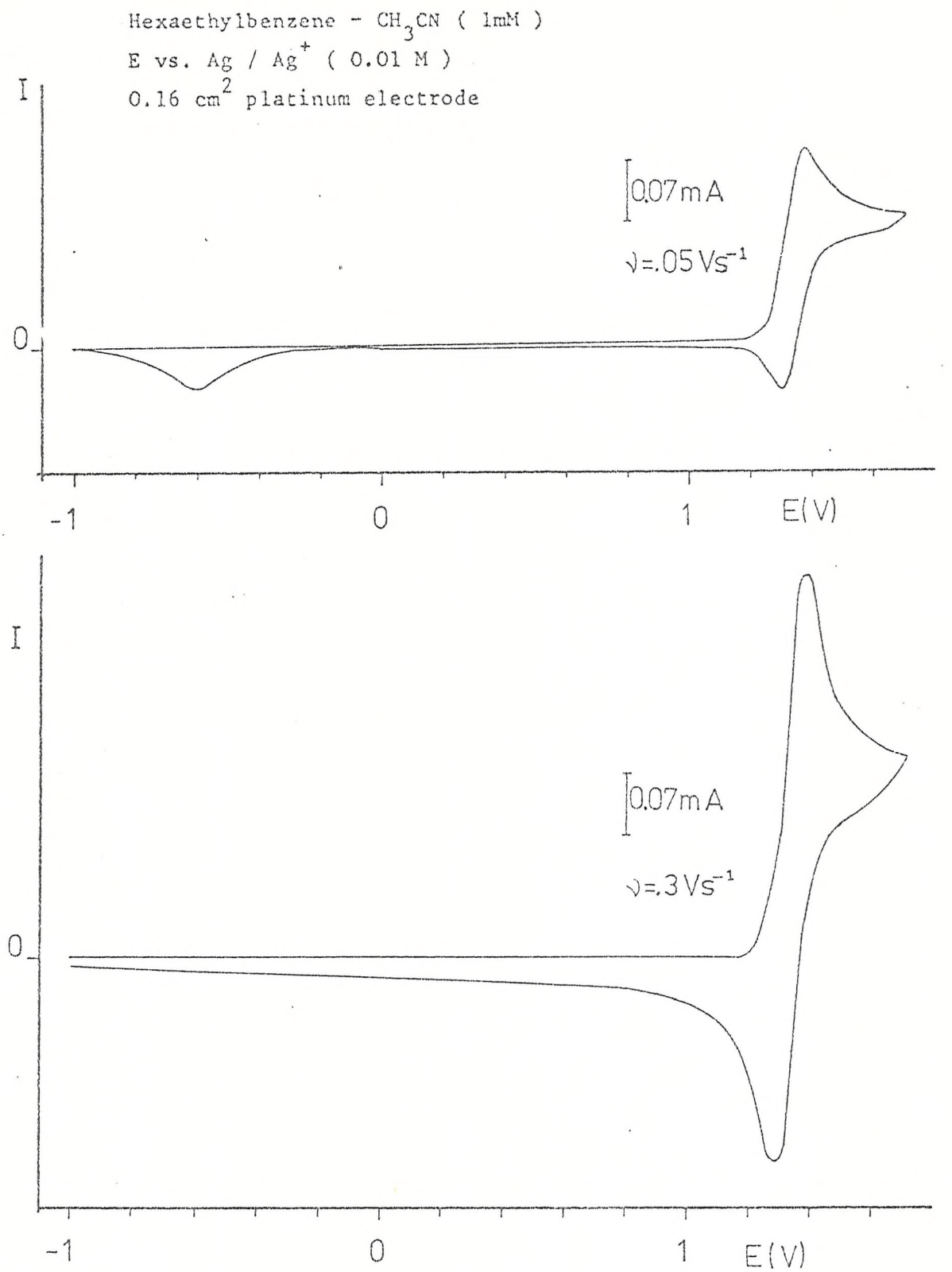

Fig. 4.1 Cyclic voltammograms of Hexaethylbenzene

From fig. 4.2, it can be observed that at low sweep rates, the current function decays as the sweep rate is increased, whereas at faster sweep rates, the decay is approximately linear and becomes independent of the sweep rate; the best fit for the experimental data, matches a k_f value of 0.75 s^{-1}.

The voltammetry of 1- Phenyloctane, 1- Phenylnonane, n- Propylbenzene and tert-Butylbenzene will be described below:

Except for the tert-Butylbenzene., which showed a second wave at +2.16 V, all the compounds showed only one peak within the range of potential 1.84 - 1.94 Volts. Those values of potential, are much higher than that observed for Hexaethylbenzene. They also exhibited a reverse broad peak at -0.60 V, which disappeared at high sweep rates. This could be indicative of a reaction of the cation radical at relatively long time. It has been reported [1,2] that such wave at -0.60 V, is due to the reduction of hydrogen ion. At very high sweep rates (after 400 Volts/s.), a reverse peak was observed at far negative potentials. All of them showed irreversible behaviour in the voltammetry.

Table 4.1 shows peak potentials against Ag/Ag^+ (0.01 M) and half peak width values for all the hydrocarbons studied in this work at sweep rate of 0.2 Volts/s.

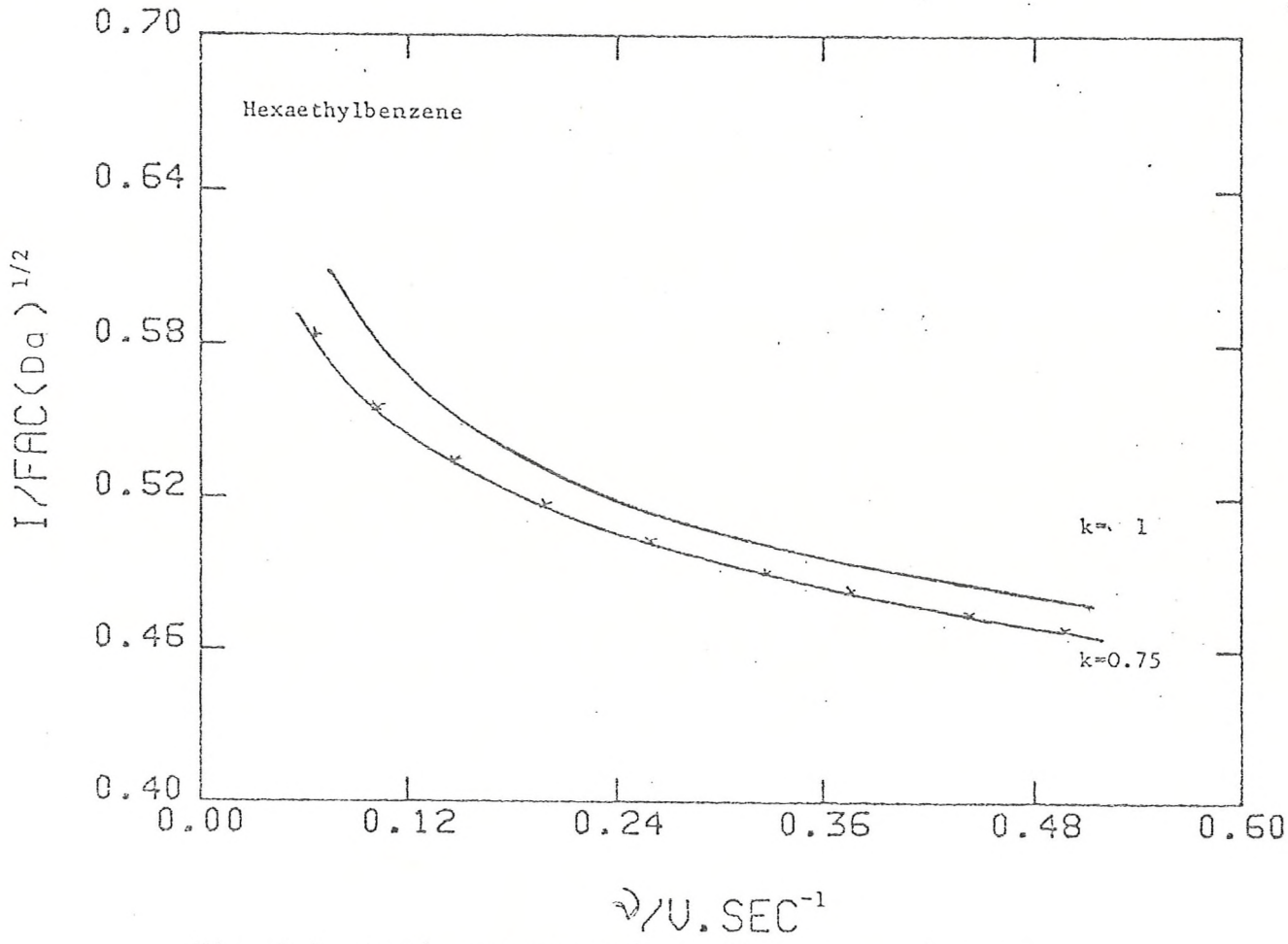

Fig. 4.2 Cyclic voltammetric working curves for the determination of the rate constant k_f.

xxx Experimental

___ Theoretical

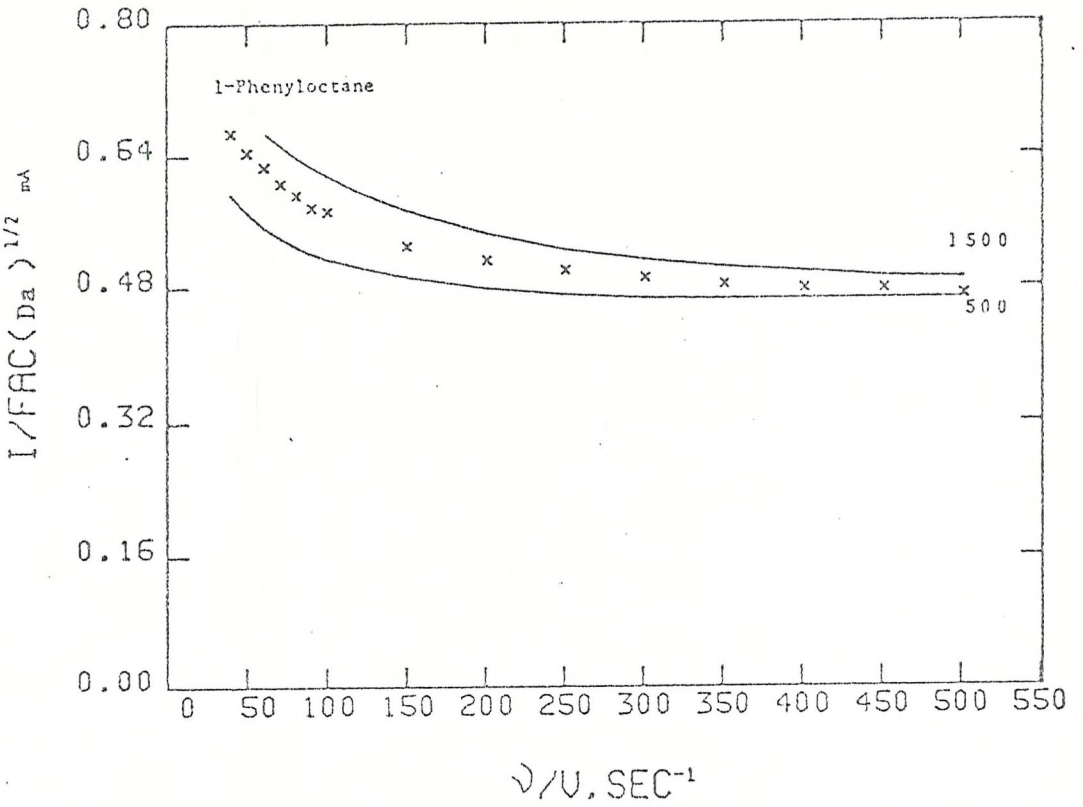

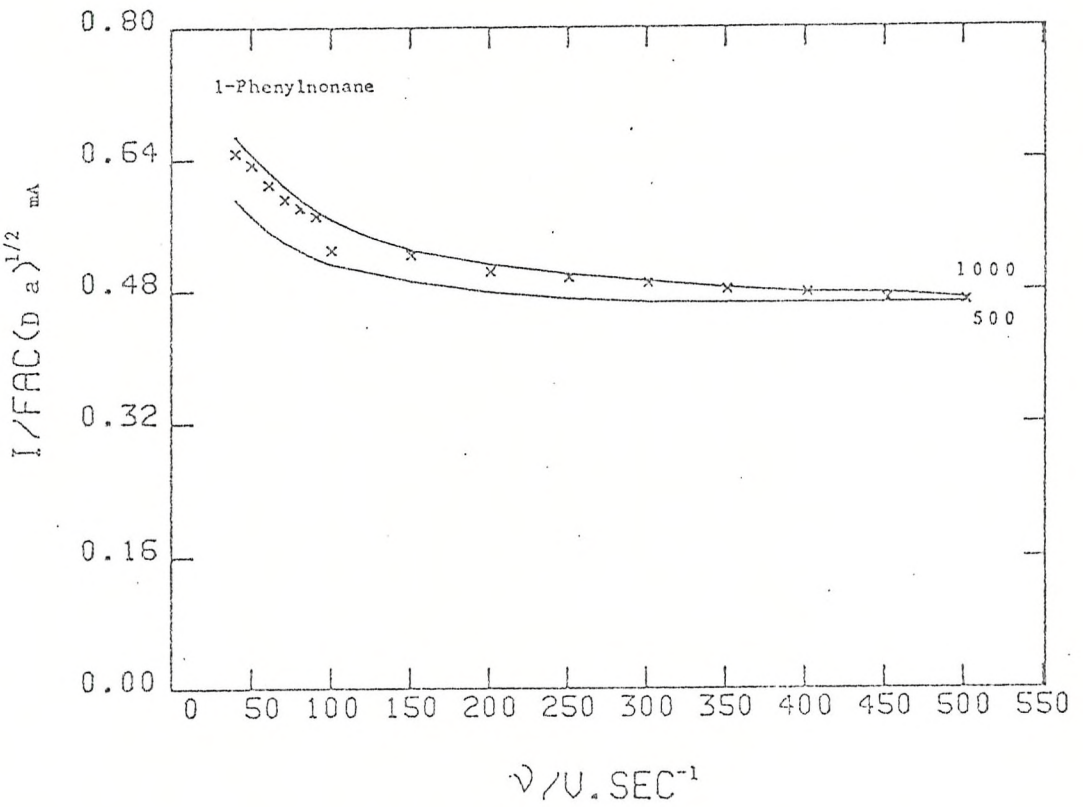

Fig. 4.3 Cyclic voltammetric working curves for the determination of the rate constant k_f .

xxx- Experimental

___ Theoretical

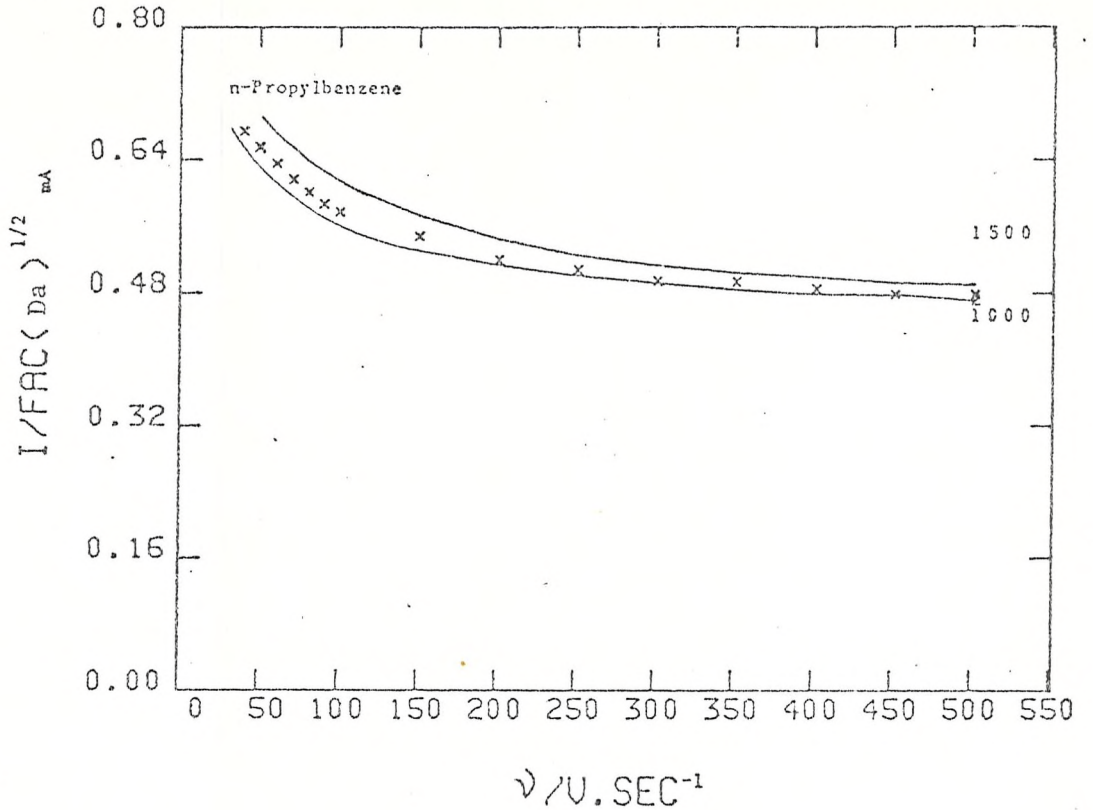

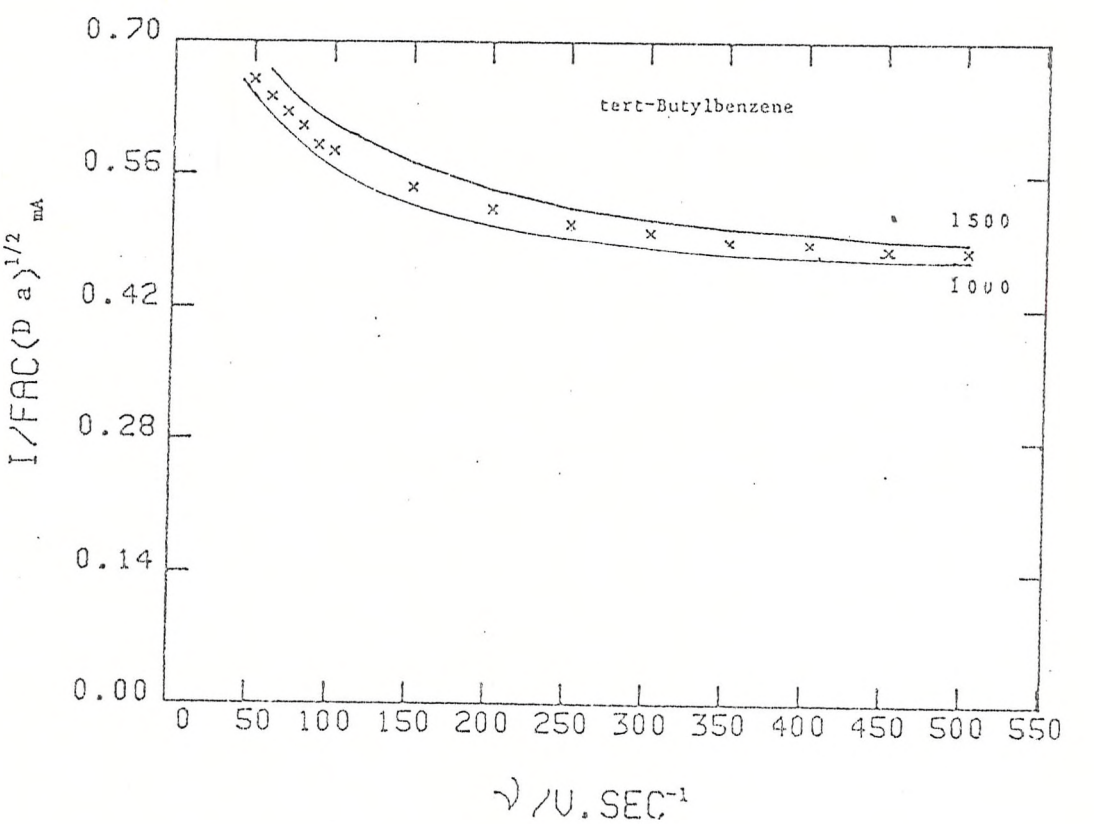

Fig. 4.4 Cyclic voltammetric working curves for the determination of the rate constant k_f.

xxx- Experimental

___ Theoretical

SUBSTRATE	Ep (Volts)	$Ep/_2$ (Volts)	$Ep-Ep/_2$ (Volts)
Hexaethylbenzene	1.360	1.300	0.060
1- Phenyloctane	1.920	1.820	0.100
1- Phenylnonane	1.850	1.770	0.080
n- Propylbenzene	1.900	1.800	0.100
tert-Butylbenzene	1.940	1.860	0.080

TABLE 4.1.- Voltammetric data for anodic oxidation of hydrocarbons.

Theoretical working curves were constructed and the best fit for a pseudo-first order rate constant was found to be within a range of 1000 to 1500 $s.^{-1}$ (Figures 4.3 and 4.4).

4.2 CHRONOAMPEROMETRY RESULTS FOR ANODIC OXIDATION OF HYDROCARBONS.

Chronoamperometry was performed using the same cell as that used for cyclic voltammetry. The setting up of the system and the choice of a suitable pulse amplitude, have been described in section 3.5. Figures 4.5. through 4.7 show the plots of I vs. $t^{-\frac{1}{2}}$ taken from the current transients obtained for the substrates under study. Theoretical working curves were constructed for various k_f

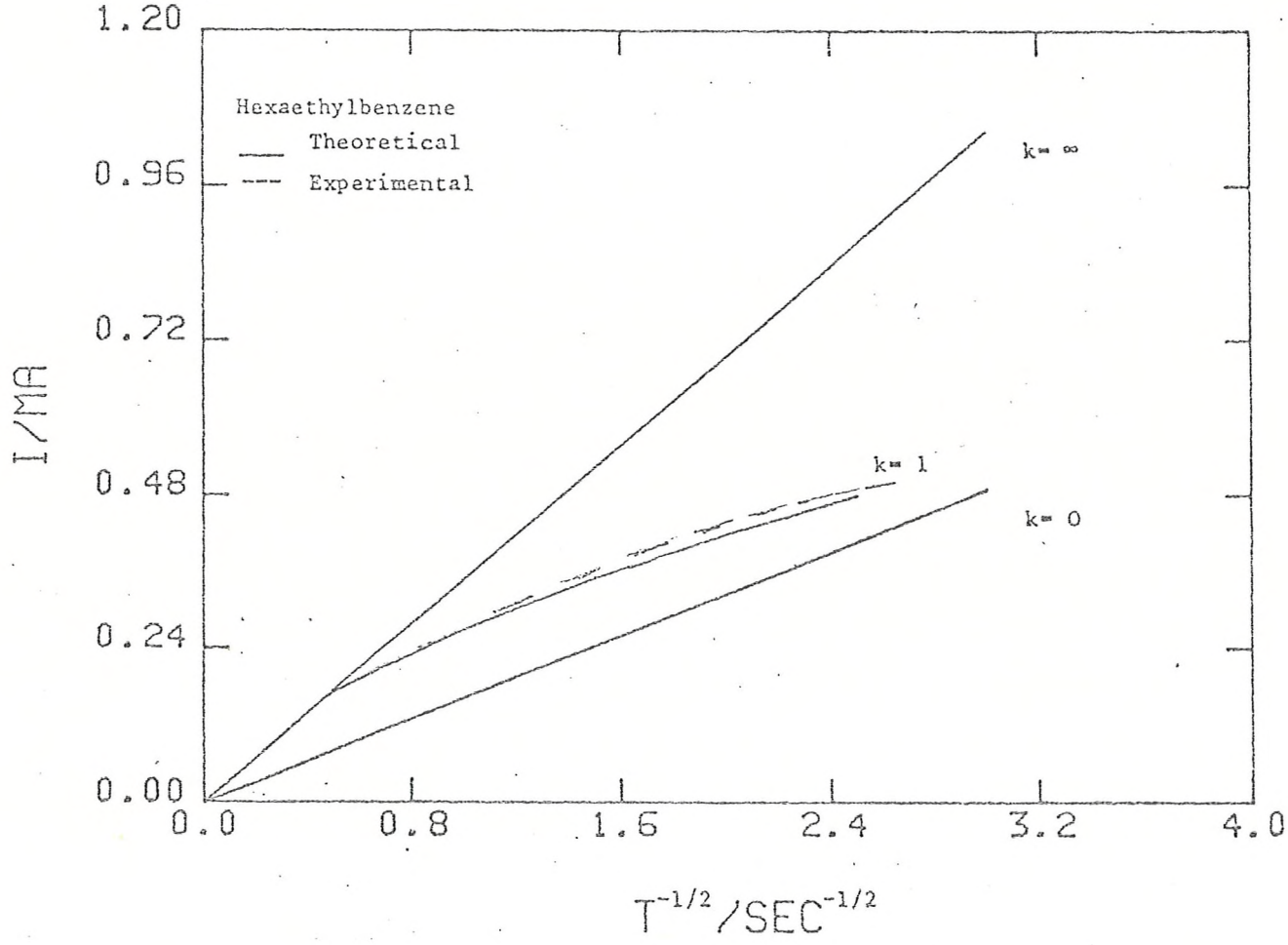

Fig. 4.5 Chronoamperometric working curves for the determination of the rate constant k_f.

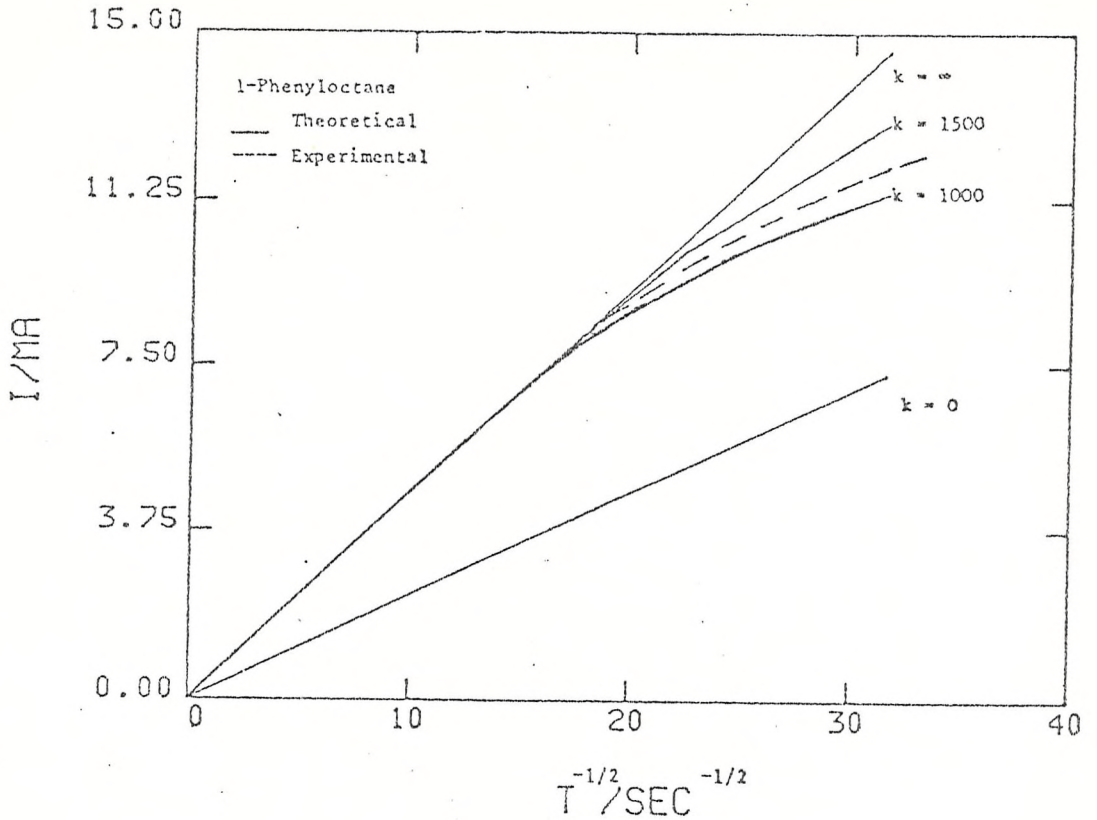

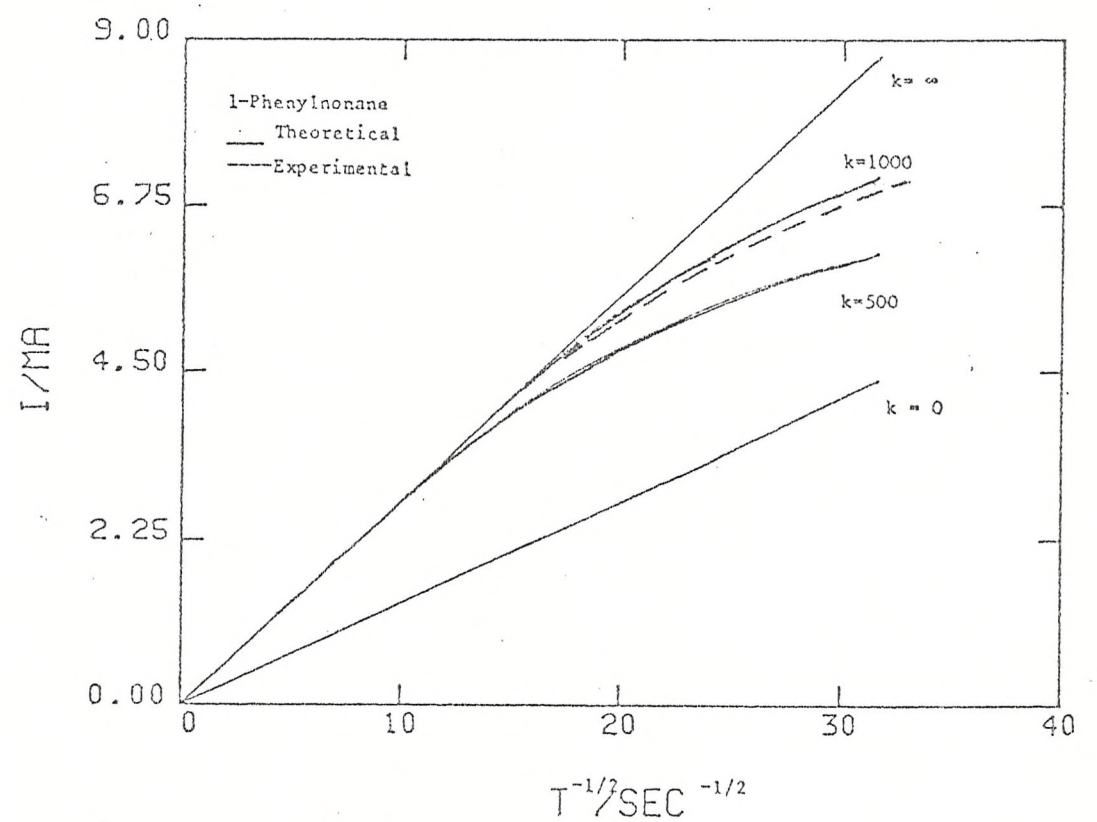

Fig. 4.6 Chronoamperometric working curves for the determination of the rate constant k_f.

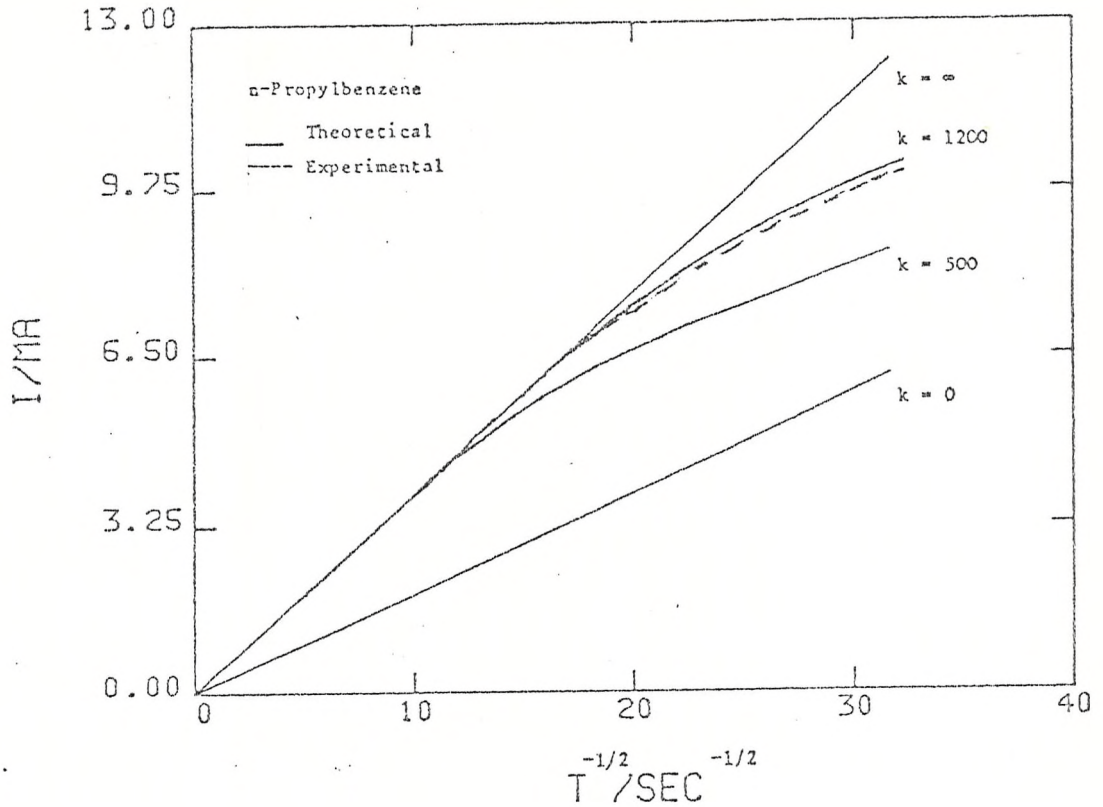

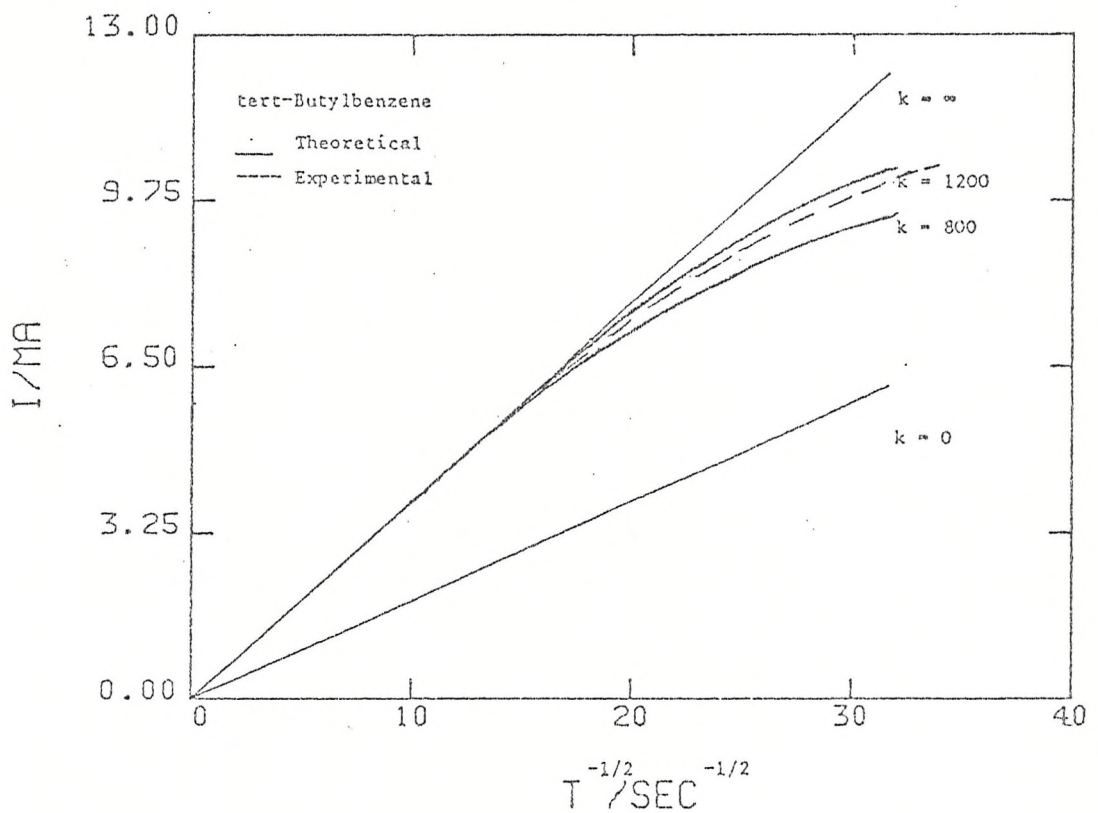

Fig. 4.7 Chronoamperometric working curves for the determination of the rate constant k_f.

according to the method described in section 2.2.3. The limiting curves corresponding to the rate constants $k_f = 0$ and $k_f = \infty$ are also shown on the plots. Semi-infinite linear diffusion and over all 2 electron process were assumed. Therefore, the boundary conditions correspond to a one electron ($k_f = 0$) and two electron process ($k_f = \infty$) respectively.

The experimental points were put into the theoretical working curves and the best fit method was used to estimate rate constant values. The value of the experimental rate constant for Hexaethylbenzene was found to be 1.5 $s.^{-1}$ and, for the other hydrocarbons it varied from 900 to 1200 s^{-1}. Table 4.2 shows the experimental conditions for the chronoamperometry.

SUBSTRATE	BASE POTENTIAL (Volts)	PULSE HEIGHT (Volts)
Hexaethylbenzene	1.200	0.300
1- Phenyloctane	1.500	0.520
1- Phenylnonane	1.700	0.320
n- Propylbenzene	1.600	0.500
tert-Butylbenzene	1.600	0.540

TABLE 4.2.- Experimental conditions for the chronoamperometric experiments.

4.3 MODULATED REFLECTANCE SPECTROSCOPY EXPERIMENTS.

All the optical experiments were performed in a cell giving an angle of incidence at the electrode of 45° (fig. 3.6). A description of the optical cell, the electrodes and the setting up procedures for the experiments, has been given in sections 3.7.1 and 3.7.2. Figures 4.8 through 4.12 show the spectra obtained during oxidation of the five alkylbenzenes discussed here.

All the data were obtained at room temperature in dry Acetonitrile and $Bu_4^n NBF_4$. Table 4.3 summarizes the characteristics for the spectra.

For all of the compounds, normalized reflectance changes, $\Delta R/R$ at wavelength believed to correspond to monitoring of the cation radical produced in the first electron transfer:

$$RH \rightleftharpoons RH^{\cdot +} + e^{-} \qquad \{4.1\}$$

were recorded as a function of time in response to a potential step as described in section 3.7.2. The theoretical transient assuming that the cation radical is stable is given[3] by:

$$\Delta R/R = \frac{4 \epsilon C A (Dt)^{1/2}}{\pi^{1/2} \cos \theta} \qquad \{4.2\}$$

Where all the parameters have been identified previously. For the plots where $\Delta R/R$ vs. $t^{1/2}$ behaved linearly, values of ϵ could be calculated from the slope. Table 4.3 shows the results for those experiments.

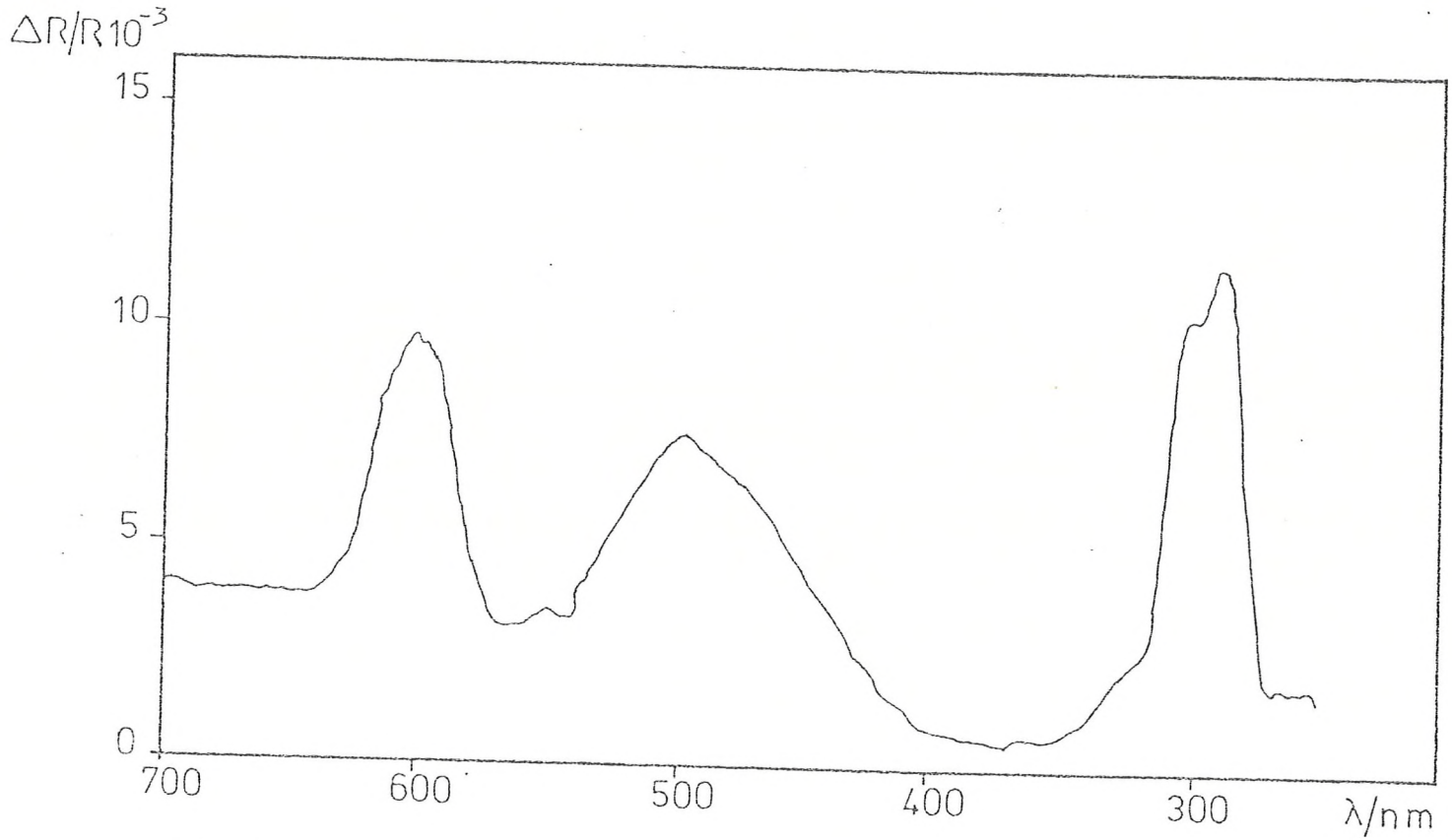

Hexaethylbenzene.Modulated Specular Reflectance Spectra

Fig. 4.8

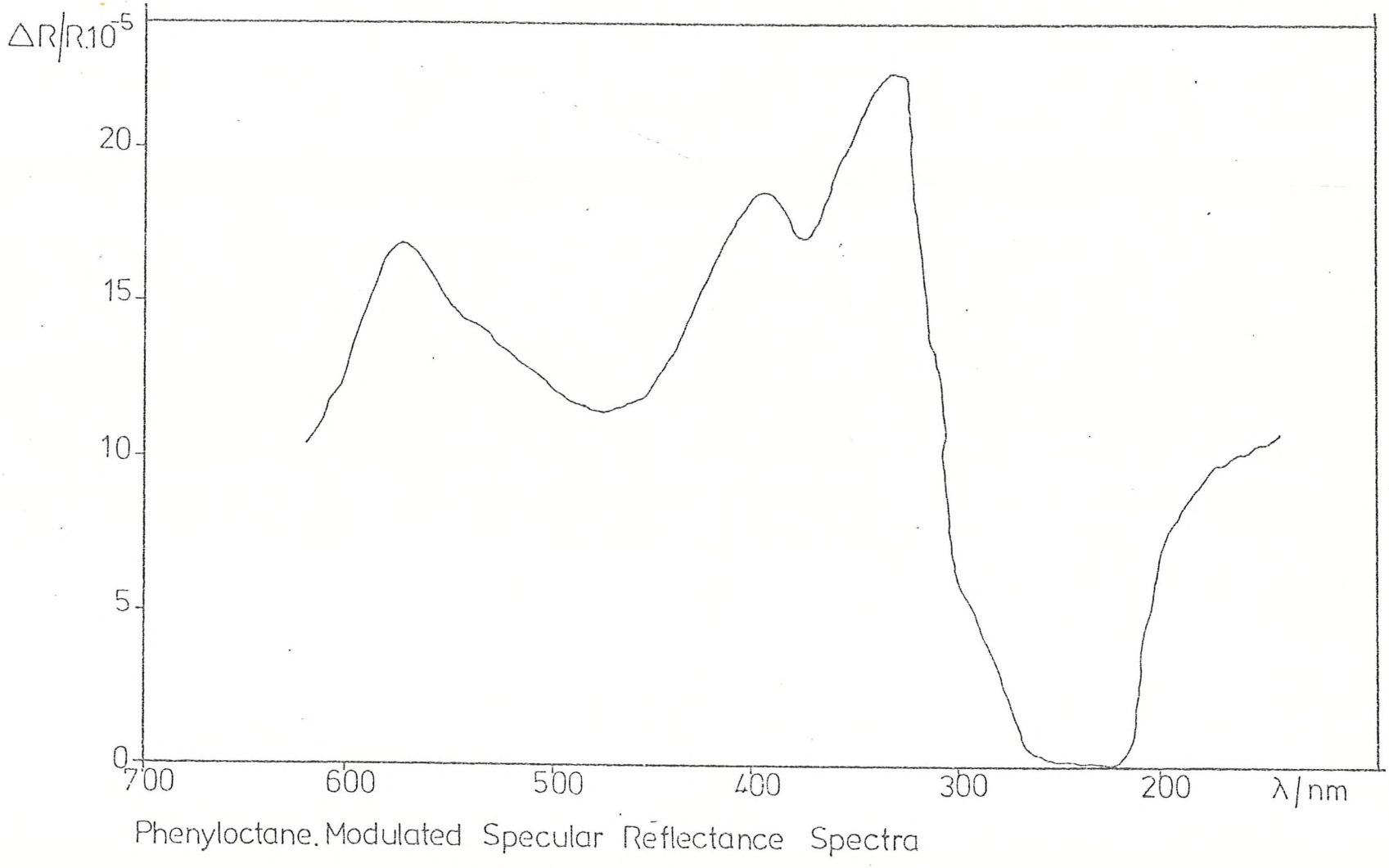
ΔR/R.10^-5
20
15
10
5
0
700
600
500
400
300
200
λ/nm
Phenyloctane. Modulated Specular Reflectance Spectra

Fig. 4.9

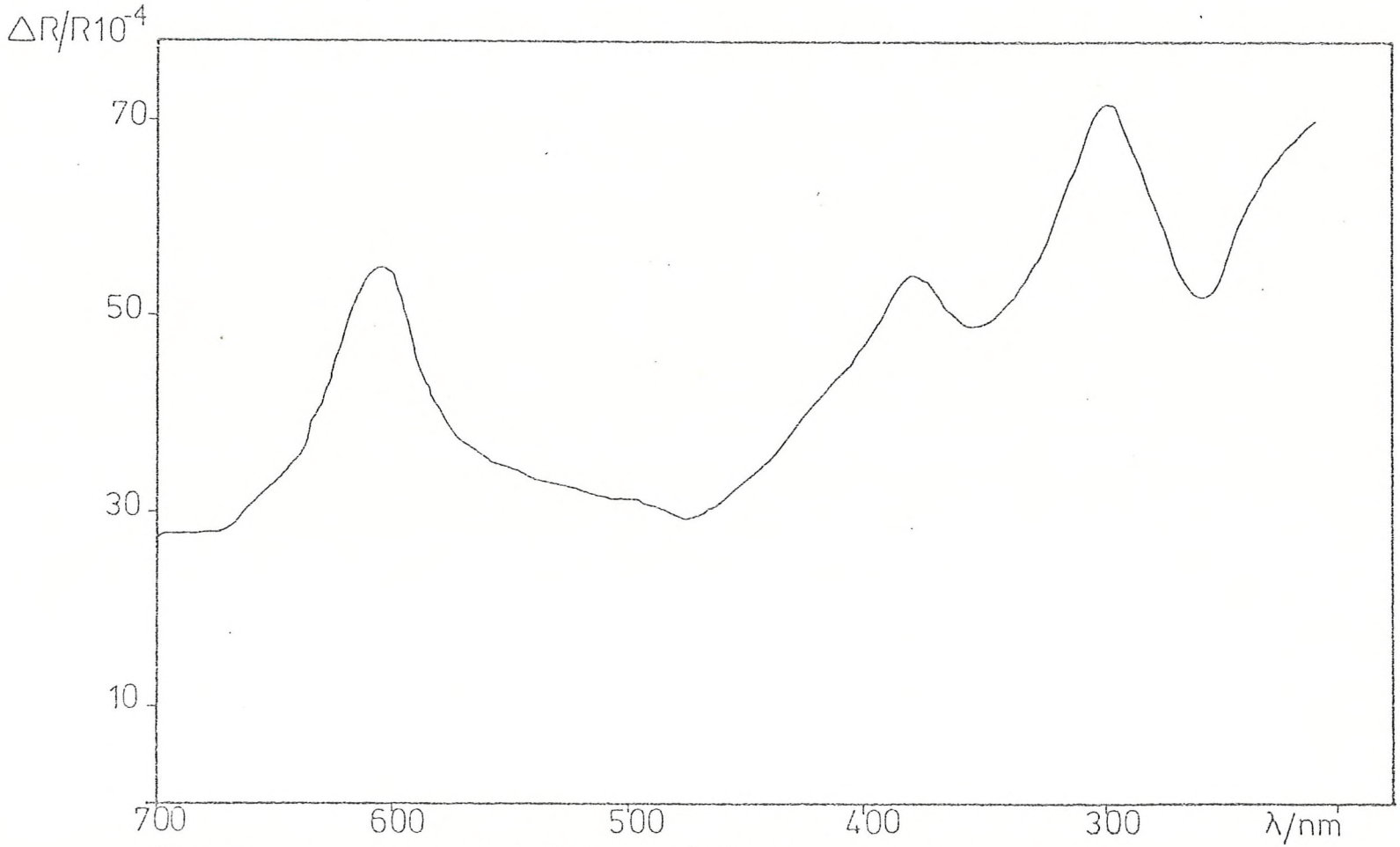

Phenylnonane. Modulated Specular Reflectance Spectra

Fig. 4.10

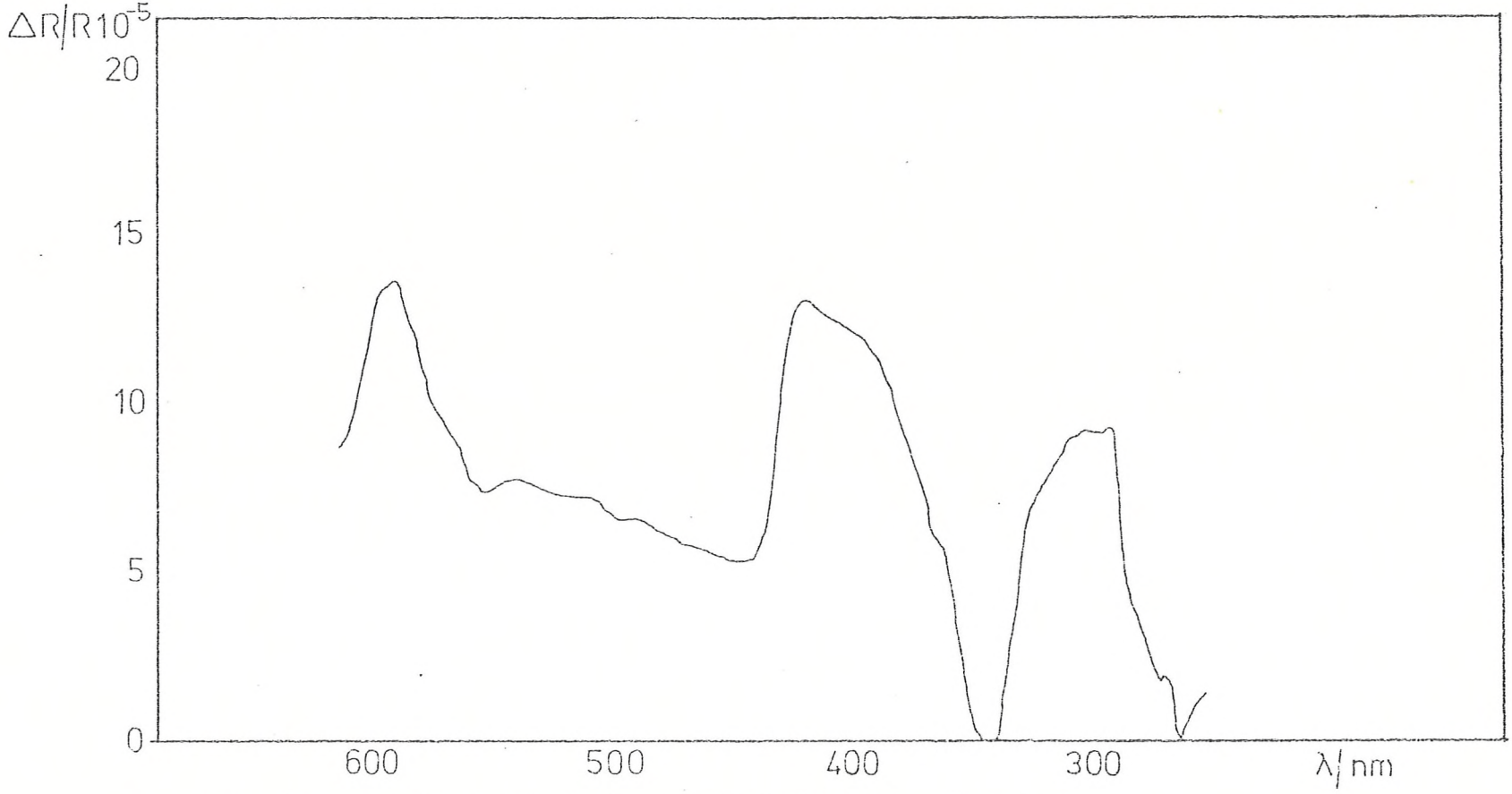

n-Propylbenzene.Modulated Specular Reflectance Spectra

Fig. 4.11

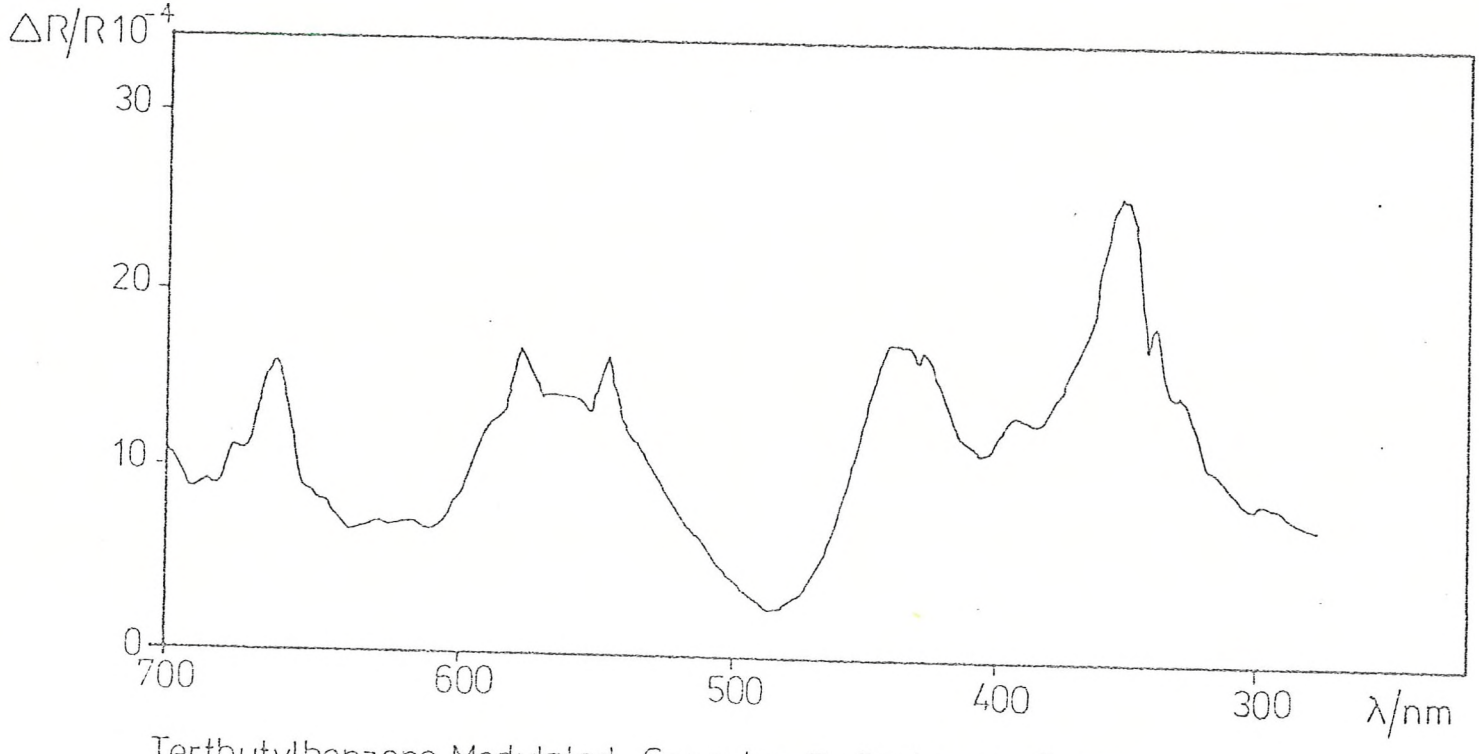

Tertbutylbenzene. Modulated Specular Reflectance Spectra

Fig. 4.12

SUBSTRATE	MODULATION RANGE (Volts)	FREQUENCY (Hz)	SPECTRAL LINES WAVELENGHTS (nm)			λ { $\varepsilon(M^{-1} cm^{-1})$ }
			λ_1	λ_2	λ_3	
Hexaethylbenzene	1.200 - 1.550	80	600	500	300	600 {3396}
1- Phenyloctane	1.500 - 2.300	80	575	400	340	575 {1800 }
1- Phenylnonane	1.700 - 2.300	80	600	400	300	600 {3650 }
n- Propylbenzene	1.600 - 2.400	80	590	400	300	590 {2240 }
tert- Butylbenzene	1.600 - 2.200	80	660	438	354	660 {1210 }
			578			578 {4823 }
			546			546 {1632 }

TABLE 4.3.- Spectral characteristics in U.V., visible region from modulated Specular Reflectance Spectroscopy.

All the optical transients are shown in figures 4.13 through 4.22.

4.4. PREPARATIVE COULOMETRY.

Preparative electrolyses on Hexaethylbenzene, 1- Phenyloctane, 1- Phenylnonane, n- Propylbenzene and tert-Butylbenzene were carried out by steady state coulometry and also using a pulse activation procedure. It was found, in all the cases, that the latter method was greatly superior. The general procedure will be described using Hexaethylbenzene as an example. Paragaph 2.6 describes all the experimental features.

4.4.1. STEADY STATE PREPARATIVE ELECTROLYSIS OF HEXAETHYLBENZENE.

Hexaethylbenzene in acetonitrile was oxidized at 1.360 V. the background current being 0.05 mA. Table 4.4 gives the initial current and the current reached after several hours of electrolysis for different amounts of Hexaethylbenzene, in 25 ml of solution, when using a 2 cm^2 working electrode.

AMOUNT OF SUBSTRATE IN 25 ml. OF SOLUTION (mol)	INITIAL CURRENT (mA)	CURRENT AFTER 10 hr. OF ELECTROLYSIS
1.25×10^{-4}	8.2	7.5
2.50×10^{-4}	13.0	10.6
1.25×10^{-3}	18.8	16.9
2.50×10^{-3}	30.0	27.1

TABLE 4.4.- Results for the steady state preparative Coulometry of Hexaethylbenzene.

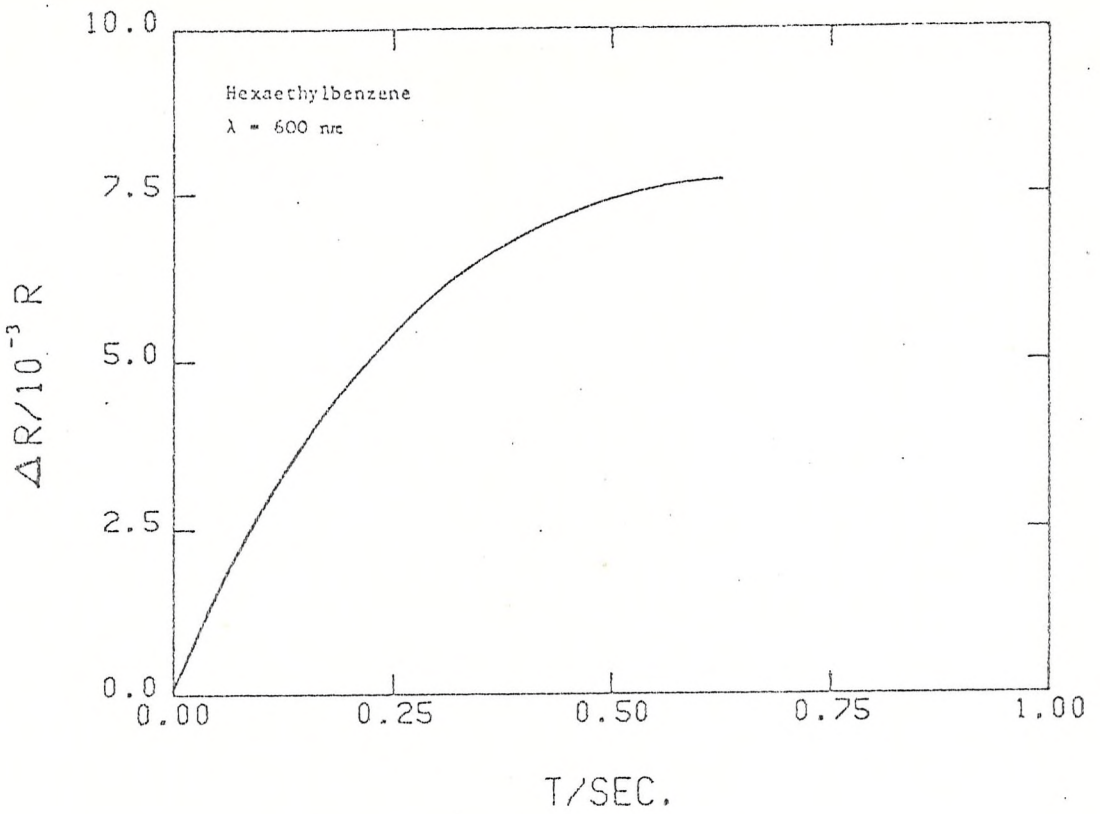

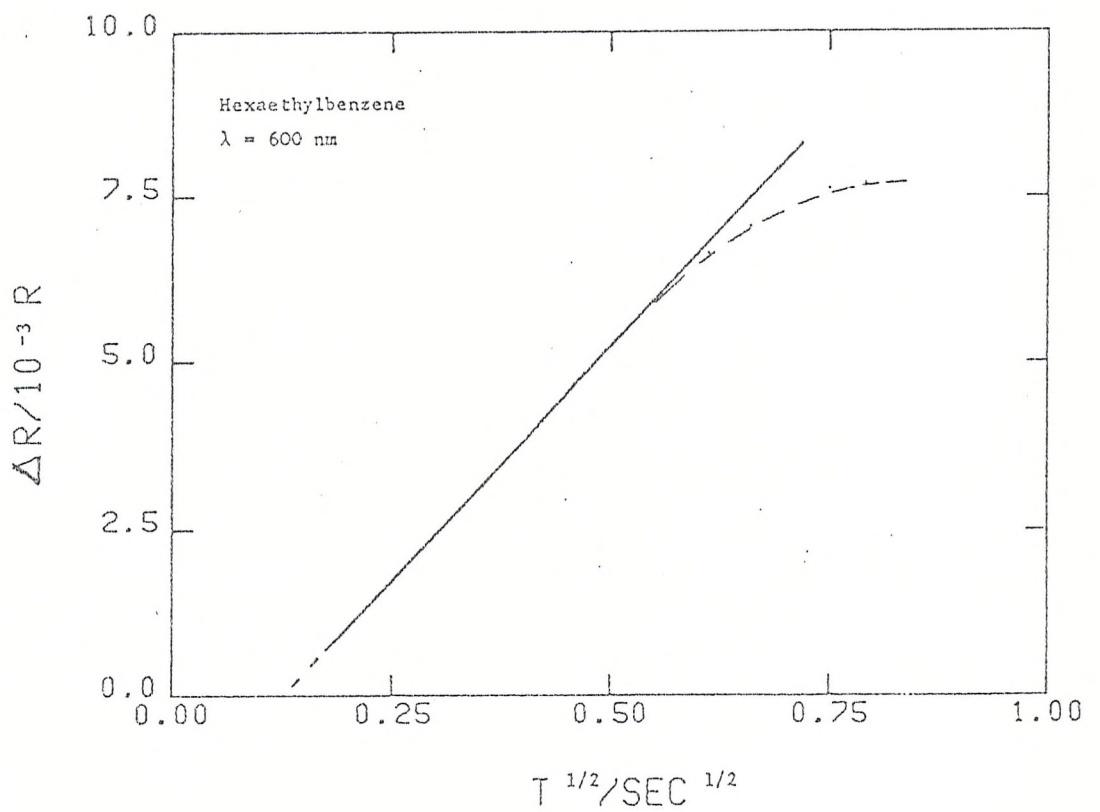

Fig. 4.13 Optical transient and absorbance vs. $t^{\frac{1}{2}}$ plot for the anodic oxidation of Hexaethylbenzene.

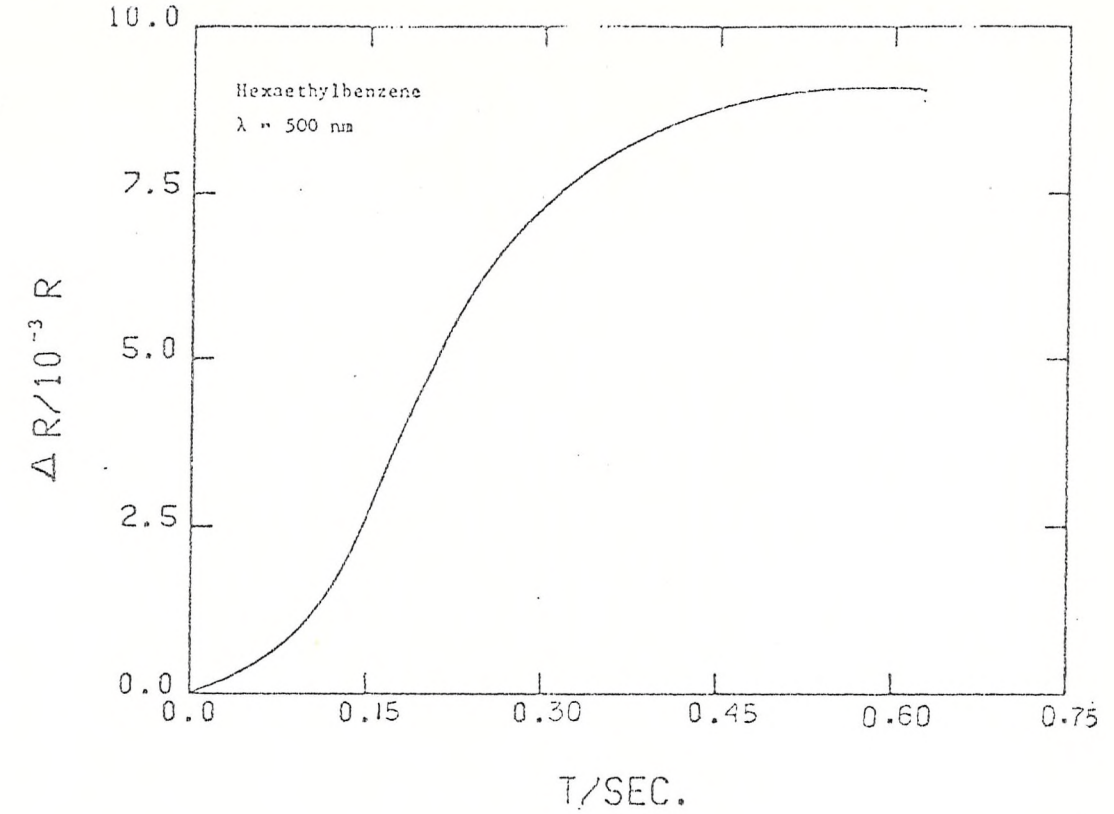

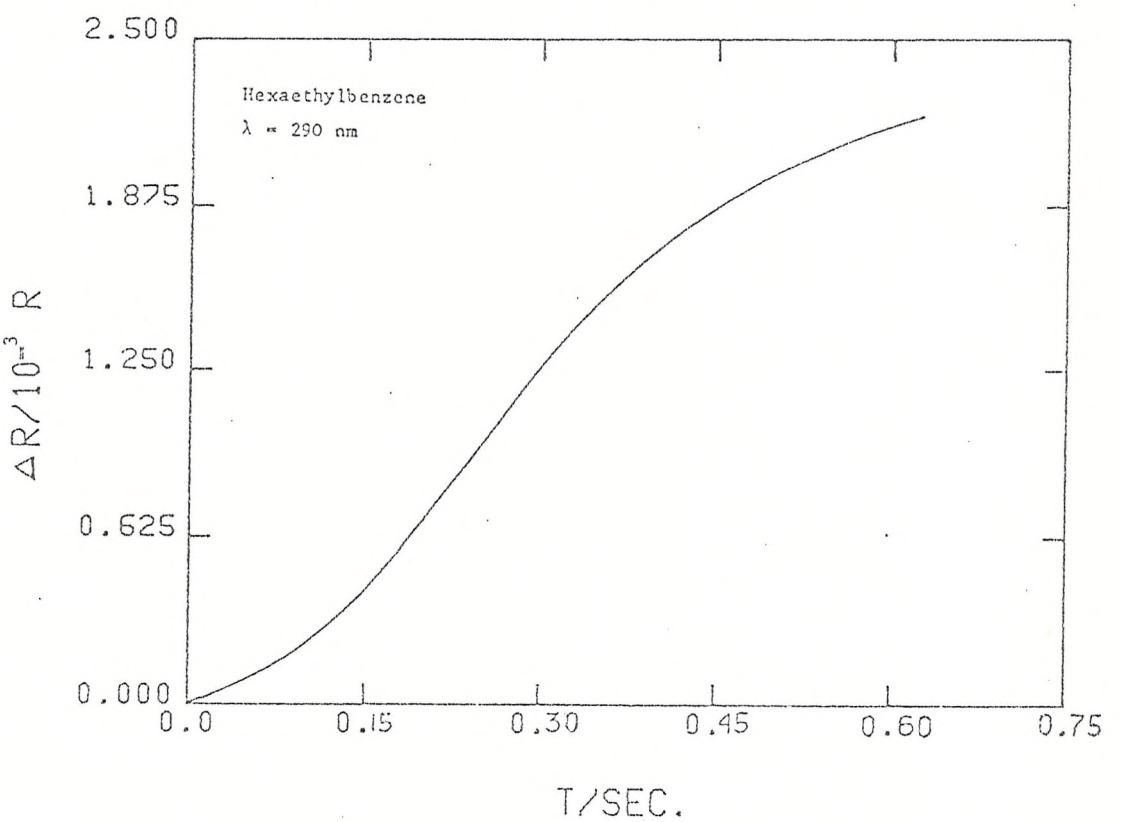

Fig. 4.14 Optical transients for the anodic oxidation of Hexaethylbenzene.

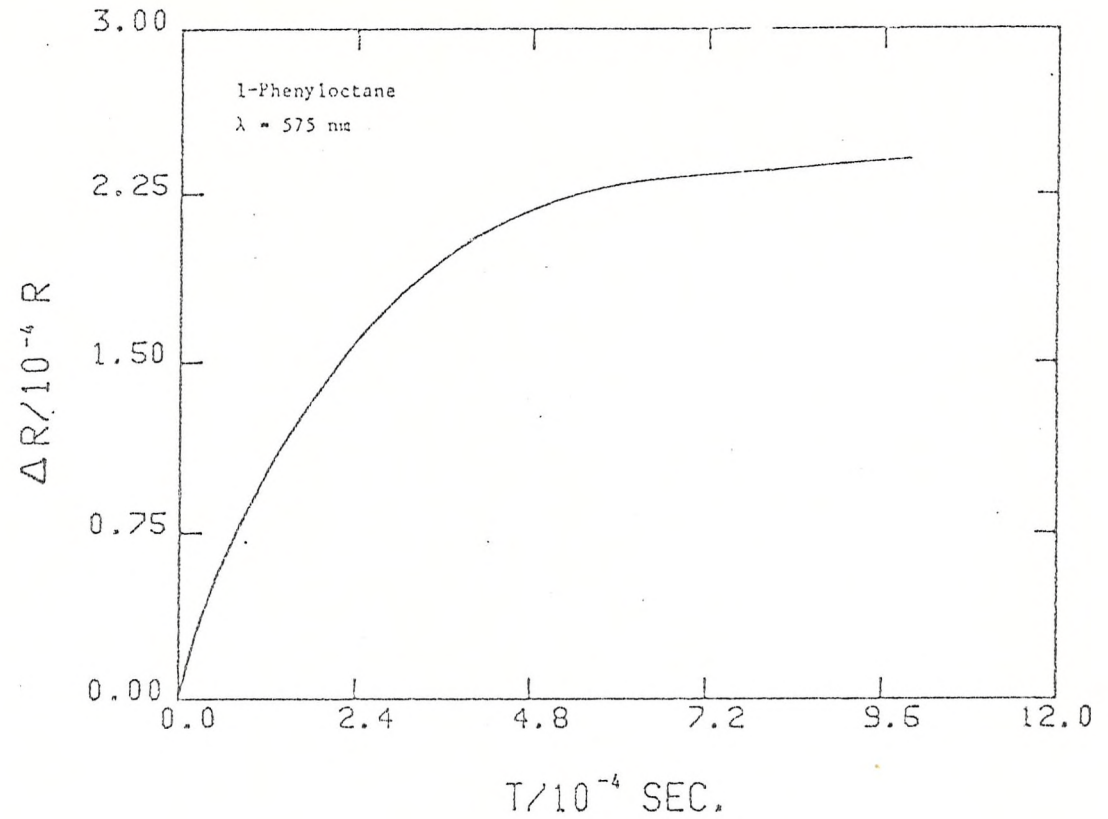

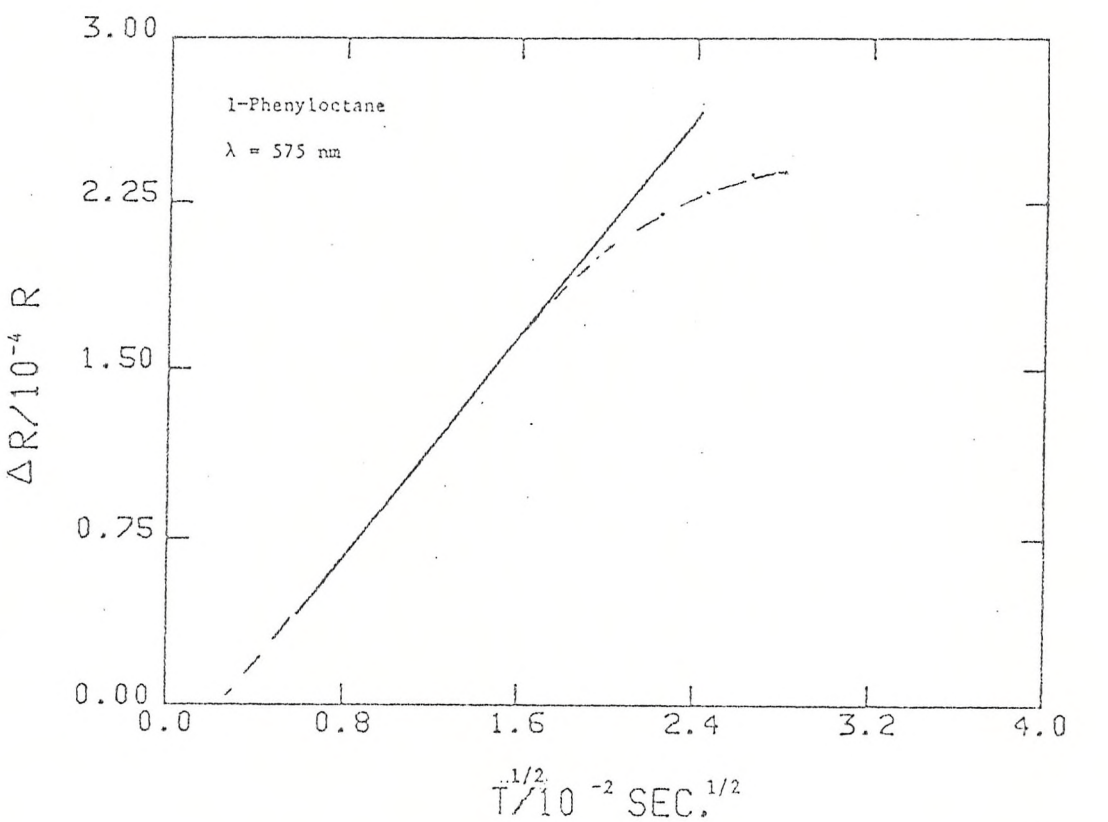

Fig. 4.15 Optical transient and absorbance vs. $t^{\frac{1}{2}}$ plot for the anodic oxidation of 1-Phenyloctane.

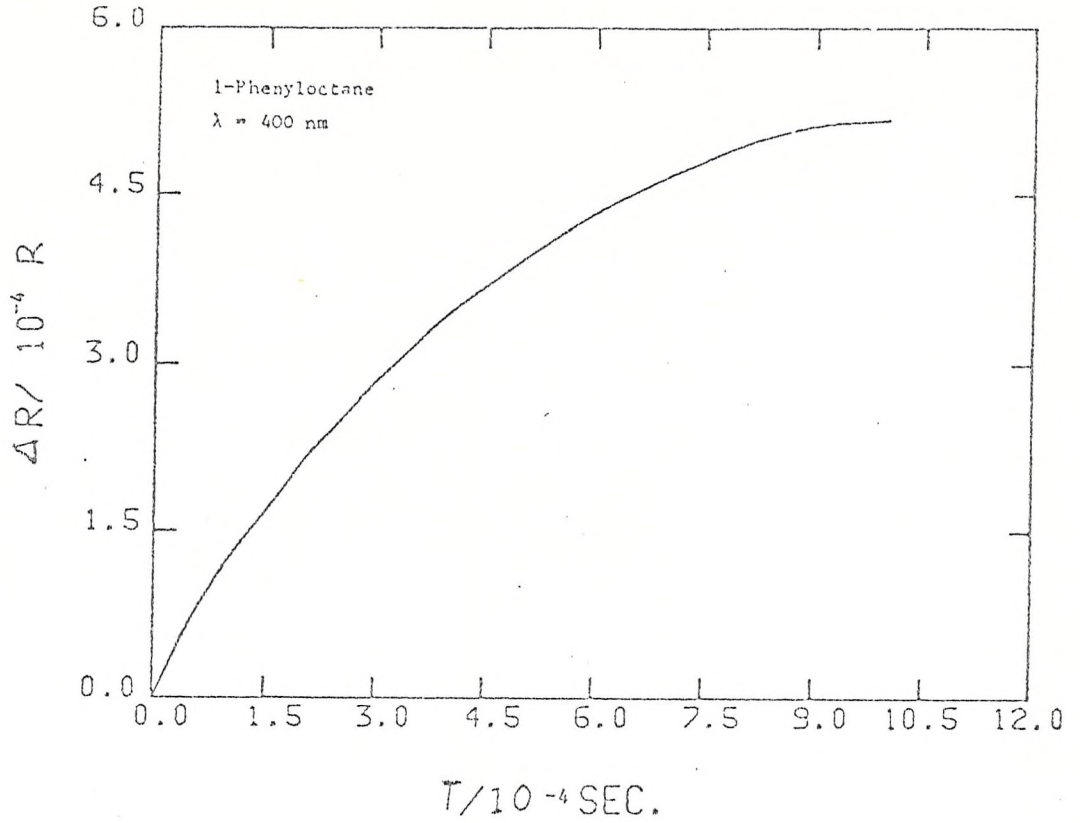

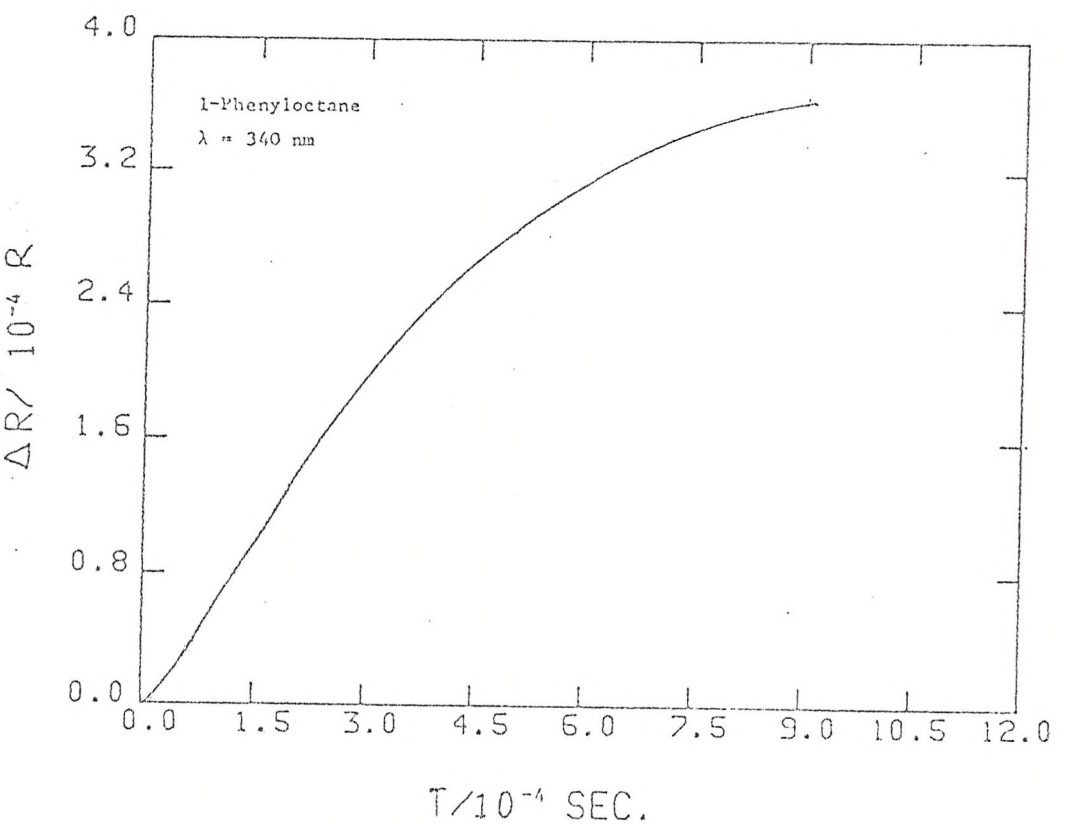

Fig. 4.16 Optical transients for the anodic oxidation of 1-Phenyloctane.

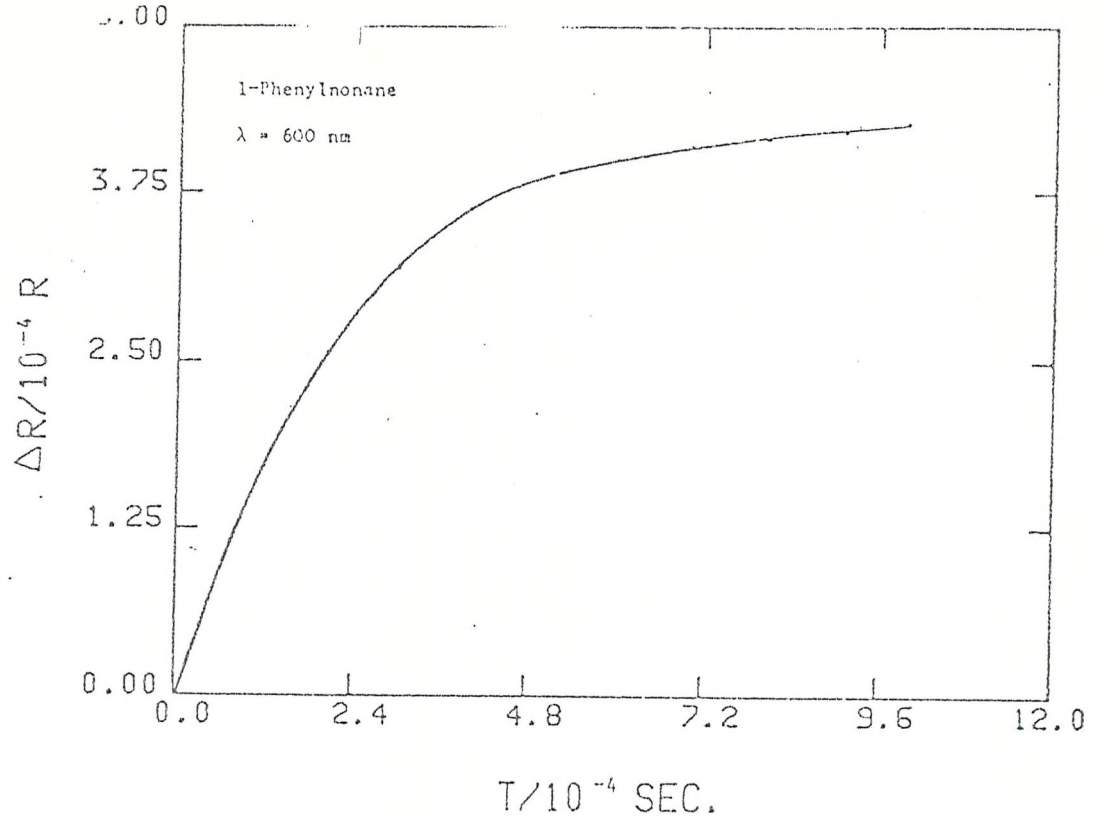

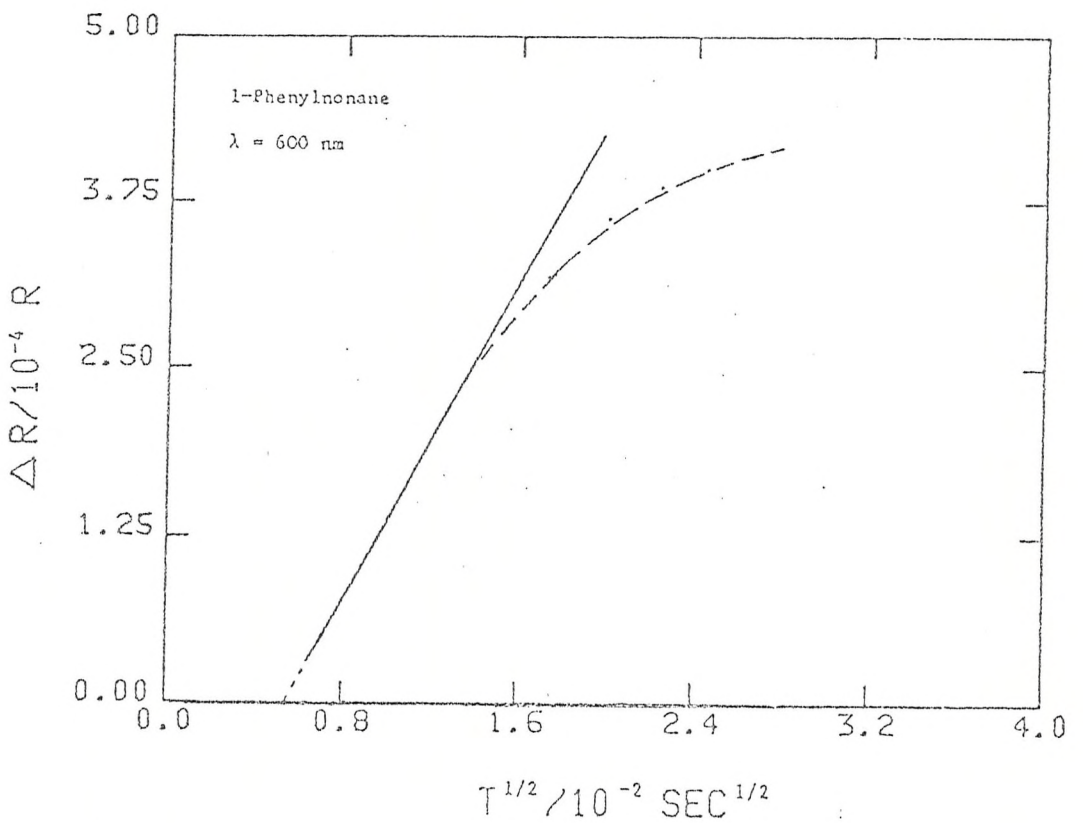

Fig. 4.17 Optical transient and absorbance vs. $t^{\frac{1}{2}}$ plot for the anodic oxidation of 1-Phenylnonane.

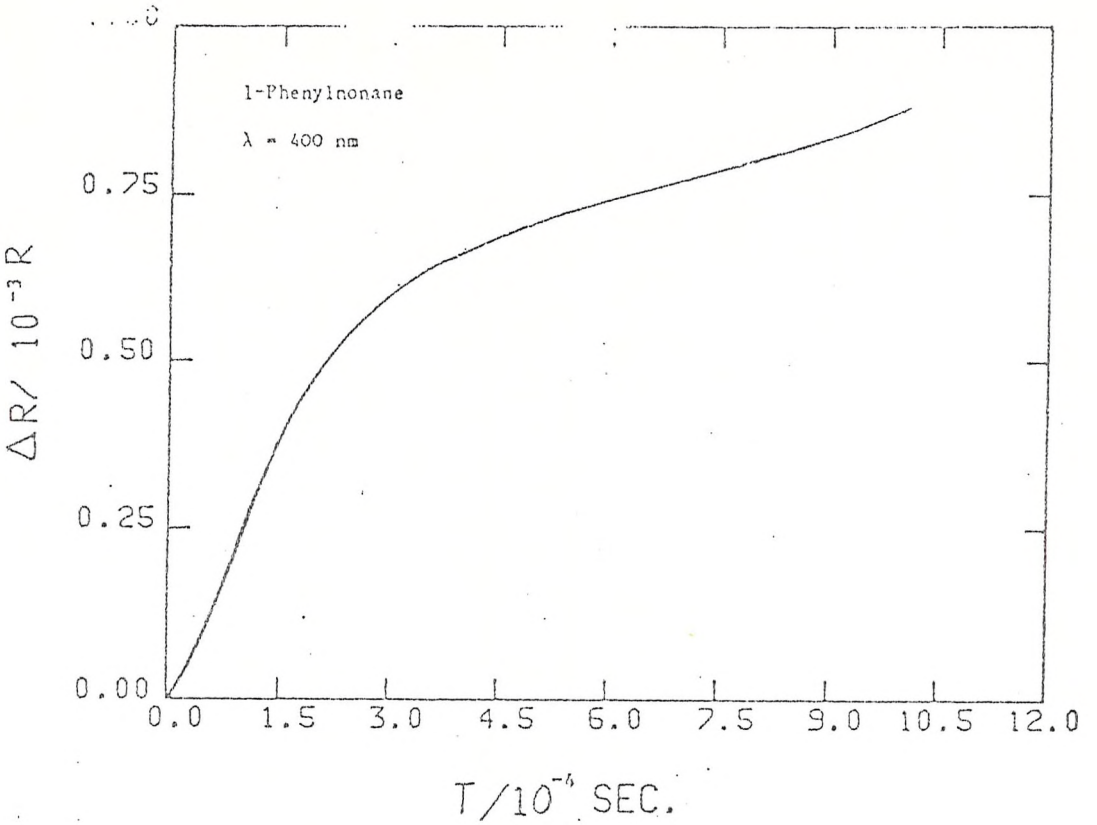

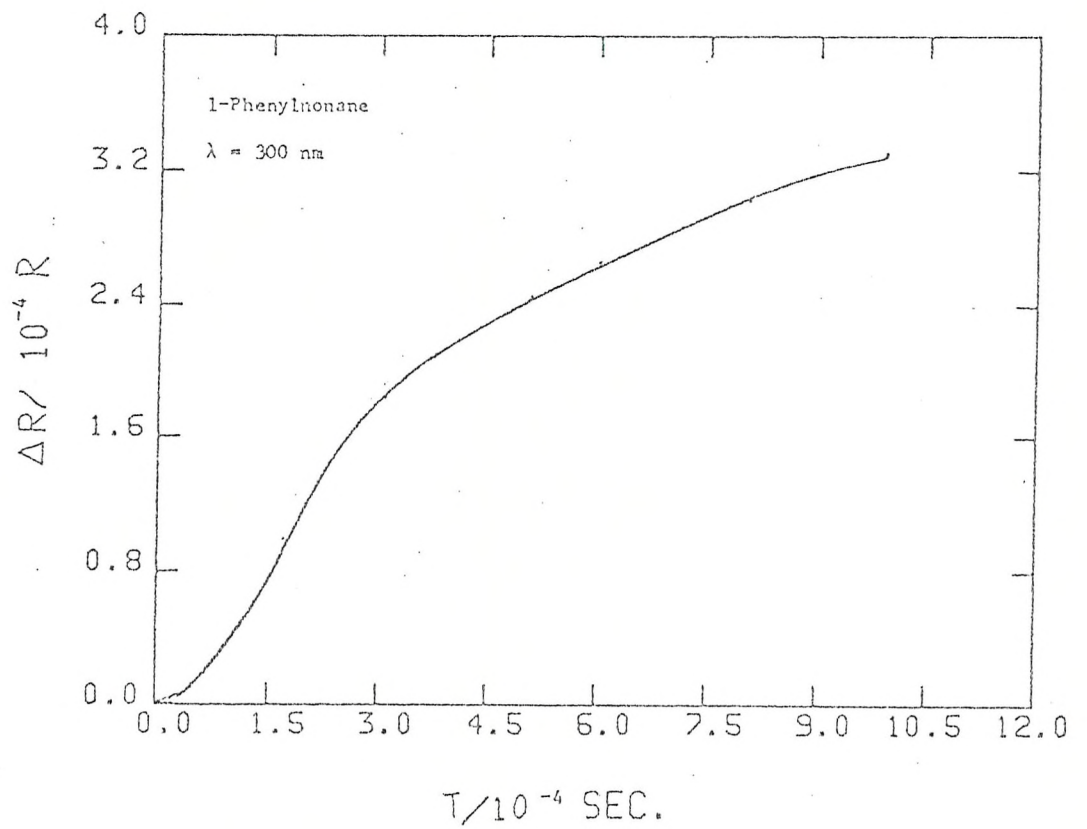

Fig. 4.18 Optical transients for the anodic oxidation of 1-Phenylnonane.

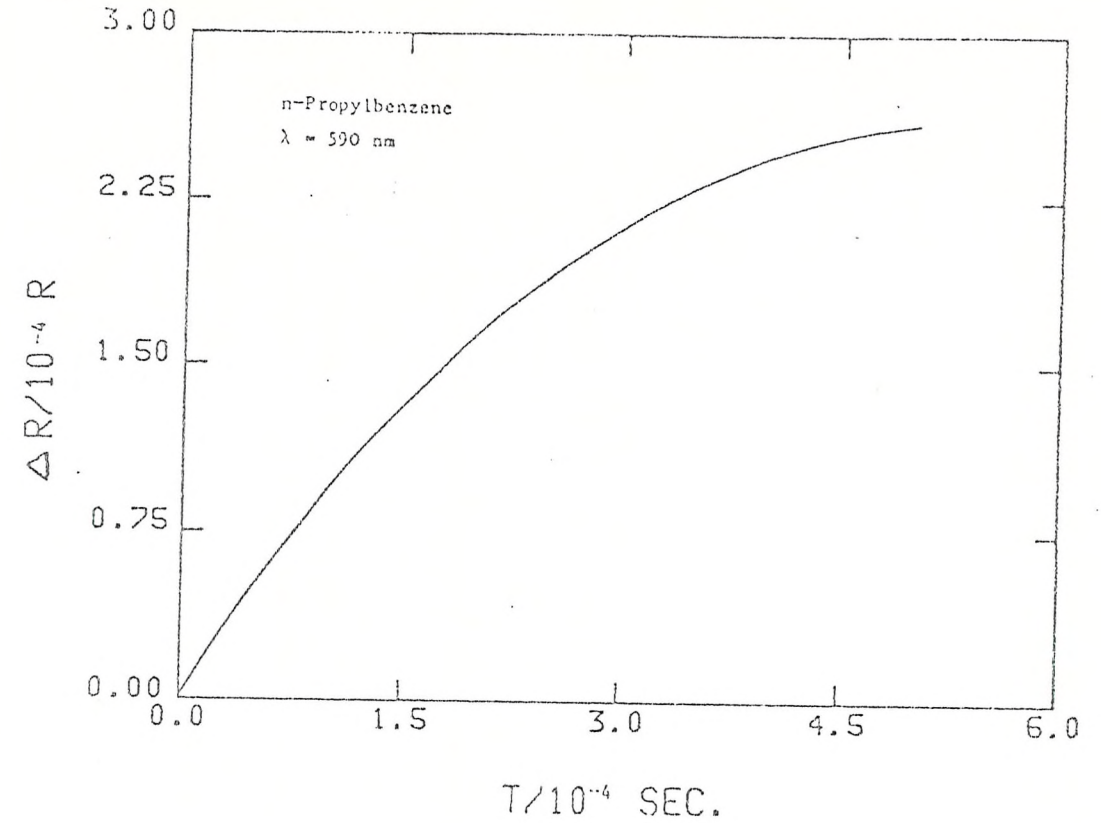

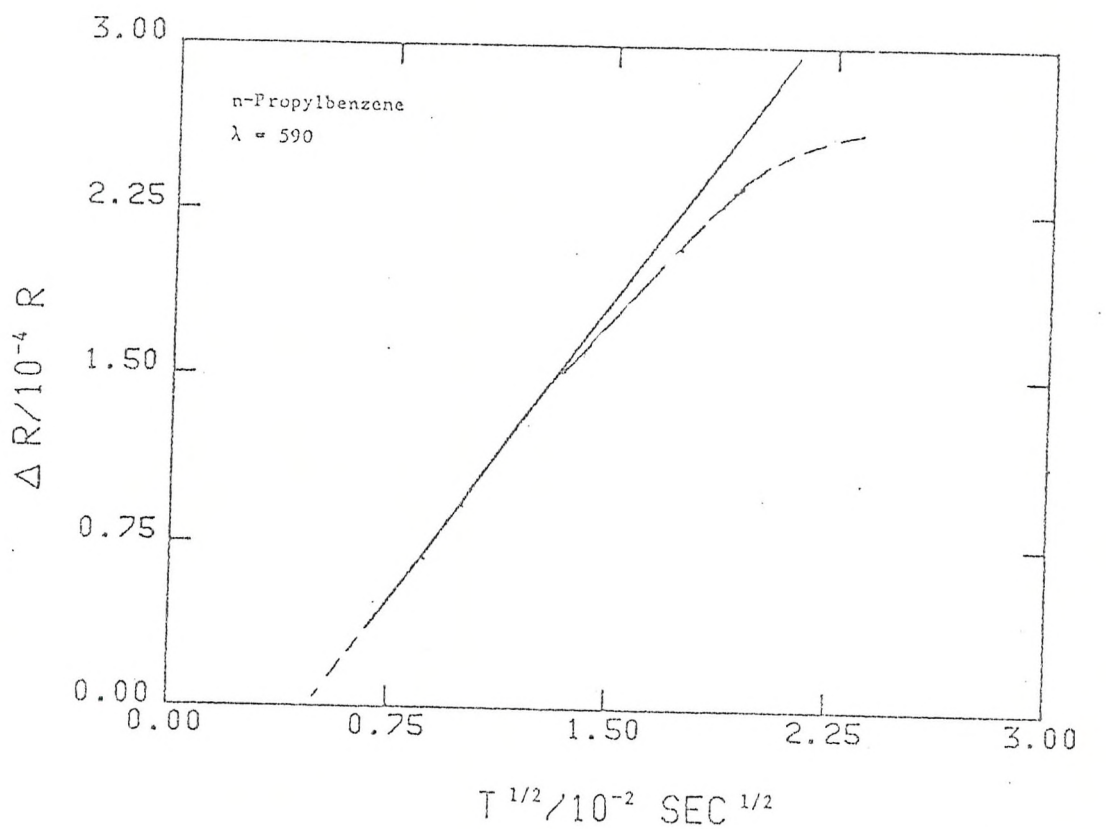

Fig. 4.19 Optical transients and absorbance vs. $t^{\frac{1}{2}}$ plot for the anodic oxidation of n-Propylbenzene.

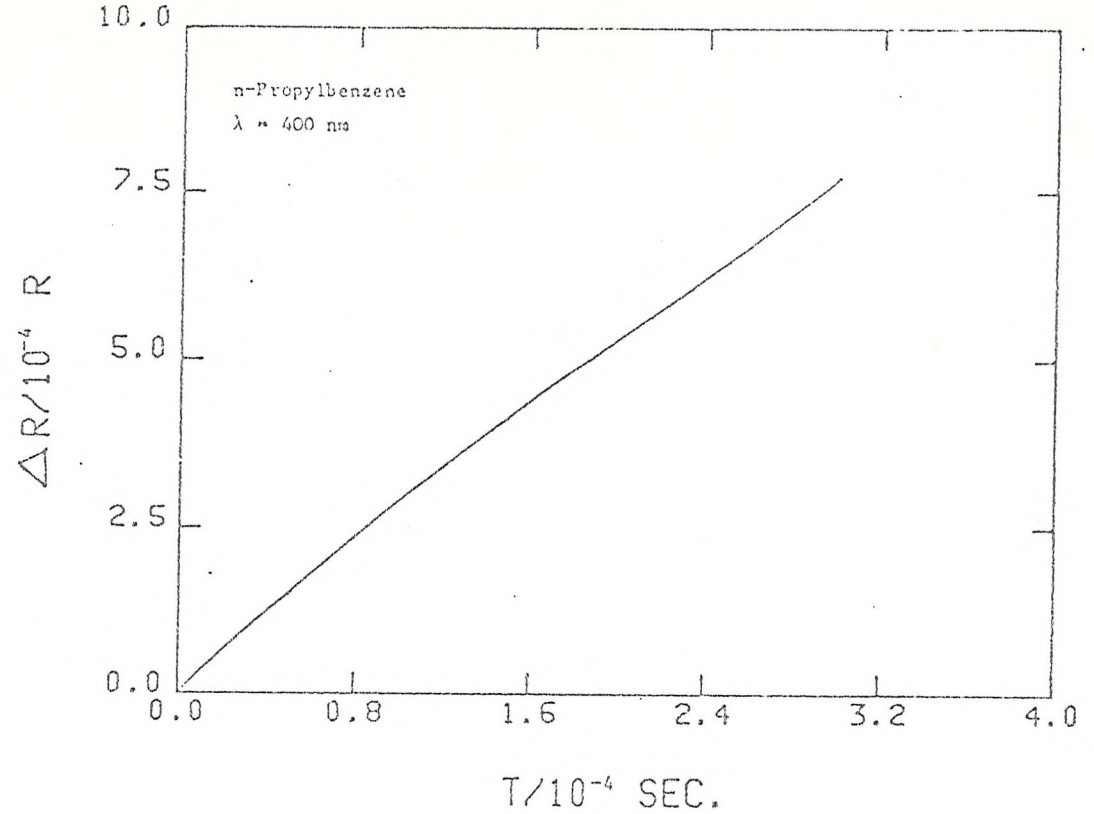

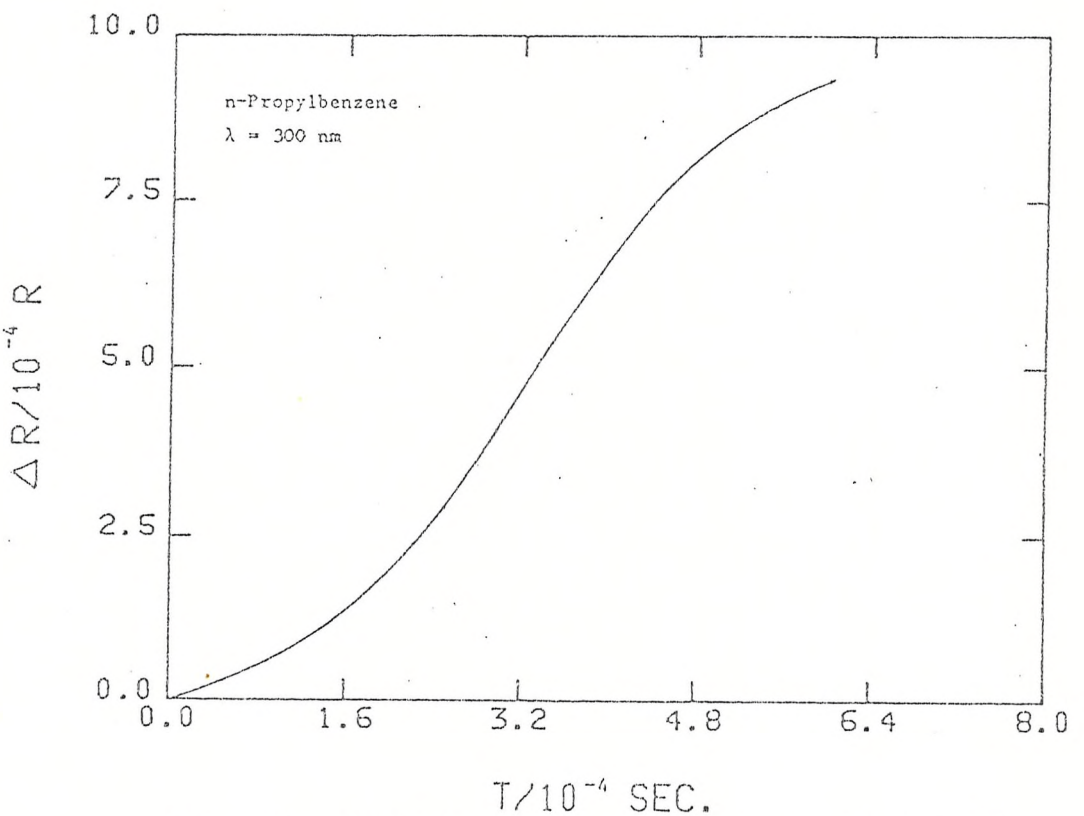

Fig. 4.20 Optical transients for the anodic oxidation of n-Propylbenzene.

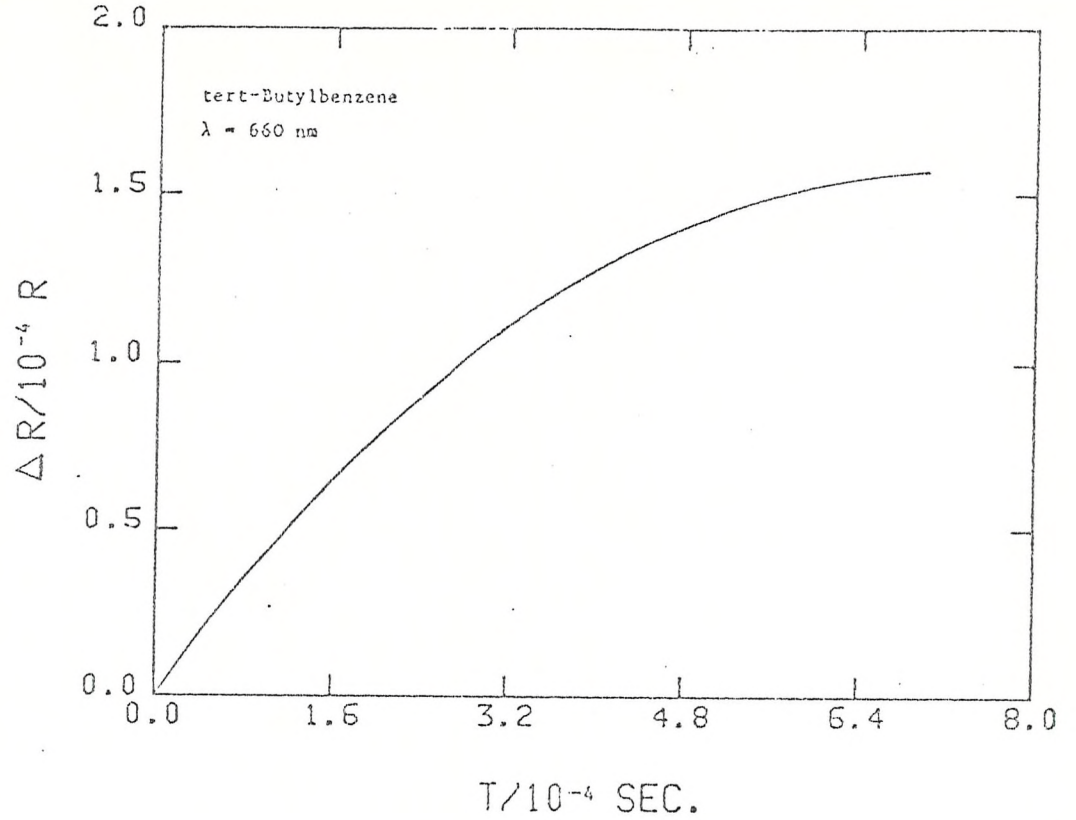

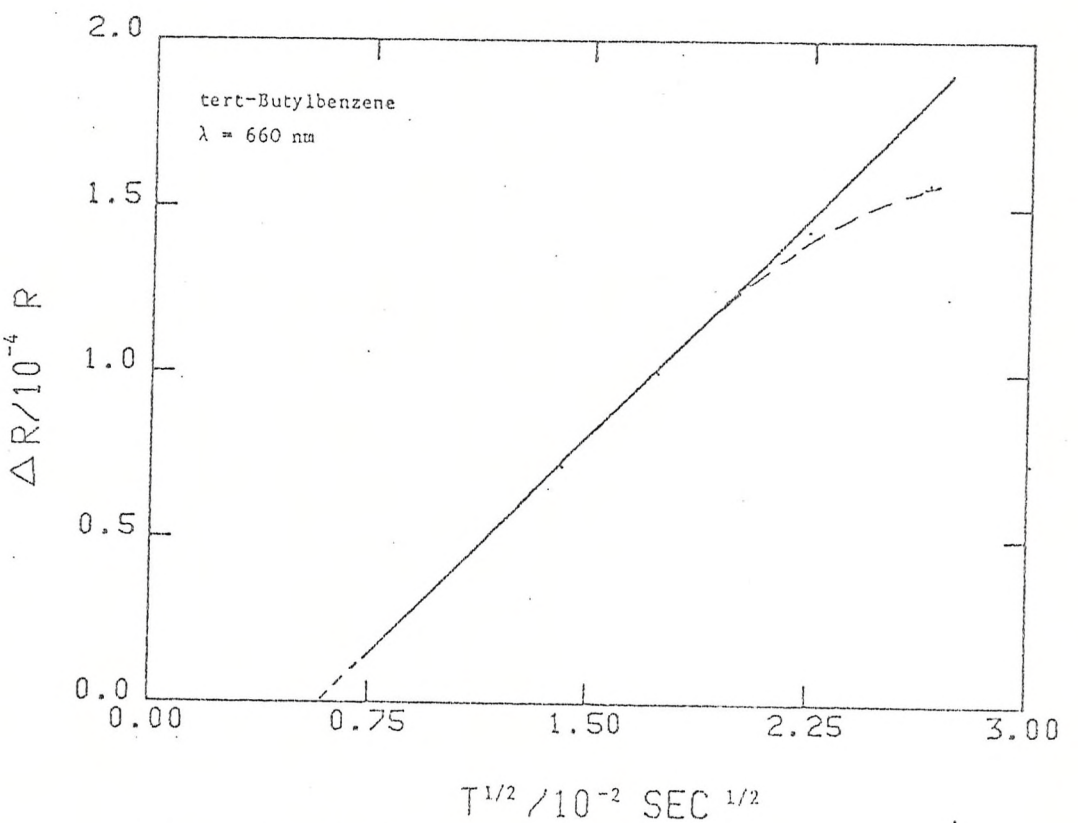

Fig. 4.21 Optical transient and absorbance vs. $t^{\frac{1}{2}}$ plot for the anodic oxidation of tert-Butylbenzene.

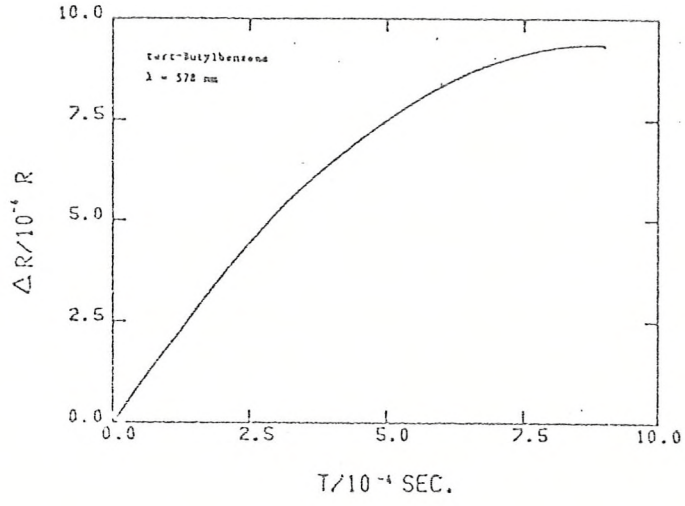

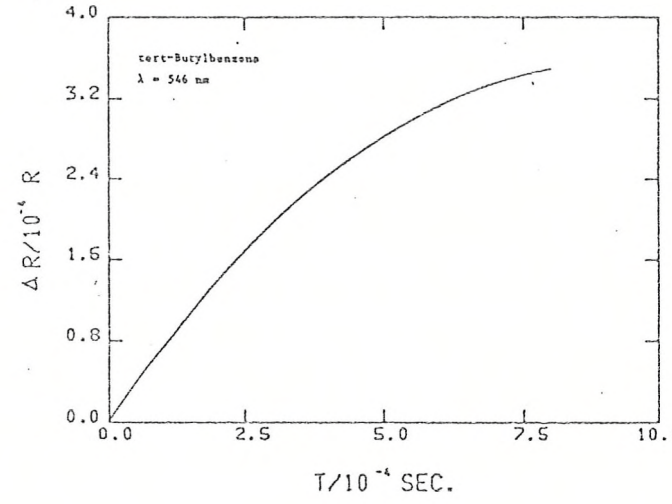

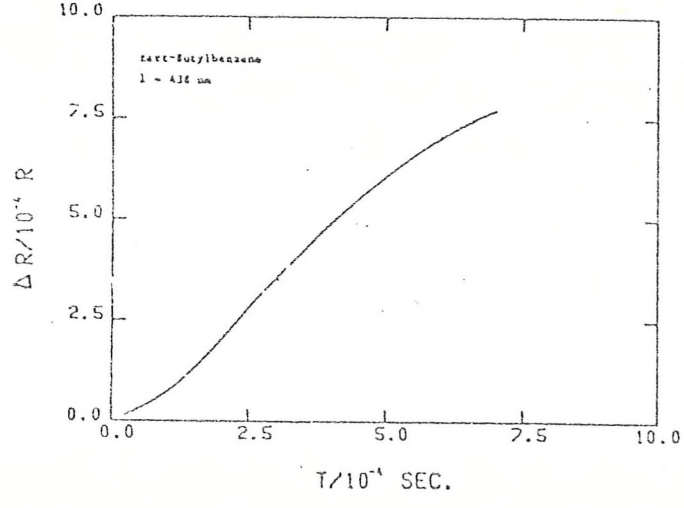

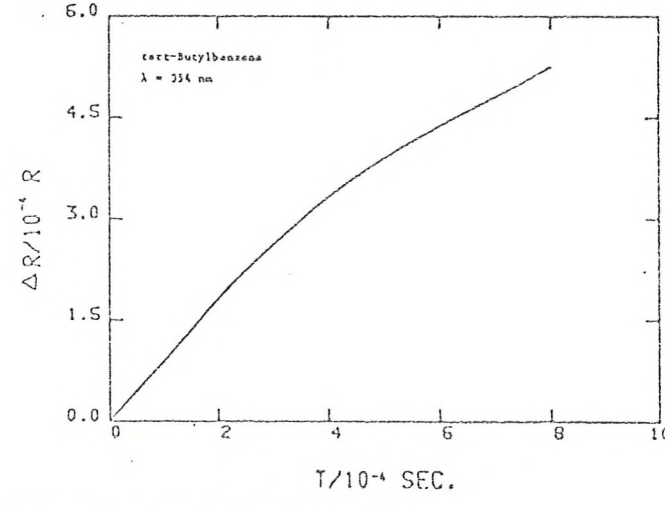

Fig. 4.22 Optical transients for the anodic oxidation of tert-Butylbenzene.

After a few minutes of electrolysis, the anolyte solution became red-brown and the catholyte was yellow. From table 4.4, it can be seen that after 10 hours of electrolysis, the current had declined only slightly from the initial value even though more charge had been passed than that required to consume all of the substrate at 2 F per mole. This may be due to catalyzed oxidation taking place.

The anolyte was quenched with water (0.2 ml.) and the solvent evaporated. The remaining solid was washed three times with distilled water and the main product was extracted from the residue overnight with diethylether, drying the extract with sodium sulphate. The filtered solution was evaporated, the residue was extracted using ethylacetate (10 ml.) and recrystallized from ethanol. The product was the starting material, Hexaethylbenzene, in high yield. This was confirmed by IR and mass spectra. In view of those results, an attempt was made to use a cation exchange resin to trap possible intermediate cation, e.g., the nitrilium ion, and thus, simplify the reaction. All the other conditions were mantained the same. After a few minutes of the electrolysis, the anolyte was brown and the catholyte yellow. Table 4.5 shows similar data to those shown in table 4.4 for this new set of electrolyses conditions. The behaviour now offers to be much simpler with a substantial fall in the current indicating consumption of substrate.

The anolyte was filtered and the resin separated, washed with CH_3CN and poured into 1M NaOH solution, leaving it to stand for 1 hour, stirring magnetically. It was then filtered. The resin was poured into CH_2Cl_2 and stand for 2 hours. The aqueous was neutralized with HCl and then extracted with the CH_2Cl_2 and dried with sodium sulphate, the solvent was evaporated, the residue taken up in ethyl-

acetate (5 ml.) and recrystallized from ethanol.

AMOUNT OF SUBSTRATE IN 25 ml. OF SOLUTION (mol)	INITIAL CURRENT (mA)	CURRENT AFTER 10 hr. OF ELECTROLYSIS (mA)
1.25×10^{-4}	8.5	0.6
2.50×10^{-4}	13.0	0.8
1.25×10^{-3}	19.0	1.0
2.50×10^{-3}	30.0	1.5

TABLE 4.5.- Effect of the presence of 2.5 g. of cation exchange resin on the electrolysis.

Preparative thin layer chromatography (TLC) was run for 0.016 g. of this recrystallized product in a 80% - 20% petroleum ether-ethylacetate mixture on a (20x20) cm^2 plate. Seven lines were observed, the most important one being scraped off from the plate, the solid poured into ethylacetate and then filtered. The solvent was evaporated and the product (0.008 g.) gathered to be analyzed. Infrared and mass spectra indicated the presence of the monoamide and the diamide with the former predominating. From the TLC results, 50% of material trapped by the resin was the amide. According to the results presented in table 4.6 the highest yield corresponded to the electrolysis carried out with 10 g. of resin and 0.025 g. of Hexaethylbenzene. From 0.025 g. (10^{-4} mol) of starting material, 6.5 mg. of amide was obtained.

For a complete conversion, 0.030 g. of amide should be obtained, therefore, the yield was 21.7% respect to the starting material. It was found that the amount of resin used during the electrolysis, played a very important role in determining the yield. Table 4.6 shows this effect.

The product remaining in solution in the anolyte was also investigated. The solvent was evaporated from the anolyte solution, the residue washed three times with water and the product extracted with diethylether. The product was found to be a dimer.

AMOUNT OF STARTING MATERIAL (g.)	AMOUNT OF RESIN (g.)	AMOUNT OF RESIDUE FROM THE RESIN (g)	AMOUNT OF RESIDUE FROM THE SOLUTION (g.)
0.240	5.00	0.018	0.197
0.120	5.00	0.016	0.098
0.050	10.00	0.020	0.026
0.025	10.00	0.013	0.008

TABLE 4.6.- Effect of the amount of resin on the yield of the amide.

4.4.2. NON-STEADY STATE PREPARATIVE ELECTROLYSIS OF HEXAETHYL BENZENE.

Hexaethylbenzene (0.100 g. , 4 x 10^{-4} mol) was oxidazed in acetonitrile by repetitively switching the potential from 0.00 V. up to the voltammetric peak potential(+1.360 V.), being a 4 s. on period and 4 s. off period. The initial current was 27 mA., and this value was mantained for a long time. After 75 coulombs were

passed, the current had dropped to 2 mA.; 95.8 mg of Hexaethylbenzene reacted and 4.5 mg remained unreacted; 9.7 g. of resin were used and 0.084 g. of residue were extracted from it. TLC was run together with a standard sample of the monoamide in a 50% - 50% ethanol - petroleum ether mixture. The separation was similar in both cases. NMR and mass spectra showed the monoamide as the main product. Traces of the diamide could be observed from mass spectra. The yield was 71.25% with respect to starting material.

4.4.3. STEADY STATE PREPARATIVE ELECTROLYSES OF THE OTHER MEMBERS OF THIS SERIES OF HYDROCARBONS.

Steady state preparative electrolyses were performed for 1- Phenyloctane, 1- Phenylnonane, n- Propylbenzene and tert-Butylbenzene under the same conditions as for Hexaethylbenzene. In all the cases, the current dropped drastically to the background value, 5 to 10 minutes after the electrolysis started. The anolyte solution was very dark and the electrode was completely poisoned. No information could be obtained from those experiments, even when the resin was used.

4.4.4. NON STEADY STATE PREPARATIVE EELECTROLYSES OF THE OTHER MEMBERS OF THIS SERIES.

As all the members of the series of hydrocarbons under study, except the Hexaethylbenzene, had a similar behaviour, all the conditions and the results for the pulsed electrolyses will be sumarized in tables 4.7 and 4.8.

SUBSTRATE	AMOUNT OF SUBSTRATE (mol)	BASE POTENTIAL[a] (Volt.)	PULSE HEIGHT (Volt.)	INITIAL CURRENT (mA)	FINAL CURRENT (mA)
1- Phenyloctane	2.7×10^{-4}	1.320	0.600	30.0	2.5
1- Phenylnonane	8.3×10^{-4}	1.070	0.700	34.0	5.0
n- Propylbenzene	1.43×10^{-3}	1.100	0.700	32.5	4.0
tert-Butylbenzene	1.30×10^{-3}	1.160	0.700	29.5	5.0

TABLE 4.7.- Experimental conditions for pulse electrolyses[b] of a series of hydrocarbons.

SUBSTRATE	AMOUNT OF RESIN (g.)	YIELD OF AMIDE RESPECT TO STARTING MATERIAL (%)
1- Phenyloctane	3.0	56.0
1- Phenylnonane	3.0	51.2
n- Propylbenzene	3.0	50.6
tert-Butylbenzene(c)	3.0	20.4

TABLE 4.8.- Yield of amide from the same amount of resin.

(a) The base potential was chosen such that no cathodic current was observed during the electrolysis.

(b) For all the experiments, the on period and the off period were equal at 0.1 s.

(c) From the anolyte solution, a considerable amount of acetamide (M.W. 59) was found.

None of the electrolyses described before, have been reported in the literature, so, to ensure whether the improvement achieved by using pulsed electrolysis could be extended to other systems, we tried the oxidation of toluene in dry acetonitrile, which has been reported in literature[2] to yield 17% of amide; the process is described in section 4.4.5.

4.4.5. NON-STEADY STATE PREPARATIVE ELECTROLYSIS OF TOLUENE.

Toluene (0.096 g., 9.3×10^{-4} mol) was oxidized in acetonitrile by modulating the potential from 0.00 V. up to the

voltammetric peak potential (2.220 V.), the potential being 0.1 s. switched on and 0.1 s. off. The initial current was 19 mA, and this value was mantained for a long time. After 63 coulombs had been passed, the current was 6.4 mA., 30 mg. of toluene reacted and 50 mg. remained unreacted (at this point, the anolyte became black, probably due to the formation of polymer). Five grams of resin were used and 48.7 mg of residue was extracted from the resin. The material was dissolved in acetone, examined by g.l.c. and compared with a standard sample of the amide. A yield of the amide of 44.21% with respect to the starting material, was found. Further studies for other compounds, following the same technique[21], gave satisfactory results, which reinforces our expectations.

4.5 DISCUSSION.

The cyclic voltammetric peak heights for the oxidation of all the members of this series, did not show simple linear proportionality to the square root of the sweep rates over the entire range of sweep rates. The deviation were towards higher currents at lower sweep speed and thus for the data processing, an ECE type of mechanism has been assumed. From the current function $Ip/\nu^{\frac{1}{2}}$, as a function of scan rate, qualitative information was obtained by comparison with the diagnostic criteria presented by Nicholson and Shain[4,5]. In all cases, a region where the current function remained almost independent of the sweep rate was observed, indicating that a simple diffusion controlled electron transfer process was taking place, i.e. the transference of the first electron to form the cation radical. At lower sweep rates, the current function was not independent of the sweep rate indicating that over that time scale, the cation radical was undergoing a chemical reaction. At

even slower sweep rates, the transference of the second electron was observed for all, except the Hexaethylbenzene, where the data were possibly affected by convection at the very slow sweep rates required. For convenience of presentation, only the data concerned with the transference of the first electron and the coupled chemical reaction are included in the graphs.

Hexaethylbenzene behaved quite differently from the other hydrocarbons of this series. The cation radical was very stable. Its life time was found to be about 10^3 times longer than the life time of the others from the results obtained in cyclic voltammetry.

If we now compare the results of the cyclic voltammetry with that of the chronoamperometry experiments performed under diffusion controlled conditions, we find that they are closely related. The current/time transients have been analyzed assuming overall a two electron process, and taking as limiting behaviour firstly a chemical rate constant equal to zero to represent a simple one - electron process and secondly, a rate constant of infinity to represent a two - electron process. At very short times, for all the hydrocarbons, the behaviour approached that for one electron oxidation, while at long times, the current function reached values which were indicative of two electron behaviour. A crossover region between the two extreme situations was exhibited by all the hydrocarbons, so, we can conclude from the cyclic voltammetry and chronoamperometry, that the anodic oxidation of Hexaethylbenzene, 1- Phenyloctane, 1- Phenylnonane, n- Propylbenzene and tert-Butylbenzene, follow an ECE type of mechanism. Whether this second electron transfer occurs in the bulk of the solution or on the electrode

surface, i.e., whether the mechanism is pure ECE or of the DISP type, can not be predicted by these techniques.

The reflectance experiments showed a tendency for all the members of this series to exhibit absorption peaks in three wavelengths regions, the first ranging between 575 and 660 nm.; the second within the interval 400 - 500 nm. and the third one from 300 - 350 nm., in the UV region . This result is in good agreement with literature. Those three regions have been assigned to cation radical [6-10], carbonium ion[11-13] and free radical [14-15], respectively, for alkylbenzenes. Qualitative information can be obtained from a comparison of the shapes of the experimental absorbance/time transients observed at different wavelengths with those reported in the literature[1] for the corresponding species. The cation radical has been found to produce a transient significantly different from those for the other intermediates. Since the cation radical is the primary species produced at the electrode surface ($RH \rightleftharpoons RH^{+\cdot} + e^-$), the absorbance increases rapidily from the time at which the anodic pulse is applied; the slope dA/dt is greatest at zero time and thereafter decreases monotonically. For the free radical and the carbonium ion, which are produced only after the delay caused by the homogeneous chemical reaction, the absorbance rise should be slower at short times. Absorbance/time transients with qualitatively the shapes expected for the carbonium ion and neutral radical were observed at wavelengths, λ_2 and λ_3. On this basis, therefore, those bands, λ_1, in table 4.3, observed for alkylbenzenes in this series, can be assigned to the cation radical. All the optical transients performed at those values of wavelength λ_1, for each compound were of the shape expected for the cation radical as described above. Furthermore, linearity was observed in the plots of $\Delta R/R$ vs. $t^{\frac{1}{2}}$, which is also indicative of the cation radical[3]. At longer times, a deviation from linearity of the absorbance could be observed. Extrapolating the

straight line observed at shorter times, the chemical rate constant, k_f, can be calculated for the decay of the cation radical. For a first order decay the following relationship holds[1]:

$$Q_{k_f} = Q_o - \int_o^t k_f \, Q_{k_f} \, dt \qquad \{4 - 3\}$$

were Q_{k_f} is the total amount of cation radical in the diffusion layer at a time t, after the start of the anodic pulse; Q_o is the amount of species that would have been present if k_f was zero. Since $A(t) = 2\,Q\,\varepsilon / \cos\theta$, we can write:

$$Q_{k_f} = A(t)_k \cos\theta / 2\,\varepsilon \qquad \{4 - 4\}$$

$$Q_o = A(t)_o \cos\theta / 2\,\varepsilon \qquad \{4 - 5\}$$

Substituting {4-4} and {4-5} into {4-3} :

$$A(t)_k \cos\theta / 2\varepsilon = \cos\theta / 2\,\varepsilon \left[A(t)_o - k_f \int_o^t A(t)_k \, dt \right]$$

$$A(t)_k - A(t)_o = - k_f \int_o^t A(t)_k \, dt$$

$$k_f = \frac{A(t)_o - A(t)_k}{\int_o^t A(t)_k \, dt} \qquad \{4 - 6\}$$

If we assume the sequence:

$$RH^{+}_{\bullet} \xrightarrow{k_f} R^{\bullet} + H^{+} \qquad \{4 - 7\}$$

$$RH^{+}_{\bullet} + R^{\bullet} \xrightarrow{k'} RH + R^{+} \qquad \{4 - 8\}$$

and if we consider the reaction {4 - 8} to be very fast, each time a cation radical molecule reacts to give the free radical, another molecule of cation radical reacts with free radicals to give the carbonium ion and the hydrocarbon, The rate of disappearance of cation radical observed in the optical experiment is given by:

$$-d\frac{\left[RH^{+}_{\bullet}\right]}{dt} = 2k_f\left[RH^{+}_{\bullet}\right] \qquad \{4 - 9\}$$

The consumption of the cation radical is expected to follow a first order decay with an apparent rate constant, k_{app},[16,17] twice as large as k_f. From equation {4 - 6}, values of k_f were estimated (see table 4.3). Table 4.10 shows the values of k_f obtained by the different methods used in this work.

As the functionalization of hydrocarbons in acetonitrile to produce amides has been carried out in this laboratory with great success[1,2,18-20], and the use of polymer bound reagents has improved the yield of the product; in this work we have extrapolated our expectations towards longer chain substituted alkylbenzenes in acetonitrile. The hexaethylbenzene was also of particular interest to be compared with the hexamethylbenzene which has been widely studied and its behaviour well known.

For preparative coulometry, hexaethylbenzene was chosen as an example because of its structural similarity with hexamethylbenzene which gave a good yield of the amide[1,2,18-20] with respect

to the starting material. The results presented for preparative electrolyses of the hydrocarbons, showed that they were oxidized in dry acetonitrile to give functionalized products, the amide being the main product when a cationic resin trapping agent was used during the electrolysis to separate physically the nitrilium ion and preventing its further reaction. When the electrolysis of hexaethylbenzene was carried out without the resin, a catalyzed oxidation took place after a small amount of starting material had reacted giving rise to the comsumption of a large amount of charge while almost the whole amount of starting material remained unreacted. Although the use of the resin made it possible to obtain the expected amide, in the case of hexaethylbenzene, the results given in table 4.4 show that it is necessary to take into account, the role that the ratio starting material/amount of resin plays in the production of the amides. Indeed, the yield of the amide obtained in this work, increased markedly as this ratio decreased, and the best yield, in the case of hexaethylbenzene was obtained when a ratio of 0.0025 was chosen. In those cases when a low amount of resin has been used, the formation of a considerable amount of dimer could be explained in two ways: either the structure of the nitrilium ion is such that exchange with the proton of the resin is slow for steric reasons and some of the nitrilium ion therefore reacts to form the dimer before being trapped by the resin, or the equilibrium constant is sufficiently low to maintain a significant concentration of nitrilium ion even though the exchange with the resin is fast. When the amount of resin used during the electrolysis is increased, this situation is avoided, no dimer is formed and, instead, a reasonable yield of the amide can be observed.

As was mentioned in paragraph 4.4.3, the other members of this series gave rise to poisoning of the electrode surface, no matter if the resin was present or not. To overcome this problem, a square wave, instead of a constant potential was applied to the working electrode, with the result shown in tables 4.5, 4.6 and paragraph 4.4.5. The duration of the pulse was chosen, according to the system under study, to produce always anodic currents. The advantages of the pulse technique can be summarized as follows:

(i) The surface of the electrode is mantained active, the poisoning and the consequent rapid fall off of the current being avoided.

(ii) If the equilibrium for the exchange of the proton of the resin is slow, the pulse technique allows the nitrilium ion time to link to the resin before its concentration increases considerably, thus inhibiting the formation of the dimer and increasing the concentration of nitrilium ion on the resin, leading to a higher yield of the amide.

(iii) By changing the length of the pulse, the concentration of nitrilium ion in the solution can be controlled.

Table 4.9 shows the yields reached by using the combination of pulse technique and resin. Table 4.10 shows a comparison between the values of rate constant, k_f, calculated by the various methods used in this work.

STARTING MATERIAL	OXIDATION POTENTIAL (VOLTS)	PRODUCT	YIELD FOR STEADY STATE COULOMETRY (%)	YIELD FOR PULSING COULOMETRY (%)
Hexaethylbenzene	1.36	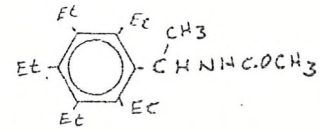	21.20	70.80
1-Phenyloctane	1.92	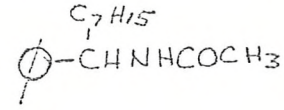		56.02
1-Phenylnonane	1.85	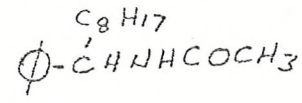		51.20
n-Propylbenzene	1.90	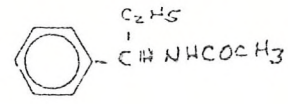		50.57
tert-Butylbenzene	1.94	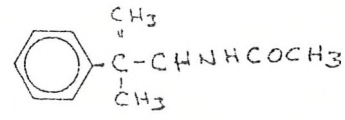		20.41
Toluene*	2.22	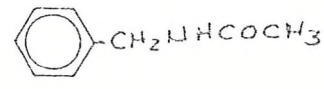	17.00	44.15

* See ref 2

TABLE 4.9.- Anodic oxidation of Alkylbenzenes in dry acetonitrile at Platinum.

SUBSTRATE	$k_{f_1}(sec^{-1})$	$k_{f_2}(sec^{-1})$	$k_{f_3}(sec^{-1})$
Hexaethylbenzene	0.75	1.5	1
1-Phenyloctane	1000	1200	900
1-Phenylnonane	1000	900	800
n-Propylbenzene	1200	1100	900
tert-Butylbenzene	1200	1100	-

TABLE 4.10.- Pseudo first order rate constant calculated by

(1) Cyclic voltammetry
(2) Chronoamperometry
(3) Modulated Specular Reflectance Spectroscopy

Using the hexaethylbenzene as an example, and from the results of this work, the following scheme can be proposed for the production of the amide.

If the transference of the second electron is taking place on the electrode surface, the carbonium ion is produced through reaction (a), whilst if it happens in the bulk solution, it will follow path (b). In any case, the production of the nitrilium ion takes place by nucleophilic attack of acetonitrile.

SCHEME I:

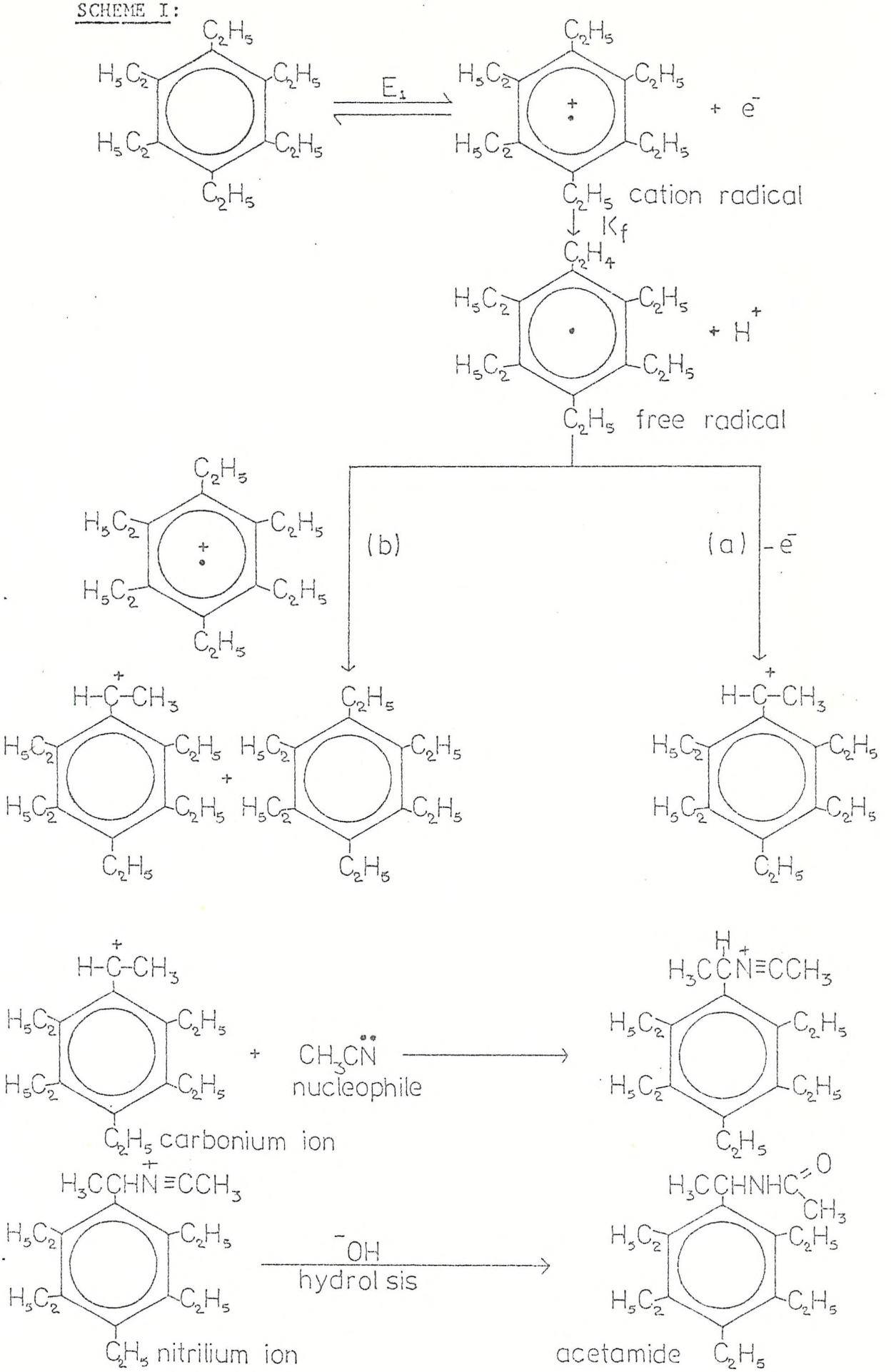
E1
+ e⁻
cation radical
Kf
+ H⁺
free radical
(b)
(a) -e⁻
carbonium ion
CH3CN
nucleophile
nitrilium ion
⁻OH
hydrolysis
acetamide

4.6. REFERENCES

(1) A. Bewick, J.M. Mellor, and B.S, Pons. Electrochim. Acta, 25, 931(1980)

(2) B.S. Pons, Ph D. thesis, Southampton University (1979).

(3) J. Strojek, T. Kuwana and S. Feldberg. J. Am. Chem. Soc., 90, 1353(1968).

(4) R. Nicholson and J. Shain. Anal.Chem. 36, 706(1964)

(5) R. Nicholson and J. Shain. Anal.Chem. 37, 178(1965)

(6) B. Badger and B. Brocklehurst, Trans. Faraday Soc., 65, 2582(1969)

(7) W. Duley, J. Faniran and J. Mc Cullough. J. Chem. Phys. 64, 2704(1976).

(8) R. Buhler and W. Funk, J. Phys. Chem. 79, 2098(1975)

(9) T. Shida and W. Hamill, J. Chem. Phys. 44, 4372(1966)

(10) L. Dorfman, Acts Chem. Res. 3, 224(1970)

(11) G. Olah, "Chemistry of Carbonium ions", Willey, New York (1973)

(12) J. Williams, Tetrahedron, 18, 1847(1962)

(13) I. Hanazaki and S. Nagakura, Tetrahedrom 21, 2241(1965)

(14) G. Porter and M. Savadetti, Spectro-Chim. Acta 22, 803(1966)

(15) P. Johnson and A. Albrecht, J. Chem. Phys. 48, 851(1968)

(16) G. C. Grant and T. Kuwana. J. Electroanal. Chem., 24,11(1970)

(17) N. Winograd, Electroanal. Chem. and Interfacial Electrochem., 43, 1 (1973).

(18) A. Bewick, G. J. Edwards and J. M. Mellor, Electrochim. Acta, 21, 1101(1976)

(19) A. Bewick, G. J. Edwards and J. M. Mellor. J. Chem. Soc. Perkin II,1952(1977)

(20) A. Bewick, G. J. Edwards and J. M. Mellor, Tetrahedron lett, 4685(1976)

(21) D. Coe , personal communication, Southampton University 1979

CHAPTER 5: ANODIC OXIDATION OF ALKOXYBENZENES.

5.1. Cyclic voltammetry results for the anodic oxidation of Alkoxybenzenes.

5.2. Chronoamperometry results for the anodic oxidation of alkoxybenzenes.

5.3. Modulated reflectance spectroscopy experiments.

5.4. Preparative Coulometry.

5.5. Discussion.

5.6. References.

5.1 CYCLIC VOLTAMMETRY RESULTS FOR THE ANODIC OXIDATION OF ALKOXYBENZENES.

Cyclic voltammetry of 1,2-dimethoxybenzene, 1,3-dimethoxybenzene, 1,4-dimethoxybenzene, 1,3,5-trimethoxybenzene, ethoxybenzene (Phenetole), 3-methylphenetole, anisole and 4-methylanisole, were carried out in the second part of this work. All voltammetric experiments were carried out using the cell described in section 3.4 and showed in figure 3.1. The composition of the solution used for voltammetry is described on the voltammograms.

Except for the 1,4-dimethoxybenzene, which behaved reversibly (fig. 5.1), all the members of this series showed irreversible behaviour. 1,2-dimethoxybenzene showed a rather complex voltammogram: at slow sweep rates (0.01 - 0.3 volts.s^{-1}), three anodic irreversible peaks were observed. As the sweep rate was increased, the value of the peak current for the first voltammetric wave increased while the peak currents for the second and third peaks decreased indicating that the latter were probably due to a further reaction of the species formed in the first process. A cathodic peak was also observed, which shifted towards more positive values as the sweep rate increased. Above 0.4 volts. s^{-1}, only one anodic peak was observed. At 50 volts. s^{-1}, a new reverse peak was observed at a potential more positive than that for the peak observed at slower sweep rates. The amplitude of this second reduction peak increased as the sweep rate was increased and concurrently there was a diminution of the peak due to the reduction of the proton, the latter peak being observed for all the members of this series.

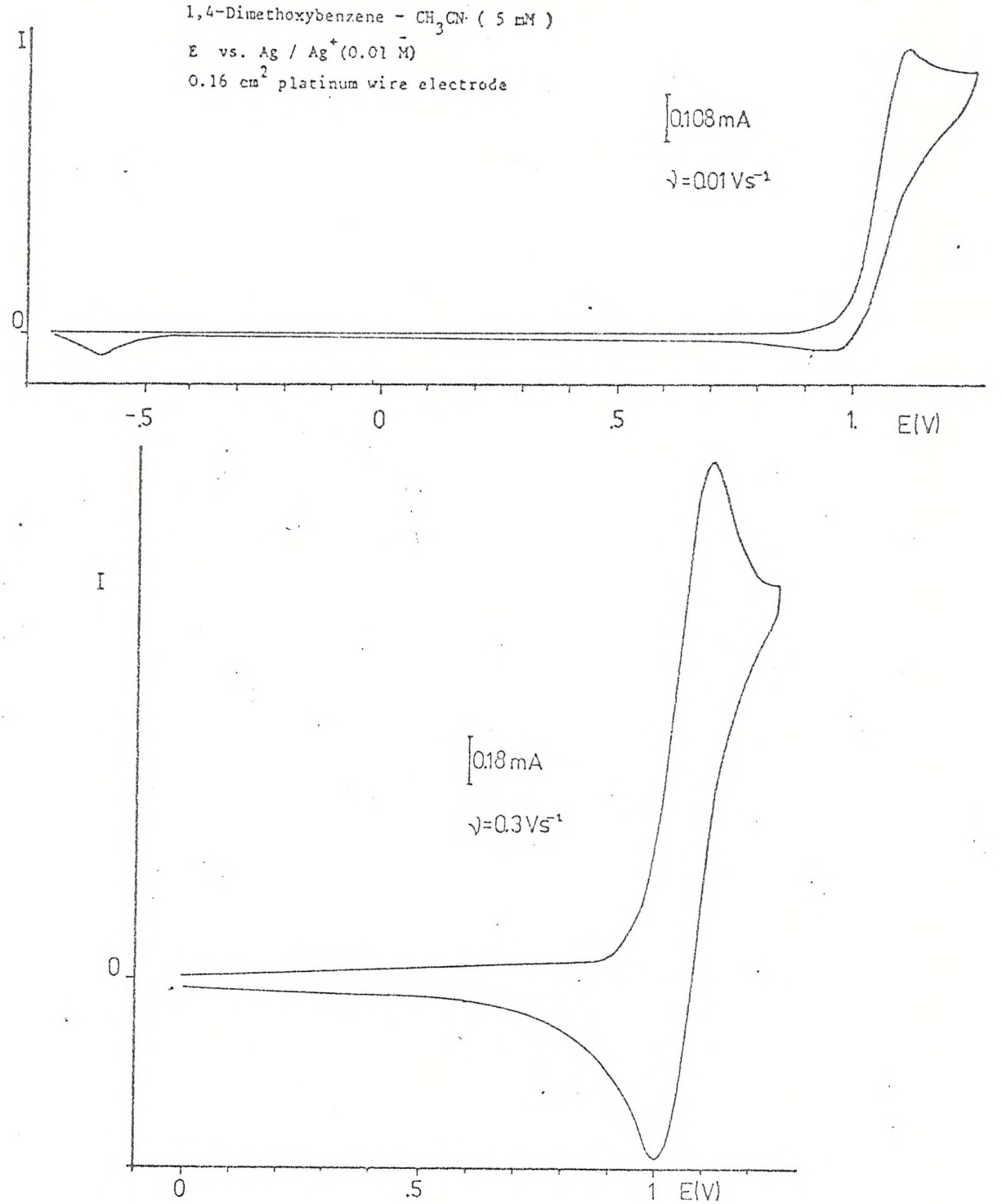

Fig. 5.1 Cyclic voltammogram of 1,4-Dimethoxybenzene

Table 5.1 shows the experimental values of peak potential and half peak widths for all the alkoxybenzenes studied in this work; all at a sweep rate of 0.2 volts . s^{-1}, against Ag/Ag^{+} (0.01M) reference electrode.

SUBSTRATE	E_p(volt)	$E_{p/2}$(volt)	$E_p - E_{p/2}$(volt)
1,2-Dimethoxybenzene	+1.23	+1.15	+0.08
1,3-Dimethoxybenzene	+1.16	+1.08	+0.08
1,4-Dimethoxybenzene	+1.00	+0.94	+0.06
1,3,5-Trimethoxybenzene	+1.16	+1.09	+0.07
Ethoxybenzene (Phenetole)	+1.40	+1.32	+0.08
3-Methylphenetole	+1.30	+1.22	+0.08
Anisole	+1.38	+1.30	+0.08
4-Methylanisole	+1.16	+1.08	+0.08

TABLE 5.1.- Voltammetric data for Anodic Oxidation of Alkoxybenzenes.

Theoretical working curves for an ECE mechanism according to the procedure described in chapter 2,were constructed.Table 5.2 shows the values of k_f giving the best fit to the data (Figs.5.2 through5.5).

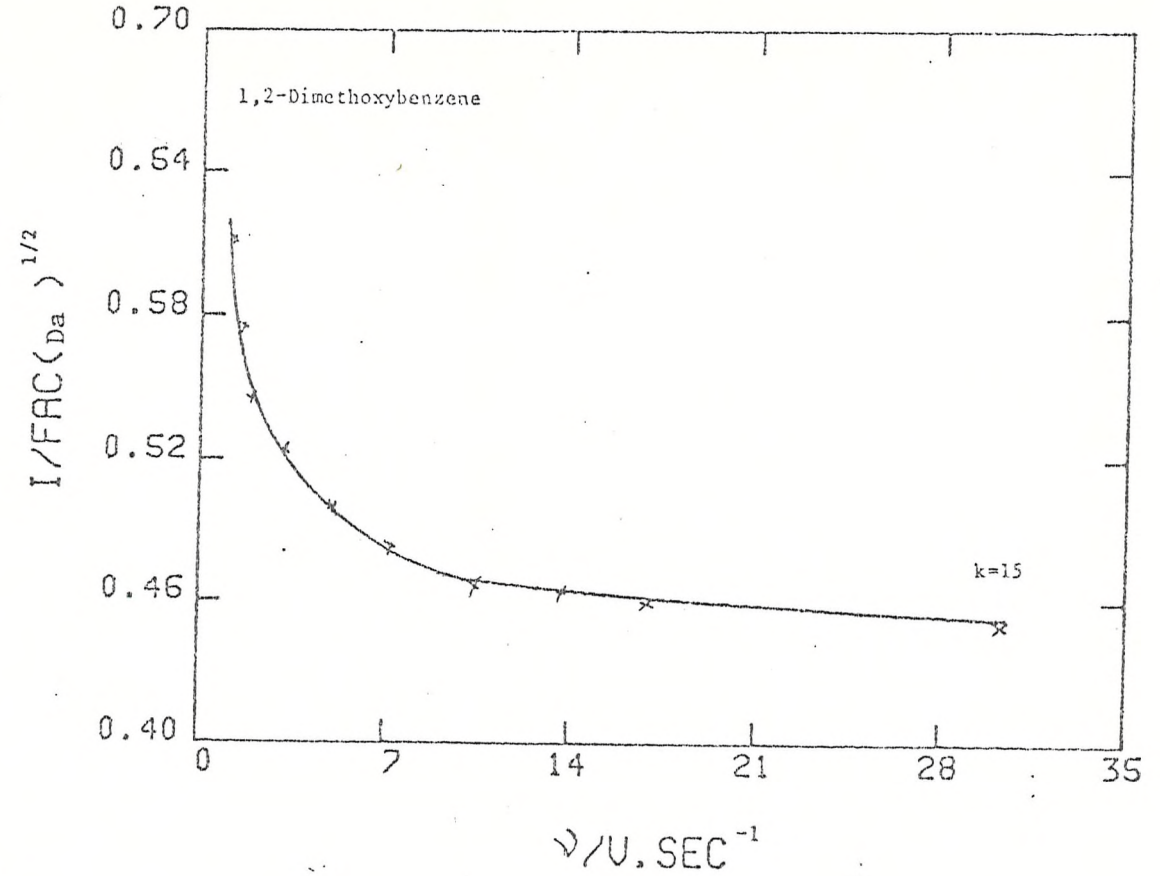

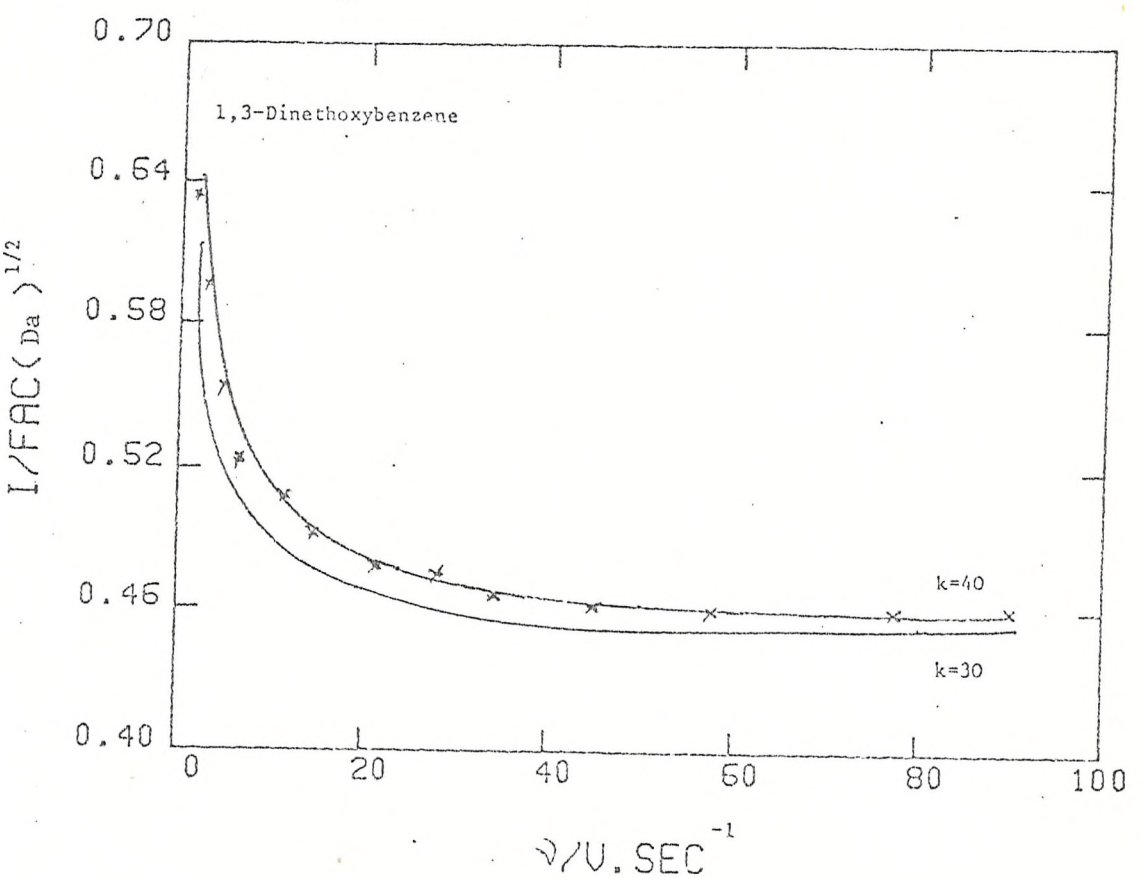

Fig. 5.2 Cyclic voltammetric working curves for the determination of the rate constant k_f .

xxx Experimental

___ Theoretical

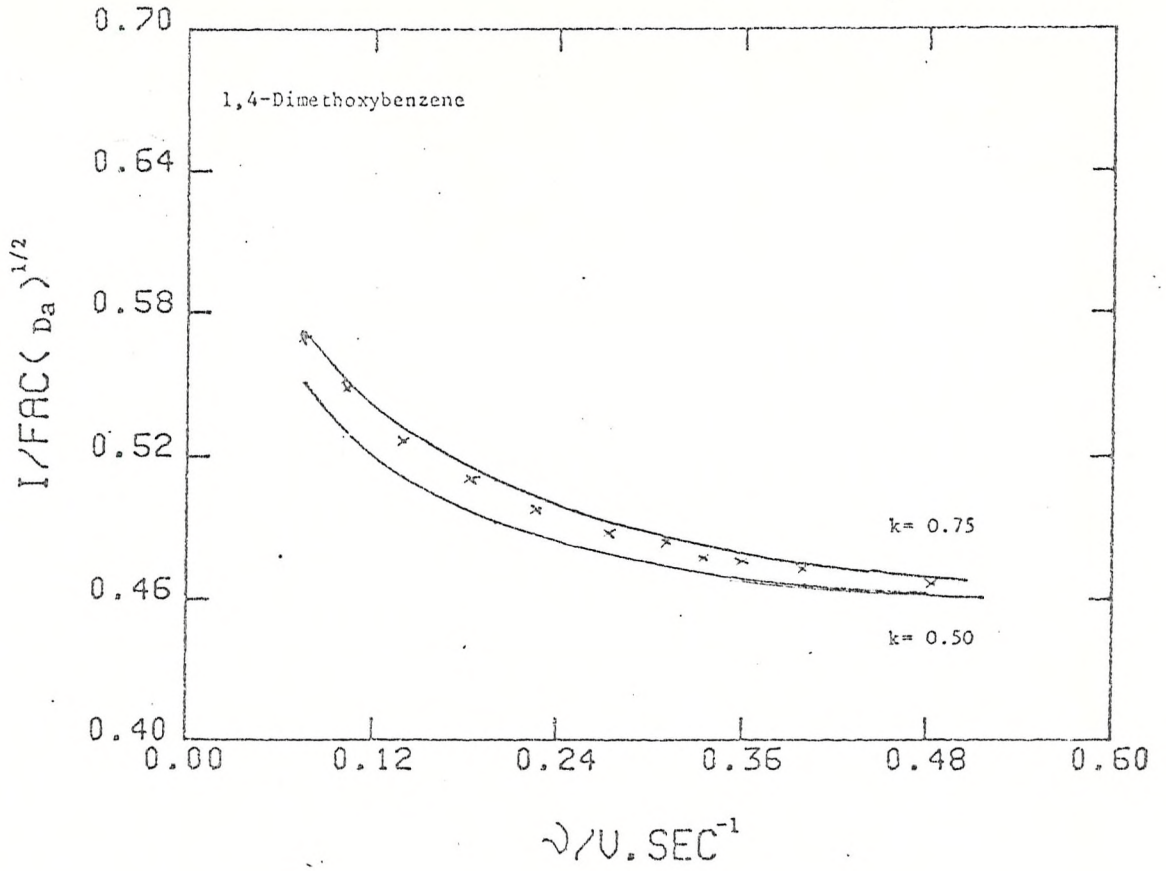

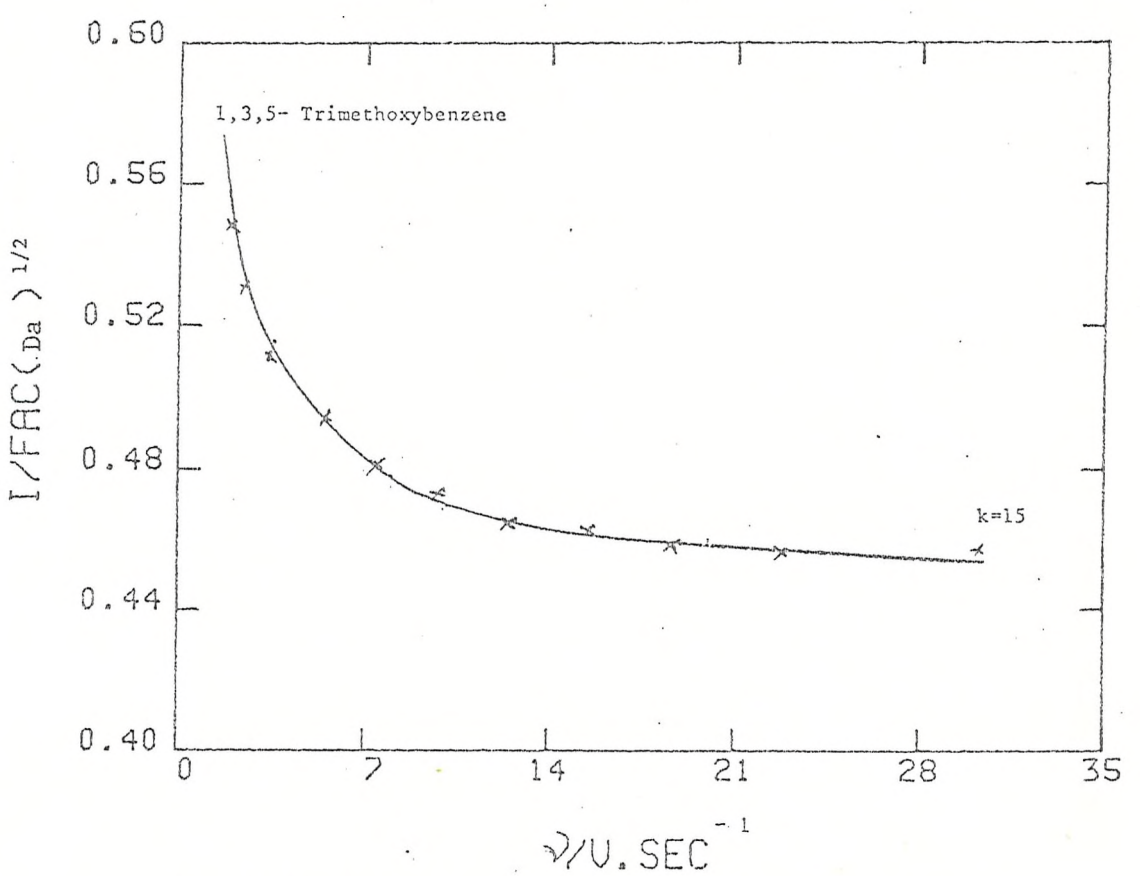

Fig. 5.3 Cyclic voltammetric working curves for the determination of the rate constant k_f .

xxx Experimental

___ Theoretical

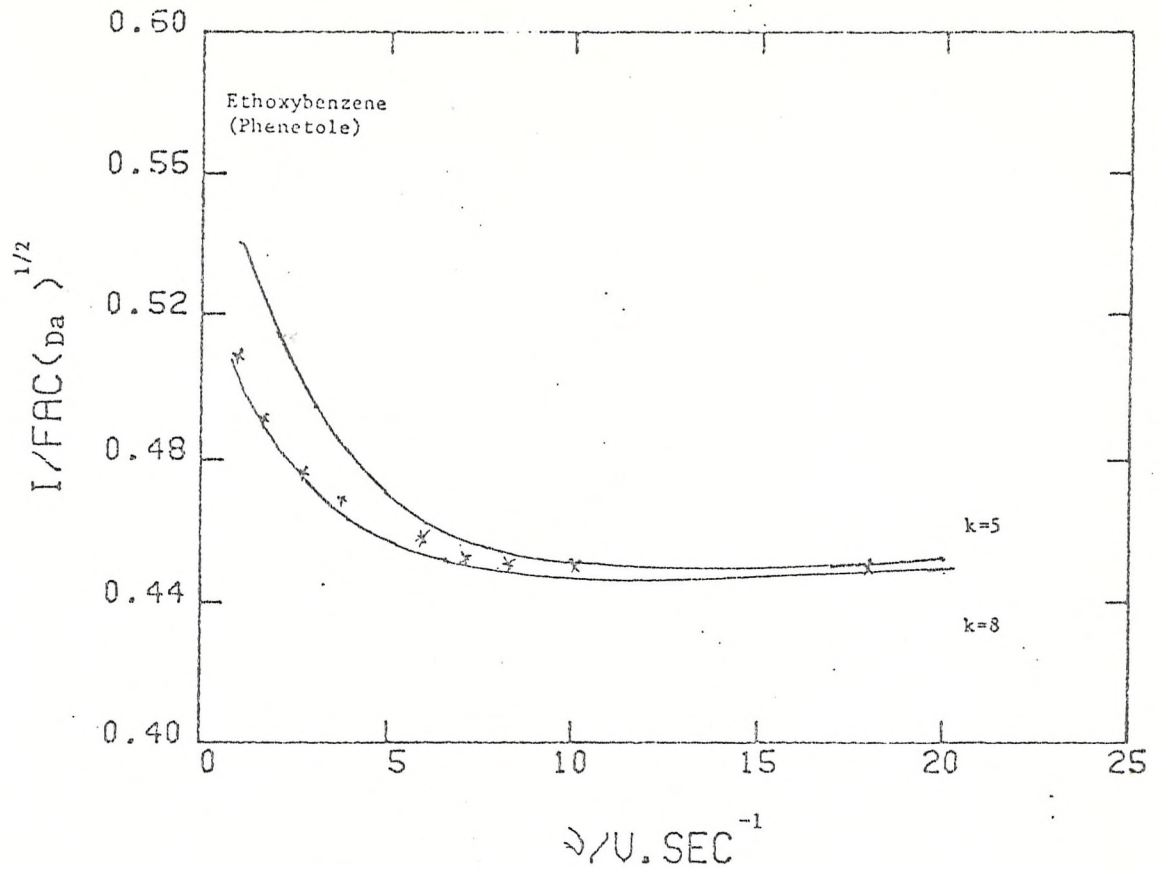

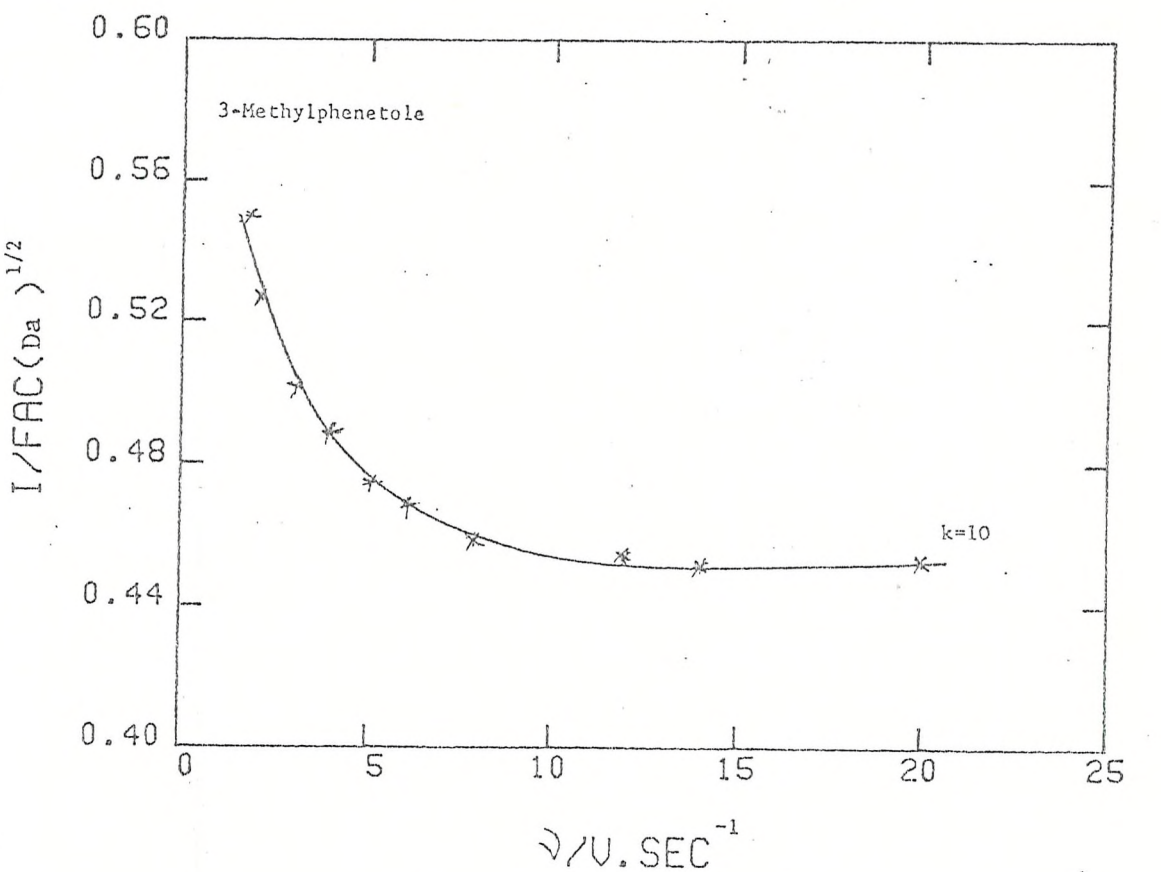

Fig. 5.4 Cyclic voltammetric working curves for the determination of the rate constant k_f.

xxx Experimental

___ Theoretical

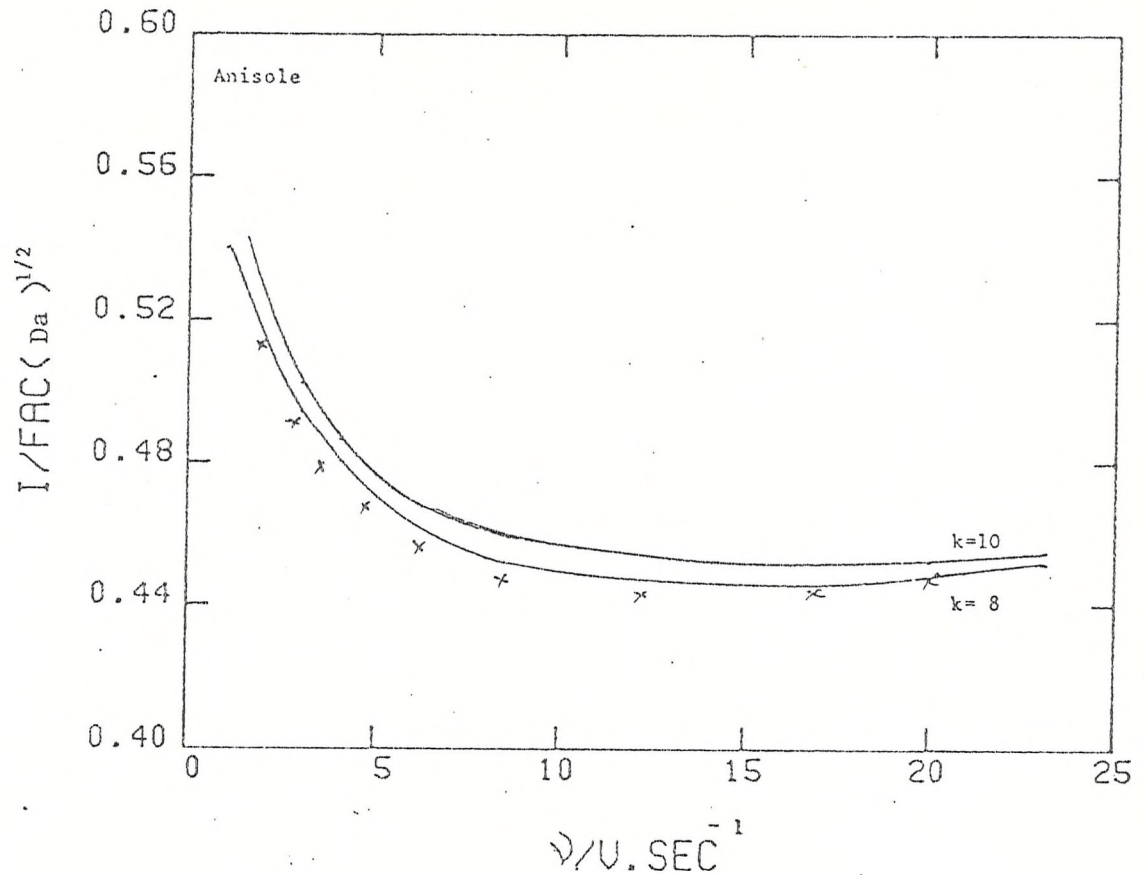

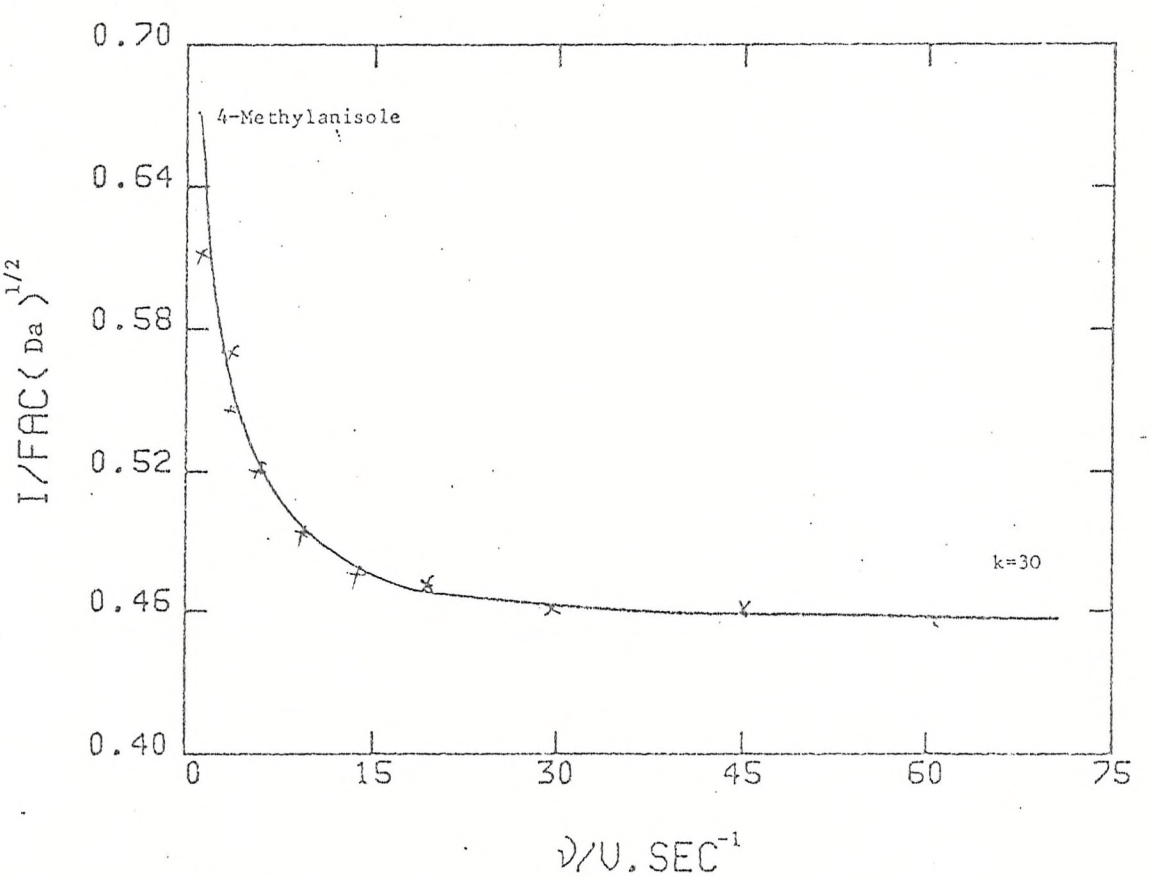

Fig. 5.5 Cyclic voltammetric working curves for the determination of the rate constant k_f.

xxx Experimental

___ Theoretical

SUBSTRATE	RATE CONSTANT (Sec^{-1})
1,2-Dimethoxybenzene	15
1,3-Dimethoxybenzene	40
1,4-Dimethoxybenzene	0.7
1,3,5-Trimethoxybenzene	15
Ethoxybenzene (Phenetole)	8
3-Methylphenetole	10
Anisole	6 - 7
4-Methylanisole	30

TABLE 5.2.- Values of pseudo-first order rate constant for the chemical reation obtained from Cyclic Voltammetry.

5.2 CHRONOAMPEROMETRY RESULTS FOR THE ANODIC OXIDATION OF ALKOXYBENZENES.

Chronoamperometry experiments were performed using the same cell as that used for cyclic voltammetry. The setting up of the system and the choice of a suitable pulse profile have been described in section 3.5. Figures 5.6 through 5.9 , show the plots of I vs. $t^{-\frac{1}{2}}$, for each case, taken from the current transients obtained for

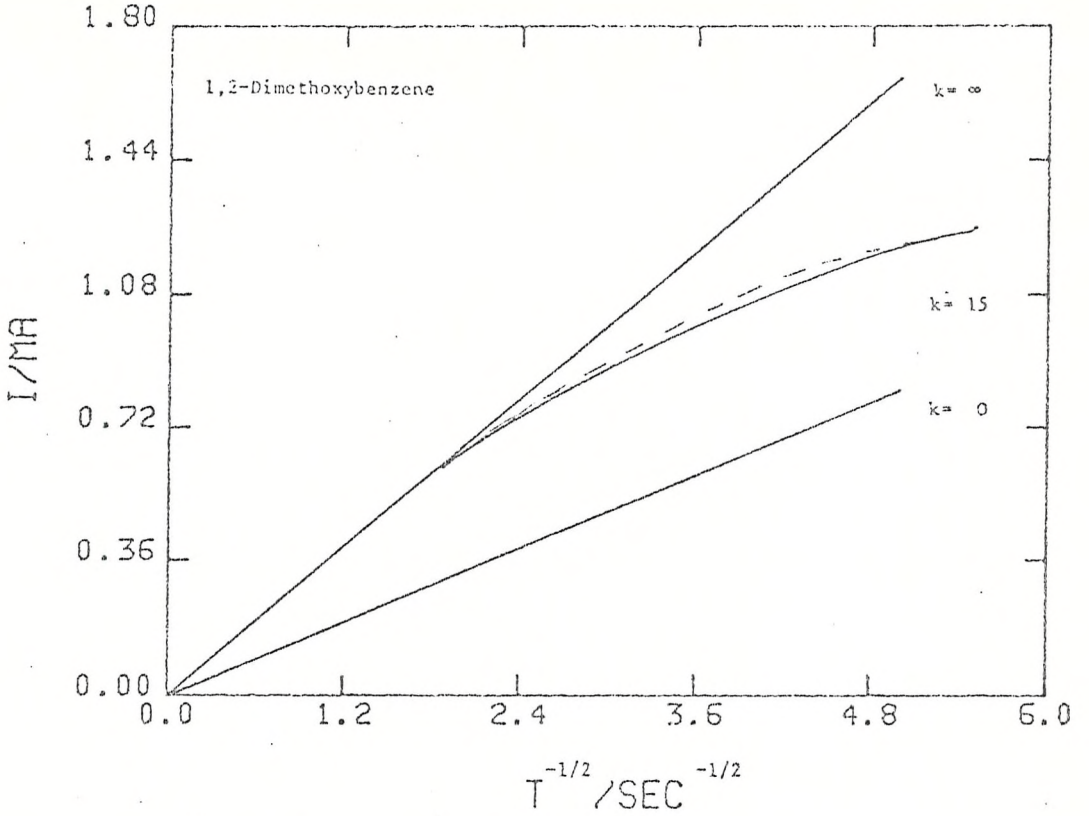

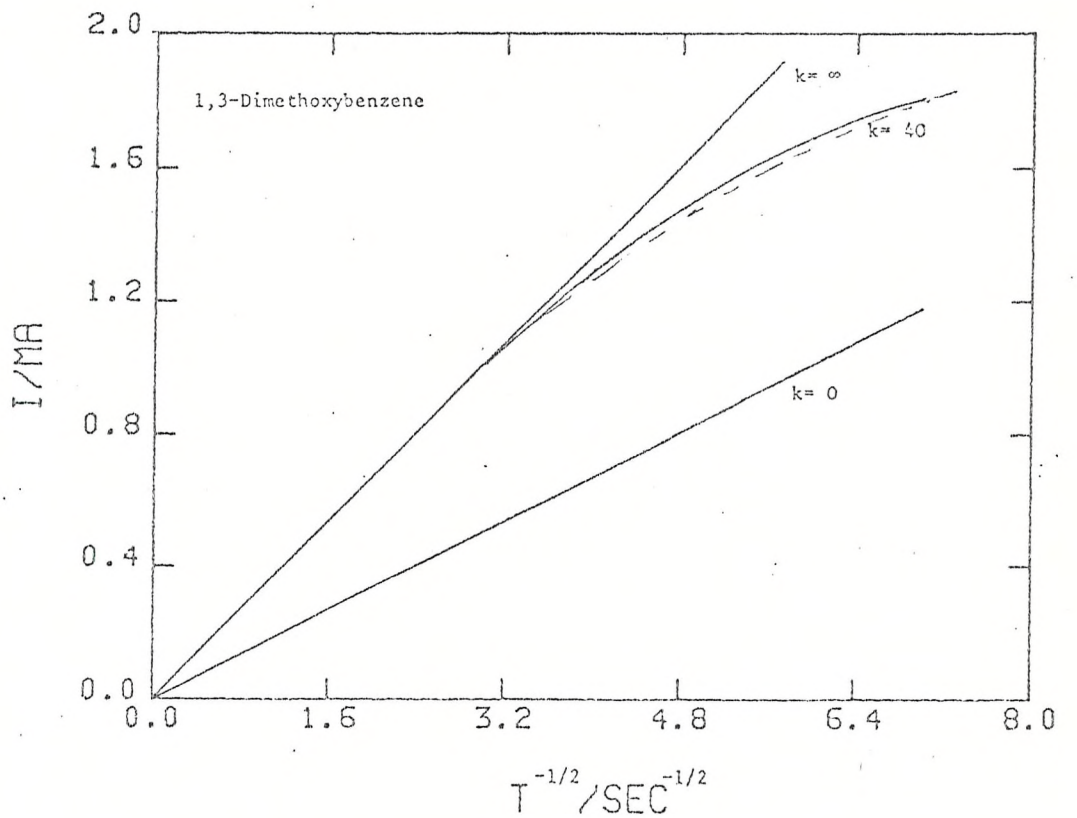

Fig. 5.6 Chronoamperometric working curves for the determination of the rate constant k_f.

xxx Experimental

___ Theoretical

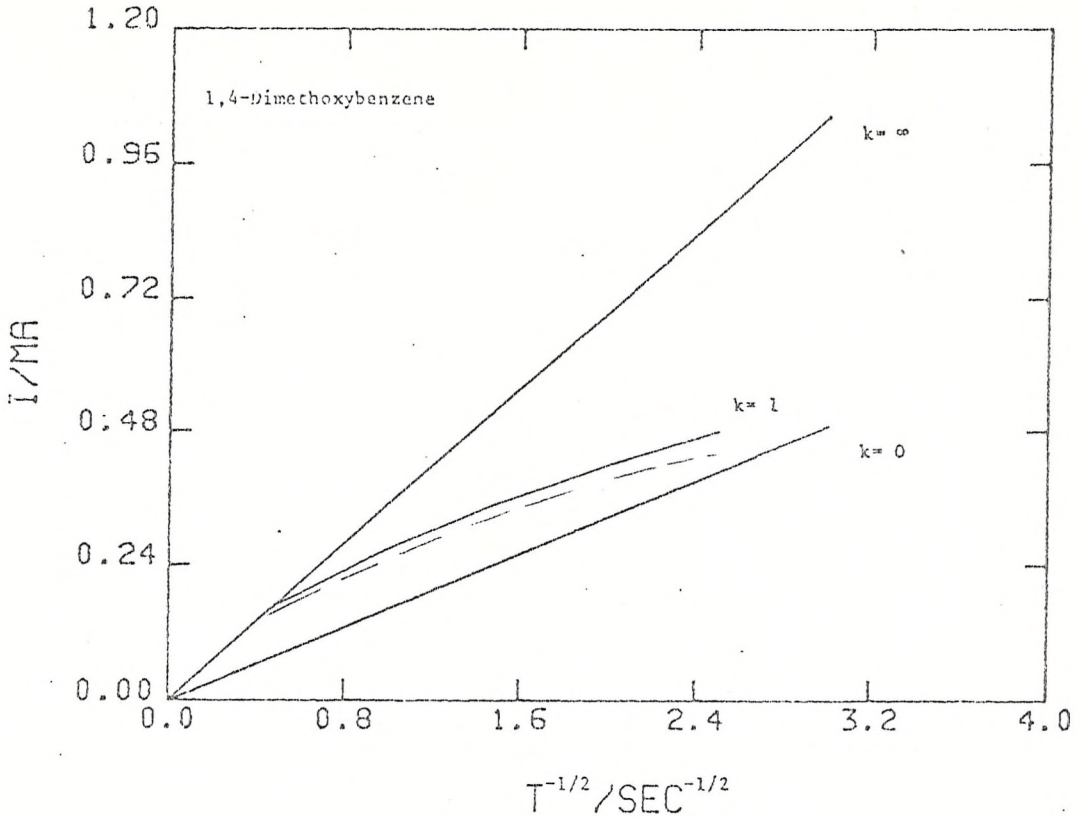

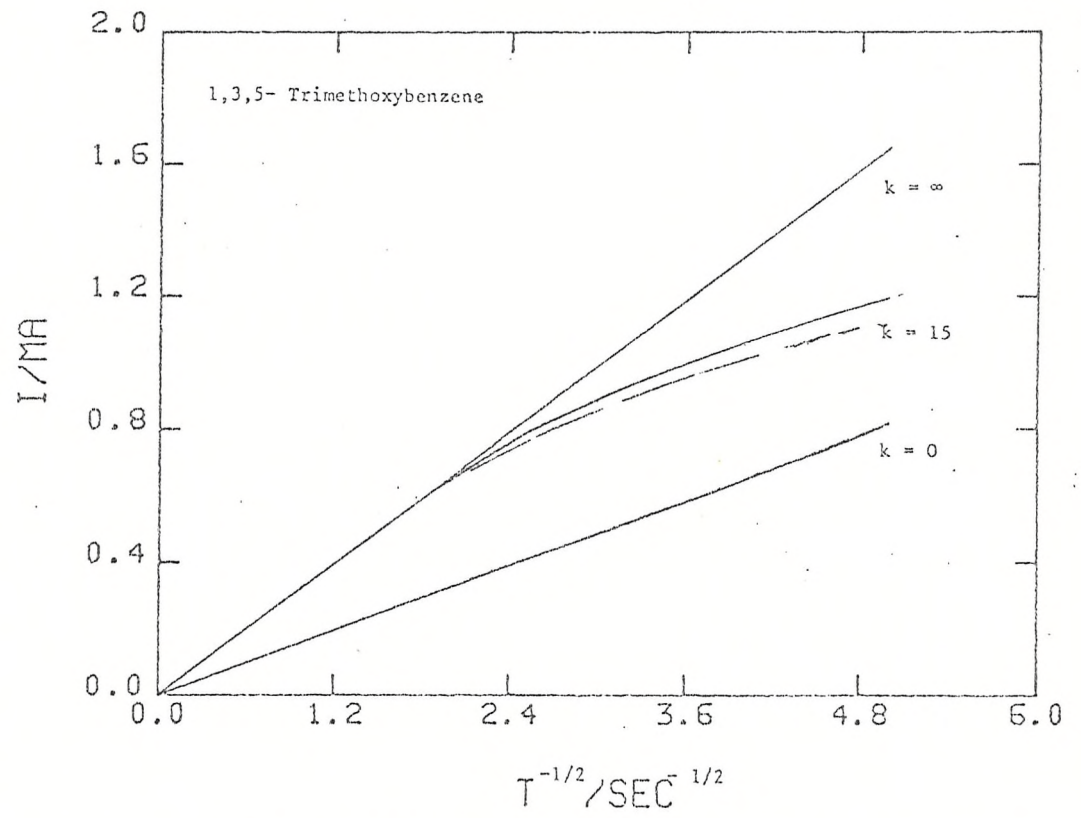

Fig. 5.7 Chronoamperometric working curves for the determination of the rate constant k_f.

xxx Experimental

___ Theoretical

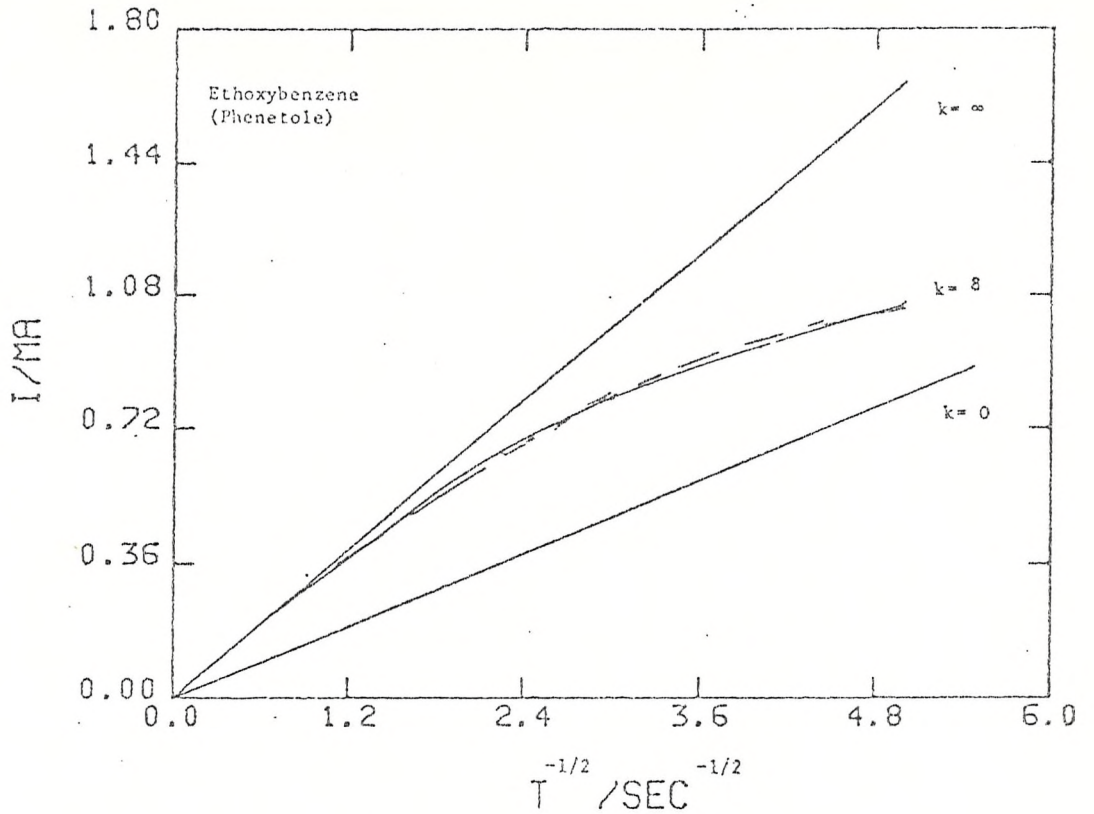

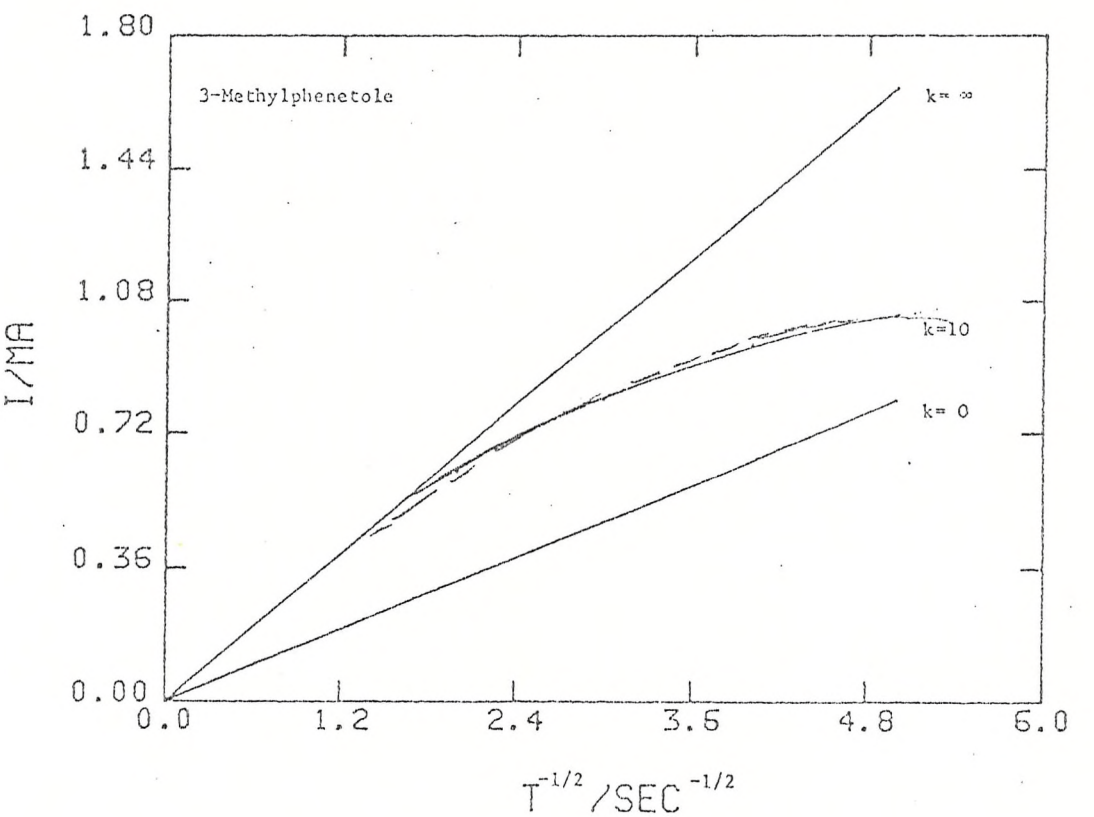

Fig. 5.8 Chronoamperometric working curves for the determination of the rate constant k_f.

xxx Experimental

___ theoretical

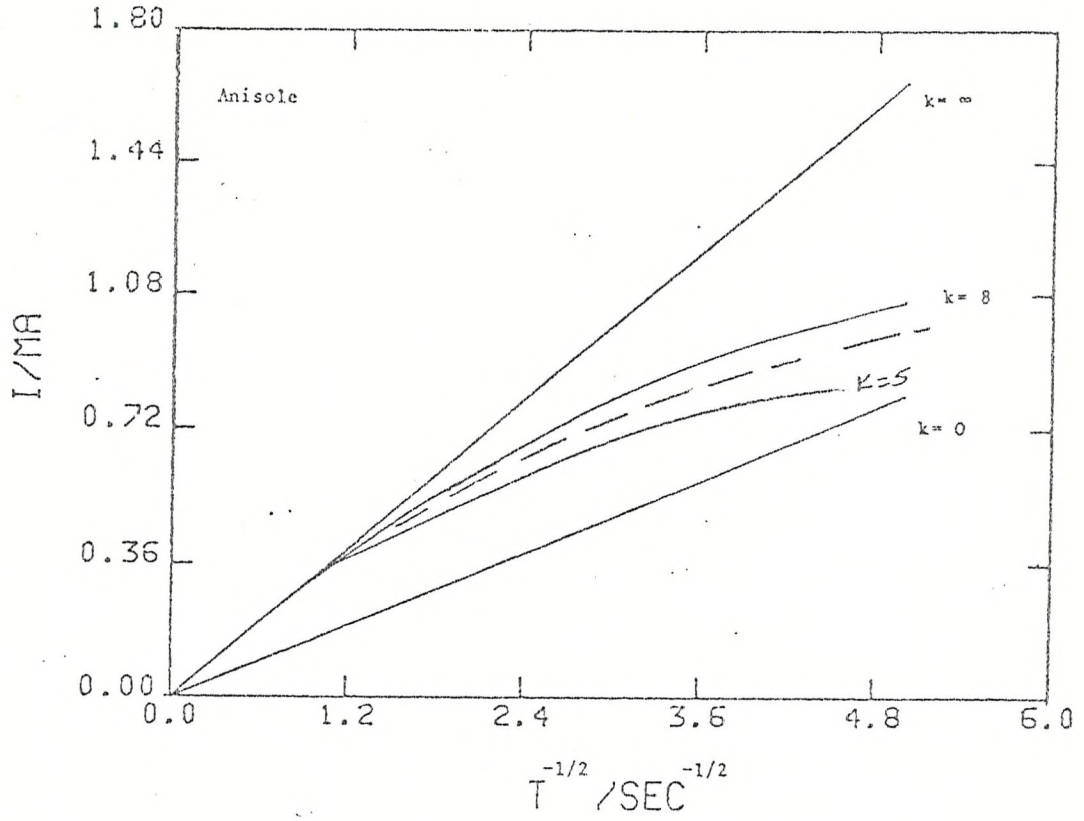

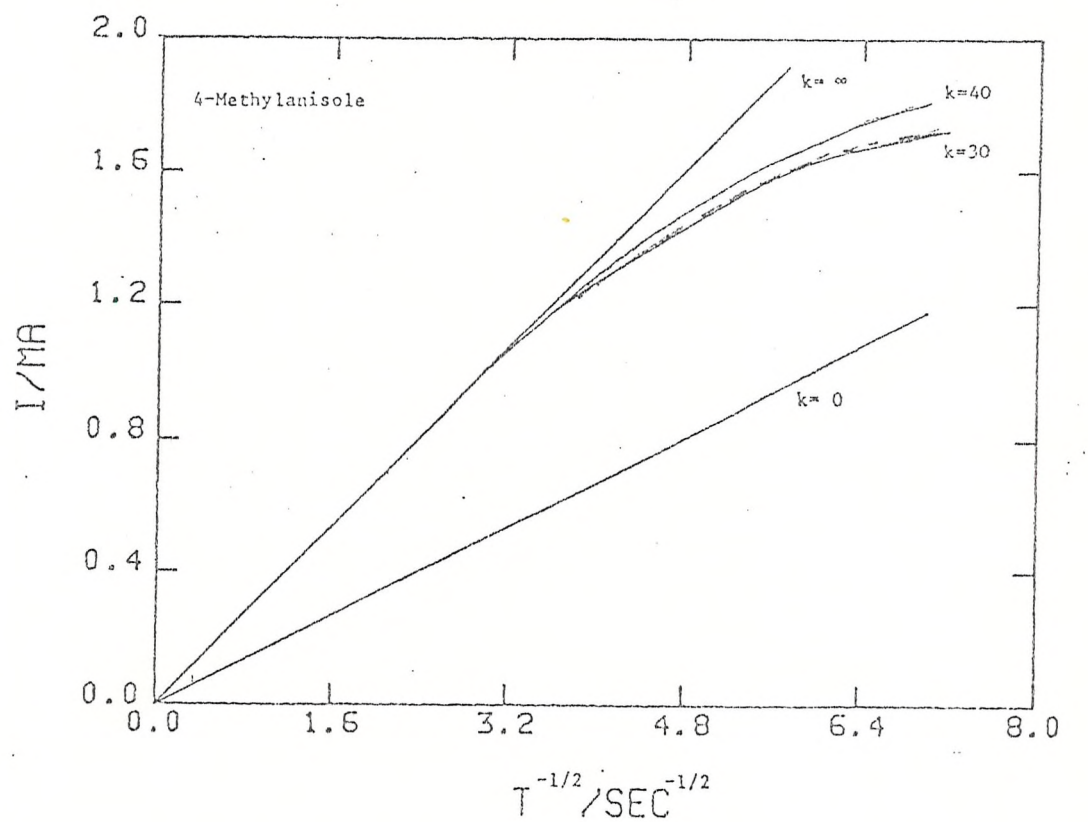

Fig. 5.9 Chronoamperometric working curves for the determination of the rate constant k_f.

xxx Experimental

___ Theoretical

the members of this series. The experimental data were treated in the same way described in chapter 4. Table 5.3 contains the experimental conditions for chronoamperometry and the values of k_f obtained from these experiments.

SUBSTRATE	BASE POTENTIAL (Volts.)	PULSE HEIGHT (Volts.)	k_f (s^{-1})
1,2-Dimethoxybenzene	+0.850	+0.480	15
1,3-Dimethoxybenzene	+0.850	+0.400	38
1,4-Dimethoxybenzene	+0.750	+0.375	0.8
1,3,5-Trimethoxybenzene	+0.680	+0.600	13
Ethoxybenzene (Phenetole)	+1.000	+0.500	8
3-Methylphenetole	+0.900	+0.500	10
Anisole	+1.100	+0.400	7
4-Methylanisole	+1.000	+0.400	30

TABLE 5.3.- Experimental conditions and pseudo-first order rate constants obtained from chronoamperometry.

5.3 MODULATED REFLECTANCE SPECTROSCOPY EXPERIMENTS.

All the optical experiments carried out for the alkoxybenzenes were performed in the same way as those for Alkylbenzenes and under the

same experimental conditions (see chapter 4).

1,2-Dimethoxybenzene did not produce reflectance spectra under the conditions of these experiments. In most of the other cases,it was possible to obtain spectra if the electrode was polished from time to time during the experiments,as it was described in chapter 3.

Figures 5.10 through 5.16 show the spectra obtained for all the members of this series, except for 1,2-Dimethoxybenzene. Table 5.4 summarizes the observed characteristics for the spectra. For all the compounds, absorbance/time transients were recorded at a fixed wavelength, believed to correspond to maximum absorption by the radical cation produced in the first electron transfer, using the method described in sections 3.1.2. and 4.3.Table 5.5 shows the results for those experiments (figures 5.17 - 5.24).

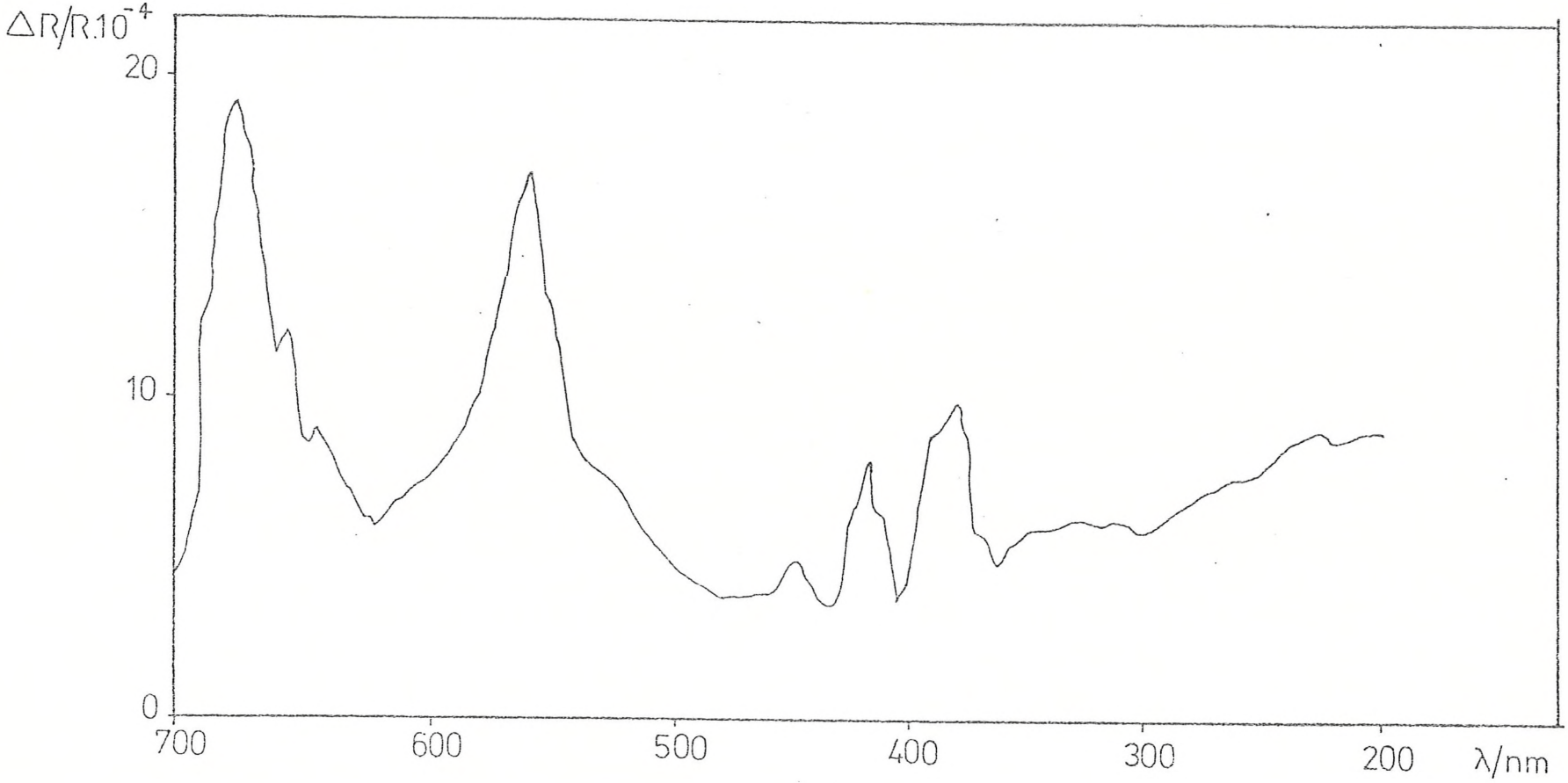

m-Dimethoxybenzene. Modulated Specular Reflectance Spectra

Fig. 5.10

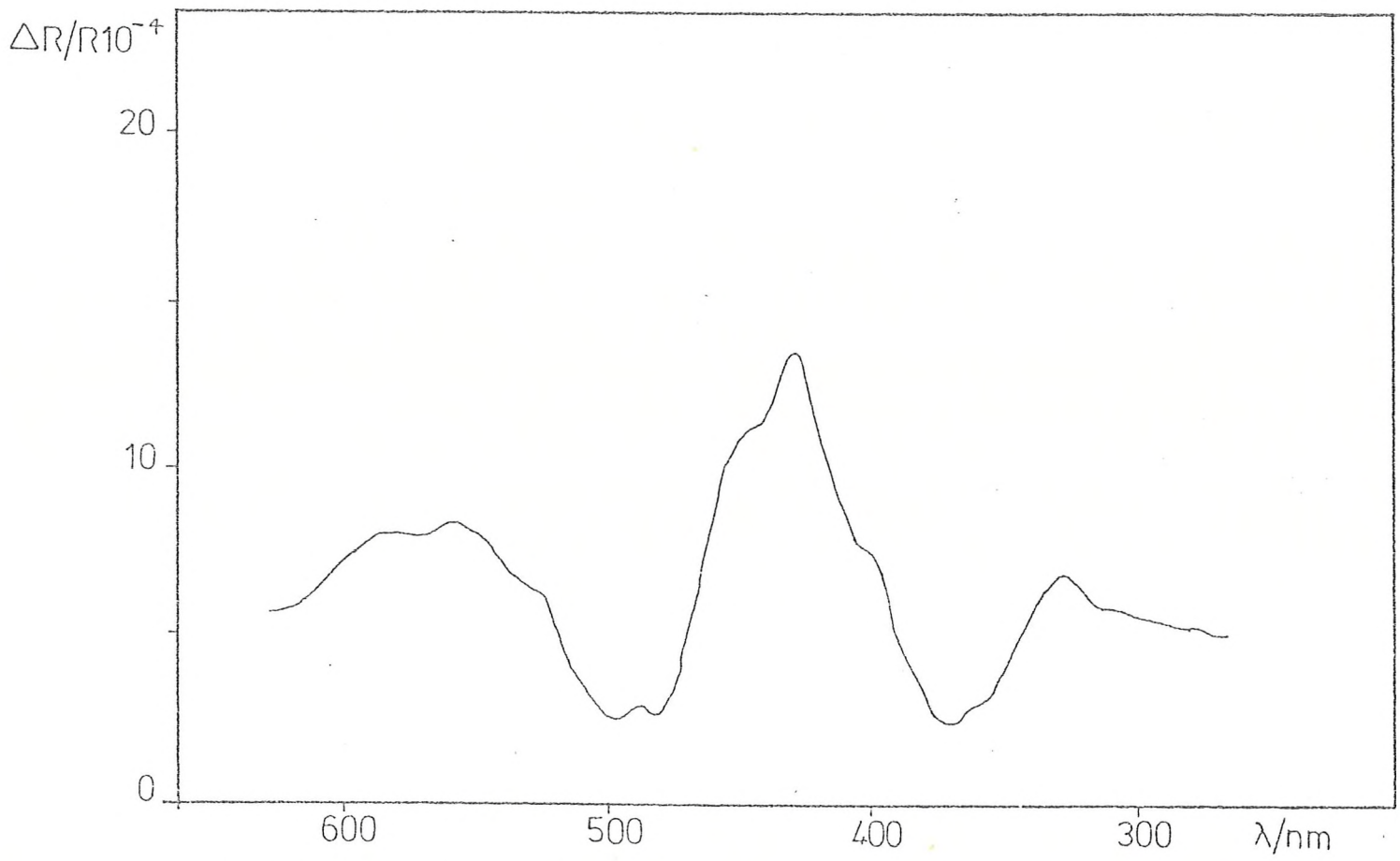

p-Dimethoxybenzene. Modulated Specular Reflectance Spectra

Fig. 5.11

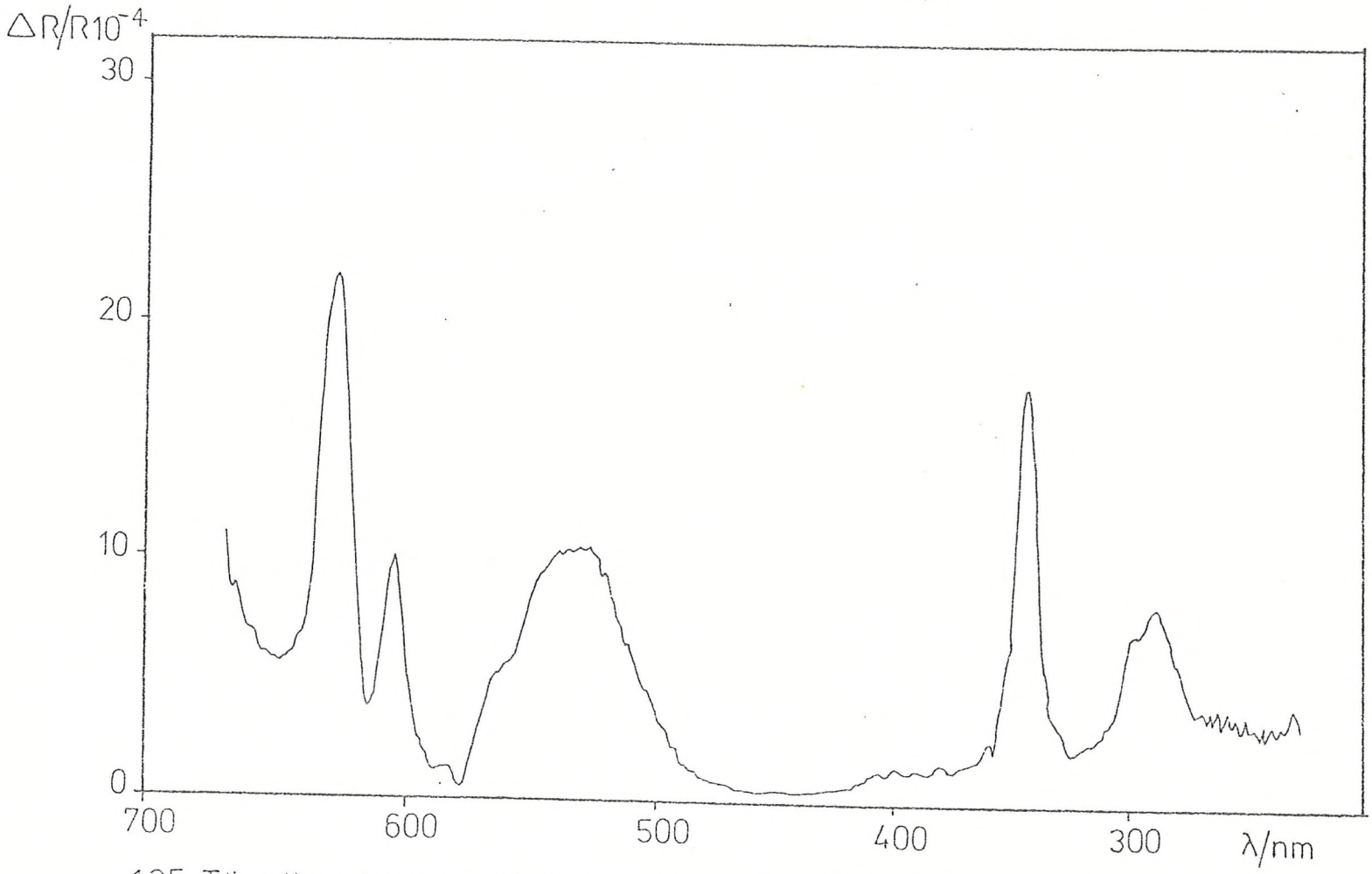

1,3,5-Trimethoxybenzene. Modulated Specular Reflectance Spectra

Fig. 5.12

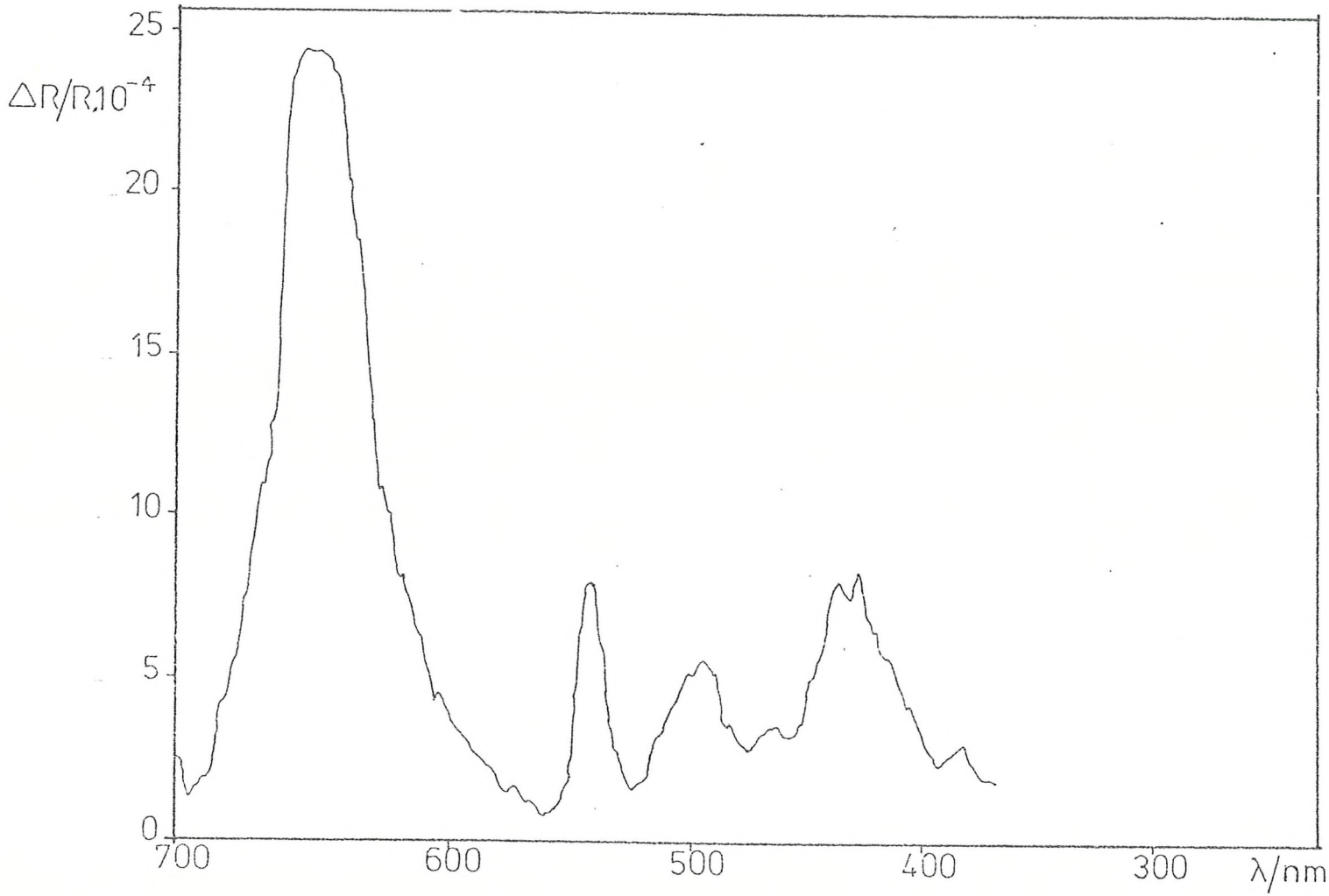

Ethoxybenzene (Phenetole). Specular Reflectance Spectra

Fig. 5.13

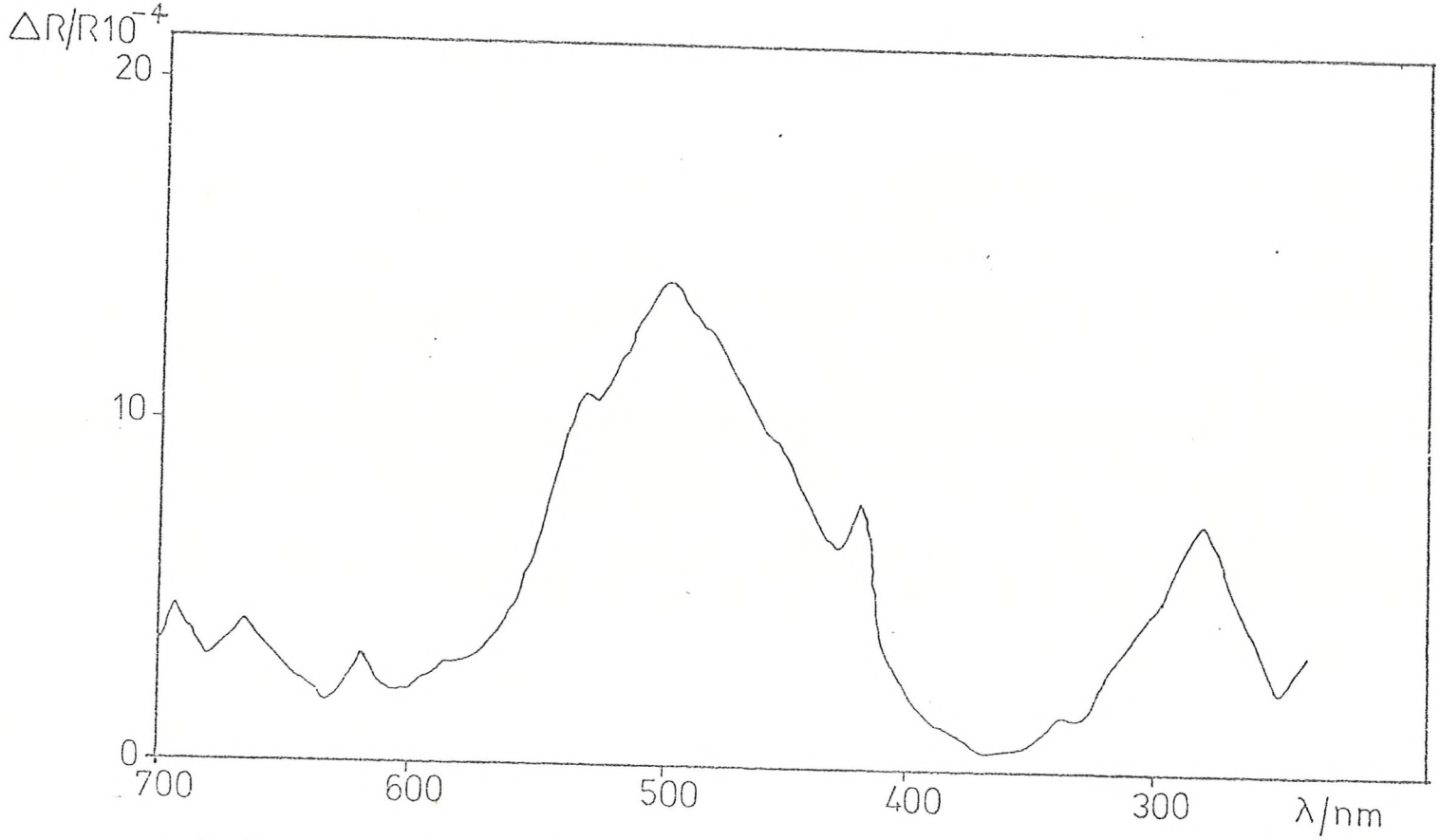

m-Methylphenetole. Modulated Specular Reflectance Spectra

Fig. 5.14

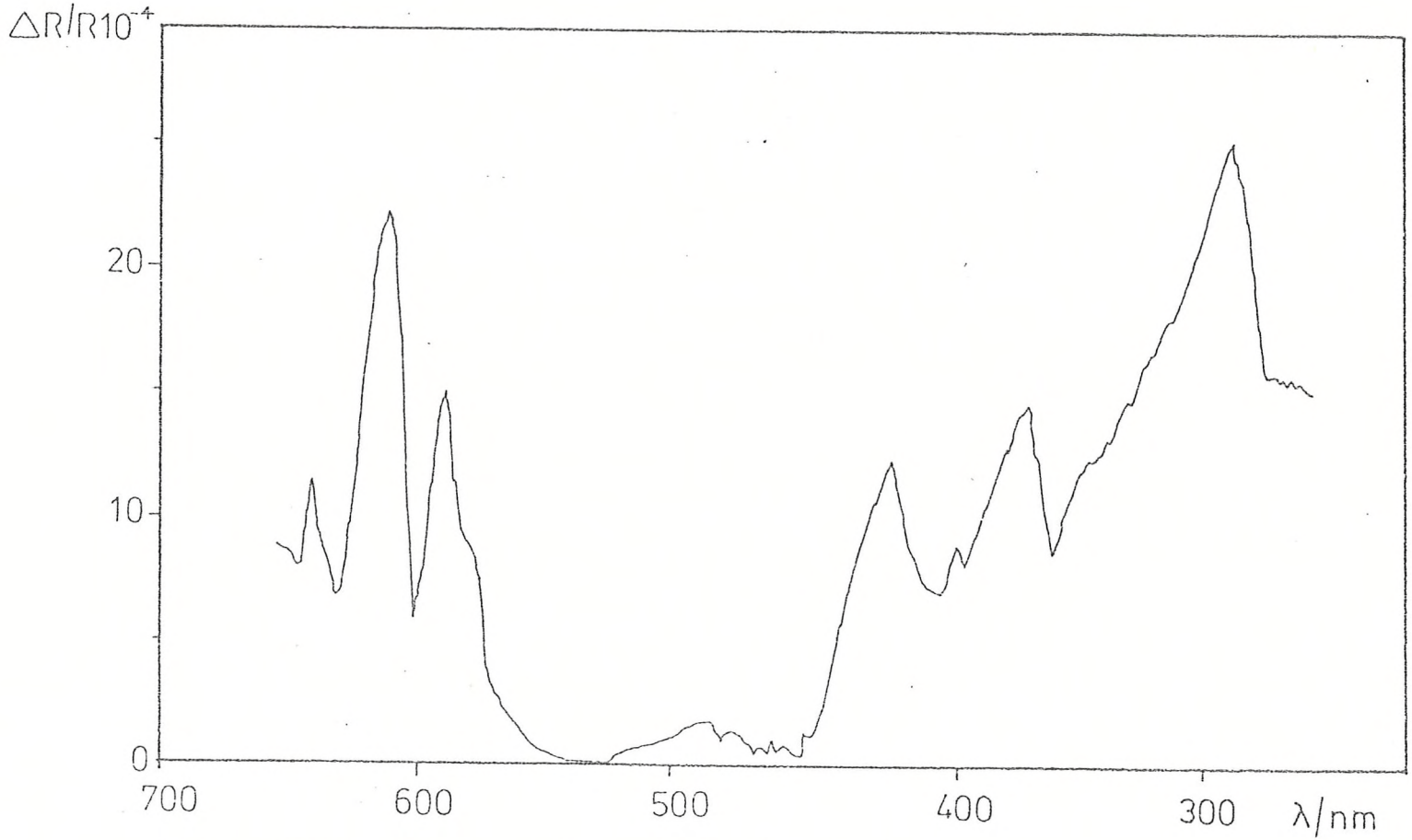

Anisole.Modulated Specular Reflectance Spectra

Fig. 5.15

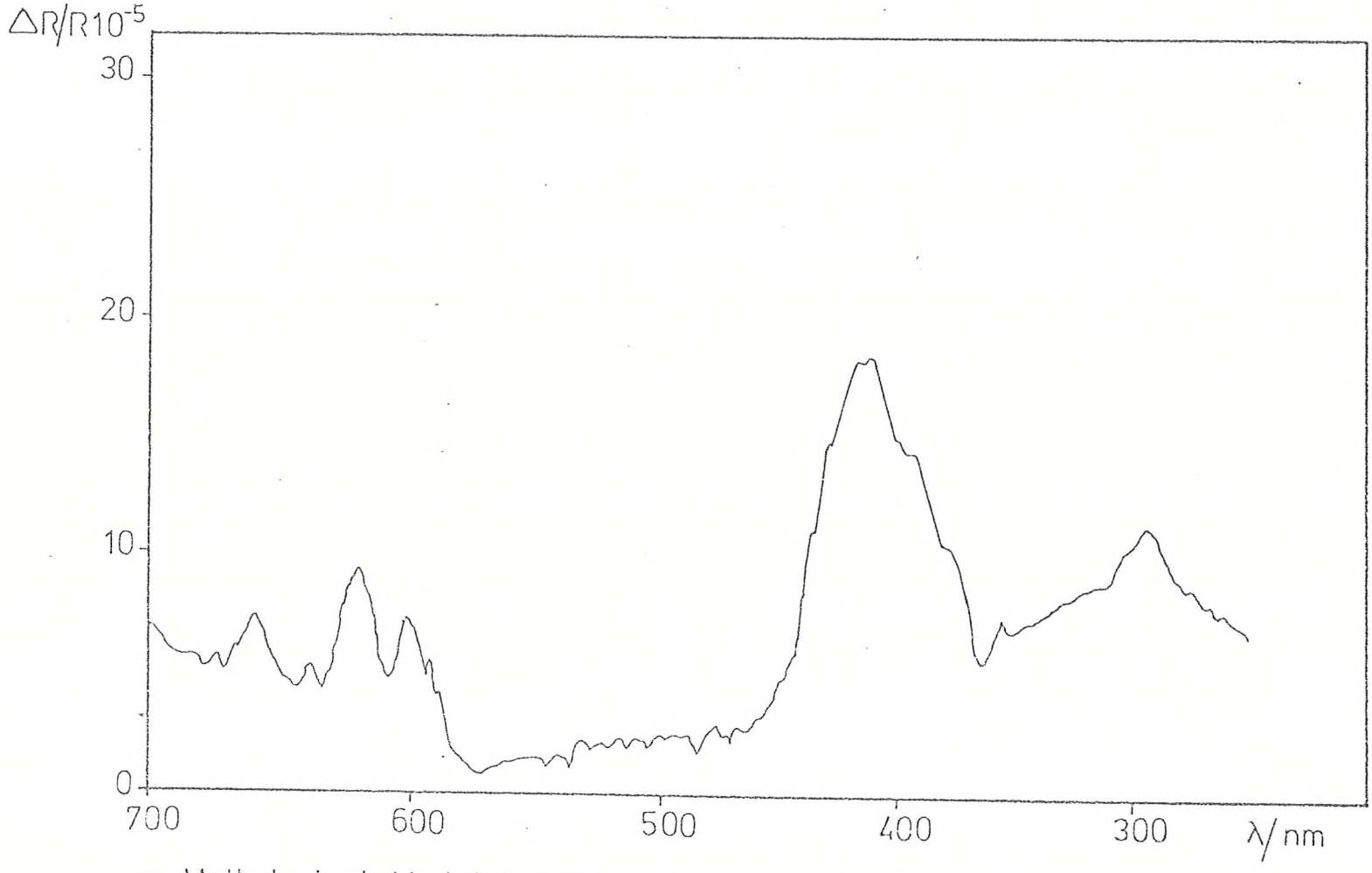

p-Methylanisole.Modulated Specular Reflectance Spectra

Fig. 5.16

SUBSTRATE	MODULATION RANGE (VOLTS)	FREQUENCY (HZ)	SPECTRAL LINES WAVELENGTHS (nm) λ_1	λ_2	λ_3
1,3-Dimethoxybenzene	+0.900 - +1.300	80	675	560 420	380
1,4-Dimethoxybenzene	+0.800- +1.200	80	(550-600)	460 430	330
1,3,5-Trimethoxybenzene	+0.700- +1.300	80	625 600	540	350 290
Ethoxybenzene (Phenetole)	+1.000- +1.500	80	650	540 500 430	
3-Methylphenetole	+0.900- +1.400	80	665 620	530 495 420	280
Anisole	+1.200- +1.500	80	650 625	540 430	325 290
4-Methylanisole	+1.000- +1.250	80	670 630	420	300

TABLE 5.4.- Spectral characteristics in the UV-visible region

...m Modulated Specular Re...ctance Spectroscopy.-

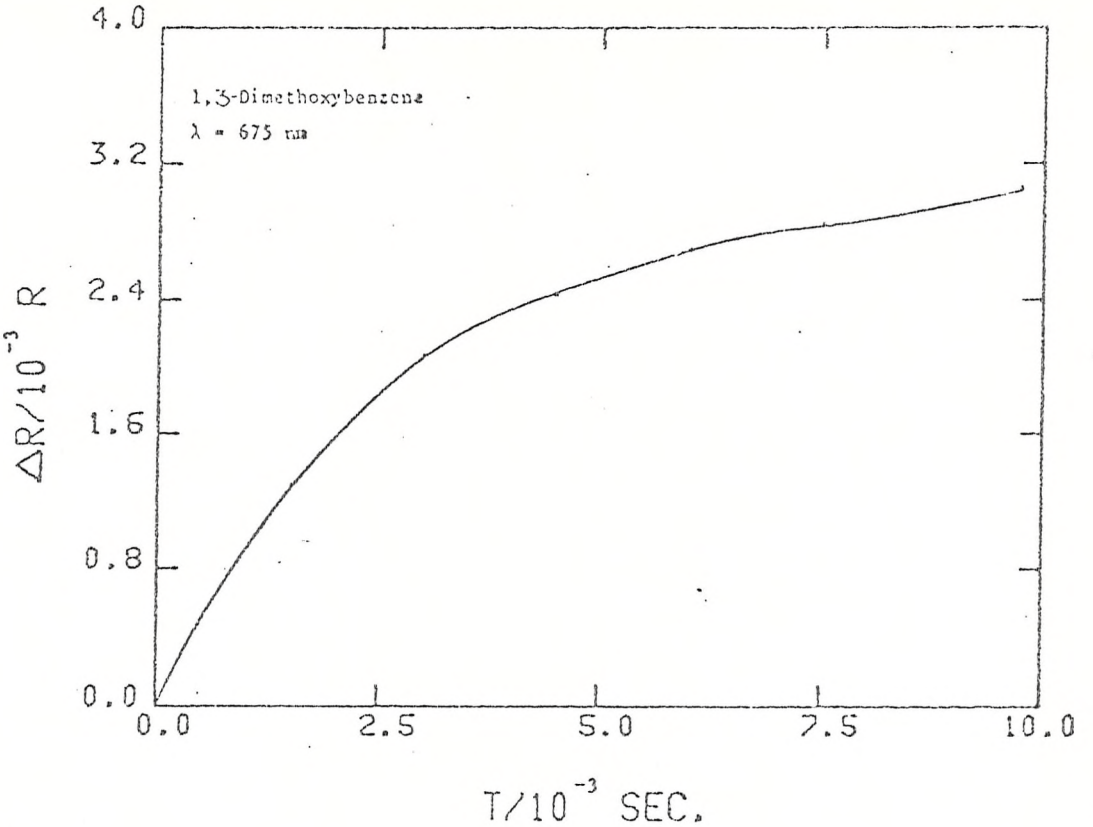

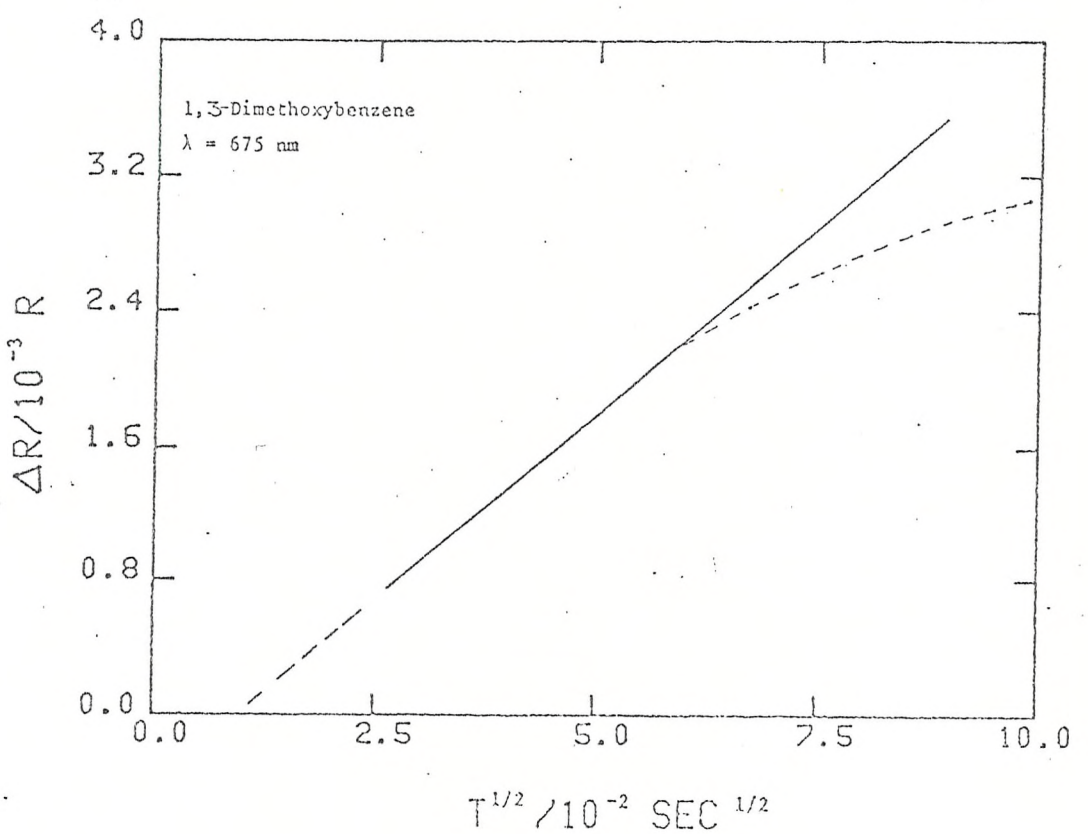

Fig 5.17 Optical transient and absorbance vs. $t^{\frac{1}{2}}$ plot for the anodic oxidation of 1,3- Dimethoxybenzene

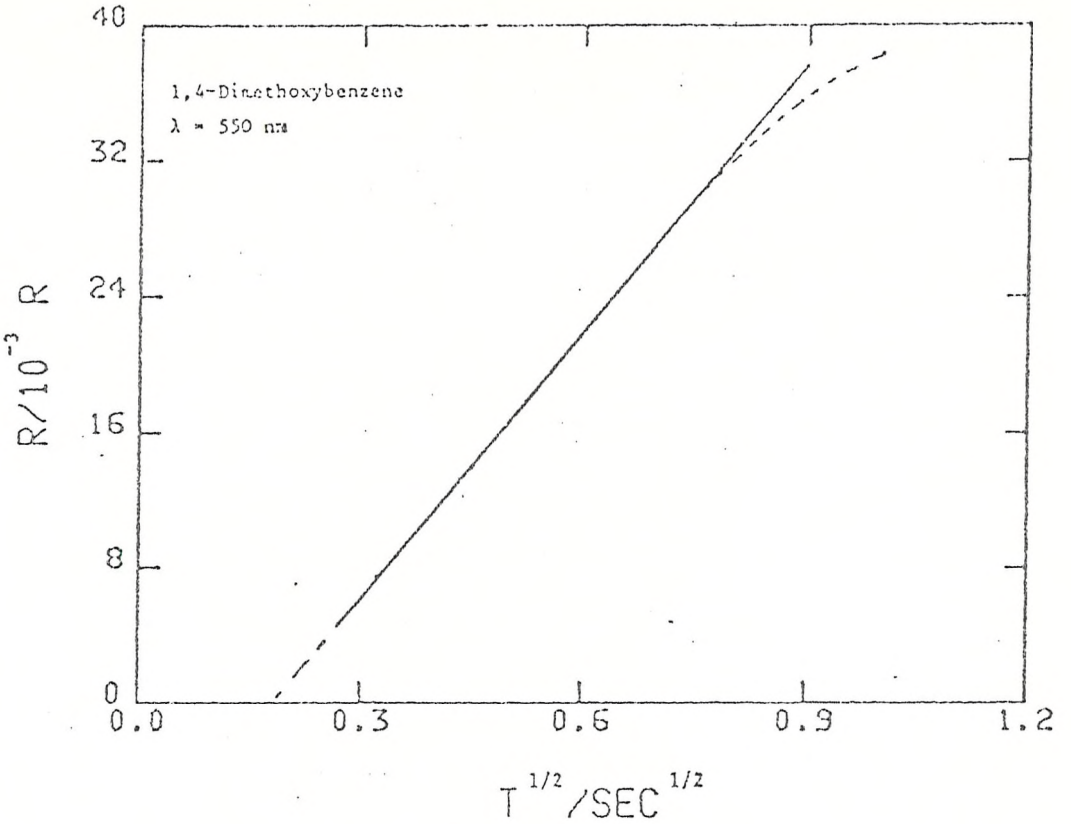

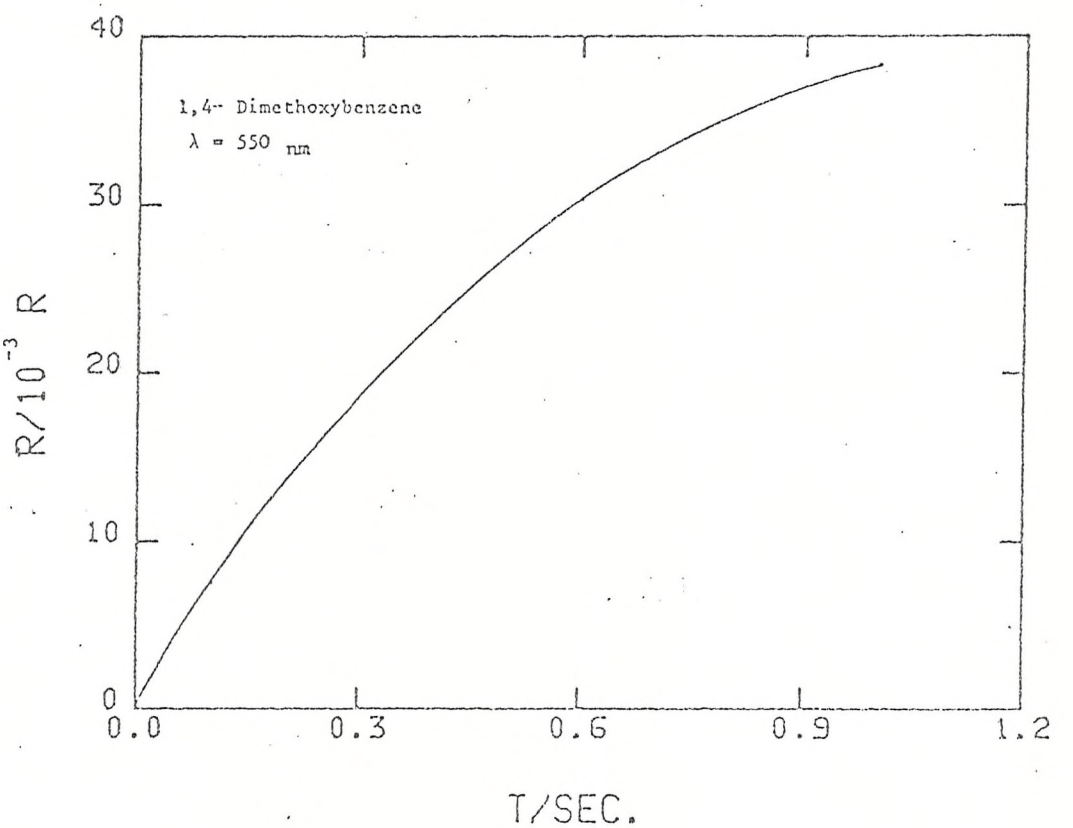

Fig. 5.18 Optical transient and absorbance vs. $t^{\frac{1}{2}}$ plot for the anodic oxidation of 1,4- Dimethoxybenzene

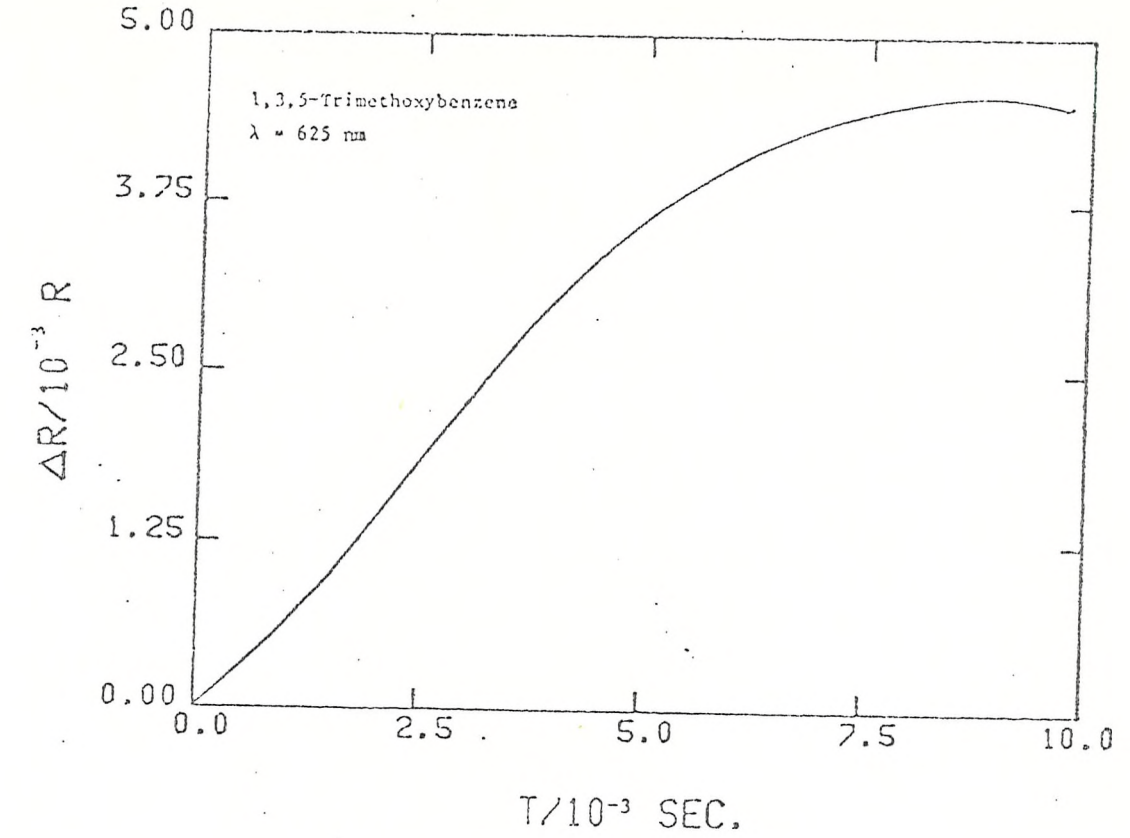

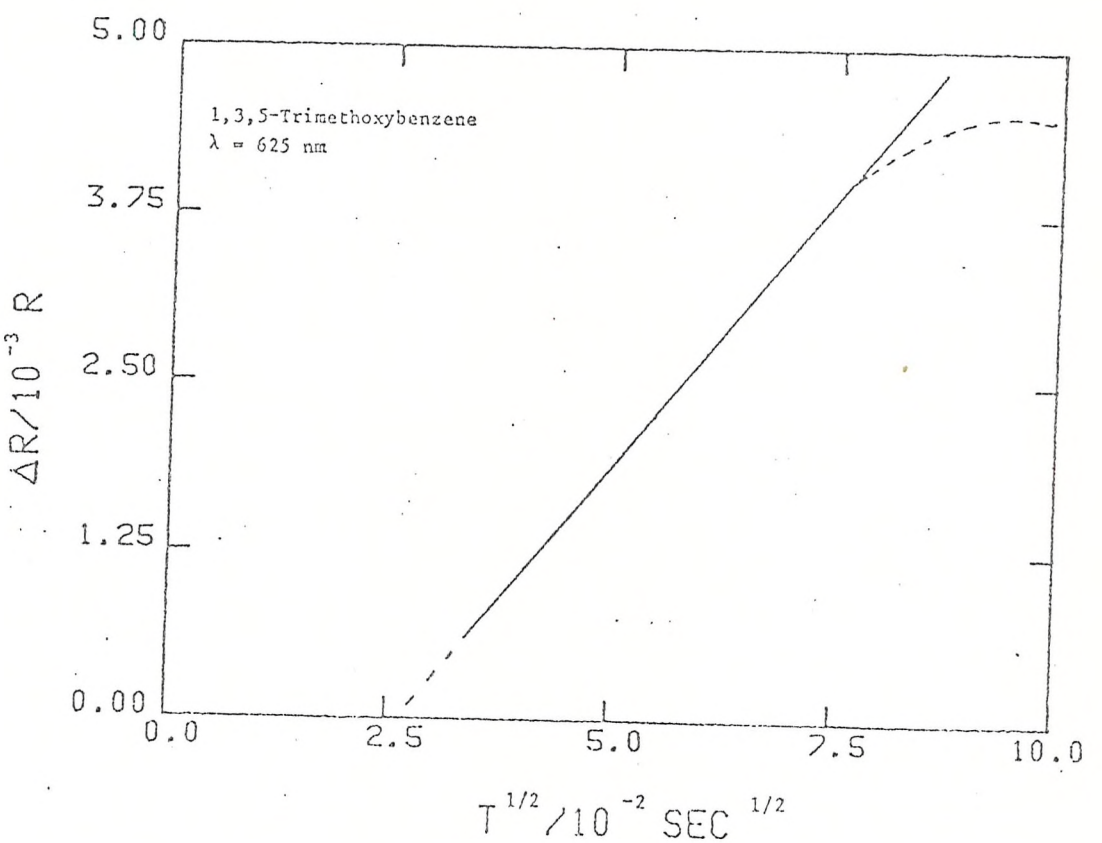

Fig. 5.19 Optical transient and absorbance vs. $t^{\frac{1}{2}}$ plot for the anodic oxidation of 1,3,5- Trimethoxybenzene

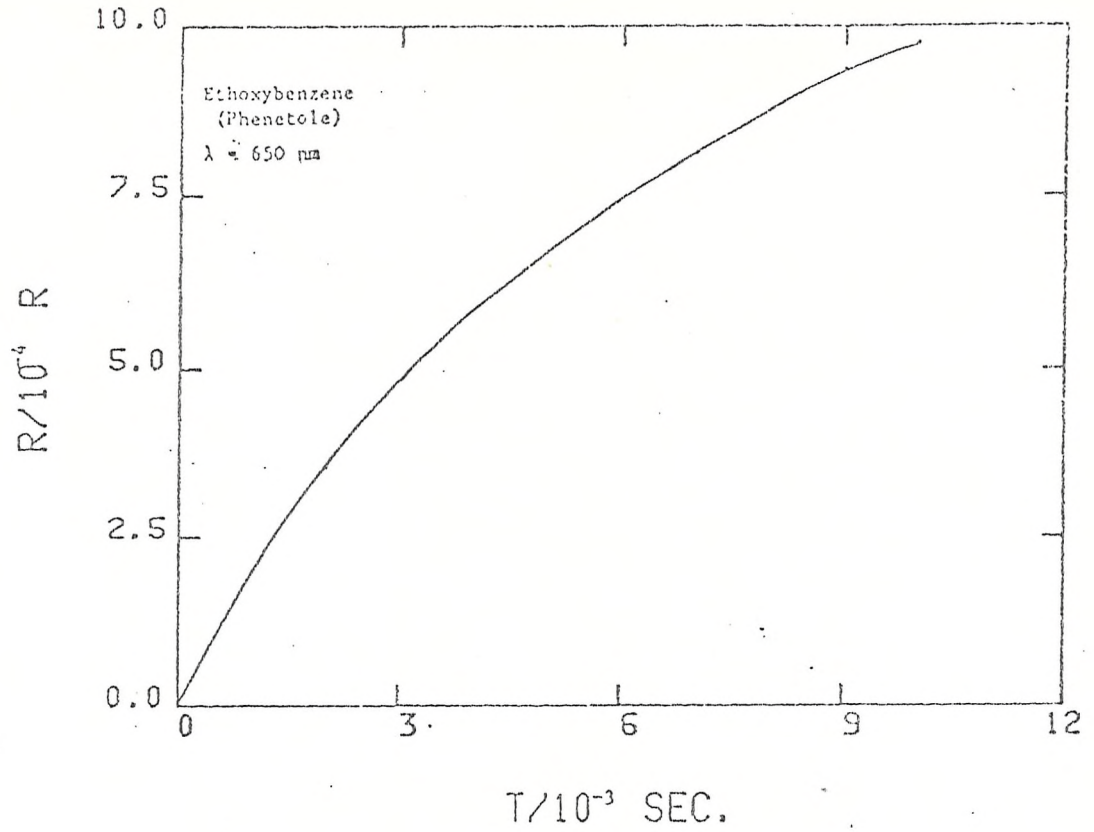

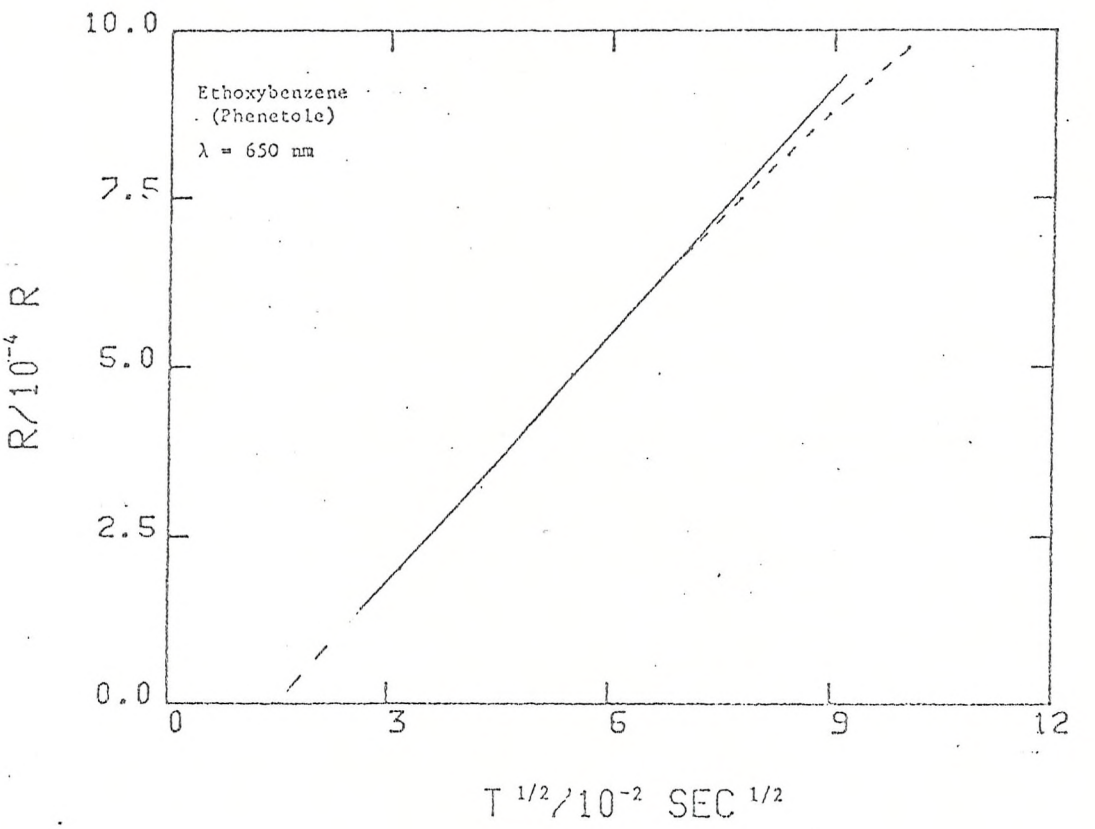

Fig. 5.20 Optical transient and absorbance vs. $t^{\frac{1}{2}}$ plot for the anodic oxidation of Ethoxybenzene (Phenetole)

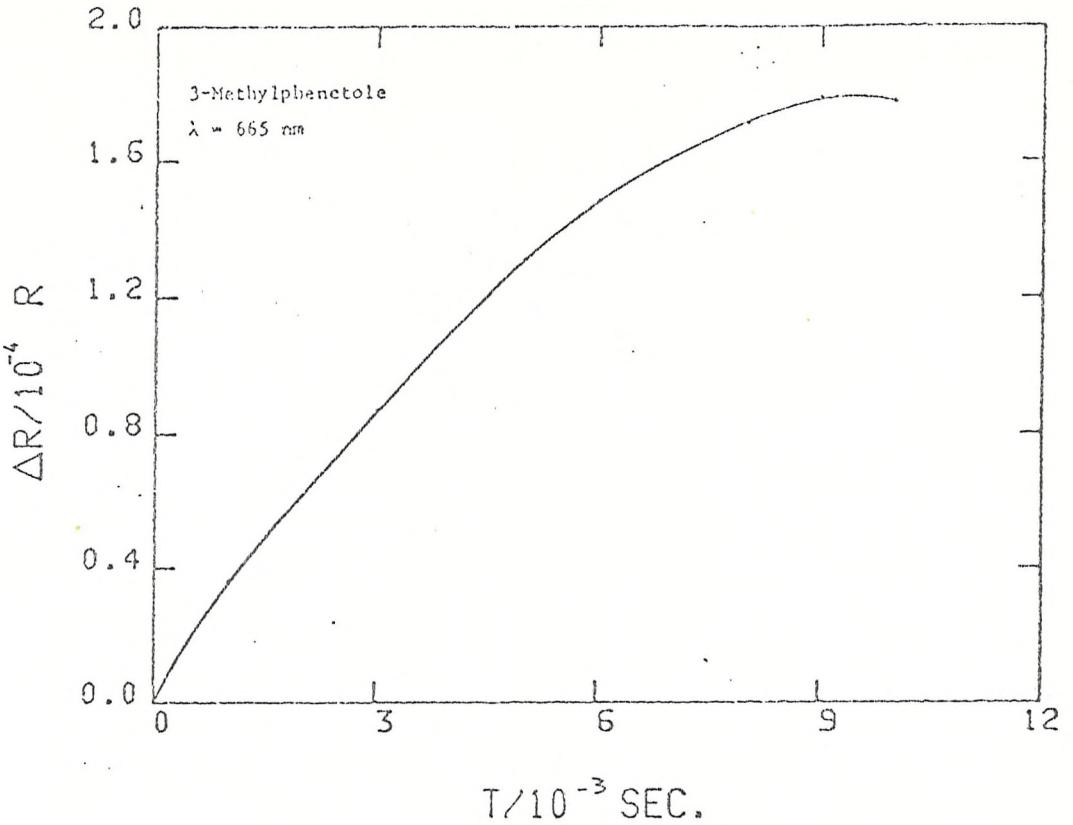

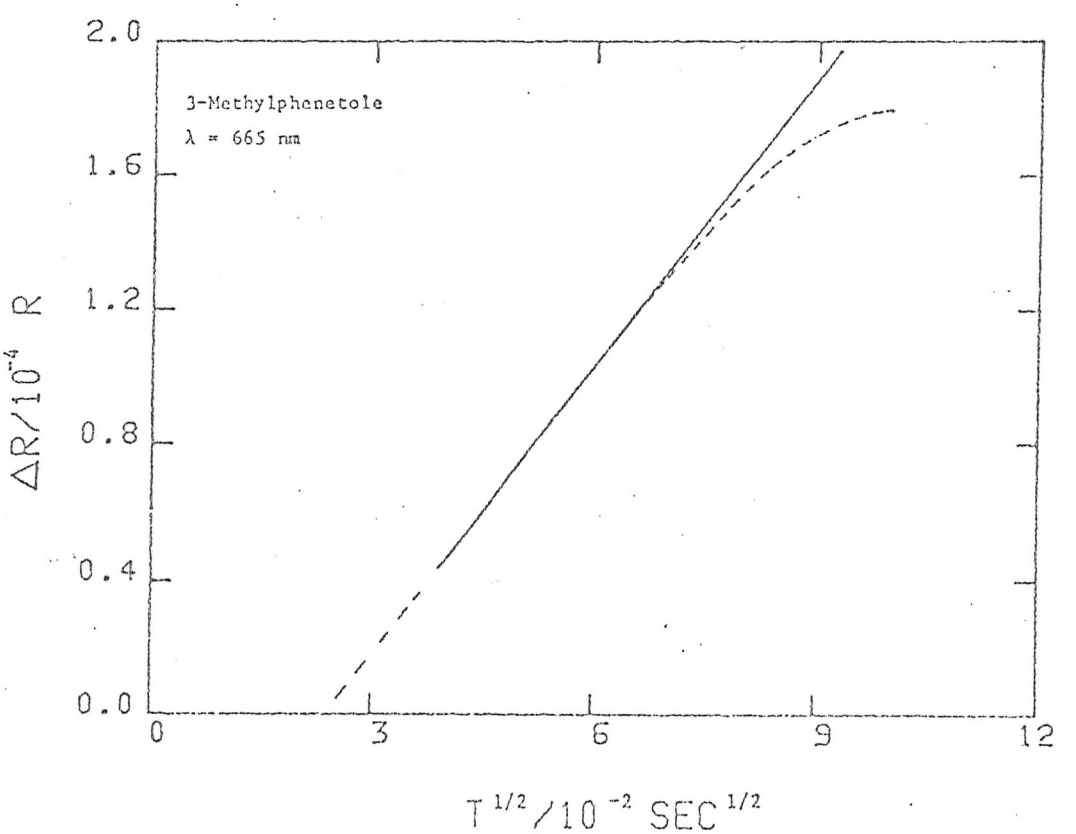

Fig. 5.21 Optical transient and absorbance vs. $t^{\frac{1}{2}}$ plot for the anodic oxidation of 3- Methylphenetole

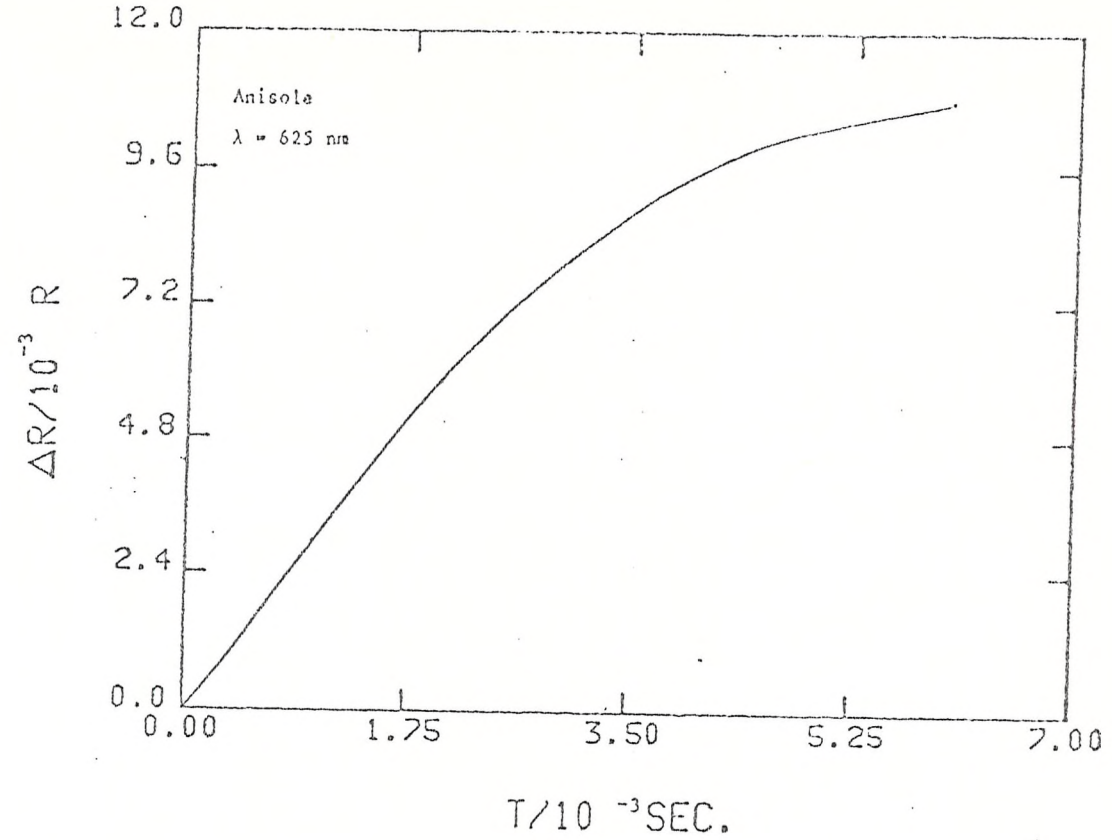

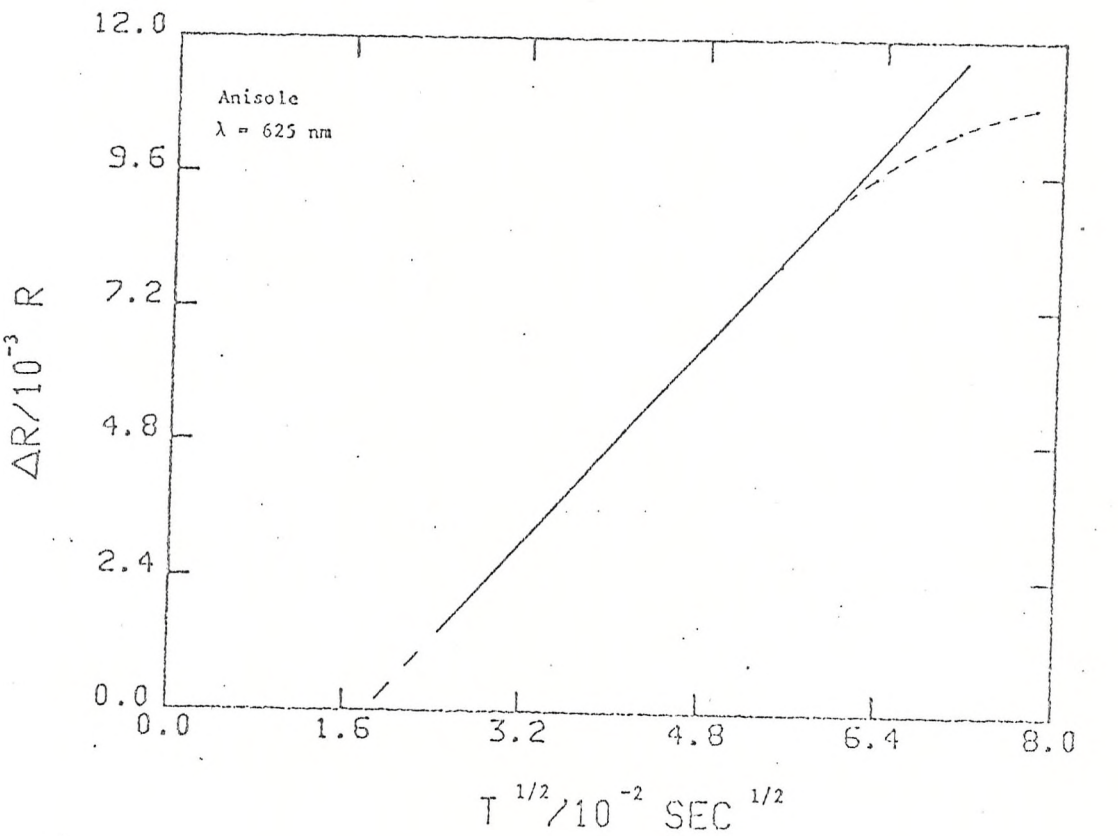

Fig. 5.22 Optical transient and absorbance vs. $t^{\frac{1}{2}}$ plot for the anodic oxidation of Anisole

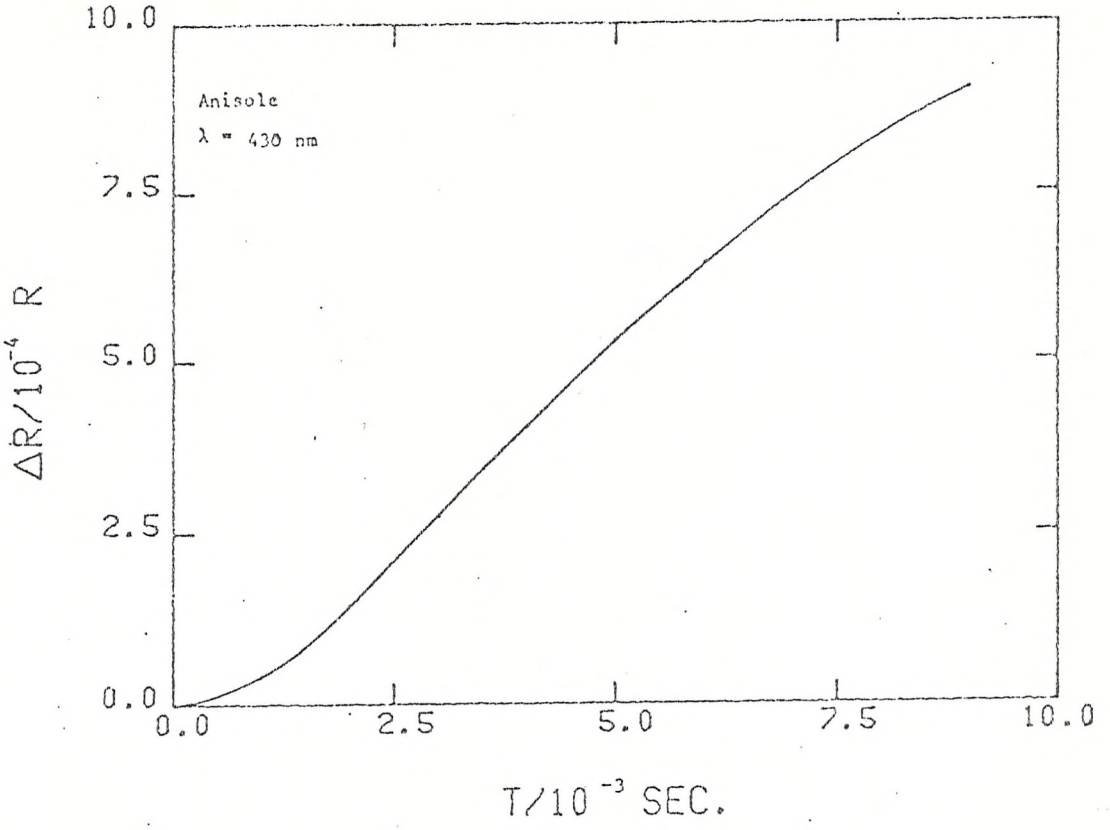

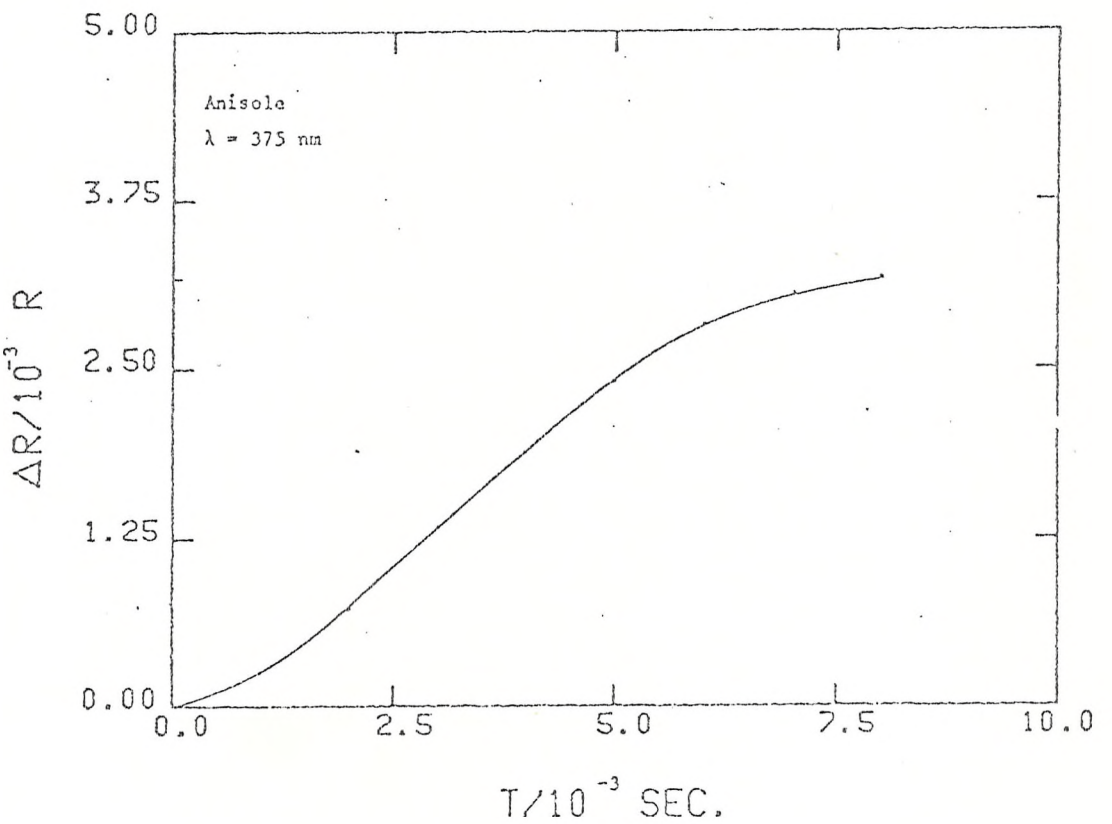

Fig. 5.23 Optical transients for the anodic oxidation of Anisole

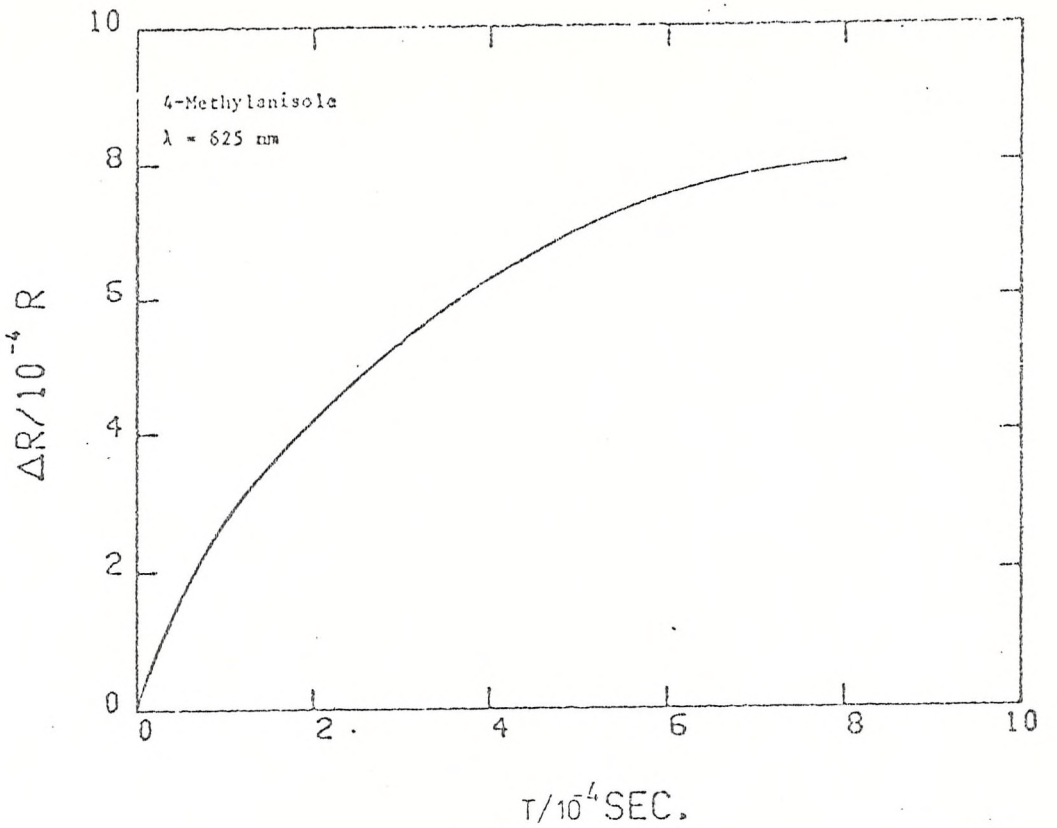

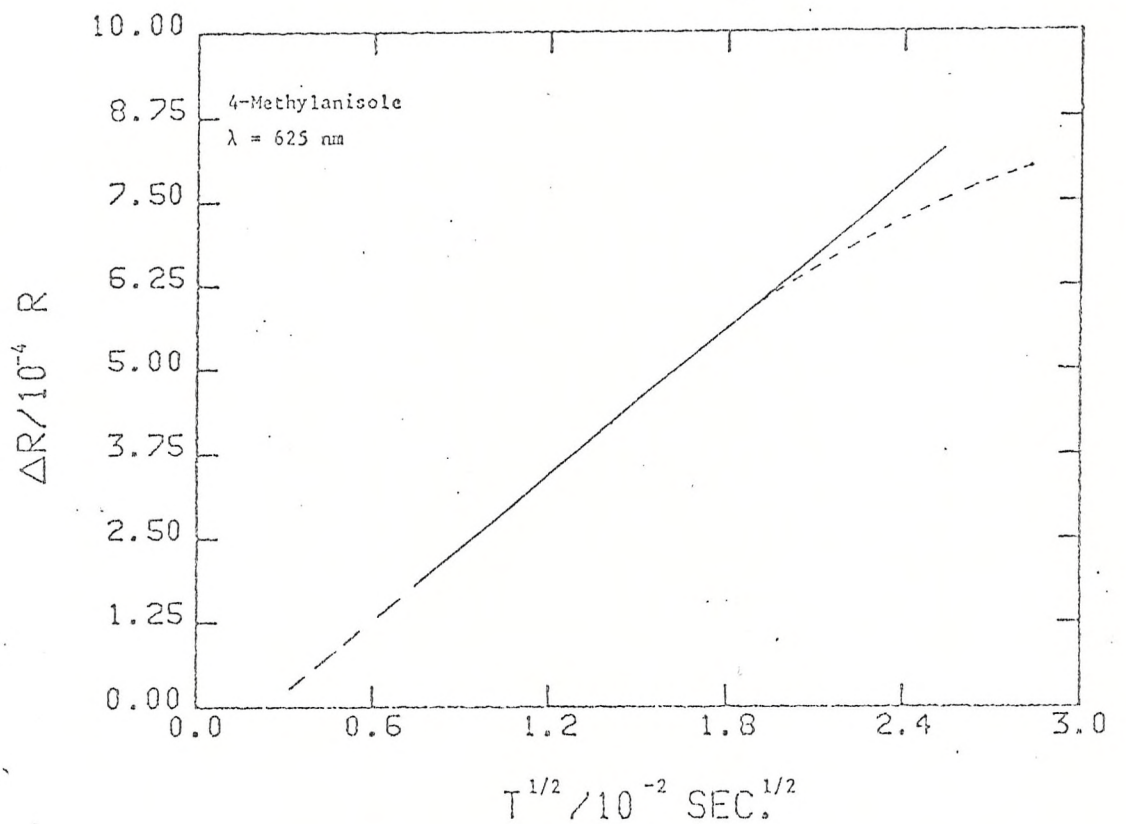

Fig 5.24 Optical transient and absorbance vs. $t^{\frac{1}{2}}$ plot for the anodic oxidation of 4-Methylanisole

SUBSTRATE	λ (nm) $\{\varepsilon(M^{-1}\ cm^{-1})\}$	k_f (s^{-1})
1,3-Dimethoxybenzene	675 {1659}	38.0
1,4-Dimethoxybenzene	550 {3135}	0.9
1,3,5-Trimethoxybenzene	625 {3504}	13.2
Ethoxybenzene (Phenetole)	650 {6839}	7.6
3-Methylphenetole	665 {5839}	9.1
Anisole	625 {6830}	8.6
4-Methylanisole	630 {1060}	30.6

TABLE 5.5.- Experimental data for the extinction coefficient and pseudo-first order rate constant.

5.4 PREPARATIVE COULOMETRY.

Preparative electrolysis was carried out on 1,4-Dimethoxy benzene in the presence of resin and using the pulse activation procedure; 35 mg. (2.53×10^{-4} mol.) of starting material was electrolyzed in acetonitrile by modulating the potential between +0.800 Volts and + 1.00 Volts with a symetrical square wave of 2 Hz. The initial current was 95 mA., and this value was mantained for a long time, the final current being 3 mA.; 30 mg. of 1,4-Dimethoxybenzene reacted and 5 mg. remained unreacted. Two grams of resin were used and 14.3 mg. of residue was extracted from the resin. The material was dissolved in diethyl ether, examined by g.l.c. coupled with a mass spectrometer, the results of this analysis suggested the formation of 2,5-Dimethoxy benzylacetamide with a yield of 34% with respect to the starting material. Preparative electrolyses of the other members of this series were not carried out.

5.5 DISCUSSION.

This series is particularly interesting for studying intermediates because of the expected stabilizing effect of electrondonating groups on the cation radicals. For that reason, perhaps, they have been very widely studied[7-19] and several schemes have been proposed for the various reactions under examination.

For all the Alkoxybenzenes examined in this work, as for the former series, cyclic voltammetry peak heights for the anodic oxidation in acetonitrile did not show simple linear proportionality to the square root of the sweep rates, therefore, the same asumptions made for the alkylbenzenes for the treatment of cyclic voltammetric

data, were also made for this series. The same tendency for one-electron transfer at short times then a crossover region, characteristic of an homogeneous reaction followed by a two-electron transfer at longer times was observed for the alkoxybenzenes in both, cyclic voltammetry and chronoamperometry experiments. 1,4-Dimethoxybenzene produced the most stable intermediate species of all in this series. In general, the alkoxybenzenes oxidized in dry acetonitrile on platinum electrode producing intermediate species more stable than those produced by the alkylbenzenes when they were oxidized under the same conditions. If we observe the I vs $t^{-\frac{1}{2}}$ plots for the alkoxy benzenes, the time scale on which the reactions take place allows one to observe clearly the transition from a one-electron to a two electron process.

In the reflectance experiments, the alkoxybenzenes showed very complex spectra, but with the same tendency observed for the alkylbenzenes to show absorption peaks in three regions of wavelengths. The spectral absorptions obtained from the reflectance experiments, are in good agreement with the literature [2-6] (see table 5. 6). Analysis of the shapes of the experimental absorbance/time transients for different wavelengths indicated for all the members of this series that a cation radical absorbing at the longer wavelengths was the primary species produced at the electrode surface; the same criteria were used as for the alkylbenzenes (see paragraph 4.5). On this basis those bands λ_1, in table 5.5, can be assigned to the cation radical.

SUBSTRATE	λ(nm){ε(M^{-1} cm^{-1})} Ref. 2	Ref. 3	Ref. 4	Ref. 5	Ref. 6	This Work
1,2-Dimethoxybenzene	290 {9300} 400 {2830}					
1,3-Dimethoxybenzene	280 460 {4000} 430 {3550}					380 420 560 675 {1659}
1,4-Dimethoxybenzene	300 {13000} 480 {9040} 460 {9540}	315 430 455			430 {4040} 460 {9540}	330 430 550 {3135}
1,3,5-Trimethoxybenzene	280 450 {4150} 580 {5710}		260			290 350 540 625 {3504}
Ethoxybenzene (Phenetole)						430 500 540 650 {6839}
3-Methylphenetole						280 420 495 665 {5839}
Anisole	280 {7240} 430 {3800}		280 {7400} 430 {3200} 810 {300}	300 491 628		290 430 540 628 {6830}
4-Methylanisole						300 420 630 {1060}

TABLE 5.6.- Comparison of the spectral bands with those reported in the literature.

1,4-Dimethoxybenzene was chosen as a model compound for detailed mechanistic analysis because of the stability of its cation radical and the availability of data in the literature for comparison.

The evidence from the cyclic voltammetry and the chronoamperometry is that all the members of this series reacted according to an ECE mechanism when they were anodically oxidized at platinum in dry acetonitrile / $Bu^n_4 NBF_4$ at room temperature.

The product analysis was made by comparison with a standard sample of the suspected product. This procedure proved that the product was coincident with the species(V) proposed in the scheme shown on the next page.

As it was stated earlier in this chapter, the first electron transfer leads to the formation of the cation radical. Unlike the cation radicals of alkylbenzenes which decay to the neutral radical by the loss of a proton, the decay of the radical cations from the alkoxybenzenes occurs by nucleophilic attack of the solvent on the cation radical to produce the species (II), which undergoes an electron transfer followed by the loss of an aromatic proton to yield species (IV).

SCHEME II

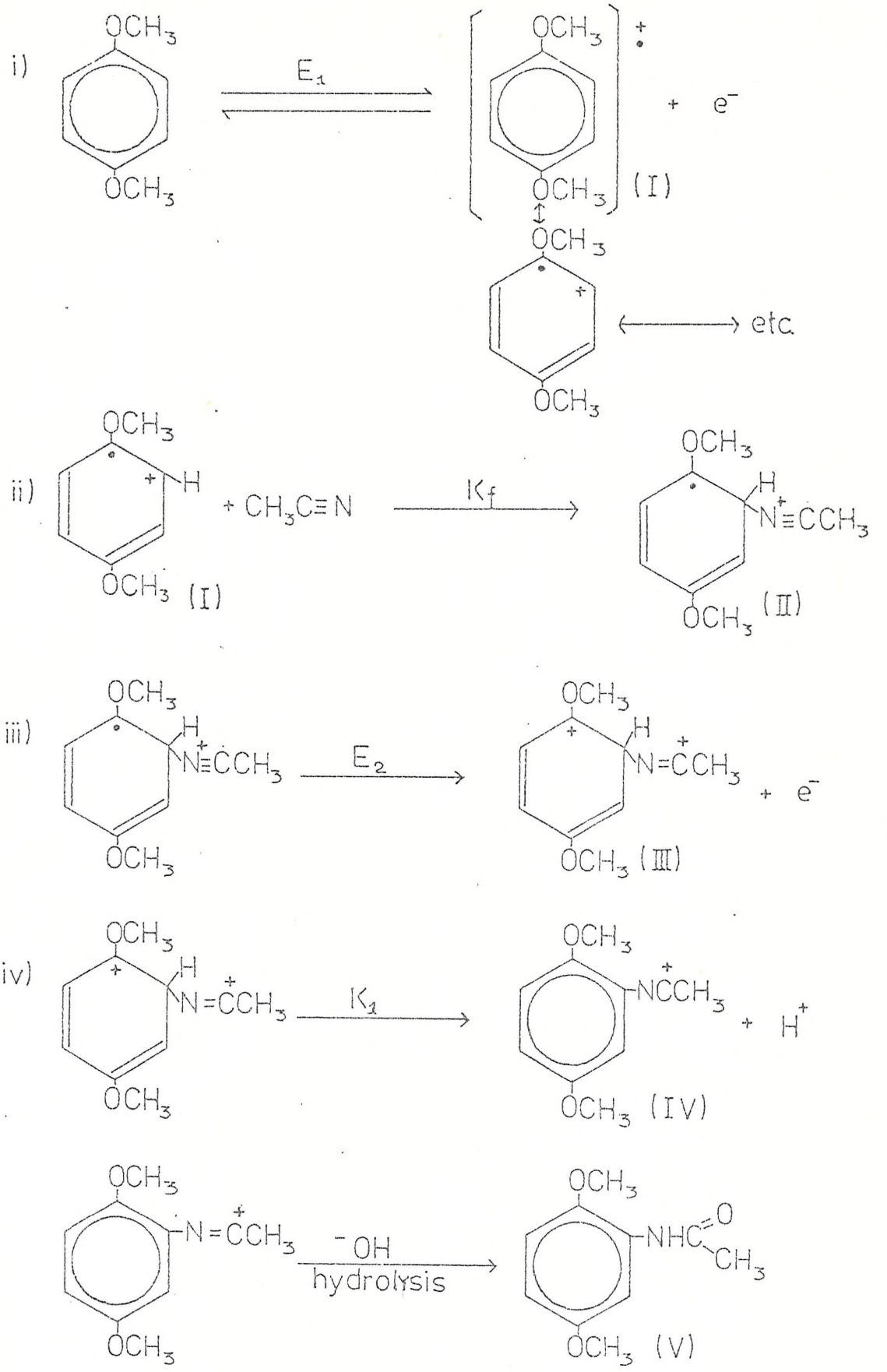
i)
E_1
+ e^-
(I)
etc.
ii)
+ $CH_3C\equiv N$
K_f
(I)
(II)
iii)
E_2
+ e^-
(III)
iv)
K_1
+ H^+
(IV)
^-OH
hydrolysis
(V)

It is interesting to note that the cyclic voltammograms showed a peak due to the reduction of a hydrogen ion, for all the members of this series; two possibilities have to be taken into account from the origin of this hydrogen ion: either (a) there is a competition for the decay of the cation radical between the nucleophilic attack proposed in scheme II, and the loss of a proton by the cation radical to produce a free radical, or (b) paths (iii) and (iv) in scheme II are sufficiently rapid for the proton loss in (IV) to be observed in the reverse scan of cyclic voltammetry at relatively slow sweep rates. If we favour possibility (a), the rate constant we are measuring for the decay of the cation radical is due to a mixture of both processes and from the observations of this work it is not possible to be certain whether the proton loss at that stage occurs on the side chain or on the nucleus, perhaps an analysis of the secondary products would enable us to discriminate. If we consider possibility (b), the rate constant refers to the kinetics of the nucleophilic reaction. Nevertheless, in the light of this work, the major product identified indicates that there is a major contribution from the nucleophilic attack on the cation radical by theacetonitrile. The last stage of the proposed mechanism is the same as that for the alkylbenzenes ; the hydrolysis of the nitrilium ion to produce the acetamide. Cyanation, methoxylation and acetoxylation of methoxybenzenes have been extensively studied [7-9, 21-24] In all these cases, the formation of the cation radical has been proposed as the primary species produced at the electrode. There is also agreement that the anodic axidation of methoxybenzenes may follow an ECE type of mechanism[20,21] and support for the assumption that the cation radical does not decay by proton

loss but by a nucleophilic attack.

For the cyanation of 1,4-dimethoxybenzene, some authors [7,25] have suggested that the decay of the cation radical is due to the attack on position 1 by the nitrile ion with the subsequent release of the methoxy group at that position to form anisonitrile. For the acetoxylation, however, nucleophilic attack on the aromatic ring has been proposed by Yoshida et al[8], furthermore, they propose a scheme in which the formation of an intermediate of the type

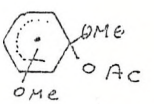

does not occur.

Eberson and co-workers have reported, for the cyanation of 1,4-dimethoxybenzene, the formation of 4-methoxybenzonitrile (40%) and 2,5-dimethoxybenzonitrile (3%). The same observations of attack at the free ring position were made in for other dimethoxybenzenes. Other authors[2] have observed the formation of dimeric species. The ocurrence of these reactions will depend, to same extent, upon the amount of positive charge[10] on certain positions on the ring. In the case of 1,4-dimethoxybenzene there is a high unpaired electron density at position 1 and 4 and, hence, if there is the formation of a dimer, it would be expected to be in those positions; the 2, 3, 5 and 6 positions, however, have a high positive charge density which makes the 1,4-dimethoxybenzene a good acid and also more vulnerable to nucleophilic attack at these positions. In this work, nucleophilic attack on the free ring positions was observed. The use of the cationic resin, allowed the nitrilium ion exchange with the proton of the resin and makes the reaction

more selective to favour the formation of the 2,5-dimethoxybenzyl-acetamide.

5.6 REFERENCES

(1) A. Bewick, J. M. Mellor and B. S. Pons. Electrochim Acta, 25, 931 (1980)

(2) P.O"Neill, S. Steenken and D. Schulte-Frohlinde, J. Phys. Chem. 79, 2773 (1975)

(3) G. Grabner, W. Rauscher, J. Zechner and N. Geltoff, J. Chem. Soc. Chem. Comm., 222 (1980)

(4) J. Holeman and K. Sehesied J. Phys. Chem. 80, 1642 (1976)

(5) T. J. Pinnavaia, P. L. Hall, S. S. Cady and M. M. Mortland, J. Phys. Chem., 78, 994 (1974)

(6) E. Ernstbrunner, R. B. Girling, W. E. L. Grossman and R. E. Hester, J. Chem. Soc. Perkin II.

(7) S. Andreades and E. W. Zahnow, J. Am. Chem. Soc. 91, 4181 (1969)

(8) K. Yoshida, M. Shigi, T. Kanbe and T. Fueno, J. Org. Chem. 40, 3805 (1975)

(9) B. Belleau and N. L. Weinberg. J. Am. Chem. Soc. 85, 2525 (1963)

(10) K. Yoshida, M. Shigi and T. Fueno, J. Org. Chem. 40, 63 (1975)

(11) M. Rakoutz, D. Michelet, B. Brossaro and J. Varagnat. Tet. Letters, 39, 3723 (1979)

(12) M. J. Manning, D. R. Henton and J. S. Swenton, Tet. Letters 1679 (1977)

(13) W. T. Dixon and D. Murphy, J. Chem. Soc. Perkin II, 1823 (1976)

(14) L. Eberson and B. Helgee. Acta Chem. Scand B29, 151 (1975)

(15) L. Eberson and B. Helgee. Chem. Scripta, 5, 47 (1974)

(16) B. Grant, N. J. Clecak, Michael Oxsen, A. Jaffe and G. S. Keller, J. Org. Chem. 45, 702 (1980)

(17) P. D. Sullivan, J. R. Bolton, and W. E. Geier Jr., J. Am. Chem. Soc. 92, 4176 (1970)

(18) D. R. Henton, R. L. McCreery and J. S. Swenton, J. Org. Chem. 45, 369 (1980)

(19) A. Laurent, E. Laurent and P. Locher, Electrochim Acta, 30, 857 (1975)

(20) L. Eberson and K. Nyberg, Acc. Chem. 6, 106 (1973)

(21) L. Eberson, M. Baizer, Ed. Organic electrochemistry, Dekker, New York 1973.

(22) N.L. Weinberg and B.Belleau, Tetrahedron Letters, 29, 279 (1973)

(23) L.Eberson,and E. Helgee, Acta Chem. Scand, B32, 313(1978)

(24) K. Yoshida and S. Nagase, J. Am. Chem. Soc.101:15 ,4268(1979)

(25) N.L. Weinberg,D.H. Marr and C.N. Wu, J.Am.Chem. Soc.,97:6,1499(1975)

CHAPTER 6 : GENERAL DISCUSION

6.1 Mechanistic considerations

6.2 Pulsed electrolysis

6.3 References

6.1 MECHANISTIC CONSIDERATIONS.-

In this work, the anodic functionalization of substituted benzenes (alkylbenzenes and alkoxybenzenes) in dry acetonitrile to produce acetamides has been described. The results show that two general reactions types are observed: side chain substitution is favoured for alkylbenzenes and ring substitutions for alkoxybenzenes. Side chain oxidation is also expected to occur for alkoxybenzenes at potentials higher than the peak potential[1]. An ECE type of mechanism has been observed in both cases. From the cyclic voltammetry, a wave due to the reduction of hydrogen ion could be observed for both, the alkyl and alkoxybenzenes, which supports the postulated reaction schemes

Consideration of the voltammetric characteristics, supplemented by coulometry and analysis of products, leads to the mechanistic schemes I and II proposed in chapter 4 and 5 for the alkyl and alkoxybenzenes respectively.

In the case of the alkylbenzenes (Scheme I), the cation radical undergoes a de-protonation to produce a neutral radical. This is oxidized either anodically or homogeneously (DISP mechanism) to a carbonium ion. This latter species is attacked by the solvent to give the nitrilium ion which is then trapped by the cationic exchange resin and then hydrolysed to the acetamide.

For the decay of the anodically generated cation radical of the alkoxybenzenes, however, two competitive pathways could be considered. Firstly, the cation radical is attacked by the acetonitrile

to produce the species (II) in scheme (II), followed by further anodic oxidation and sucessive proton release thus leading to the nitrilium ion which is also trapped by the resin and then hydrolyzed to yield the annular acetamide. Alternatively, the cation radical could lose a proton, probably from the side chain, to produce species similar to those proposed in scheme I. Indeed, the use of the resin permits the selectivity of the product because the most stable of the species (in this case it is expected to be the annular substituted species) will be trapped by the resin. If paths (iii) and (iv) in scheme (II) are fast enough, we would be able to observe from cyclic voltammetry, the reduction of the hydrogen ion released in path (iv).

The rate constants for the decay of the cation radicals of the alkylbenzenes are much higher than those for the decay of the alkoxybenzenes cation radicals. That is indicative of the stabilizing effect of the methoxy groups on the cation radicals.

6.2 PULSED ELECTROLYSIS.-

The anodic oxidation of organic molecules, is often hampered to a greater or lower extent by the problem of electrode fouling. This is often severe when non aqueous media are used. A technique which is frequently used to try to overcome this problem during steady state electrolyses is periodically to pulse the working electrode to a high anodic potential in order to oxidize off the adsorbed species which are inhibiting the desired reaction. This method is often succesful[2-4] In the present work fouling was observed for many of the substrates and the simple pulsed activation method

described above was found to have little effect. However, it was found that dramatic improvements could be obtained by combining a different kind of pulsed electrolysis procedure with the use of an ion exchange resin in the anolyte to trap cationic intermediates. In this method, instead of pulsing the electrode to a potential considerably more positive than that required for the normal oxidation, the electrode was pulsed to a less positive value. It was found that the best results were obtained if the pulsing took the form of a square wave with equal periods at the normal oxidation potential and at the more negative value, the latter being chosen to be as negative as possible without leading to appreciable cathodic currents. A good example of the efficacy of this method is seen in the oxidation of Toluene. The literature value for the yield of benzylacetamide obtained at a steady potential and without the benefit of the resin is 3%[6]; a similar electrolysis in the presence of the resin led to a yield of 17%.[5] However, as reported in table 4.9, the yield in this work using pulsed electrolysis and resin was 44%

It is clear that the pulse technique used in this work does not overcome the electrode fouling by oxidizing off adsorbed species. In conjunction with the resin trapping agent, it appears to provide optimum conditions for the trapping of intermediates thus minimising further undersirable reactions leading to adsorbable poisoning species. The rather lengthy cathodic period of the square wave, seems to be necessary for the complete trapping on the resin of the species produced in relatively high concentration during the anodic period. It is interesting to note that, in the case of Hexaethylbenzenes, pulsed electrolysis in the absence of resin was suf

ficient to overcome electrode fouling but the presence of the resin was necessary to achieve a good yield of the desired amide product. It is likely that this technique, or variants of it, could be used in many cases to obtain good product yields.

Thus it is clear that the variations of chemistry observed in this work are mainly due to the differing structures and stabilities of the radical cation species, produced in the primary electron transfer reaction at the anode. The important factors are clearly the lifetime of the cation radical before it decays by proton loss (which will be related to its acid strength), and its susceptibility towards nucleophilic attack, which will be determined by the charge distribution in the ion.

6.3 REFERENCES

(1) T. Matsue, M. Fujihira and T. Osa., Bull Chem. Soc.Japan, 52, 3692 (1979)

(2) M. Fleischmann, J.N.Petrov and W.F.K.Wynne-Jones.,Electrochemistry Proceedings of 1st Australian conference, Pergamon London,1964.

(3) M. Fleischmann and F. Goodbridge, Discussion Faraday Soc., 45 , 254 (1968)

(4) G.J. Edwards, Southampton University, PhD. thesis, 1977.

(5) B.S. Pons, Southampton University, PhD. thesis 1979

(6) see reference given in ref 5 for Toluene.

APPENDIX

Infrared spectrum observed for the product of oxidation of Hexaethylbenzene.-

Wavenumber (cm^{-1})	Group
3100 - 3200	Secondary amide
1375 - 1400	$-CH_3$
2890	Tertiary C - H
1400 - 1500	Skeletal vibrations C-C
3000 - 3100	Aromatic C - H
1540 - 1870	C = O (amide)
1515 - 1650	Amide I band (N-H)
3400 - 3500	Free N-H stretch
1405 - 1450	CH_2 - N (amides)
1000 - 1100	Aromatics

Mass spectrum for the product of oxidation of 1,4-Dimethoxybenzene.-

Fractions (M.W.)	Loss of
180	$-CH_3$
165	$-CH_3$, $-CH_3$
164	$-OCH_3$
152	$-C(=O)CH_3$
150	$-CH_3$, $-CH_3$, $-CH_3$
149	$-OCH_3$, $-CH_3$
122	$-NHC(=O)CH_3$, $-CH_3$
107	$-NHC(=O)CH_3$, $-CH_3$, $-CH_3$

NMR spectrum for the product of oxidation of 1,4-Dimethoxybenzene in dry acetonitrile.

SPECTRUM N°	
DATE	
OPERATOR	
SAMPLE N°	
IDENTIFIED	

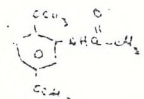

Standard Sample.

^1H	60	90	MHz
^{19}F	56.4	84.6	MHz

SOLVENT	$CDCl_3$
	N
	–
REF STD	TMS
	10
	–
	–
	–
	0
	½

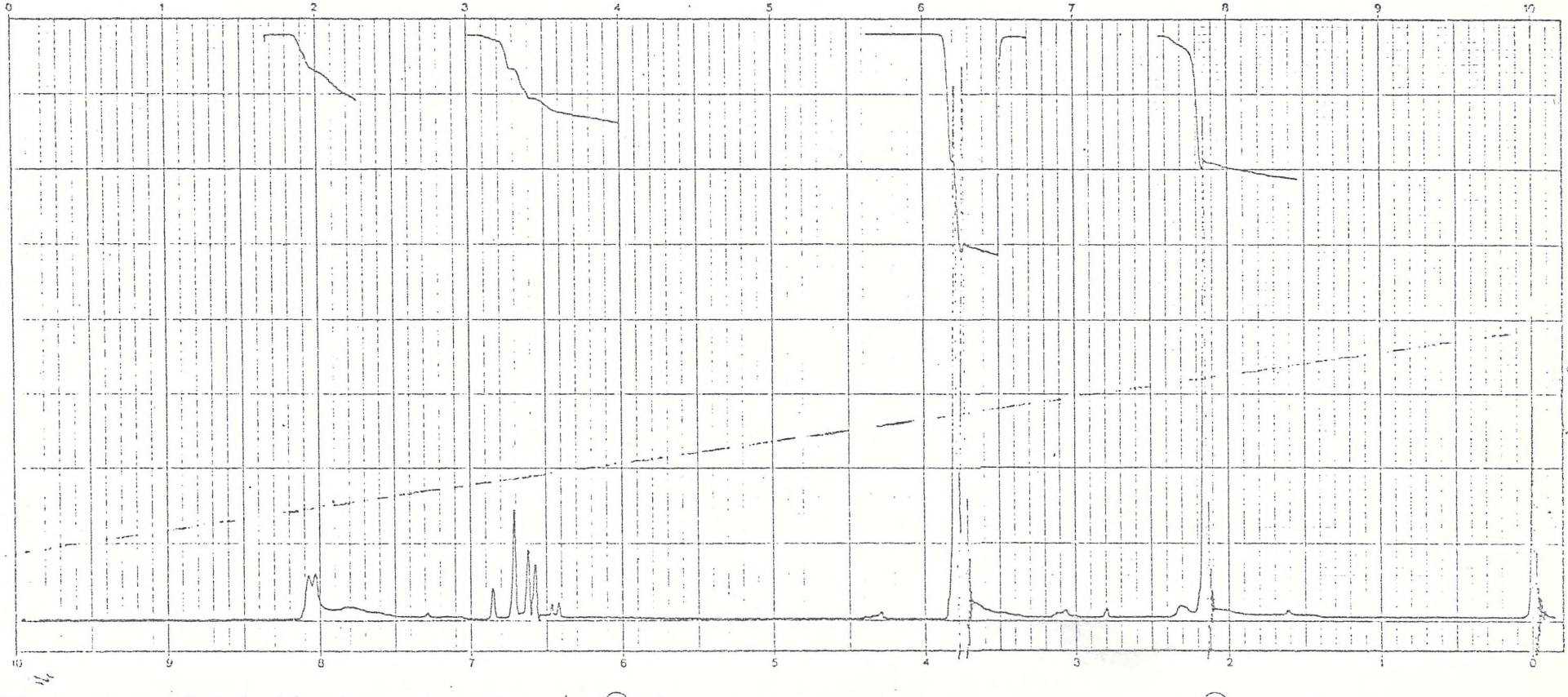

64°-620

NMR spectrum of 2,5- Dimethoxy benzyl acetamide (standard sample)

Mass spectrum for the product of oxidation of Hexaethylbenzene.*

The spectra shows mainly a mixture of the mono and the diamide (M.W. of monoamide: 303 and the diamide: 360).

Fractions (M.W.)	Loss of
303 - 360	mono and diamide respectively.
261 - 318	$- CH_2CO$
260 - 317	$- COCH_3$
246 - 303	$-NCOCH_3$
244	$2\ (-HNCOCH_3)$
245 - 302	$-HNCOCH_3$
234 - 291	$-CNCOCH_3$
232 - 289	$-COCH_3\ ,\ C_2H_4$
220 - 277	$-CONHC-,\ C_2H_4$
217 - 274	$COCH_3, C_2H_4,\ CH_3$
216 - 273	$NHCOCH_3\ ,\ C_2H_5$

This spectrum was taken for the product extracted from the resin. The characteristics of the spectra for the product extracted from the anolite solution are shown on next page.

Mass spectrum for the product of oxidation of Hexaethylbenzene.-

If we assume that the actual structure of the dimer(M.W. 549) is:

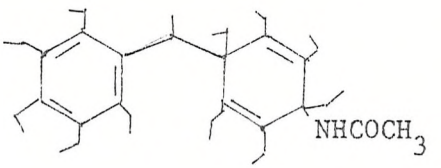

Fractions (M.W.)	Loss of
477	$-CH_2NHCOCH_3$
448	$-CH_2NHCOCH_3$, $-C_2H_5$
317	$NHCOCH_3$, 6 (C_2H_5)
315	6(C_2H_5) , 4 (CH_3)
304	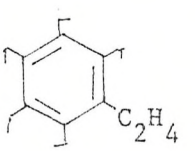
246	" , $NHCOCH_3$
245	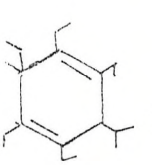 $NHCOCH_3$
247	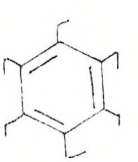 , 2 (C_2H_4)

234

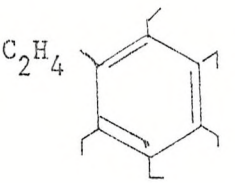

,

$-CH_2CO-, -C_2H_4$

232

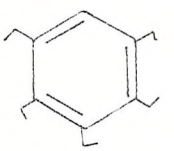

,

$-CH_2NHCOCH_3$, $-C_2H_4$

219

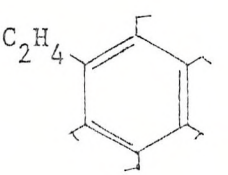

,

$-CH_2CO-$, $-C_2H_4$, $-CH_3$

Mass spectrum for the product of oxidation of 1-Phenyloctane.-

Fractions (M.W.)	Loss of
232	$-CH_3$
220	-NHCO
218	$-C_2H_5$
217	2 ($-CH_3$)
204	$-C_3H_7$
190	$-C_4H_9$
189	$-NHCOCH_3$
176	$-C_5H_{11}$
174	$-CH_3$, $NHCOCH_3$
162	$-C_6H_{13}$
148	$-C_7H_{15}$
135	$-CH(C_7H_{15})$
90	$-C_7H_{15}$, $NHCOCH_3$
77	$-(C_7H_{15})CHNHCOCH_3$

Mass spectrum for the product of oxidation of 1-Phenylnonane.-

Fractions (M.W.)	Loss of
246	$-CH_3$
231	$2(-CH_3)$
218	$-C_3H_7$
204	$-C_4H_9$
203	$-NHCOCH_3$
190	$-C_5H_{11}$,$-CHNCOCH_3$
176	$-C_6H_{13}$
162	$-C_7H_{15}$
148	$-C_8H_{17}$
135	$-CH(C_8H_{17})$
77	$-CH(C_8H_{17})NHCOCH_3$

Mass spectrum for the product of oxidation of n-Propylbenzene.-

Fractions (M.W.)	Loss of
162	$-CH_3$
148	$-C_2H_5$
147	2 ($-CH_3$)
135	$-CHC_2H_5$
134	$-COCH_3$
119	$-NHCOCH_3$
106	$-CHNHCOCH_3$
105	$-C_2H_5$, $-COCH_3$
77	$CH(C_2H_5)NHCOCH_3$ or $NHCOCH_3$, CHC_2H_5

Mass spectrum for the product of oxidation of Tertbutylbenzene.-

Fractions (M.W.)	Loss of
176	$-CH_3$
161	2 ($-CH_3$)
148	$-COCH_3$ or -NHCO
146	3 ($-CH_3$)
133	$-NHCOCH_3$
119	$-CH_2NHCOCH_3$
107	$-CCH_2NHCOCH_3$
103	$-NHCOCH_3$, 2 ($-CH_3$)
92	$-CCH_2NHCOCH_3$, CH_3
77	$-CCH_2NHCOCH_3$, 2 ($-CH_3$) or $-C(CH_3)_2CH_2NHCOCH_3$